DEVELOPMENT OF MICROSYSTEM TECHNOLOGY SUITABLE FOR BACTERIAL IDENTIFICATION AND GENE EXPRESSION MONITORING

DISSERTATION

ZUR ERLANGUNG DES AKADEMISCHEN GRADES

doctor rerum naturalium

vorgelegt dem Rat der Biologisch-Pharmazeutischen Fakultät der
Friedrich-Schiller-Universität Jena

von

Andriy Ruryk
geboren am 08. März 1971 in Lviv/Ukraine

Jena, im August 2004

Referees

1. __________________________

2. __________________________

3. __________________________

Day of the open defence: __________________________

Content

ABBREVIATIONS

Bkgd	Background signal
BSA	Bovine serum albumin
CCD	Charged-coupled device
cDNA	Complementary deoxyribonucleic acid
CV	Coefficient of variation
DDT	Dithiothreitol
DEPC	Diethyl pyrocarbonate
DMSO	Dimethylsulfoxid
dNTPs	Deoxynucleoside triphosphates
DSM	Deutsche Sammlung von Mikroorganismen
DTT	Dithiothreitol
EDTA	Ethylenediamine tetraacetic acid
EPPS	N-[2-hydroxyethyl]piperazine-N'-3-ethanesulfonic acid
FITC	Fluorescein isothiocyanate
GAPS	Gamma aminopropyl silane
G+C	Guanine plus cytosine content
HEPA	High efficiency particulate air
IMET	Institut für Mikrobiology und experimentelle Therapie
IPTG	Isopropyl-β-D-galactopyranoside
IS	Insertion sequence
mRNA	Messenger ribonucleic acid
rDNA	Ribosomal deoxyribonucleic acid
rRNA	Ribosomal ribonucleic acid
nDxA	Normalized spot intensity(ies)
ORF	Open reading frame
PAAG	Polyacrylamide gel
PBS	Phosphate buffered saline
PCR	Polymerase chain reaction
PM	Perfect match
PMT	Photo-multiplier tube
SD	Standard deviation
SDS	Sodium dodecyl sulphate
S/N	Signal-to-noise ratio
SNP	Single-nucleotide polymorphism
sRef	Background corrected reference intensity
SSC	Standard saline citrate
TIFF	Tag image file format
Tn	Transposon element
UV	Ultraviolet light

Introduction

The prospective microbiology tasks and the biology of antibiotic production by actinomycetes.

The main focus of prospective microbiology as an established research direction within life sciences over recent decades has been seeking a wider exploitation of the biological resources of medical, biotechnological and agricultural importance. Micro-organisms are well known as an inexhaustible source of novel biologics owing to the unlimited breadth of their metabolic possibilities. Based on the unique properties of their enzymes and enzymatic complexes this is reflected, on one hand, by the extreme ecological niches they can adapt to and optimally live in. Another line of survival strategy led to the redirection of significant living resources into the development of the effective defence mechanisms supporting population maintenance under mesophilic conditions and thus in a highly competitive environment. Based on current data on biological systematics it is a recognized fact that the main part of diversity of living forms on our planet is devoted to the microbial world, by which we usually mean representatives of Eubacteria and Archebacteria kingdoms. Moreover, at the moment we only know approximately 1% of all microbial isolates for which it turned out to be possible to define the selective cultivation methods (Vandamme *et al*., 1996). Given the aforementioned enormous diversity of properties and products of only the known bacteria, the main potential of biological diversity is expected to be disclosed in the near future as a result of development of efficient screening and isolation programs for as yet unknown microbes. Hence, the tasks of prospective microbiology are currently approached from both sides: firstly, by screening and searching for bacterial strains with new biochemical and biosynthetic properties, and secondly by modifying/broadening the above properties of already known strains. A significant part of these efforts has been devoted to actinomycetes. This is a group of morphologically and phylogenetically diverse gram-positive bacteria which share a common, and the most prominent, characteristic feature of high genomic DNA guanine-plus-cytosine (G+C) content (>55 mol%) (Hopwood *et al*., 1999). Their members, which are soil inhabitants, represent the typical example of aforementioned adaptation to the highly competitive mesophilic environment through the development of specific defence mechanisms, namely the production of a special class of secondary metabolites, antibiotics. This ability was extensively used for the commercial production of these bioactive molecules

for over half a century. In parallel, a lot of effort has been directed to an elucidation of the antibiotic biosynthesis process. Species *Streptomyces coelicolor* A3(2) represents the most extensively studied member. The above research has also led to complete sequencing and annotation of the whole genome of this organism, and the first among actinomycetes. Thus, the typical antibiotic biosynthesis process proceeds through the following scenario (Chater K.F., 1993): vegetative growth initiates under permissive conditions which allow, for example, spores to germinate on the substrate. Subsequent genome replication with cellular mass doubling, but without cellular division, lead to a spread of multinucleate substrate mycelia tangles. Upon entering into non-permissive conditions (i.e. growth component limitation), upward extension of aerial mycelia above the substrate occurs. They develop cross walls, which afterwards separate formed spores. In parallel, a biochemical transition from primary to secondary metabolism occurs. Thus, as a rule, antibiotics and other important secondary metabolites are produced by streptomycetes upon the onset of morphological differentiation into surface-grown and aerial-grown cultures and are uncoupled with vegetative growth. *S. coelicolor* A3(2) produces red-pigmented tripyrrole undecylprodigiosin (Red), lipopeptide calcium-dependent antibiotic (CDA) and deep-blue pigmented polyketide actinorodin (Act) (Hopwood D.A., 1999). Extensive investigation of the genetic control of their production has paved the way to the elucidation of complex biosynthetic pathways encoded by physically clustered genes located contiguously on the bacterial chromosome and regulated co-ordinately. This regulation usually occurs through pathway-specific transcriptional regulator(s); their encoding genes are normally clustered with biosynthetic genes as well as the genes conferring resistance to the own antibiotic. In addition, the above regulators are themselves subject to control by pleiotropic regulatory genes (Hopwood *et al*., 1995, Kieser *et al*., 2000). The whole scheme turned out to be true for the production of most antibiotics known to date (Bate *et al*., 1999; Distler *et al*., 1987; Geistlich *et al*., 1992; Gramajo *et al*., 1993; Narva *et al*., 1990; Raibaud *et al*., 1991; Wilson *et al*., 2001). Moreover, the availability of the fully sequenced 8.7 Mb long *S. coelicolor* genomic sequence has recently allowed simultaneous and global assessment of the transcription of antibiotic biosynthetic genes and their regulatory pathways using DNA microarrays (Huang *et al*., 2001). These experiments confirmed the general dependence of antibiotic production on the growth phase as well as coordinated regulation of biosynthetic genes. By correlation of temporal changes in expression with chromosomal position it was possible to identify the physical boundaries of biosynthetic loci, to infer the extent of known clusters, and to discover new groupings of physically contiguous and co-ordinately expressed genes that may have

related functions. Interestingly, transcriptional profiles of sigma factors and other pleiotropic regulatory proteins were affected in some instances by the mutations of the genes of pathway-specific regulators. It could imply a kind of feedback control of the biosynthetic pathway over the transcription of this class of regulators. An example concerned the afsR2/afsS multipathway regulator transcriptional profile in cells with mutated Act pathway-specific regulator actII-ORF4. In addition, a competition between both different antibiotic biosynthesis pathways and antibiotic and spore pigment production pathways was shown. This also might imply some higher-level interactive regulatory network.

However, some exceptions from this general scheme of antibiotic production by actinomycetes are well known. One of the most important of them is the production of clinically important macrolide antibiotic erythromycin by its major producer *Saccharopolyspora erythraea*. The differences regard the production mode and thus the regulation of biosynthesis cluster genes. The striking feature is that the erythromycin production is coupled with the vegetative growth of *S. eryhtrea* and that the *ery* cluster, obviously, lacks the pathway-specific regulator (Reeves *et al*., 1999; Reeves *et al*., 2002). The completed analysis of the erythromycin gene cluster resulted in mapping of the genes involved in the biosynthesis of the polyketide ring, the biosynthesis and attachment of mycarose to the macrolide ring and the biosynthesis and attachment of desosamine to the macrolide ring. Additionally, three genes encoding modifying enzymes were mapped within the cluster, one of them, encoding C-12 hydroxylase, marking the right flank border of the cluster (Stassi *et al*., 1993). Two more ORFs, *ery*BI, which is not essential for erythromycin A biosynthesis and encoding putative -glucosidase, and orf5, encoding a putative type II thioesterase, were also shown to be located in the *ery* gene cluster. At the left flank border two genes were mapped and shown to be transcribed in opposite directions: *erm*C encoding rRNA methylase, which confers resistance to the host organism and *ery*CI. Based on a border location of the latter gene, its co-localization with the self-resistance gene, analysis of data on mutation suppression experiments and those elucidating effects of multiple copies present in cells, some authors hypothesized this gene to be a sought-after pathway-specific regulatory gene (Vara *et al*., 1989, Hanel *et al*., 1993). *Ery*CI locus mutations cause the accumulation of 3α-mycarosyl-erythronolide B, the intermediate in ery biosynthesis that just lacks attached deoxysugar and thus precedes a formation of the first antibiotically active substance erythromycin D. There are conflicting data in the literature regarding putative functions of EryCI product. Some authors point to the strong resembling of putative regulatory gene from *Bacillus stearothermophillus* at the protein sequence level (Hanel *et al*., 1993); others assign a

transaminase function to this product, based on comparisons to the homologues from other amino sugar pathways, i.e. the strong relationship between EryCI enzyme and deduced TylB protein (61% identity). The latter participates in the biosynthesis of D-mycaminose, an analogue of D-desosamine in tylosine that is not deoxygenated at C-4 (Summer *et al*., 1997). In support of the hypothesis, one possible regulatory role of at least one of the *ery* cluster genes suggests the finding of pathway-specific regulatory genes for two other macrolide antibiotics: picromycin cluster has one regulator (Wilson *et al*., 2001) and tylosin cluster has five regulators (Bate *et al*., 1999). It has been shown that these regulatory genes are contiguous with or contained within their respective clusters. Moreover, a mutant with knocked-out former regulator was unable to convert macrolactones (10-deoxymethynolide and narbonolide) to glycosylated products, in analogy to above reports regarding *ery*CI mutants of *S. erythraea*. In addition, the erythromycin gene cluster of *Aeromicrobium erythreum* has been recently reported (Brikun *et al*., 2004). The 55.4-kb cluster contains 25 *ery* genes where homologues were found for each gene in the *ery* cluster of *S. erythraea*. Among four new predicted *ery* genes, two were internally positioned homologues of the *ery* genes of *S. erythraea*. The two others were found at the ends of the *ery* cluster, one of them being a MarR-family transcriptional repressor (ery-ORF25). Unfortunately, until now an involvement in erythromycin biosynthesis has been experimentally documented for only the gene located at opposite end of cluster. Hypothesis of involvement of *ery*-ORF25 product awaits further experiments. The same is also true of a final clarification on presumed functional units on *ery*CI-flanking regions of *S. erythraea*. It is still theoretically possible, if early mappings are correct (Vara *et al*., 1989), that the *ery* cluster of *S. erythraea* may represent a rare case in which essential antibiotic biosynthesis/regulatory gene(s) fall(s) well outside the boundaries of the biosynthesis gene cluster. Taken together with above notion of coupling between vegetative growth and *ery* production in *S. erythraea*, this situation points to the large biological and commercial interest in understanding the regulatory mechanisms operating in this bacteria which control the level of production of this valuable antibiotic. One of the most recent reports on transcriptional monitoring of the production cultures of wildtype and classically improved strains of *S. erythraea* using DNA microarrays of sequenced actinomycete *S. coelicolor* showed that the overproducer expressed the entire 56-kb *ery* cluster for several days longer that the wildtype strain (Lum *et al*., 2004). This gave one more piece of evidence for the presence of regulatory mechanisms exerting their effects on the level of the whole cluster. It is obvious that further analysis of this global view on comparative gene expression will be of great aid in the elucidation of *S. erythrea* regulatory pathways. On

the other hand, given the known differences in regulatory mechanisms between *S. coelicolor* and *S. erythraea,* as well as their production of different antibiotics, the necessity of using DNA microarrays with *S. erythraea's* own genes is also clearly evident.

Current taxonomy issues on actinomycete bacteria

A current developmental stage of bacterial taxonomy, polyphasic taxonomy, arose 35 years ago and aims at the integration of different kinds of data and information (phenotypic, genotypic and phylogenetic) on micro-organisms, essentially indicating a consensus type of taxonomy (Vandamme *et al*., 1996). Genotypic information is derived from cellular nucleic acids, whereas phenotypic information is derived from proteins and their functions, different chemotaxonomic markers, and a wide range of other expressed features (i.e. morphological, serological, etc.).

It is generally accepted that the results of the chemotaxonomic analyses of cellular compounds are extremely useful for delineating genera within the order *Actinomycetales* (Embley *et al*., 1994; Stackebrandt *et al*., 1995). Given the role these bacteria play and thus the efforts put in various isolation programs of rare or novel actinomycetes, certain achievements have been reported. For example, between 1990 and 2000 approximately 35 new genera of actinomycetes were described, 24 of them being monotypic. Because of the use of improved chemotaxonomic and molecular techniques, 10 of these genera were established via the reorganisation of combinations for members of previously described genera (Rainey *et al*., 1995; Stackebrandt *et al*., 1995; Klatte *et al*., 1994). In addition, novel taxa have been isolated from different environmental and clinical samples and their taxonomic positions have been clarified by means of polyphasic approaches (Groth *et al*., 1996; Kleespies *et al*., 1996; Nakamura *et al*., 1995; Yassin *et al*., 1996). However, generally speaking, the procedure itself is inefficient, as it is based on pure culture isolation and thus on the cultivation of bacteria. This always leads to an under-representation of samples, as it is impossible to optimize growth conditions for all actinomycete entrants. Therefore, culture-independent techniques have been developed, and this has become possible through both the recognition of a suitability of molecular chronometers in bacterial systematics, and recent great technological advance of the methods of molecular biology.

Molecular chronometers are represented by macromolecules with universal distribution and function among bacteria whose genes do not transmit horizontally and are characterized by varied molecular evolutionary rate. The most well-documented example so far is the fact that

deep phylogenetic relationships between living organisms, and thus their identification, can be deduced from sequence comparisons of rRNA molecules and from some of their sequence signature features (Gutell *et al*., 1994, Woese, 1987). Comparisons of the 16S rRNA sequences have revealed the phylogenetic framework of bacterial classification. As an increasing number of rDNA or rRNA nucleotide sequences became available, the comparison of homologous sequences could yield oligonucleotide stretches which are specific to the taxa being compared. These oligonucleotides could be labelled and used as probes in hybridization experiments with samples from known and unknown isolates. By using these specific sequences in PCR techniques, the target DNAs could be amplified and thus the detection level was drastically enhanced (Ludwig *et al*., 1999). By this means, tens of thousands of rRNA sequences became available. In combination with much-improved methods for inferring phylogenies, the rRNA tree quickly attained a status of "gold standard" for determining microbial relationships. Most importantly, the development and application of this so-called full rRNA cycle of PCR, cloning-assisted sequence retrieval followed by phylogenetic analysis, specific probe design and *in situ* cell hybridization, achieved its main goal, namely the uncoupling of microbial detection and identification from the need of cultivation. Some important drawbacks of the approach have also been noticed. If PCR amplification is used for 16S rRNA gene amplification it can result in both equalized and biased representation of the members of the analyzed mixture, regardless of the initial proportions of the templates (Suzuki *et al*., 1996, Wang *et al*., 1997). Obviously, no PCR conditions can be optimized for amplification of all 16S rRNA genes in complex mixtures. In addition, a library of obtained fragments should be constructed and checked for the presence of chimeric 16S rRNA sequences. These recombinant ("shuffle-gene") products are generated when a DNA strand of one gene anneals with complementary strand of a homologous gene to prime the next cycle of DNA synthesis (Brakenhoff *et al*., 1991, Meyerhans *et al*., 1990). In fact, this often occurs in amplifications of mixtures of 16S rRNA genes, due to the highly conserved structure of these sequences; it is dependent on the mixture complexity and genes of a lower presentation are mostly affected by this process (Liesack *et al*., 1991, Kopczynski *et al*., 1994). In particular, a high rate of chimeric product formation was shown when 16S rRNA gene fragment amplification from genomic DNAs of actinomycete bacteria was investigated (Wang *et al*., 1997). The results of the analysis of obtained sequences lead to the erroneous reporting of novel lines of evolutionary descent, give a false impression of biodiversity within microbial communities, and reduce the quality of centralized sequence databases. Another problem is represented by the fact that most bacteria have multiple copies of rRNA genes and their

sequences have commonly been found to be heterogeneous (Clayton *et al*., 1995). Therefore, the phylogenetic position of an organism cannot always be ascertained, as the rDNA sequences of different copies may fall in different clades on the phylogenetic tree. Moreover, these heterogeneous copies often take part in the above process of chimeric product formation even when single bacterial genomic DNA is used as a template in PCR (Wang *et al*., 1997).

The establishment of the above approach has raised important additional considerations and caused great discussion among specialists, which regard a correspondence of the trees above to real microbial phylogeny and, related to this, the importance of microbial species and thus taxa in general, definition. These considerations have arisen from the facts that rRNAs alone provide a narrow window on the microbial genome and that the individual protein-coding genes which give rise to all variety of phenotypic/chemotaxonomic characteristics as structural or enzymatic markers often disagree irreconcilably with the rRNA trees. Two possible reasons have been suggested for an explanation of the latter disagreement: a steady process of an accumulation of spontaneous mutations randomly distributed over the genome, and lateral (horizontal) gene flow, which has recently become a competitive model for the origin of microbial biodiversity in general (Charlebois *et al*., 2003). It has become clear that there is no way of defining a species that will correspond to both a phenotypically recognized entity and an evolving unit and will have, even approximately, the same meaning for all bacterial taxa (Vandamme *et al*., 1996). Therefore, a need to compare the structural features of many genomic regions between different environmental isolates, their pure cultures, and other bacterial population samples for proper identification has been recognized. Experiments exploring such “whole-genome trees” have recently been performed in order to extract the bulk phylogenetic signals that are inherent in the genome and to overcome the noise and bias of single-protein analyses. It has been shown that input data for these trees can be the proportions of genes or proteins that genomes hold in common or the mean pairwise similarities between shared proteins. Finally, it has become apparent that whole-genome trees largely converge on the rRNA-sequence tree, thus showing the utility of the aforementioned approach for further bacterial systematics and isolation programs. “Largely” means that it is preferred to adjust this convergence in every individual case using the additional chronometer sequences most suitable for the taxa to be compared, based on their current phylogenetic definition and ranking. It is due to another dimension of the microbial taxonomic assignment problem, which concerns the resolution power of phylogenetic information recorded within the chronometer sequence. It is well known that 16S rRNA sequences are most appropriate for determining inter-, and sometimes intra-, generic relationships (Fox *et al*., 1992). In regard

to actinomycete bacteria, Stackebrandt *et al*. have proposed their new classification system, in which phylogenetically neighbouring taxa at the genus level are clustered into families, sub-orders, ordersand sub-classes, with an introduction at the end a new class *Actinobacteria*. The authors mentioned the above problem of adjustment of 16S rRNA phylogenies and thus pointed out that the pattern of signature nucleotides, but not necessarily each individual nucleotide, is indicative of the membership of a taxon to a higher taxon and that other shared genes from organisms which cluster together by 16S rRNA comparison should be analyzed (Stackebrandt *et al*., 1997). Resolution on lower and higher ranking levels can be done based on the analysis of sequences resulting from, and thus reflecting, the higher and lower evolutionary rates respectively. Both types of sequences are present within eubacterial rRNA gene clusters and can be successfully used for the purposes above, including a significant focus on the identification of actinomycete clade's representatives. These are sequences of intergenic 16S-23S rRNA spacer and 23S rRNA gene (Barry *et al*., 1991, Stackebrandt *et al*., 1991, Jensen *et al*., 1993, Yoon *et al*., 1998, Guertler *et al*., 1996, Trebesius *et al*., 1994, Manz *et al*., 1992, Roller *et al*., 1992). Another range of gene sequences, such as those encoding for RNA polymerase beta-sub-unit or δ^{70}-type sigma factors and DNA gyrase B sub-unit, has shown their suitability for bacterial identification (Gruber *et al*., 1997, Mollet *et al*., 1997, Yamamoto *et al*., 1998).

In summary, a need to interrogate multiple genomic fragment sequences and/or their positions within microbial genomes and thus the development and application of corresponding technological tools in order to perform reliable detection and assignment of new important entrants of different environmental niches, especially soil consortia, has become a focus of intensive investigation. In should, however, be kept in mind that the successful solution of the problems above will only pave the way, and that a further puzzle, the isolation of pure cultures of those bacteria for the biotechnological purposes, will need to be solved.

DNA microarrays: new frontiers in prospective microbiology

Flat high-density arrays of oligonucleotides or complementary DNAs represent one of the most powerful and versatile tools which have resulted from demands of the current developmental stage of modern biology, namely, its stage as system biology, after a row of full genomes, including the human one, became available and functional genomics came into play. These arrays consist of many microscopic spots, each of which contain numerous identical single- or double- stranded deoxyribonucleotide polymer molecules attached at

specific locations on a surface. These immobilized sequences can range in length from ten or twenty bases up to one or two thousand. The utility of these spots arises from the tendency of their component bases to pair up or hybridize with a matching partner, having a complementary sequence in a process which occurs on the surface and is determined by the rules of molecular recognition. As there are four bases, the probability P of a single base matching a given molecule of X bases long is X/4; the probability of a two-base sequence matching is $1/4^2$xX-1 and, thus, for an *n* base sequence, it becomes $1/4^n$x(X-*n*). If X represents a very large piece of DNA, for example 10^6 bases, and *n* is a modest number, such as 20, the probability that the entire sequence of 20 bases will match some location in the chain by chance alone is only $1/4^{20}$x(10^6-20), or less than one in a million. Thus, even a sequence as short as 20 bases can uniquely bind to and, by this means, identify a given gene, provided that the sequence is carefully chosen so that it does not appear in several genes (e.g. in a promoter, conserved domains, or microsatellites) (Graves *et al*., 1999).

With this background, it is easy to see how an array of different sequences can be used to identify one or more pieces of DNA or RNA in a solution. These unknown molecules are all tagged and represent the assay's targets; they are exposed to an array containing hundreds or thousands of different sequences, each in a known location (probes). When the array is examined, one can tell which molecules are present in the assayed sample by determining which spot's acquired tags used. Microarray methodological format originates from Southern blotting (Southern, 1974) which represents first approach to immobilize the DNA molecules under investigation onto solid support in a spatially-addressable manner. Recently, the use of glass as a substrate and fluorescence for detection, together with the development of new technologies for synthesizing or depositing nucleic acids on the substrate above at very high densities, have allowed the miniaturization of nucleic acid arrays with a concomitant increase in experimental parallelism/throughput and information content (Fodor *et al*., 1991, Pease *et al*., 1994, Schena *et al*., 1995).

DNA chip technologies are distinguished by the sizes of arrayed DNA fragments, the methods of arraying, the chemistries and linkers for attaching DNA to support, and the hybridization and detection methods. Two DNA chip formats currently in wide use are the *in situ* synthesized oligonucleotide arrays (Pease *et al*., 1994) and that of the cDNA array format (Schena *et al*., 1995).

Concerning the former, a company called Affymetrix has established a method of combining an oligonucleotide synthesis and photolitographic computer chip synthesis to generate DNA chips carrying 65 000 – 400 000 different oligonucleotides; these represent up to 9 000 genes

on a 1.6-cm^2 glass surface. In DNA photolitography, UV light is shone through holes in masks in order to direct the parallel, stepwise synthesis of oligonucleotides (Lockhart *et al*., 1996). At each step in the synthesis, oligonucleotides requiring, for example, cytosine in the next position are deprotected by light directed to the appropriate positions by a mask. The chip is then flooded with activated cytosine nucleotides which couple to the deprotected positions; uncoupled cytosines are then washed away. On the next step, another mask is applied and the deprotection and coupling steps are carried out with adenosine, for example. Repetition of this cycle 100 times, with 100 different masks, allow synthesis of complete array of thousands of 25-mer oligonucleotides in parallel.

cDNA microarrays represent the array format developed at Stanford University and widely accepted by academic investigators. These arrays are made by robotic deposition of DNA spots that are approximately 50-250 μm in diameter onto an activated glass surface. Usually, PCR-amplified inserts from cDNA libraries are arrayed; long synthetic oligonucleotides (50-70 bases) are nowadays also widely used. An average density of this type of array is 10 000 spots per microscopic glass, which represents up to 10 000 genes on an area of 3.6 cm^2.

Although is possible to synthesize or deposit DNA fragments of unknown sequence, the most common implementation is to design arrays based on specific sequence information, a process sometimes referred to as "downloading the genome onto a chip" (Lockhart *et al*., 2000). At the moment there are several variations on this basic technical scheme: the hybridization reaction may be driven (for example, by an electric field; Edman *et al*., 1997); other detection methods (Gray *et al*., 1997) besides fluorescence can be used; and the surface can be made of materials other than glass such as plastic, silicon, gold, gel or a membrane, or may even be comprised of beads at the ends of fibre-optic bundles (Walt *et al*., 2000, Michael *et al*., 1998, Ferguson *et al*., 1996). Nonetheless, the key element is always the process of a parallel hybridization to localized, surface-bound nucleic acid probes with a subsequent counting of bound molecules.

The drawbacks of *de novo* sequencing with the use of oligonucleotide arrays can be illustrated by following example. An array of 4^7 = 16 384 all possible sevenmer oligonucleotides could be constructed and a fairly short piece of DNA (e.g. 1000 bases) then tagged and applied to the array. The spots that acquired the tags (statistically, about 1 in 16) could then be located. Each sevenmer sequence is decoded from its location and, from an analysis of the overlapping short sequences, the original long sequence could be reconstructed. Researchers quickly realized, however, that if a given short sequence appeared more than once in the encompassing long sequence undergoing analysis, one would have a branch point in the

reconstruction diagram and could not assign an overall sequence without ambiguity (Khrapko *et al*., 1989). This application has thus largely fallen out of favour, although resequencing in order to look for mutations or polymorphisms in a region, the "normal" sequence of which is already known, is still considered to be a worthwhile goal. Therefore, arrays are widely applied to genomic studies, including resequencing. Such studies primarily involve the search for single-nucleotide polymorphisms (SNPs), which may have considerable importance in causing an overt disease, predisposition to disease, and the antibiotic resistance of microbial pathogens, etc. (Drmanac *et al*., 1998, Gingeras *et al*., 1998). It is thus evident that the experimental and computational methods take as much advantage from sequence information as possible. In this context, the goal of functional genomics is not just to provide a catalogue of all the genes and information about their functions, but to reveal a genetic potential of components which work together, and the way they do it, to consisted of functioning cells and organisms. Microarrays allow us to approach functional genomics through the monitoring of gene expression (mRNA abundance). The collection of genes transcribed from genomic DNA, referred to as the expression profile or "transcriptome", is one of the major determinants of cellular phenotype and function. The transcription of genomic DNA to produce mRNA is the first step in the process of protein synthesis, and differences in gene expression are responsible for phenotypic differences, as well as indicative of cellular responses to environmental stimuli. Unlike the genome, the transcriptome is highly dynamic and changes rapidly and dramatically in response to perturbations or even during normal cellular events occurring through cell cycle progression. In terms of understanding the function of genes, knowing when, where and to what extent a gene is expressed is central to understanding the activity and biological roles of its encoded protein. In addition, changes in the multi-gene patterns of expression can provide clues about regulatory mechanisms, broader cellular functions, and biochemical pathways.

All this has resulted in multiple attempts to use the DNA microarray format for increased throughput, speed and sensitivity of both detection and sequence interrogation of reliable chronometers, mainly 16S rRNA, from a plethora of microbes and whole microbial genomes for bacterial identification and typing, as well as gene expression monitoring experiments in order to reveal genomic traits responsible for the synthesis of biotechnologically important products and for their regulation on a transcriptional level. The microarrays currently used in environmental studies can be divided into three major classes on the basis of the type of probes arrayed (Zhou *et al*., 2002). Firstly, phylogenetic oligonucleotide arrays (POAs) or cDNA arrays contain probes derived from rRNA genes (16S and 23S) and 16S-23S rDNA

intergenic spacer region and are primarily used for the detection and typing of bacterial isolates, as well as for the phylogenetic analysis of microbial community composition and structure (Cook *et al*., 2004; Adamchyk *et al*., 2003; Stin *et al*., 2003; Call *et al*., 2003; Keramas *et al*., 2003; Koizumi *et al*., 2002; Rudi *et al*., 2002; Wang *et al*., 2002; Wilson *et al*., 2002; Small *et al*., 2001). The results of the use of PCR amplification from conserved regions of rRNA sequences with subsequent labelling of obtained fragments and their hybridization to tethered specific oligonucleotide probes has shown the dependence of sensitivity and specificity of the assay on oligonucleotide sequences, length, attachment mode, position within PCR fragment, and overcoming an inhibition of PCR by soil contaminants. A detection limit of a few to tens of genome equivalents has been reported (Keramas *et al*., 2003). Importantly, the results of direct detection of intact 16S rRNA from unpurified soil extracts has been shown with the detection limit of 0.5 μg of total RNA, corresponding to approximately $7.5x10^6$ cell equivalents of RNA (Small *et al*., 2001). Secondly, functional gene arrays (FGAs) contain oligonucleotide or cDNA probes for genes encoding key or characteristic enzymes involved in various biogeochemical cycling processes, and are useful for the detection of corresponding host cells, monitoring their physiological status as well as functional activities of microbial communities in natural environments (Denef *et al*., 2003; Bodrossy *et al*., 2003; Taroncher-Oldenburg *et al*., 2003; Dennis *et al*., 2003; Wu *et al*., 2001). Optimized set-ups based on 70-mer oligonucleotides showed detection limits of single copy genes from an organism contributing to 1% of the total community (Denef *et al*., 2003) or 10 pg of DNA, equivalent to approximately 10^7 copies per target per microarray with 87% sequence identity threshold value, and a target-to-probe perfect match-to-mismatch binding free energy ratio of 0.56 (Taroncher-Oldenburg *et al*., 2003). On mRNA level, the induction of specific catabolic genes of strain diluted into a constructed mixed microbial community has been detected at the level of 10^5 cells/ml against a background of 10^8 cells/ml (Dennis *et al*., 2003). Thirdly, whole genome arrays of defined strains using oligonucleotides representing each ORF can be constructed (Snyder *et al*., 2004; Watanabe *et al*., 2004; Bjorkholm *et al*., 2001; Kato-Maeda *et al*., 2001), as well as community genome arrays (CGAs) using whole genomic DNA isolated from pure culture member micro-organisms (Zhou *et al*., 2002). The former types of array are usually fabricated based on the whole genome sequence of type strain, and then the phylogenetically important differences in genome content between the above strain and its new or known isotypes or closely related species are detected via the co-hybridization of both genomic DNAs, labelled by different tags/dyes; this type of array seems to be of paramount importance for delineating

closely related strains or monitoring the evolution of sub-clones of bacteria with high genome plasticity occurring within narrow time. The latter types of array allow the monitoring of physiological activity and the population dynamics of cultivable component of the communities. The technological advantages of DNA microarray format regarding the high parallelism and resolution of the assay will lead to a broadening of possible set-ups from different sides. For example, among recent interesting modifications one could mention restriction site tagged (RST) microarrays (Zabarovsky *et al*., 2003) and quantitative oligonucleotide microarray fingerprinting (Willse *et al*., 2004). RST arrays allow increased sensitivity of strain discrimination by approximately two orders of magnitude using as probes and targets assayed the constructed libraries of fragments which link genome restriction sites for specified endonucleases; the proof-of-principle has been demonstrated on two closely-related *E.coli* strains differing by less than 0.1% in their 16S rRNA sequences (Zabarovsky *et al*., 2003). On the other hand, the high resolution power of oligonucleotide fingerprinting using the array of nonamers has been shown through reliable discrimination between 25 closely related *Salmonella enterica* strains (Willse *et al*., 2004).

Therefore, an evident trend for DNA microarrays becoming an important and integral part of polyphasic bacterial taxonomy comes into focus. As a tool which allows interrogating bacterial genetic content at genome-wide scale in highly parallel manner, it provides a possibility of substituting, to a large extent, a broad array of methods which deliver information on bacterial phenotypic traits, as all these traits are encoded by or indexed in the genome. The information obtained indicates the differences between two genomes regarding their contents, the location of the same functional units, and/or their copy numbers. By this means it will represent comprehensive complementary information to that of the single-nucleotide features of taxonomically relevant sequences which can be inferred from other type of microarrays. Moreover, DNA arrays are used not only for the above static features of both types of genetic information (structure), but also for the investigation of its dynamics (expression into RNA). This will give an additional dimension to the bacterial delineation process, which will allow the comparison of different physiological circuits and their regulatory pathways in response to an array of environmental stimuli.

In regard to modification or increase of the biosynthetic capacity of the known microbial producers, the genome-wide expression monitoring of cells grown under specifically selected conditions allows the evaluation of those genes whose expression is responsible for the narrow points of metabolic pathways of interest. These genes represent molecular targets for subsequent manipulations. The necessary directed alteration of activity of the genes above can

be achieved by means of site-directed mutagenesis, gene inactivation, gene fusion, introduction of additional gene copies, and other tools of recombinant DNA technology, as well as the mathematical modelling of metabolism and metabolic flux analysis. The use of array information in this current research direction, called pathway engineering, is at an early stage. The first results have been obtained with genetically manipulated *E. coli* cells. Arrays containing probes for the genes involved in central metabolism, key biosyntheses, some regulatory functions, and stress response, have been used to investigate the physiological responses to protein overproduction and metabolic fluxes in recombinant cells (Oh *et al*., 2000, Gill *et al*., 2001). Investigation of the differences in expression levels for 30 genes involved in xylose catabolism in the parent, strain B, and the engineered strain, KO11, revealed an increased expression of those genes (Tao *et al*., 2001). This has been proposed as a basis for the increased growth rate and glycolytic flux in ethanologenic KO11 strain. The efficiency of the metabolic engineering approach regarding known pathways and regulation circuits for the construction of strains with improved production of antibiotics, amino acids, lipids, and other low-molecular weight compounds or their altered spectrum, has been shown for a broad range of bacteria (Kennedy *et al*., 2003; Long *et al*., 2002, Sohn *et al*., 2001, Moore *et al*., 2000, de Graaf *et al*., 2001, Korycka-Machala *et al*., 2001, Ogawa-Miyata *et al*., 2001, Paradkar *et al*., 2001, Marin-Sanguino *et al*., 2000).

Seven years ago, when the presented work was initiated, there were no clearly established microarray technologies of the format where pre-synthesized DNA probes are positioned and immobilized on the activated support available to study entire groups of DNA molecules of interest in one go. As this was absolutely necessary to cope with the highly complex biological questions to be solved, it was first crucial to develop and evaluate a suitable technology. Therefore, a relatively large part of this thesis is devoted to the development of the technology used for the elucidation of the biological aspects presented here.

The work was focused on the representatives of the actinomycete bacteria, as the richest source of bacterial secondary metabolites known at present. As a suitable molecular chronometer the 16S-rRNA sequence was used for the following reasons: 1) the largest collection of these sequences in public databases; 2) published single-nucleotide sequence differences relevant for delineation of actinomycete bacteria at genera level and above; 3) the prevalence of rRNA fraction in total cellular RNA.

For a cellular transcriptional profiling on a genome-wide scale, a response of the cells of erythromycin–producing strain *Saccharopolyspora erythraea* DSM 40517 to the shift from rich to semi-synthetic growth medium was chosen.

Aims

16S rRNA sequence interrogation

- Selection and design of the suitable PCR primers and oligonucleotide probes.
- Development of microarray format optimized for the probing of single-nucleotide differences.
- Evaluation of the developed array format on rDNA/rRNA from pure test bacterial cultures.

Expression monitoring

- Development of microarray format which allows the fabrication, hybridization and analysis of cDNA arrays suitable for genome-wide expression monitoring of bacteria with high G+C content un-sequenced genomes.
- Evaluation of the developed array format on the test system, including *Saccharopolyspora erythraea* cell response to the cultivation media composition shift.

Materials and Methods

Materials

- **Bacterial strains**

***Actinomycetales* strains**	***Escherichia coli* strains**
Actinomadura madurae IMET9585, *Agrococcus jenensis* HKI085, *Agromyces mediolanum* HKI108, *Amycolatopsis orientalis* IMET7653, *Bogoriella caseilytica* HKI088, *Demetria terragena* HKI089, *Gordonia amarae* IMET7518, *Janibacter limosus* HKI083, *Nocardioides albus* IMET7807, *Nocardiopsis dassonvilei* IMET 9605, *Saccharomonospora viridis* IMET 9550, *Saccharopolyspora hirsuta* IMET 9709, *Streptomyces griseus* IMET40235, *Streptomyces globisporus* 1912, *Saccharopolyspora erythraea* DSM 40517 *Streptomyces griseus* IMET3933	***JM101*** *[F', traD36, lacIq, lacZΔM15, proA+B+ lsupE, Δ(hsdM-mcrB)5, (rkmk-McrB-), thi, Δ(lac-proAB)] (Sambrook et al., 1989),* ***DH5α****[supE44 ΔlacU169 (ϕ80 lacZΔM15) hsdR17 recA1 endA1 gyrA96 thi-1 relA1] (Sambrook et al., 1989),* ***TOP10*** *[F- mcrA D(mrr-hsdRMS-mcrBC) f80lacZDM15 DlacX74 deoR recA1 araD139 D(ara-leu)7697 galU galK rpsL (StrR) endA1 nupG] (Invitrogen)*

- **Nucleic acids**

Type	**Nucleic acids**
sequencing primers (M13/pUC 24-mers)	*universal (5'CGCCAGGGTTTTCCCAGTCACGAC3'),* *reverse (5'AGCGGATAATTTCACACAGGA3')*
Random hexamers	*Commercially available from Amersham*
Plasmids	*pBlueScript KS+ (MBI Fermentas),* *pUC118 (MBI Fermentas)*
DNA size markers	*DNA cut with either of endonucleases: Hind III or Pst I or Eco91I (MBI Fermentas),* *100 bp DNA ladder (Promega)*

- **Media**

For the cultivation of	**Type**	**Composition**
Actinobacteria strains	M 79	Dextrose – 10.0 g Bacto-peptone – 10.0 g Casein hydrolysate – 2.0 g Yeast extract – 2.0 g NaCl – 6.0 g Distilled water – 1000 ml
	56 (Oatmeal agar)	Oat flakes – 10.0 g Oatmeal – 10.0 g Agar – 15.0 g Tap water – 1000 ml Final pH 7.0-7.2
	53 (Yeast extract-malt extract agar)	Yeast extract – 4.0 g

For the cultivation of	Type	Composition
		Malt extract – 10.0 g Dextrose – 4.0 g Agar – 20 g Distilled water – 1000 ml
	89 (Bennett's saccharose agar)	Meat extract – 1.0 g Yeast extract – 1.0 g Casein peptone – 2.0 g Saccharose – 10.0 g Agar – 20.0 g Distilled water – 1000 ml
	BHI (Brain heart infusion)	Commercially available from Difco
	R-(rich) medium (Yamada K. and K. Komagata 1972)	Bacto peptone (Difco) - 10.0g Yeast extract – 5.0 g Casamino acids (Difco) – 5.0 g Meat extract (Difco) – 2.0 g Malt extract (Difco) – 5.0 g Glycerol – 2.0 g $MgSO_4x7H_2O$ – 1.0 g Tween 80 - 0.05 g Agar – 20.0 g Distilled water – 1000 ml
	Magadi 2	I. Glucose – 10.0 g Pepton – 5.0 g Yeast extract – 5.0 g K_2HPO_4 – 1.0 g $MgSO_4x7H_2O$ – 0.2 g To be dissolved in 500 ml of distilled water and incubated at 121°C for 15 min; next, 20 g of agar to be added per 1000 ml of formed solution II. NaCl – 40.0 g Na_2CO_3 – 10.0 g To be dissolved in 500 ml of distilled water and incubated at 121°C for 15 min.; Solutions I and II to be cooled to 60°C, mixed and plated. Final pH 9.7
	Minimal Czapek medium	Soluble starch – 30 g L-asparagin – 0.5 g K_2HPO_4 – 1.0 g $MgSO_4x7H_2O$ – 0.5 g KCl – 0.5 g $FeSO_4$ – 0.01 g Distilled water – 1000 ml After autoclaving the volume was divided into 200 ml portions with subsequent addition per each portion: 50% glucose – 16 ml 50% NH_4NO_3 – 0.8 ml 25% KH_2PO_4 – 1.2 ml
	SSM (semi-synthetic medium)	Glucose – 20 (40,75) g NaCl – 5 g KH_2PO_4 – 0.8 (0.4, 1.2) g NH_4NO_3 – 2g Distilled water – 990 ml, to mix with 10 ml of trace-salt solution (100x): $MgSO_4x7H_2O$ – 100 g $FeSO_4x7H_2O$ – 2 g $ZnSO_4x7H_2O$ – 1 g

For the cultivation of	Type	Composition
		$CuSO_4x5H_2O$ – 0.4 g $CoCl_2x6H_2O$ – 0.1 g HCl (37%) – 1 ml Distilled water – 1000 ml.
Escherichia coli strains	LB-medium	Bacto-trypton – 10.0 g Yeast exstract – 5.0 g NaCl – 10.0 g Agar – 15.0 g (optional) Distilled water – 1000 ml
	LAXI-medium	LB-medium Ampicillin – 100 µg/ml Xgal – 40 µg/ml IPTG – 20 µg/ml
	2xTY medium	Bacto-trypton – 16.0 g Yeast extract – 10.0 g NaCl – 5.0 g Distilled water – 1000 ml

- **Compounds**

0.5 M EDTA (Roth), pH 8.0: prepared according to Sambrook *et al*., 1989

2x modified Kirby mixture: 1%(w/v) sodium-triisopropylnaphthalene sulphonate, 6%(w/v) sodium 4-amino salycilate, 6% (v/v) phenol equilibrated with 50 mM Tris-HCl, pH 8.3

3 M sodium acetate (Merck), pH 5.2: prepared according to Sambrook *et al*., 1989

3-aminopropyl-trimethoxysilane (Sigma)

6% PAAG (Long Ranger gel solution, BioProducts, Rockland, Maine, USA)

9M LiCl: 381.6 g LiCl (Merck), bidistilled water till 1 l

10% ammoniumpersulfat: 1 g ammoniumpersulfat, 10 ml bidistilled water

10 M ammonium acetate (Merck): prepared according to Sambrook *et al*., 1989

10.3% sucrose: 10.3 g sucrose, 100 ml of bidistilled water

20% (w/v) SDS (Roth): prepared according to Sambrook *et al*., 1989

38% stock solution of acrylamide, 2% bisacrylamide (Roth)

Borohydride solution: 1.3 or 2.6 g of Na_2BH_4 dissolved in 375 ml of PBS + 125 ml of 100% ethanol

Chloroform/isoamyl alcohol (24:1) (Roth)

DEPC (Serva)

Deoxynucleoside triphosphate mix (dNTPs), 2 mM: mixture of 20 µl of each dNTP (Amersham) was dissolved in 920 µl of DEPC-treated water

DMSO (Merck)

Ethidium bromide (Roth) (10 mg/ml): prepared according to Sambrook *et al*., 1989

Glutardyaldehyde (Fluka)

Glycerol (Sigma)

HCl (Roth)

Poly-l-lysine (0.1%) (Sigma)

Lysozyme (Roth) (20 mg/ml) in TE, pH 8.0

mineral oil (Sigma)

Nucleoside triphosphates: 0.5 M solutions of GTP, ATP, CTP each (Boehringer Mannheim)

Phenol, chlorophorm, phenol:chlorophorm (1:1), ethanol, isopropanol, methanol (Roth)

RNA fragmentation buffer: 40 mM Tris-acetate, pH 8.1, 100 mM potassium acetate, 30 mM magnesium acetate

Solution I: 50 mM glucose, 25 mM tris/HCl, pH 8.0, 10 mM EDTA

Solution II: 0.2 N NaOH, 1%SDS, freshly prepared

Solution III: 3M sodium acetate, pH 5.2

- **Buffers**

20xSSC, pH 7.0: prepared according to Sambrook *et al*., 1989.

20xSSPE, pH 7.4: prepared according to Sambrook *et al*., 1989.

Phosphate-buffered saline (PBS): prepared according to Sambrook *et al*., 1989.

Spotting buffers:

Spotting solution (TeleChem International, Inc.)

3x SSC: prepared according to Sambrook *et al*., 1989.

Hybridization buffers:

UniHyb buffer (TeleChem International, Inc.)

SSPE-T buffer: 0.9 M NaCl, 60 mM NaH_2PO4, 6 mM EDTA, pH 8.0, 0.0005% Triton X-100, 100 µg/ml herring sperm DNA (Lockhart *et al*., 1996)

modified Church buffer: 0.5 M NaH_2PO4, pH 7.4, 1% BSA, 1 mM EDTA, pH 8.0, 5% SDS (Church *et al*., 1984)

ACES 2.0 buffer: 0.5 M NaH_2PO_4, pH 7.2, 0.5% Tween 20, 1% caseine, 0.02% sodium azide (Life Technologies)

EPPS buffer: 1M NaCl, 30 mM EPPS (Sigma), 3 mM EDTA.

Washing buffers:

Cell biomass washing

STE buffer: 150 mM NaCl, 100 mM Tris-HCl, pH 8.0, 100 mM EDTA, pH 8.0 TE buffer: 10 mM Tris-HCl, pH 8.0, 1 mM EDTA, pH 8.0

Array hybridizations

Oligonucleotide arrays

2x SSC, 0.2%SDS

2xSSC

Shotgun library arrays

1xSSC, 0.03% SDS

0.2xSSC

0.05xSSC

Electrophoresis buffers:

TAE buffer (50x)

242 g Tris-base, 57,1 ml acidic acid, 100 ml 0.5 M EDTA, pH 8.0, bidistilled water till 1000 ml.

TBE buffer (10x)

108 g Tris-base, 55 g boric acid, 40 ml 0.5 M EDTA, pH 8.0, bidistilled water till 1000 ml

- **Microscopic glass slides**

Both homemade, activated microscopic slides and commercial ones were used ((i) Poly-Prep (Sigma) polylysine slides, (ii) SSC-100 silylated slides (TeleChem), and (iii) Esco selected microscope slides (Erie Scientific)).

- **Plastic consumables**

96- and 384-well microtiter plates (Nunc), Slide racks and boxes (Roth), and Cover slips (circle and square cover glasses, silanized [Ingen Laboratories]) were used.

- **Enzymes kits**

Name	**Provided by**
DNase I	New England Biolabs
Taq polymerase	AGS
Pwo polymerase kit	Boehringer Mannheim
Ligase and its buffer	MBI Fermentas
Restriction endonucleases and their buffers	MBI Fermentas
RNase inhibitor	MBI Fermentas
T7 RNA polymerase	Boehringer Mannheim

- **DNA and RNA molecular labels and stains**

Cy3- or Cy5-conjugated dCTP were provided by Amersham. SybrGreen I and II were provided by Molecular Probes.

- **Nucleic acid purification columns**

Microcon 30 columns were provided by Amicon.

- **Nucleic acid labelling and purification kits**

The QIAquick PCR purification kit and Plasmid Mini Prep kit are available at Qiagen. NucleoSpin Extraction Kit was purchased from Clontech. Fluorescence labelling kit was bought from Boeringer Mahnheim. Label IT Labelling Kits was provided by Mirus, PanVera Corporation. ThermoSequenase fluorescent-labelled primer sequencing kit is available at Amersham.

- **Hybridization chambers, spotting pins**

Glass hybridization chambers were purchased from TeleChem and Clontech. Stealth Micro-Spotting (split) Pins were from TeleChem.

- **Software**

The following software was used: (i) GCG, version 9.0-Unix (GCG), (ii) ArrayVision 4.0 (Imaging Research), (iii) DNAsis (Pharmacia), and (iv) BLAST 2.0 (NCBI).

- **Additional devices**

Robocycler (Stratagene), GeneAmp PCR System 9600 (Perkin Elmer), Slab Gel Dryer SGD2000 (Savant), M35 X-OMAT Processor (Kodak), DU 640 spectrophotometer (Beckman), LI-COR4000 (LI-COR Biosciences), OmniGrid arrayer (GeneMashines), ScanArray 3000 (General Scanning), Bench-top centrifuge (Eppendorf), Laboratory centrifuge 4K10 (Sigma), CCD camera (PCO CCD imaging), Laboratory Rotationshaker (Infors), Labsonic (Braun Melsungen), Thermomixer (Eppendorf), Mini Oven MK II (MWG-Biotech)

Methods

- **Morphological, physiological and chemotaxonomical characterization of freshly isolated eubacterial strains**

Pure cultures isolated from soil obtained from Kreta island were characterized according to methods presented in Groth *et al*., 1997.

- **Genomic DNA isolation from *Actinomycetales***

Pre-cultures were made by inoculation of the material from frozen stocks (rich medium + 5%DMSO) into 2 ml of liquid M79, M89, M53, M56 or Magadi 2 (for the corresponding strains) and incubation for 24 hours at 28°C or 32-34°C (for *Saccharopolyspora hirsuta, Nocardiopsis dassonvilei* and *Gordona amarae*) with shaking. This material was transferred into 20 ml of corresponding media and incubation was continued for 48-72 hours as described above. Afterwards cells were harvested by centrifugation at 5000xg, 4°C for 10 min and washed with equal volume of STE buffer. Approximately 1 g (wet weight) of cell biomass was resuspended in 5 ml of TE buffer, 0.5 ml of freshly prepared lysozyme solution (20 mg/ml) was added and the suspension was mixed gently and incubated at 37°C for 30-60 min with gentle mixing after every 15 min. Then 1.4 ml of 0.5 M EDTA, pH 8.0 and 0.8 ml of 10% SDS were added and mixed. Incubation continued for one hour. After cooling down to room temperature, the solutions were transferred into 50 ml centrifuge tubes and mixed for at least 10 min with an equal volume of equilibrated phenol (pH 7.5). After centrifugation (5000xg, at room temperature for 15 min), the aqueous phase was transferred into clean centrifuge tubes using wide-born pipettes. The extraction was repeated twice. Then the aqueous phase was mixed with 0.2 volume of 10M CH_3COONH_4 and subsequently with 2 volumes of absolute ethanol at room temperature. Genomic DNA was collected by a centrifugation at 5000xg for 10 min. DNA pellet was washed twice with 70% ethanol, dried and resuspended in 1 ml of TE buffer.

- **Total RNA isolation**

Pre-cultures of actinomycetes and incubation procedure were performed as described above. Approximately 1 g of mycelium collected (growth for 72h) was treated by 2 mg/ml lysozyme at 37°C till protoplast formation (approximately for 30-60 min depending on a strain). Equal volumes of 4.5-5.5 mm glass balls and 2xmodified Kirby solution were added (Hopwood *et al*., 1985). Samples were vigorously vortexed for 2 min. 5 ml of phenol/chloroform was added and vortexing was repeated for 1 min. After centrifugation at 4390 x g for 10 min at 4°C the aqueous phase was extracted by phenol/chloroform twice. Then the nucleic acids were precipitated by isopropanol, washed with 80% ethanol, air dried and dissolved in 100 µl TE, pH 8.0 (DEPC-treated). After an additional phenol/chloroform extraction and ethanol precipitation nucleic acid pellet was resuspended in 1x DNase I reaction buffer containing10 µg DNase I per ml of buffer and incubated for approximately 1 h at room temperature to remove genomic DNA. After two phenol/chloroform extractions and one ethanol precipitation

the total RNA was resuspended in 100 µl of DEPC-treated water. Sample quality and quantity were checked by agarose-gel electrophoresis and photometrically. Samples were stored at -80°C.

- **Nucleic acid sequence analysis**

For 16S rDNA sequence retrieval and multiple alignment the Wisconsin Package version 9.0-Unix was used. The use of the enclosed Prime program for primer searching was not successful enough and PCR primers were selected from aligned sequences manually.
In the case of DNA cloning and sequencing retrieved sequences were proved through the BLAST 2.0 program.

a) Selection of primers for PCR amplification and sequencing of 16S-rRNA gene fragments

To select appropriate primers the PileUp program (multiple comparison package) was used under GCG default parameters to align 97 complete and partial 16S-rRNA gene sequences. This set of rRNA sequences included a broad range of type strains of the class *Actinobacteria* representatives including those used in this work, uncharacterized or uncultured representatives of the same class, some of uncharacterized Gram-positive bacterial species with a high (G+C) content and *E. coli* strains as references. No special adjustments to the default aligning parameters were made due to highly conserved structure of the given gene sequence. The resulting alignment was checked manually. Short conserved fragments were analyzed with a maximum of 2 mismatches across the aligned sequence set and located on stretches separated by approximately 500 bp. Finally, seven suitable oligonucleotide sequences were chosen as primers for the DNA amplification and sequencing reactions. Primers were named according to the following scheme:

rRNAfX – for forward primers,
rRNArX – for reverse primers,
where X = 0,1,2,3.

b) Selection and design of the oligonucleotide probes interrogating specific positions of the 16S rRNA gene sequence.

The aim of this step was to select a set of DNA stretches with single nucleotide variation within the conserved sequences for a majority of the analyzed sequences and positioned within various secondary structure motives (bulges, loops, and stems) of 16S rRNA. A major

part of these variability points was represented by taxonomically relevant "signatures" described by Stackebrandt *et al*. (Stackebrandt *et al*., 1997). Then the oligonucleotide probes were designed according to the requirements of the length, G+C content and melting temperature.

- **Polymerase chain reactions**

Different fragments of 16S rRNA gene were amplified in order to obtain both DNA probes for subsequent spotting and labelled DNA targets to be hybridized to microarrays using various combinations of forward and reverse primers selected in the course of work. Optimization of PCR conditions was done on Robocycler (Stratagene) using its ability to form temperature gradient across the termoblock. Reactions were performed according to the manufacturer's instructions. In addition to the annealing temperature, concentrations of the following components were optimized: bacterial genomic DNA, $MgCl_2$ or $MgSO_4$, primers, deoxynucleoside triphosphates, DMSO and Taq polymerase or Pwo polymerase. After this specific PCR fragments were obtained on Perkin Elmer 9600 cycler in 50 µl PCR mixtures using following annealing temperatures:

T = 45°C for rRNAf2-r1 and rRNAf2-r0 primer pairs,
T = 55°C for rRNAf0-r2, rRNAf1-r2, rRNAf1-r1, rRNAf1-r0, rRNAf3-r0, rRNAf3-r1, rRNAf0-r0 primer pairs;
T = 59°C for rRNAf0-r1 primer pair.

The use of aminomodified primers or those with 5' end-coupled fluorescent dyes did not need any special modifications to the above amplification protocol.

DNA labelling by PCR incorporation of FITC-conjugated dUTP was performed using Fluorescence labelling kit (Boeringer Mahnheim) according to the manufacturer's instructions. For this purpose only primer pair rRNAf0-r2 was used.

To obtain single stranded PCR fragments, asymmetric PCR reactions were performed with molar ratios of primers 1:50, 1:100 or using just one necessary primer.

DNA fragments for manufacturing of shotgun-library array were generated by PCR using vector sequences as common primers. M13/pUC 24-mer sequencing primer (CGCCAGGGTTTTCCCAGTCACGAC) and reverse sequencing primer (AGCGGATAATTTCACACAGGA) were used. PCR was performed in 96 microtiter plates. As a template, either DNA from plasmid miniprep isolations, or cell lysates from the frozen stocks of the clone library were used. In the latter case, 30 µl of the glycerol cell suspension was sonicated at 100W for 10s. 0,5 µl of this suspension was applied to PCR reaction. For the

optimal amplification of *Actinomycetales* G+C-rich sequences the following dNTPs mix was used: 0.28 mM of each, dGTP and dCTP, 0.14 mM of each, dATP and dTTP. Cycling conditions used were as follows: 96°C for 10 min; 94°C for 40 sec, 53°C for 30 sec, 72°C for 1 min (5 cycles); 94°C for 30 sec, 48°C for 30 sec, 72°C for 1 min (25 cycles); final extension step at 72°C for 10 min.

- **Transformation of *E. coli* cells**

200 µl of the competent Ca^{2+} cells of relevant *E. coli* strains (DH5α or JM 101) were transformed according to the protocol described by Sambrook *et al*., 1989.

- **Plasmid DNA minipreps from *E.coli* cells**

Plasmid DNA minipreps were isolated according to the protocol described by Sambrook *et al*., 1989.

- **Cloning of PCR fragments**

Blunt-end PCR fragments made with the primer pair rRNAf0-rRNAr2 were cloned into EcoRV digested pBlueScript KS+ vector DNA, according to the protocol described by Sambrook J. *et al*., 1989. Recombinant constructs were named as follows: pB – PCR primer pair – numbering component of IMET or HKI strain designation, e.g., pBf0-r2.108 (cloned rRNA f0-r2 fragment of *A. mediolanus* HKI108 (see Materials, Bacterial strains)).

- **Sequencing of PCR fragments of 16S rDNA**

Sequencing of cloned inserts was performed using the ThermoSequenase fluorescent-labelled primer sequencing kit (Amersham) according to the manufacturer's instructions. As a template plasmid DNA was used. The resulting single-stranded fragments labelled by either universal 24 or reverse 24 IRD800-5'end labelled primers were resolved on LI-COR4000 (LI-COR Biosciences) according to the manufacturer's instructions. The sequences were read using cognate ImageAnalysis V2.10 software.

- **Direct chemical labelling of total RNA**

This was done by chemical coupling of the dye molecules to guanine residues of RNA chain with the use of Label IT Labelling Kits (Mirus, PanVera Corporation, Madison, USA) according to the manufacturer's instructions.

- **RNA fragmentation**

Total RNA (labelled and unlabelled) was fragmented to the average length of 100 bp according to DeSaizieu *et al*. (DeSaizieu *et al*., 1998).

- **Primer design for cDNA labelling**

In order to improve priming efficiency from mRNA fraction of *Saccharopolyspora erythraea* DSM 40517, cells in reverse transcription labelling reaction available *Streptomycetales* rRNA operon sequences were tested for restriction endonuclease sites using the DNAsis program (Pharmacia). Those not occurring within the above sequences but in turn cutting the protein coding sequences were selected and used for primer design. As a result, the following nine 6-mers, two 7-mers and one 8-mer were used in the 1:1 mixture with random hexamers (Amersham) in all cDNA first strand synthesis/labelling reactions (5'-3' direction): GACGTC, GTGCAC, GGATCC, GCGCGC, CTCGAG, AGCCGT, CTGGAG, CAGCTG, GTCGAC, CGGWCCG, GCGGCCGC.

- **RNA labelling**

Fluorescent labelling of total cellular RNA of *Saccharopolyspora erythraea* DSM 40517 was performed according to the protocol described by Richmond C.S. *et al*. (Richmond C.S. *et al*., 1999).

Cloned 16S rDNA fragments were FITC-labelled via *in vitro* transcription from T7 promoter of pBlueScript KS+ plasmid using T7 RNA polymerase kit (Boehringer Mannheim) according to the manufacturer's instructions.

- **Quantification of nucleic acids and labelling efficiencies**

Nucleic acids and their labelled counterparts were quantitated on DU 640 spectrophotometer (Beckman) according to the manufacturer's instructions. To calculate their averaged labelling efficiency the molar ratios of nucleic acid bases and dye molecules in labelled fractions were found based on their molar extinction coefficients.

- **Activation of solid support surface for DNA coupling**

Structured and unstructured silicon and glass wafers activated by gelatine and polylysine coatings were a kind gift from IPHT, Jena.

Borofloat-33 aldehyde activated slides were a kind gift from A. Tretyakov and V. Klujeva. They were cleaned and activated according to the following protocols:

- in protocol N1 glass surface cleaning was performed using cerium oxyde and subsequent sonication followed by an acidic activation step, aminosilane coupling, drying and aldehyde activation.
- in protocol N2 glass surface was cleaned by soap solution, hot tap water and sonication, activated by the treatment in water solution of potassium hydroxide, followed by aminosilane coupling in methanol under sonication and aldehyde activation.
- in protocol N3 sodium hydroxide instead of potassium hydroxide, methanol solution instead of water solution and ethanol medium for aminosilane coupling were used compared with protocol N2.

For polylysine slide preparation the same Borofloat-33 slides were treated according to P. Brown's lab protocol (http://brownlab.stanford.edu/protocols.html) with the following modifications: cleaning and activation were performed for 24 h in 10% KOH in 56% methanol with subsequent vigorous 5-times washing in bidistilled water at room temperature (5 min each) with a third washing performed at 95°C.

- **DNA sampling for array fabrications**

In order to obtain equimolar amounts of DNA in each spot, 3819 library fragments were averaged and divided into 7 (500, 1000, 1500, 2000, 2500, 3000 and 3500 bp) and 16 groups, according to their size and concentration respectively, after visualization via gel electrophoresis. Selected representative extremes among the representatives of each group were additionally quantitated photometrically. This was used to adjust the concentrations of all fragments to approximately 600 nM. Finally doubled concentrations were used for arraying on glass slide to compensate for deviations. Spotting samples were prepared in 3xSSC in a final volume 10 µl. Oligonucleotide probes spotting samples were prepared in either Spotting Solution (TeleChem) or 3xSSC; concentrations ranged from 0.78 to 400 µM.

- **Array fabrication**

Immobilization of DNA probes on glass surface was done as described in Figures 1 and 2.

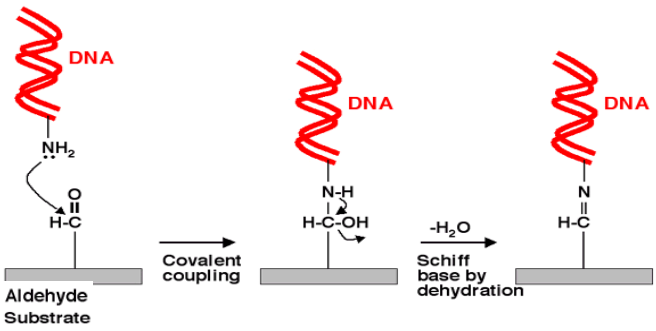

Figure 1. Aldehyde coupling chemistry. A six carbon linear (aliphatic) amine is added to each DNA molecule (double-stranded PCR products or single-stranded oligonucleotides). The aliphatic amine on the amino-modified DNA acts as a nucleophile, attacking the carbon atom on reactive aldehydes covalently attached to the surface of the slide. DNA attachment proceeds via an unstable intermediate that converts quickly to a Schiff base. Schiff's base formation occurs at neutral pH provided by 3xSSC solution or Telechem

spotting solution and room temperature as the printed DNA dries on the surface of the substrate. To minimize fluorescent background, the unreacted aldehyde groups were reduced to non-reactive primary alcohols by treatment with sodium borohydride ($NaBH_4$).

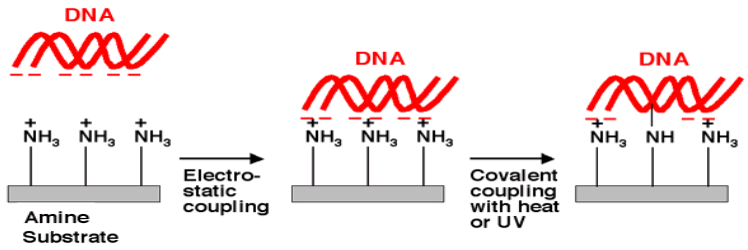

Figure 2. Coupling chemistry with the use of primary aminogroups. The surface amines carry a positive charge at neutral pH, allowing attachment of native DNA through the formation of ionic bonds with the negatively charged phosphate backbone of DNA. Electrostatic attachment is supplemented by treatment of the printed substrate with ultraviolet light, which induces free radical-based coupling between thymidine residues on the DNA and carbons on the alkyl amine.

Volumes of 10 µl of sampled DNA were transferred into 96- or 384 well microtiter plates. Volumes of 1-5 nl were spotted onto polylysine-coated Borofloat-33 slides using Micro-Spotting Pins and OmniGrid arrayer according to manufacturer's instructions. The spotting processes were programmed by cognate OmniGrid 2.0 software. Slides with printed shotgun-library fragments were processed according to Brown P. *et al.* (http://brownlab.stanford.edu/protocols.html). Oligonucleotide arrays were fabricated according to the following methods:

- volumes of 8 µl of TeleChem's Spotting buffer containing oligonucleotide DNA were transferred into 96 well microtiter plate and spotted as described above. After spotting slides were kept in a slide box with the lid slightly ajar in a humid chamber (50-60% humidity) at room temperature for 24 hours. Then slides were washed twice with vigorous stirring for 2 min each at room temperature in 0.2% SDS, twice in dH_2O for 2 min each at room temperature, once in dH_2O for 2 min at 95°C and cooled to room temperature (1-2 min). Then they were treated at room temperature for 5, 10 or 30 min in sodium borohydride solution (see Materials) and washed in 0.2% SDS three times for 1 min each at room temperature, twice in dH_2O for 1 min each at room temperature. The slides were then immediately dried by centrifugation (500xg for 2 min). The treatment by 6-amino-1-hexanol in DMF for 2-3 hours before denaturation step as a means of reducing the aldehyde groups was also tested .
- in the case of 3xSSC spotting buffer and PCR products as probes, the above procedure was modified as follows: incubation in 95°C H_2O for 5 min, rinsing in 0.2% SDS for 2 min, doubled short rinsing in H_2O and centrifugation (500xg for 2 min). Slides were stored in the dark at room temperature.

- **Array hybridization**

Oligonucleotide arrays prepared on microscopic glass were hybridised with 20 nM – 2 μM of the fluorescently labelled target nucleic acids in 2.5 – 10 μl for 0.5 – 12 hours at 36–56°C. Secondary structures of the long nucleic acid targets (RNA or PCR fragments) were denatured by pre-incubation for 2 min in boiling water (PCR fragments) or 5 – 10 min at 65°C (RNA) and immediate chilling on ice. Hybridizations were performed in the hybridization chamber casette according to the manufacturer's recommendations. Casette was quickly and firmly closed and placed into an appropriately heated water bath.

After hybridization slides were washed in 2xSSC, 0.2% SDS for 15 min at room temperature and then in 2xSSC for 5 min. After washing the slides were centrifuged at room temperature (500xg, 2 min) for drying. In special cases washing was prolonged to 30 min – 1 h and 37°C was used as washing temperature. After centrifugation slides were ready for the analysis. In the case of shotgun-library arrays they were pre-hybridized in the glass hybridization chamber (Clontech) containing 1.5 ml of 1x pre-hybridization buffer (4xSSC, 0.2% SDS, 1% BSA, 5xDenhardt's solution, 100 μg/ml sheared salmon sperm DNA) for 30 min at 64°C. It was followed by washing in 4xSSC, 0.2% SDS for 10 min at room temperature with vigorous stirring and centrifugation in a rack at 500xg for 2 min. Then 20 μl of hybridization mixture (4xSSC, 0.2% SDS, Cy3- and Cy5-labelled cDNA) were incubated in boiling water for 2 min, spun on bench-top centrifuge, spotted in the centre of an array and covered by a 22x22 cm cover slip avoiding air bubbles. Slides were assembled and kept at hybridization temperature as described above. Arrays were hybridized at 64°C for 24 h. After hybridization they were washed in 1xSSC, 0.03% SDS for 10 min, 0.2xSSC for 5 min and rinsed in 0.05xSSC followed by immediate centrifugation in a rack for 2 min at 500xg. Slides were used for fluorescent scanning directly or stored in a closed slide box at room temperature.

- **Hybridization data retrieval**

Three different methods of data retrieval were used depending on the fluorescent label the targets were labelled with. In the case of FITC and SybrGreen I or II 5 μl of TE buffer, pH 8.0 were spotted onto the centre of the washed array and covered by a cover slip. The resultant fluorescence signals were checked either by means of an epifluoprescence microscope (Olympus) with subsequent recording onto photographic film (Kodak) or by a cooled CCD camera system (PCO CCD imaging) with recording of resultant 12 bit files in TIFF format by cognate SensiControl software. Slides were irradiated for different time periods: 1 – 10 msec using the microscope and 20 – 300 msec using the CCD camera. In some cases TE buffer was

substituted by antifading mounting solution (90% glycerol, 10% PBS, 9 mM *p*-phenylenediamine) to prevent photobleaching of FITC.

For the background sources investigation the following modifications were applied:

1) content of a mounting solution was 2xSSC, 2.5 mM $MgSO_4$ (to prevent possible denaturation of the formed resultant duplexes); 2) for RNA targets RNAse was used additionally in above SSC+$MgSO_4$ solution at 100 μg/ml final concentration for 10 min.

In the case of cyanine dyes (Cy3 and Cy5) slides were scanned on the ScanArray 3000 epifluorescent confocal scanning device in two steps: at first quick pre-scanning at low resolution in order to define a precise location of the array as well as appropriate laser power and PMT power for the given array. Then the scanning procedure was repeated at high resolution (10-20 μm/pixel) and adjusted scanning parameters. The resulting 16 bit files were stored in TIFF format by cognate ScanArray3000 software. For the evaluation of the approximate density of active aldehyde groups, slides were scanned using Cy3 channel (usually laser power at 90% level and PMT voltage at 100% level).

- **Data analysis**

Obtained TIFF-format files were exported into the ArrayVision 4.0 software program (Imaging Research Inc.) and analyzed according to the manufacturer's recommendations. Background-subtracted signals were subjected to the normalization procedure. This procedure was accomplished by calculating spot signal intensities as multiples of the reference intensities. In the case of oligonucleotide arrays for both one-target hybridizations- or two-target co-hybridizations data, these reference intensities were presented by either those of blank spots or mean intensities of all array spots. In the case of differential expression monitoring, the latter values were used for normalization. In addition, in data analysis on expression monitoring these normalized signal intensities were further compared by means of a statistical data segmentation (ArrayVision User guide). It was accomplished by a combination of the resulting ratio scores (obtained by division of Cy5-signals by Cy3-signals), the difference scores (obtained by subtraction of Cy3-signals from Cy5-signals), and the distribution scores (z-values of the difference scores which were calculated as the difference value between signal intensity of the given spot and the mean of all spots divided by their standard deviation). Finally, the elemental displays of the resulting data were made in order to select only spots characterized by values of three above parameters surpassing the applied thresholds. The spots present in all three elemental displays were collected into the summary elemental displays.

Results

A relatively large part of this section is devoted to the development of the microarray technology used for the studies of biological tasks of my thesis. The key steps concern the fabrication of miniaturized substrates, the surface treatment to immobilize the molecules of interest, the positioning of the biomolecules (probes), the preparation of the labelled biomolecules (targets) to be used for hybridization, and finally the quantification and analysis of the data obtained.

A broad set of oligonucleotide probes encompassing 500 bp at the 5' end of the 16S-rRNA gene sequence were designed and tested. The suitable PCR primers were derived from the same gene region. The resulting amplified fragments were immobilized on solid supports and hybridized with labelled oligonucleotides and a wide spectrum of long-labelled nucleic acids of a different complexity. On the other hand, immobilized oligonucleotides were hybridized to the same spectrum of targets.

1.1 Taxonomical assignment of newly isolated strains

It was possible to isolate 132 eubacterial strains as pure cultures from 1 g of used soil sample from Crete, which turned to be cultivable upon the dilution plate technique and on selective media used. They were numerated N1 through N132. Based on growth and morphological characteristics, eight of them (N3, 4, 6, 8, 13, 39, 45 and 62) were selected for further analysis as those possibly belonging to the *Actinomycetales* order. According to the chemotaxonomical (i.e. cell wall component analysis, lipid analysis, DNA base composition, DNA-DNA hybridization, and 16S rDNA sequence determination and analysis) as well as biochemical and physiological characteristics obtained, these isolates were assigned to the following genera: N3, 4 and 62 – *Aureobacterium*; N6 – *Curtobacterium*; N8 – *Arthrobacter*; N13 and 39 – *Arthrobacter globiformis*-group; N45 – *Micrococcus*. Thus, all of them belong to the same large sub-order *Micrococcineae*. Regarding the family's assignment, one half of the strains belonged to the family *Microbacteriaceae* (N3, 4, 6, 62) and the other half to the family *Micrococcaceae* (N8, 13, 39, 45).

1.2 Primers designed for PCR amplification of 16S-rRNA gene fragments

The 16S- rRNA gene sequence was investigated in order to find conserved stretches suitable for the design of PCR primers. These primers had to be optimal both for the amplification of the fragments used for immobilization on the supports and for hybridization. The seven PCR primers evaluated are shown in Table 1.

Table 1. Designed PCR primers. Locations within 16S rDNA are given according to *E.coli* sequence numeration (Brosius J. *et al*., 1978).

Direction	Name	Sequence (5‘-3‘ direction)	Location
Forward	rRNA f0	GTGCTTAACACATGCAAGTCGA	44-65
	rRNA f1	GGGAGGCAGCAGTGGGGAAT	346-365
	rRNA f2	ATTGGGCGTAAAGAGCT	563-579
	rRNA f3	TTAGATACCCTGGTAGTCCA	788-807
Reverse	rRNA r0	TACGGCTACCTTGTTACGACTT	37-58 bp 3' extension of *E.coli* 16S rRNA gene sequence
	rRNA r1	CACGACACGAGCTGACGACA	1059-1078
	rRNA r2	ACCGCGGCTGCTGGCACGTAGTT	509-531

The four forward and the three reverse primers were used in different combinations. They provided high specificity and efficiency of the amplification on DNA from both test pure cultures and all newly isolated *Actinomycetales* strains. The results of the use of rRNA f0-r2, rRNA f1-r2 and rRNA f2–r1 fragments as DNA probes for immobilization and hybridization on microarrays are presented below.

Oligonucleotide probes interrogating the 16S-rRNA gene sequences

Sets of 15-20 mer-probes spanning 500 bp of the 5‘ end of the 16S-rRNA gene sequence are presented in table 2 and figures 3, 4. Their design aimed at interrogation of the positions of single-nucleotide variation responsible for the taxonomic delineation within the newly-established *Actinobacteria* class above the genus level (Stackebrandt *et al*., 1997). It concerned all probes except rRNA p15.111, rRNA p15.112, rRNA p15.111.1, rRNA p15.112.1 and rRNA p15.13.1. In general, 11 of these signature positions were included into research. The majority of them were derived from double-stranded helical motives of 16S-rRNA secondary structure (signatures 139, 239, 293, 370, 371, 390, 391); the others were derived from single-stranded loops (signatures 280, 328, 381, 415) (see figure 4). Substitutes were located at different positions within the probe sequences and reached the 5‘ and 3‘ extremities in the design of probe sets rRNA p15.4.X and p15.5.X (X designates number of

every probe included in given set). In addition, the latter sets also consisted of probes with the internal two-nucleotide differences. Some probes (rRNA p15.111/112, rRNA p15.13.X.r) did not carry any specific taxonomic information and were selected for test purposes only.

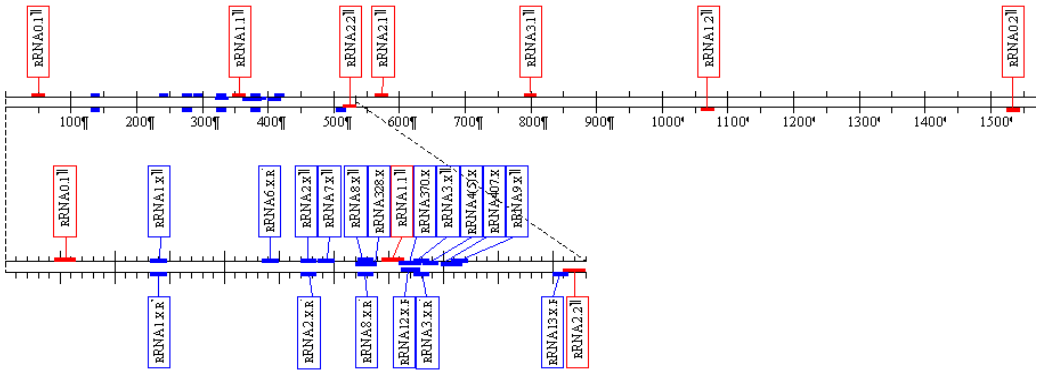

Figure 3. Locations of the designed primers and probes within the sequence of domain I of 16S rRNA. Sequence of E. coli 16S rDNA was used as an eubacterial type example (Brosius J. *et al*., 1978). Primers are shown in red, and probes are shown in blue colour.

Table 2: Oligonucleotide probes. "r" designates that the sequence is derived from the antisense strand of the 16S rDNA. The others are from complementary sense strand. Nucleotide substitutions are presented in lowercase, bold letters. Interrogated signature positions are additionally red-coloured. Locations within 16S rDNA are given according to the *E.coli* sequence numeration (Brosius J. *et al*., 1978).

Name	Sequence (5'-3' direction)	Location	Signature position	G+C (%)
rRNAp 1.1	TGCCCTG **g** ACTCTGG	132-146	139	66.7
rRNAp 1.2	TGCCCTG **c** ACTCTGG			66.7
rRNA p1.3	TGCCCTG **t** ACTCTGG			60.0
rRNA p1.4	TGCCCT**t** **c** ACTCTGG			60.0
rRNA p2.1	ACCAAGGCG **a** CGACG	271-285	280	66.7
rRNAp 2.2	ACCAAGGCG **t** CGACG			66.7
rRNA p2.3	ACCAAGGC**t** **t** CGACG			60.0
rRNA p3.1	ATGGGCG **c** AAGCCTG	374-388	381	66.7
rRNAp 3.2	ATGGGCG **g** AAGCCTG			66.7
rRNAp 3.3	ATGGGCG **a** AAGCCTG			60.0
rRNA p4.1	**c**AAGCCTGA **t** **g** CAGC	381-395	381, 390 and 391	60.0
rRNA p4.2	**g**AAGCCTGA **t** **g** CAGC			60.0
rRNA p4.3	**a**AAGCCTGA **c** **g** CAGC			60.0
rRNA p4.4	**g**AAGCCTGA **t** **c** CAGC			60.0
rRNA p5.1	AAGCCTGA **t** **g** CAGC**a**	382-396	390 and 391	53.3
rRNA p 5.2	AAGCCTGA **t** **g** CAGC**g**			60.0
rRNA p5.3	AAGCCTGA **c** **g** CAGC**a**			60.0
rRNA p5.4	AAGCCTGA **t** **c** CAGC**a**			53.3
rRNA p15.1.1	TTTTTTTTTTTTTTTTGCCCTG **g** ACTCTGG	132-146	139	66.7
rRNA p15.1.2	TTTTTTTTTTTTTTTTGCCCTG **c** ACTCTGG			66.7
rRNA p15.1.3	TTTTTTTTTTTTTTTTGCCCTG **t** ACTCTGG			60.0

rRNA p15.1.4	TTTTTTTTTTTTTTTTGCCCTT c ACTCTGG			60.0
rRNA p15.2.1	TTTTTTTTTTTTTTTACCAAGGCG t CGACG	271-285	280	66.7
rRNA p15.2.2	TTTTTTTTTTTTTTTACCAAGGCG a CGACG			66.7
rRNA p15.2.3	TTTTTTTTTTTTTTTACCAAGGCt t CGACG			60.0
rRNA p15.3.1	TTTTTTTTTTTTTTTATGGGCG c AAGCCTG	374-388	381	66.7
rRNA p15.3.2	TTTTTTTTTTTTTTTATGGGCG g AAGCCTG			66.7
rRNA p15.3.3	TTTTTTTTTTTTTTTATGGGCG a AAGCCTG			60.0
rRNA p15.6.1	TTTTTTTTTTTTTTTCGCG g CCTATCAGCT	235-249	239	66.7
rRNA p15.6.2	TTTTTTTTTTTTTTTCGCG c CCTATCAGCT			66.7
rRNA p15.6.3	TTTTTTTTTTTTTTTCGCG a CCTATCAGCT			60.0
rRNA p15.6.4	TTTTTTTTTTTTTTT CGCG t CCTATCAGCT			60.0
rRNA p15.7.1	TTTTTTTTTTTTTTTGTAGCCGG c CTGAGA	285-299	293	66.7
rRNA p15.7.2	TTTTTTTTTTTTTTTGTAGCCGG t CTGAGA			60.0
rRNA p15.7.3	TTTTTTTTTTTTTTTGTAGCCGG g CTGAGA			66.7
rRNA p15.7.4	TTTTTTTTTTTTTTTGTAGCCGG a CTGAGA			60.0
rRNA p15.8.1	TTTTTTTTTTTTTTTACTGAGA c ACGGCCC	321-335	328	60.0
rRNA p15.8.2	TTTTTTTTTTTTTTTACTGAGA t ACGGCCC			66.7
rRNA p15.8.3	TTTTTTTTTTTTTTTACTGAGA g ACGGCCC			66.7
rRNA p15.9.1	TTTTTTTTTTTTTTTGGGATGA c GGCCTTC	408-422	415	66.7
rRNA p15.9.2	TTTTTTTTTTTTTTTGGGATGA a GGCCTTC			60.0
rRNA p15.9.3	TTTTTTTTTTTTTTTGGGATGA g GGCCTTC			66.7
rRNA p15.9.4	TTTTTTTTTTTTTTTGGGATGA t GGCCTTC			60.0
rRNA p15.1.2.R	TTTTTTTTTTTTTTTCCAGAGT g CAGGGCA	132-146	139	60.0
rRNA p15.1.3.R	TTTTTTTTTTTTTTTCCAGAGT a CAGGGCA			60.0
rRNA p15.2.1.R	TTTTTTTTTTTTTTTCGTCG t CGCCTTGGT	271-285	280	66.7
rRNA p15.2.2.R	TTTTTTTTTTTTTTTCGTCG a CGCCTTGGT			66.7
rRNA p15.3.1.R	TTTTTTTTTTTTTTTCAGGCTT g CGCCCAT	374-388	381	66.7
rRNA p15.3.2.R	TTTTTTTTTTTTTTTCAGGCTT c CGCCCAT			66.7
rRNA p15.3.3.R	TTTTTTTTTTTTTTTCAGGCTT t CGCCCAT			60.0
rRNA p15.8.1.R	TTTTTTTTTTTTTTTGGCCGT a TCTCAGTC	321-335	328	60.0
rRNA p15.8.2.R	TTTTTTTTTTTTTTTGGCCGT g TCTCAGTC			66.7
rRNA p15.12.1.R	TTTTTTTTTTTTTTTCCCATTG t g CAATAT	363-379	370 and 371	40.0
rRNA p15.13.1.R	TTTTTTTTTTTTTTTCACGTAGTT t GCCGG	503-517		60.0
rRNA p15.13.2.R	TTTTTTTTTTTTTTTCACGTAGTT g GCCGG			66.7
rRNA p15.111.1	TTTTTTTTTTTTTTTAGGCAGC a GTGGGGA	349-363		66.7
rRNA p15.112.1	TTTTTTTTTTTTTTTAGGCAGC g GTGGGGA			73.3
rRNA p15.111	TTTTTTTTTTTTTTTGGGAGGCAGC a GTGGGGAAT	346-365		65.0
rRNA p15.112	TTTTTTTTTTTTTTTGGGAGGCAGC g GTGGGGAAT			70.0
rRNA p15.328.1	TTTTTTTTTTTTTTTGGACTGAGA t ACGGCCCAGA	319-338	328	60.0
rRNA p15.328.2	TTTTTTTTTTTTTTTGGACTGAGA c ACGGCCCAGA			65.0
rRNA p15.328.3	TTTTTTTTTTTTTTTGGACTGAGA g ACGGCCCAGA			65.0
rRNA p15.370.1	TTTTTTTTTTTTTTTGGAATATTG c ACAATGGGCG	361-380	370	50.0
rRNA p15.370.2	TTTTTTTTTTTTTTTGGAATATTG g ACAATGGGCG			50.0
rRNA p15.370.3	TTTTTTTTTTTTTTTGGAATATTG t ACAATGGGCG			45.0
rRNA p15.407.1	TTTTTTTTTTTTTTTACGCCGCGTG g GGGATGAAG	397-416	407	70.0
rRNA p15.407.2	TTTTTTTTTTTTTTTACGCCGCGTG a GGGATGAAG			65.0
rRNA p15.407.3	TTTTTTTTTTTTTTTACGCCGCGTG c GGGATGAAG			70.0
rRNA p15.407.4	TTTTTTTTTTTTTTTACGCCGCGTG t GGGATGAAG			65.0

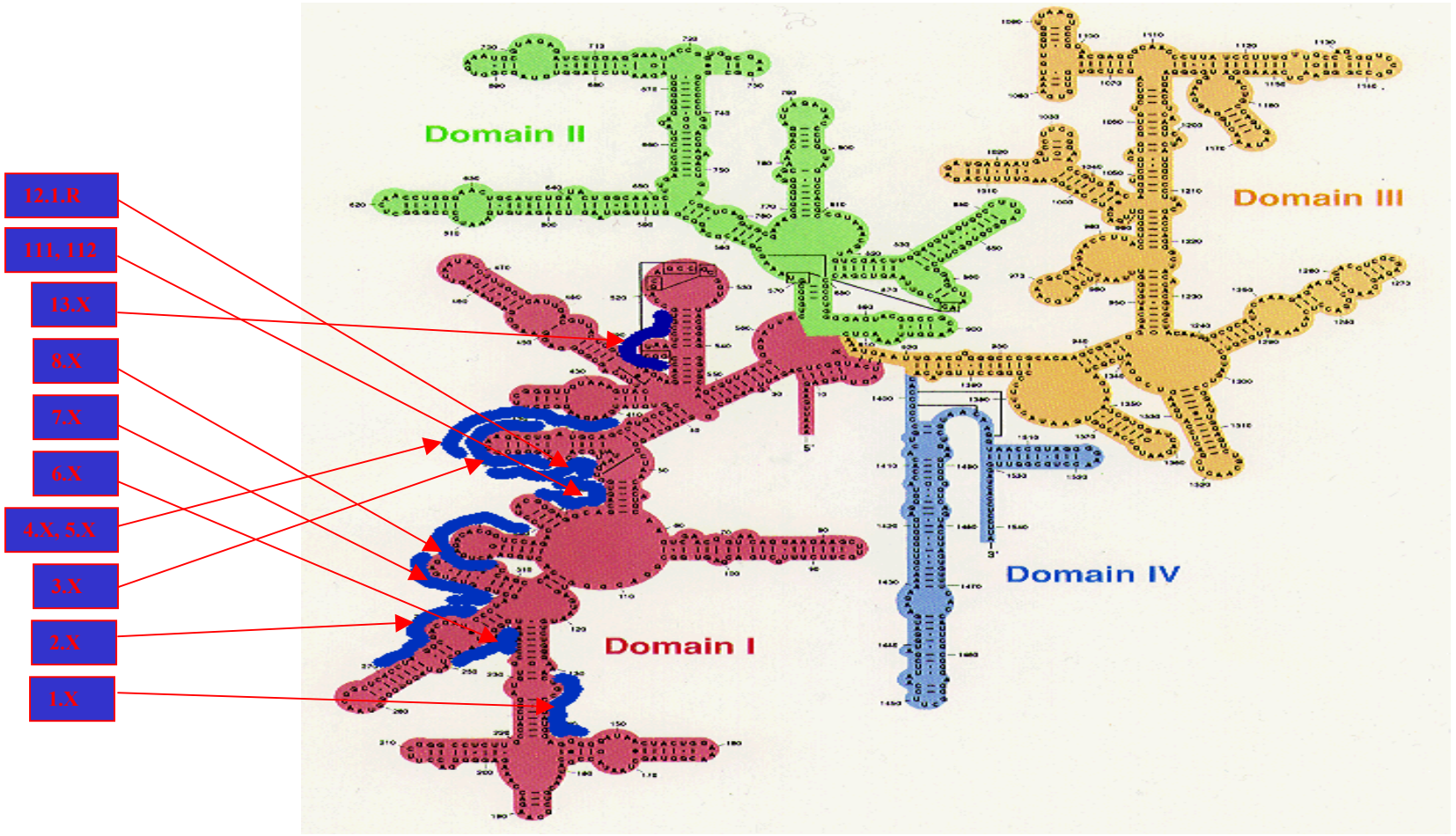

Figure 4. Locations of the designed probes in the context of a secondary structure of domain I of eubacterial 16S rRNA. Those for rRNA p15.328.X, 370.X and 407.X are not shown due to space limitation.

Solid supports

All of the solid supports used during the course of this work were based on silica (SiO_2), i.e. materials with external silanol groups. However, due to their different chemical compositions and modifications (coatings) they had varying surface properties which had to be tested for their suitability in array technology.

A broad range of glass slides was used (European and American format of microscopic slides). Beside glass slides, silicon and glass wafers were also investigated. The best results were obtained with Borofloat-33 glass upon its activation by polylysine, and commercially available silylated slides with active aldehyde groups.

Activation of the solid-support surface

For the immobilization of pre-synthesized DNA probes, the surface of solid support had to be activated. The following activation strategies were tested:

- **Activation by gelatine-carrying linkers**

The layer thickness was in the range of 100-200 nm. The structure of this gel could be modified by uniform or patterned (through non-transparent mask) UV irradiation. In the latter case, gelatine square pads separated by hydrophobic spacers were produced. The unstructured wafers were not suitable for the hybridization experiments, as the gelatine layer was unstable under the hybridization and washing conditions used.

The structured gelatine wafers were stable under the above conditions. They were further functionalized by polylysine coats in order to increase the density of DNA binding sites.

- **Polylysine coating**

Hybridization experiments between *in vitro* transcribed and labelled RNA and immobilized PCR fragments showed comparable results from arrays prepared on activated microscopic slides and structured glass wafers in regard to spot size, shape, and the dynamic range of hybridization signals. The background level was higher in the case of microscopic slides. A linear correlation between DNA- and salt concentrations of spotting samples and resultant hybridization signals was demonstrated for 1 – 3 μM concentration range of 500 bp long rRNA f0-r2 fragments. On silicon wafers, significantly decreased hybridization signals as well as a low quality of spot shapes and spot patterns were observed. Thus, a choice for the surface of the further evaluation cycle was made for microscopic glasses, due to their

affordability, handling, and broad customary possibilities of use concerning spotting densities and patterns.

Different microscopic slides were tested upon polylysine activation, e.g. Borofloat-33, Gold Seal (Sigma) and Esco pre-cleaned (Erie Scientific) microscopic slides. Sigma pre-activated, ready-to-use slides were also included and served as a control. The effect of the storage time of slides was tested for Borofloat slides. The results are shown in figure 5. Arrays were hybridized with both labelled oligonucleotide and PCR fragment.

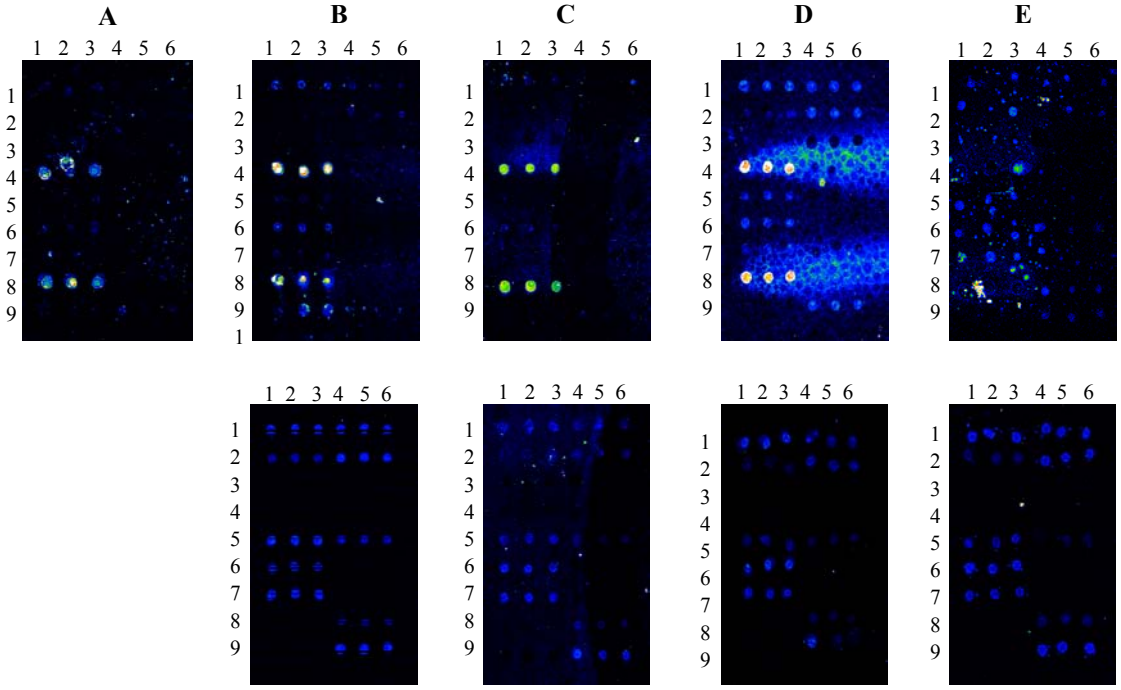

	1 2 3	4 5 6
1	rRNA f0-r2.108, 3.0 µM	rRNA f0-r2.108, 1.5 µM
2	rRNA f0-r2.108, 0.75 µM	rRNA f0-r2.108, 1.5 µM
3	*N. tabaccum* ChlD, 0.5 µg/µl	λDNA/HindIII, 0.5 pM
4	rRNA p15.1.1, 100 µM	3xSSC
5	rRNA f0-r2.108, 1.5 µM	rRNA f0-r2.108, 3.0 µM
6	rRNA f0-r2.108, 3.0 µM	*N. tabaccum* ChlD, 0.5 µg/µl
7	rRNA f0-r2.108, 0.5 µg/µl	3xSSC
8	rRNA p15.1.1, 100 µM	rRNA f0-r2.108, 0.75 µM
9	λDNA/HindIII, 0.5 pM	rRNA f0-r2.108, 3.0 µM

Figure 5. **Comparison of different poly-L-lysine activated slides.** The test consisted of Borofloat-33, Gold Seal (Sigma) (C) and Esco pre-cleaned (Erie Scientific) (D) microscopic slides which were activated (according to the protocols described in Methods) and Sigma polylysine pre-activated slides (E). Two different Borofloat-33 slides were tested: after two days (A) and two weeks (B) of storage upon preparation. The spots were made from the 3xSSC-based solutions of indicated concentrations and according to the pattern shown in the table. The upper row shows the results of the hybridization with Cy5-end labelled rRNA 1.1; the lower row shows the results of hybridization with Cy3-end labelled rRNA f0-r2.40517 fragment.

The results of the former hybridization showed that the maximal dynamic range of data was obtained using 15-day old Borofloat-33 slides. The specific hybridization signals obtained from positive control spots (rRNA f0-r2.108 fragment and rRNA p15.1.1 oligonucleotide, see figure 5) were significantly greater than those obtained with 2-day old Borofloat-33 slides or Gold Seal slides. The results obtained from the Esco pre-cleaned slides were characterized by the highest specific hybridization signals from above spots but the attachment and/or hybridized duplex stability on this type of slide was poor (see figure 5). Based on these results 2-day old Borofloat-33 slides were excluded from further experiments. The results of the latter hybridization showed roughly the same background and specific hybridization signals for all types of slides; the only exception was the highest consistency of DNA spots obtained on the Borofloat-33 slides. Based on above results and considering affordability factor, the Borofloat-33 slides were chosen for further evaluation.

- **Silanization of microscopic slides by alkylaminosilanes (Corning's gamma-aminopropyl silane slides).**

The next step consisted of the comparison between Corning's gamma-aminopropyl silane slides and polylysine-activated Borofloat 33 slides which had passed the preceding tests.

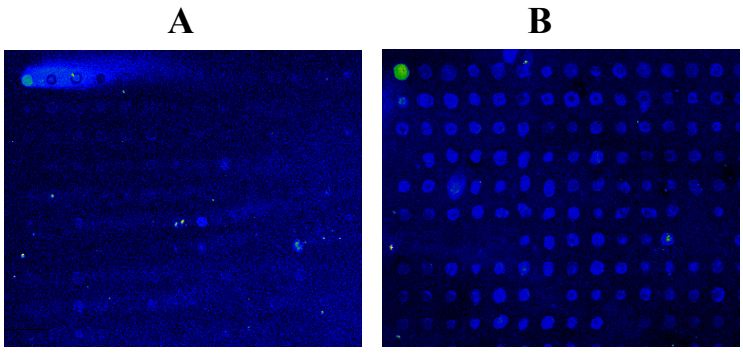

Figure 6. Comparison between ready-to-use gamma-amino-propyl silane activated slides (Corning) (A) and poly-L-lysine activated Borofloat-33 slides (B).

An array of PCR fragment shotgun library of the *S. erythraea* DSM 40517 genomic DNA was prepared on both slides. The arrays were hybridized with 1 µg of each, Cy3- and Cy5-labelled cDNAs, prepared from the corresponding total RNAs isolated from the cells grown in rich (M79) and semi-synthetic (modified Czapek) media respectively. Signal detection was performed at the indicated scanning parameters. The results showed significantly decreased DNA-retention ability, increased background signals and lower hybridization signals from silanized slides.

In summary, Borofloat 33 slides activated by polylysine coating proved to be optimal for the immobilization of long and unmodified polynucleotide probes (PCR fragments).

1.2.1 Aldehyde coupling

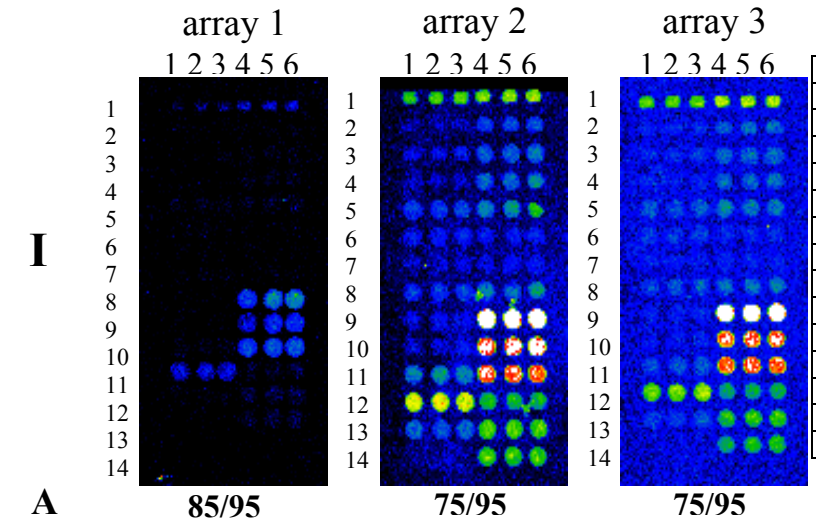

	1 2 3	4 5 6
1	**rRNA p15.1.1**	rRNA p15.6.1
2	rRNA p15.1.2	rRNA p15.6.2
3	rRNA p15.1.3	rRNA p15.6.3
4	rRNA p15.1.4	rRNA p15.6.4
5	**rRNA p15.2.1**	**rRNA p15.7.1**
6	rRNA p15.2.2	rRNA p15.7.2
7	rRNA p15.2.3	rRNA p15.7.3
8	rRNA p15.3.1	rRNA p15.7.4
9	rRNA p15.3.2	**rRNA p15.111.1**
10	rRNA p15.3.3	rRNA p15.112.1
11	rRNA p15.8.1	**rRNA p15.9.1**
12	**rRNA p15.8.2**	rRNA p15.9.2
13	rRNA p15.8.3	rRNA p15.9.3
14		rRNA p15.9.4

Figure 7. Correlation between silylated slide properties and hybridization results. Four different types of silylated slides were used for the oligonucleotide probe immobilization, as indicated in table B. The perfect match probes of each group (colour-coded) for the *A. mediolanus* HKI108 PCR fragment used as a target are given in bold. Lane I shows the resulting scans at 20 nm resolution of the arrays 1-3; lane II shows scans at 50 nm resolution of the areas surrounding arrays 2 and 3. Signal detection was performed at the scanning parameters given in lane A.

The activation strategy of aldehyde coupling to Borofloat-33 slides and silicon wafers was done using an additional final glutaraldehyde coupling reaction to the aminosilanized surfaces (see Methods). Slides activated by this method are said to be silylated. The resulting active aldehyde groups were well suited for the immobilization of aminomodified probes. A correlation between specific and background signals obtained after hybridization and signals recorded from the activated glass surface was found. The results are presented in figure 7. 15-mer oligonucleotide probes were spotted and immobilized on commercial slides with 300-400 greyscale units of fluorescence signal of glass DNA-binding layer (arrays N1) and prepared

silylated slides with 4000, 7000 and 14000 values of the above parameter (arrays N2-4, respectively). The DNA on the arrays was hybridized with Cy3-end labelled rRNAf0-r2.108 PCR fragment. The results devoted to the arrays 1-3 are quantified in supplementary tables 3-5 respectively. Statistics summarizing the three times repeated assay are given in the table 3.1. Background subtracted fluorescent signals from each array element were normalized to the mean signal value, as described in Methods. Background values (Bkgd), reference mean signal values (sRef) and signal-to-noise (S/N) ratio values were statistically evaluated: mean value (Mean) with the standard deviation (SD), coefficient of variation (CV), and total value across the array (Total) are shown. The same evaluations are presented for all further similar calculations.

Table 3.1: Results obtained on commercial and prepared silylated slides upon hybridization with Cy3-end labelled rRNAf0-r2.108 PCR fragment (averaged over three arrays of each type).

Array 1			
	Bkgd	sRef	S/N
Mean	9.63×10^{-6}	1.44×10^{-5}	2.074
SD	2.30×10^{-5}	10^{-4}	3.92
CV	239.176	3.87×10^{-6}	256.621
Total	8.09×10^{-4}	0.001	189.753
Array 2			
	Bkgd	sRef	S/N
Mean	1.43×10^{-4}	8.98×10^{-4}	4.123
SD	3.17×10^{-4}	10^{-4}	4.826
CV	221.519	10^{-4}	117.038
Total	0.012	0.075	346.362
Array 3			
	Bkgd	sRef	S/N
Mean	1.23×10^{-4}	7.79×10^{-4}	3.932
SD	1.51×10^{-4}	10^{-4}	5.088
CV	122.768	5.45×10^{-6}	129.409
Total	0.010	0.065	330.277

Table shows drastically increased values of all measured parameters when the hybridization results of array 1 were compared with those of arrays 2 and 3. In fact, 15- and 12-fold increases in the background level and 75- and 65-fold increase in the specific hybridization level were noted for arrays 2 and 3 respectively. Moreover, array 1 was scanned at the higher laser power, i.e. at 85% of the maximum value compared with the 75% used for the arrays 2 and 3. Signals from rRNA p15.111.1 and rRNA p15.112.1 spots were at the measurement

saturation level in the case of arrays 2 and 3. The values for array 3 were lower then those for array 2. Further increase of the fluorescence signal of the DNA-binding layer of glass surface (arrays 4, 14000 greyscale units) led to a sharp decrease of background level. The specific hybridization signals showed a much less pronounced decrease, as can be noted by simple visual comparison of images obtained from areas surrounding arrays 3 and 4 (Lane II). This led to the higher dynamic range of data noted for array 2.

Regarding the fabrication details, arrays 2 and 4 were activated by overnight incubation in 10% water solution of KOH and array 3 was activated under the same conditions, although KOH was dissolved in methanol. Moreover, 3% aminosilane in 95% methanol was usually used but in the case of array 4 the aminosilane concentration was decreased to 1%.

Thus, the effects of modification of slide activation protocol and their obvious impacts on the final DNA binding layer assembly were observed. The in-house preparation of silylated slides showed its unsuitability regarding a uniformity of aldehyde coating across the surface of Borofloat-33 slides (figure 7 represents rather typical examples). Among each set of 15-mer probes assayed, the perfect complements showed the highest hybridization signals.

Further investigation was focused on commercial silylated slides and aldehyde in-house-activated glass wafers. The results of a hybridization of 20-mer oligonucleotides immobilized on both surfaces with *in vitro* transcribed RNA target are shown in figure 8. Data regarding hybridization results of perfect match probes rRNA p15.111 are quantified in table 6 and 7 for the slides and wafers respectively.

Table 4.1: Averaged over three arrays, comparison between wave-guide wafer and Borofloat-33 slide.

Results on wave-guide wafer.				
	Area - mm^2	Bkgd	sRef	S/N
Mean	28.003	0.196	2.305	36.423
SD	$1.22x10^{-6}$	0.145	10^{-4}	24.702
CV	$4.34\ x10^{-6}$	74.334	$1.29\ x10^{-6}$	67.82
Total	1540.145	10.764	126.757	2003.245
Results on Borofloat-33 slide.				
	Area - mm^2	Bkgd	sRef	S/N
Mean	17.05	0.253	0.252	3.325
SD	10^{-4}	0.099	10^{-4}	1.971
CV	10^{-4}	38.994	10^{-4}	59.277
Total	579.717	8.615	8.552	113.039

The hybridization signals were background corrected and normalized to the mean value of overall spot fluorescence value. Only signals of the spots unaffected by highly varying background fluorescence were used for quantifications in the case of Borofloat-33 slides. The corresponding statistics are given in tables 4.1. The hybridization results obtained on the wafer were characterized by a uniform and approximately 30% lower background level when compared with the slides.

Table 5.1: a correlation between hybridization results presented in tables 6.1 and stock concentrations of oligonucleotide probes used for spotting, as well as discrimination values between match- and mismatch probe signals.

Support	Stock concentrations of oligonucleotide probes											
	50 µM			25 µM			12.5 µM			6.25 µM		
	Averaged hybridization signal values											
	p15.11 1 (A)	p15.11 2 (B)	A/B	p15.11 1 (A)	p15.11 2 (B)	A/B	p15.11 1 (A)	p15.11 2 (B)	A/B	p15.11 1 (A)	p15.11 2 (B)	A/B
Wafer	1.66 ± 0.438	0.73 ± 0.114	**2.3**	2.23 ± 0.398	1.00 ± 0.302	**2.2**	1.07 ± 0.214	0.41 ± 0.070	**2.6**	0.53 ± 0.246	0.26 ± 0.179	**2.1**
Slide	3.38 ± 0.309	0.30 ± 0.099	**11.2**	1.93 ± 0.443	0.31 ± 0.049	**6.3**	0.94 ± 0.113	0.21 ± 0.065	**4.4**	0.40 ± 0.131	0.13 ± 0.142	**3.1**

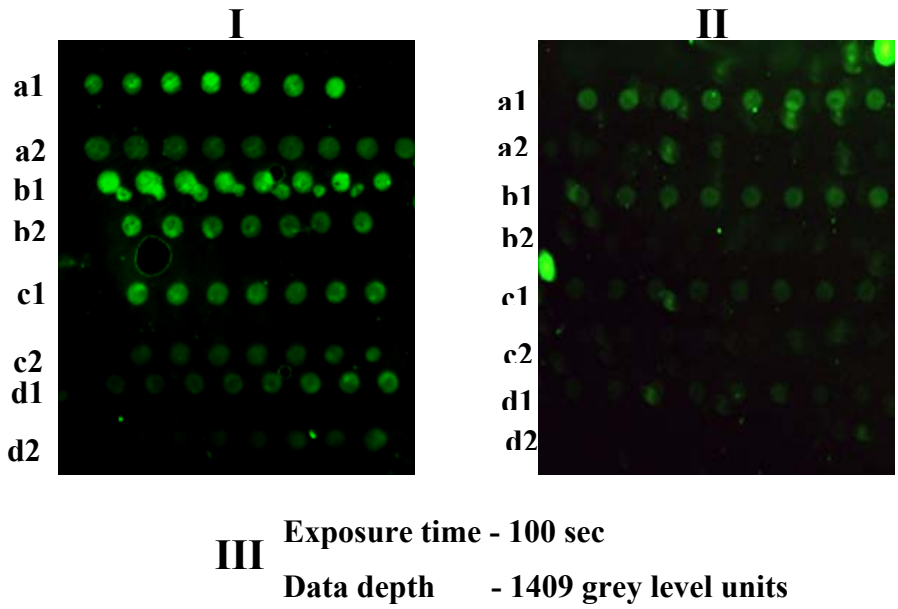

Figure 8. **Comparison between a glass wafer (I) and a Borofloat-33 glass slide (II) activated by aldehyde.** Line 1 shows signals of spots of immobilized 20-mer oligonucleotides rRNA p15.111 (perfect match); line 2 shows signals of spots of 20-mer oligonucleotides rRNAp15.112 (single mismatch). Spots were prepared from 50µM (line a), 25µM (line b), 12.5µM (line c) and 6.125µM (line d) probe solutions prepared in 1xTelechem spotting solution respectively. Signal detection was performed by a CCD camera-based detection system under the conditions given in panel III.

The dynamic range of hybridization signals relative to interspot surface obtained on the wafer was approximately 10 to15 times (mean and total signal-to-noise ratios respectively) greater

than that on the slide. A correlation between resultant hybridization signals obtained in spots of match (rRNA p15.111) and mismatch (rRNA p15.112) probes and their stock concentrations used for spotting (figure 8), as well as the discrimination match/mismatch ratios for above hybridization signals, are given in table 5.1. This data shows that the discrimination factor between match and mismatch probes linearly correlated with the probe stock concentration in the slide hybridization and was unchanged in the case of the wafer.

The results showed the superior characteristics of the commercial silylated slides. They were selected for further evaluation in a set-up consisting of the covalent attachment of aminomodified oligonucleotide probes and the subsequent use of resultant arrays in hybridizations for single base difference detection. Based on results obtained, batches of these slides showing a self-fluorescence level greater than 2000 greyscale units were used in the subsequent experiments. An aging effect of these slides was also investigated (see figure 12).

Preparation of immobilization probes

Both PCR fragment- (primers are given in table 1) and oligonucleotide probes (table 2) were tested and used for different immobilization strategies and on different activated supports.

1.2.2 PCR fragments

Both unmodified and aminomodified primers were used. PCR fragments amplified with unmodified primers were immobilized on poly-L-lysine activated slides. Those made with primers with an aminolink were used for the immobilization on silylated slides (see Methods). Varying PCR fragment concentrations were tested. The results obtained on Borofloat-33 polylysine slides are presented above (see “Activation of the solid-support surface/Polylysine coating”). The results concerning silylated slides are shown in figure 11 (see ”Immobilization on of DNA probes”).

1.2.3 Oligonucleotide probes

Oligonucleotide probes contained an aminolink at 5‘ end as an attachment site to aldehyde activated supports. The effects concerning a spacer between the aminolink and the specific probe sequence, probe length, and their concentrations were tested.

Spacer effect. As a spacer, 15-dT homooligonucleotide was tested. The typical results of this kind of test are given in figure 9. A comparison of the hybridization results of spotted probe

sets rRNA p1-5.X (without spacer) and rRNA p15.2.X (with spacer) (table 2) are demonstrated. Both arrays were hybridized with the rRNAf0-r2.7653 PCR fragment under the same conditions. No significant differential hybridization between and within sets of probes was observed upon the hybridization with the former sets of probes, thus masking the discrimination between perfect match and mismatch probes. In contrast, in the latter case a clear discrimination between those two types of probes was shown.

A

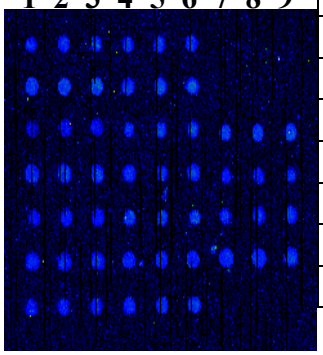

B

	1 2 3	4 5 6	7 8 9
1	rRRNA p15.1.1	rRRNA p15.4.1	
2	rRRNA p15.1.2	rRRNA p15.4.2	
3	rRRNA p15.1.3	rRRNA p15.4.3	rRRNA p15.5.1
4	rRRNA p15.1.4	rRRNA p15.4.4	rRRNA p15.5.2
5	rRRNA p15.2.1	rRRNA p15.3.1	rRRNA p15.5.3
6	rRRNA p15.2.2	rRRNA p15.3.2	rRRNA p15.5.4
7	rRRNA p15.2.3	rRRNA p15.3.3	

C

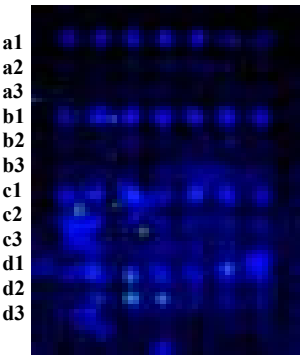

D

Laser power - 85%
PMT - 90%

Laser power - 80%
PMT - 85%

Figure 9. Investigation of the spacer effect. A: results of hybridization to the array of 15-mers without spacer, spotted according to the pattern shown in table B. C: the results of hybridization to the array of rRNA p15.2.X set (with a spacer): line 1: spots of rRNA p15.2.1 probe (perfect match); lines 2 and 3: spots of rRNA p15.2.2 and rRNA p15.2.3 probes, respectively (single mismatches). Spots were prepared from 100 µM (line a), 50 µM(line b), 25 µM (line c) and 12.5 µM (line d) probe solutions in 1xTelechem spotting solution. Signal detection was performed at the scanning parameters given in Lane D.

Thus, the use of immobilized oligonucleotides with 15-dT spacer increased the hybridization specificity and sensitivity of single-nucleotide discrimination assays.

Effects of probe length. Oligonucleotide probes of 15 and 20 bp length were used. The results obtained indicated that increasing the probe length led to increased sensitivity (higher hybridization signals) but compromised the specificity (lower match/mismatch discrimination) of the assays. Typical results are presented in figure 7. Therefore, the main part of experiments focused on the optimization of hybridization conditions for arrays of 15-mer probes with 15-dT spacer, in order to increase the detection limit of this set-up and keeping its superior specificity.

Effects of probe concentration. Dilution series ranging from 0.78 µM to 200 µM in spotting buffer were tested. The results are given in figures 8-10. A linear correlation between probe concentration and hybridization signal, as well as match/mismatch discrimination ratio, was

observed. The optimal values and saturation points for both parameters were dependent on the type of hybridization target used (PCR fragment or RNA, see below).

Immobilization of DNA probes

The composition of probe solutions and support surface properties, as well as deposition technology, should ensure small deposited volumes of DNA probes and the conditions necessary for effective covalent bond formation between corresponding chemical moieties of an array surface and probes. In addition, a negligible unspecific target attachment to the DNA spots and interspot areas upon hybridization is required.

The following immobilization procedures were tested:

1) The immobilization of PCR fragment- and oligonucleotide aminomodified probes on aldehyde supports.
2) Polynucleotide probe immobilization on polylysine supports.

In the case of first procedure, the protocols of Schena *et al*. (1996) and of TeleChem were tested. The former protocol was modified for oligonucleotide immobilization, i.e. the incubation time after spotting was extended to 24 h. Testing was performed on commercial silylated slides with fluorescence level of DNA binding layer at around 5000 greyscale units. The results are shown in figure 10. In the case of use of the TeleChem spotting buffer, no specific hybridization signals were obtained from the spots of the two lowest concentrations. This reduced the overall dynamic range of the hybridization signals by approximately 10 times in comparison with spots prepared in 3xSSC solution (supplementary tables 8, 9 and 10, 11 on data concerning protocols provided by TeleChem and Shena *et al*. for the first and second washings, respectively). The harsh conditions applied for the probe stripping were not sufficient to remove unspecifically bound target material. SybrGreen II signals were only detected from the spots prepared from commercial spotting solution. The data on rRNA p15.1.1 probe hybridization signals is presented in table 6.1.

A linear correlation between hybridization signals and oligonucleotide stock concentrations within 3.125 – 50 μM was obtained. Upon hybridization with PCR fragment, an increase of probe concentration by a factor of 4 resulted in an increase of the hybridization signal by a factor of 2 (table 6.1). This did not depend on the number of washings, their stringency, or detection parameters.

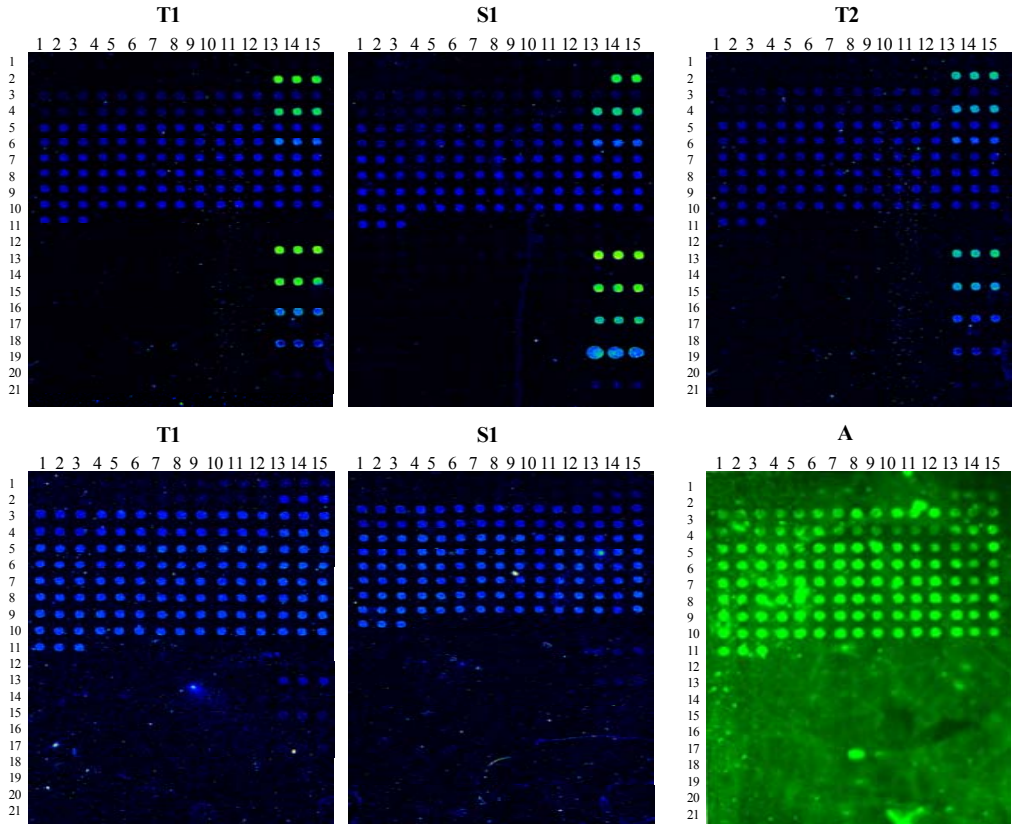

Figure 10. Investigation of two protocols for an immobilization of aminomodified DNA on silylated slides. Probes were obtained from the campus manufacturer (rRNA p15.3.X.r, rRNA p15.8.X.r, rRNA p15.13.X.r sets and rRNA p15.12.1.r) and from commercial vendor (Interactiva) (rRNA p15.1.1) and spotted according to a pattern given in table B. The spots were made from probe solutions prepared in 1xTelechem spotting solution (upper half, lines 1-10) and 3xSSC buffer (lower half, lines 12-21). The concentrations of probe solutions were as follows: 200 µM (lines 1, 2, 12, 13), 50 µM (lines 3, 4, 14, 15), 12.5 µM (lines 5, 6, 16, 17), 3.125 µM (lines 7, 8, 18, 19) and 0.780 µM (lines 9, 10, 20, 21). The prepared arrays were processed according to the protocol provided by TeleChem (T) and that of Schena *et al*. (S). Cy3 end labelled rRNAf0-rRNAr2.9550 PCR fragment (upper row) and Cy5 chemically labelled total *Streptomyces globisporus* 1912 RNA (lower row, except A) were used as targets. The results obtained after standard protocol are given in panels 1. In addition, arrays hybridized with PCR fragment were subjected to the washing process at more stringent conditions (37°C, 3 h) and the corresponding results are given in panels 2. A: the result of staining by SybrGreen II and detection on CCD camera.

	1	2	3	4	5	6	7	8	9	10	11	12	13	14	15
1	p15.3.1.r			p15.3.2.r			p15.3.3.r			p15.11.1.r			p15.11.2.r		
2	p15.2.1.r			p15.2.2.r			p15.13.1.r			p15.13.2.r			**p15.1.1**		
3	p15.3.1.r			p15.3.2.r			p15.3.3.r			p15.11.1.r			p15.11.2.r		
4	p15.2.1.r			p15.2.1.r			p15.13.1.r			p15.13.2.r			**p15.1.1**		
5	p15.3.1.r			p15.3.2.r			p15.3.3.r			p15.11.1.r			p15.11.2.r		
6	p15.2.1.r			p15.2.2.r			p15.13.1.r			p15.13.2.r			**p15.1.1**		
7	p15.3.1.r			p15.3.2.r			p15.3.3.r			p15.11.1.r			p15.11.2.r		
8	p15.2.1.r			p15.2.2.r			p15.13.1.r			p15.13.2.r			**p15.1.1**		
9	p15.3.1.r			p15.3.2.r			p15.3.3.r			p15.11.1.r			p15.11.2.r		
10	p15.2.1.r			p15.2.2.r			p15.13.1.r			p15.13.2.r			**p15.1.1**		
11															
12	p15.3.1.r			p15.3.2.r			p15.3.3.r			p15.11.1.r			p15.11.2.r		
13	p15.2.1.r			p15.2.2.r			p15.13.1.r			p15.13.2.r			**p15.1.1**		
14	p15.3.1.r			p15.3.2.r			p15.3.3.r			p15.13.1.r			p15.13.2.r		
15	p15.2.1.r			p15.2.2.r			p15.13.1.r			p15.13.2.r			**p15.1.1**		
16	p15.3.1.r			p15.3.2.r			p15.3.3.r			p15.11.1.r			p15.11.2.r		
17	p15.2.1.r			p15.2.2.r			p15.13.1.r			p15.13.2.r			**p15.1.1**		
18	p15.3.1.r			p15.3.2.r			p15.3.3.r			p15.11.1.r			p15.11.2.r		
19	p15.2.1.r			p15.2.2.r			p15.13.1.r			p15.3.2.r			**p15.1.1**		
20	p15.3.1.r			p15.3.2.r			p15.3.3.r			p15.11.1.r			p15.11.2.r		
21	p15.2.1.r			p15.2.2.r			p15.13.1.r			p15.13.2.r			**p15.1.1**		

Table 6.1: Background corrected and averaged (over three repetitive spots) hybridization signals from rRNA p15.1.1 probe spots with Cy3 end labelled rRNAf0-rRNAr2.9550 PCR fragment, obtained upon comparison of both protocols used for silylated slides processing under two washing condition sets. 1, standard washing conditions; 2, higher stringency conditions (37°C, 3h); N.D., not determined due to increased size of corresponding spots (see figure 10).

Array fabrication protocol	Spotting buffer	Number of washings	Concentrations of probe stocks used for spotting [μM] 200	50	12	3.125	0.78
TeleChem	TeleChem	**1**	14.1 ± 1.89	10.3 ± 0.35	4.6 ± 0.55	2.2 ± 0.13	1.5 ± 0.24
		2	12.2 ± 1.87	8.0 ± 0.44	3.6 ± 0.33	2.0 ± 0.39	1.2 ± 0.17
	3xSSC	**1**	17.6 ± 1.94	10.7 ± 0.83	5.0 ± 0.71	2.3 ± 0.32	0.2 ± 0.04
		2	13.2 ± 1.09	8.2 ± 0.54	4.5 ± 0.24	2.1 ± 0.27	0.1 ± 0.11
Shena M. *et al.*	TeleChem	**1**	18.7 ± 4.43	9.9 ± 0.75	4.7 ± 0.29	2.3 ± 0.30	1.7 ± 0.10
		2	10.9 ± 2.46	9.6 ± 1.17	3.5 ± 0.17	1.8 ± 0.17	1.4 ± 0.14
	3xSSC	**1**	29.8 ± 8.35	15.9 ± 2.74	9.2 ± 2.10	N.D.	0.2 ± 0.14
		2	18.0 ± 2.07	8.6 ± 5.07	4.9 ± 0.86	N.D.	0.2 ± 0.09

The results concerning PCR fragment immobilization are shown in figure 11. rRNA f0-r2 and comprising 150 bp-long rRNA f1-r2 PCR fragments of *S. globisporus* 1912 and *S. viridis* 9550 were tested. The arrays were hybridized with varying amounts of oligonucleotide- and PCR fragment targets. The results were as follows: no proper probe immobilization from 3xSSC stock solutions following the protocol of Shena *et al*., 1996 was obtained (data not shown). The results obtained from the use of the protocol provided by TeleChem are quantified in the supplementary tables 12 and 13 (for 0.1- and 1.0 μM target concentrations respectively). Averaged fluorescence values for the each DNA probe are given in table 7.1. The table shows that upon hybridization under 0.1 μM concentration of PCR-fragment target (figure 11, I, A), the highest signals from both rRNA f0-r2- and rRNA f1-r2 probes were obtained at spots prepared from the stocks of two lowest concentrations, i.e. 0.375, 0.75 μM for rRNA f0-r2- and 1.25, 2.5 μM for rRNA f1-r2 fragments, respectively. They were 4 times greater when compared with the signals from the highest concentration stocks, i.e. 6 μM for rRNA f0-r2- and 20 μM for rRNA f1-r2 fragments. The use of 10 times higher target concentration (figure 11, I, B) resulted in signal uniformity: the highest and the lowest stringency signals differed by factors 1.4-1.6 for rRNA f0-r2 fragments and 1.2-1.4 for rRNA f1-r2 fragments. Despite a higher than 99% identity between *S. globisporus* 1912 and *S. viridis* 9550 sequences of rRNA f0-r2 fragments, consistently higher signals were obtained from whole match *S. viridis* 9550 fragments (with few exceptions). The results of oligonucleotide hybridization showed opposite results regarding the response to different target concentrations used: at 0.2 μM target concentration (figure 11, II, A) only the spots made from three highest stock

concentrations of match rRNA f0-r2.9550 probe, i.e. 6, 3 and 1.5 µM, showed detectable hybridization signals.

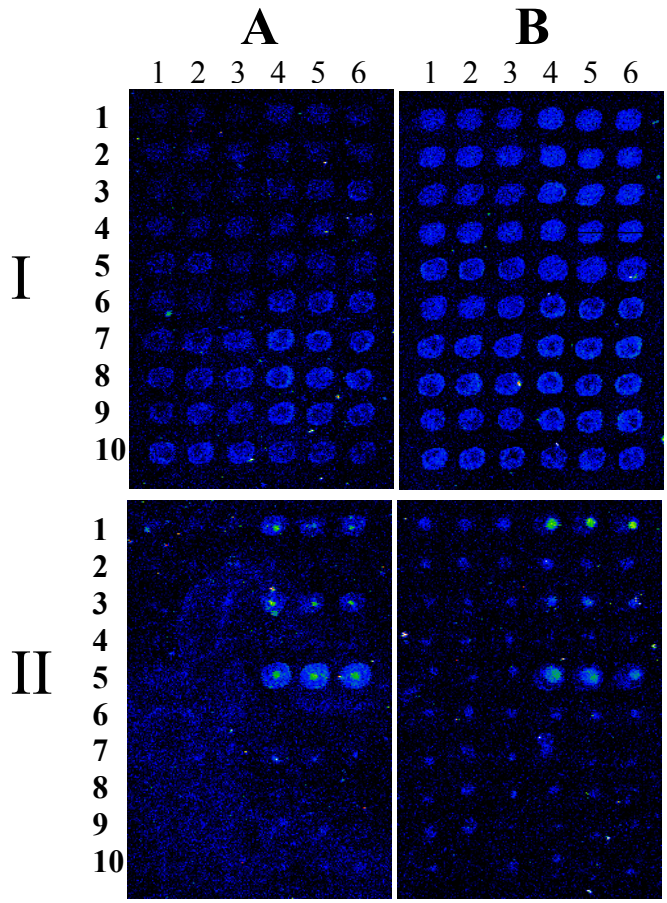

C

	1 2 3	4 5 6	
1	f0-r2.1912	f0-r2.9550	6.0 µM
2	f1-r2.1912	f1-r2.9550	20.0 µM
3	f0-r2.1912	f0-r2.9550	3.0 µM
4	f1-r2.1912	f1-r2.9550	10.0 µM
5	f0-r2.1912	f0-r2.9550	1.5 µM
6	f1-r2.1912	f1-r2.9550	5.0 µM
7	f0-r2.1912	f0-r2.9550	0.75 µM
8	f1-r2.1912	f1-r2.9550	2.5 µM
9	f0-r2.1912	f0-r2.9550	0.375 µM
10	f1-r2.1912	f1-r2.9550	1.25 µM

D

I: laser power - 85%
PMT - 95%

II: laser power - 80%
PMT - 90%

Figure 11. Comparison of oligonucleotides and PCR fragments as targets upon their hybridization with arrays of immobilized PCR fragments. Spotting pattern is given in panel C. Signal detection was performed at the scanning parameters given in panel D.

Table 7.1: Hybridization signals obtained from spots of rRNA f0-r2 and rRNA f1-r2 PCR fragments of *S. globisporus* 1912 and *S. viridis* 9550 hybridized with Cy3-end labelled rRNA f0-r2.9550 PCR fragment.
1-5 correspond to the following order of probe stocks used for spotting: 6.0, 3.0, 1.5, 0.75 and 0.375 µM for rRNA f0-r2 and 20.0, 10.0, 5.0, 2.5 and 1.25 µM for rRNA f1-r2 fragments, respectively).

Target con-centration	Probe stock concentration	rRNA f0-r2 1912	rRNA f0-r2 9550	rRNA f1-r2 1912	rRNA f1-r2 9550
0.1 µM	1	0.281 ± 0.085	0.592 ± 0.117	0.490 ± 0.074	0.508 ± 0.181
	2	0.356 ± 0.377	0.761 ± 0.228	0.558 ± 0.127	0.883 ± 0.291
	3	0.669 ± 0.215	0.588 ± 0.108	0.403 ± 0.044	1.435 ± 0.082
	4	1.069 ± 0.326	2.151 ± 0.555	1.181 ± 0.337	2.122 ± 0.370
	5	1.075 ± 0.256	1.806 ± 0.540	1.780 ± 0.179	0.924 ± 0.152
1.0 µM	1	0.609 ± 0.028	1.080 ± 0.093	0.858 ± 0.042	1.110 ± 0.125
	2	0.657 ± 0.015	1.298 ± 0.070	0.822 ± 0.080	1.024 ± 0.059
	3	0.876 ± 0.129	1.034 ± 0.011	0.845 ± 0.025	1.147 ± 0.337
	4	0.984 ± 0.075	1.380 ± 0.181	1.171 ± 0.164	1.230 ± 0.163
	5	0.770 ± 0.020	1.112 ± 0.194	0.967 ± 0.188	1.152 ± 0.399

The resulting dynamic range was decreased upon the use of 10-fold higher target concentration due to increased background signals from all probes (figure 11, II, B).

Concerning polynucleotide probe immobilization on polylysine supports, the results obtained on Borofloat-33 polylysine slides are presented above (see "Activation of the solid-support surface/polylysine coating").

Based on results above, the immobilization of unmodified PCR fragments on polylysine slides for subsequent hybridization with long polynucleotide targets and immobilization of aminomodified PCR fragments on silylated slides for subsequent hybridization with oligonucleotide targets were selected as optimal set-ups.

Labelling efficiency for hybridization target molecules

To determine the labelling efficiency, different fluorescent dyes were incorporated into target nucleic acids (see Materials and Methods). The dye incorporation was determined as a molar ratio of dyes per one mole of target molecules (in the case of total cellular RNA or its cDNA complement, the same value per 100 bp of RNA is indicated). The results were as follows (table 8.1):

Table 8.1: The efficiency of different fluorescence-labelling methods.

Target	Labelling reaction	Fluorescent dye	Dye incorporation
PCR fragment	PCR, end-labelled primer	FITC, Cy3, Cy5	1
PCR fragment, 500 bp long	PCR, dye-modified dNTP	FITC	5
RNA, 500 bp long	*In vitro* transcription	FITC	3.5
Total RNA	Chemical coupling	Cy3, Cy5	1.5
cDNA	Reverse transcription	Cy3	4
		Cy5	2.9
oligonucleotide	Chemical coupling after synthesis	FITC, Cy3, Cy5	1

Reverse transcription of the RNA into cDNA showed a 1.5- and 2.5 times greater efficiency for Cy5- and Cy3 incorporation respectively than a direct chemical coupling to RNA molecules. The latter procedure, in turn, allowed equal incorporation of both dyes. In comparison, 67% of this labelling efficiency was obtained by incorporation of labelled nucleotides using PCR. It resulted in a 1.5 times higher label incorporation compared with *in vitro* transcription of plasmid DNA. The latter two labelling reactions were performed using fluoresceine isothiocyanate (FITC) as dye. Symmetric PCR for the cyanine dye-labelling was not tested. Asymmetric PCR to create Cy3-labelled single-stranded DNA target failed upon the use of both the end-labelled primer and the labelled-nucleotide incorporation. The chemical coupling of cyanine dyes to total RNA was shown to be the most convenient, fastest, and most unbiased in regard to the use of different fluorophores.

Array hybridization

To perform optimal hybridization and washing reactions, all contributing factors such as temperature, time, buffers, hybridization volume, and concentrations of hybridizing counterparts were investigated and optimized.

The results regarding hybridizations where oligonucleotides took part as at least one hybridization counterpart were as follows:

Hybridization buffer and slide ageing. The results given in figure 12 are devoted to the effects of buffer content and aging of silylated slides (supplementary tables 14-16, data obtained upon hybridization in UniHyb buffer on old slides, were not quantified due to low quality of data). The summarized results are given in table 9.1.

Table 9.1: Summarized results of investigation on effects of a hybridization buffer and slide aging.

Slides and hybridization buffers	Background level across the array		Hybridization signal value across the array		Signal-to-noise ratio value	
	Mean	Total	Mean	Total	Mean	Total
Old slide, SSPE-T buffer	2.9	61.1	1.0	22.0	2.2	47.2
New slide, SSPE-T buffer	0.5	12.5	0.3	7.6	3.5	80.7
New slide, UniHyb buffer	0.8	22.9	1.1	32.3	5.2	155.6

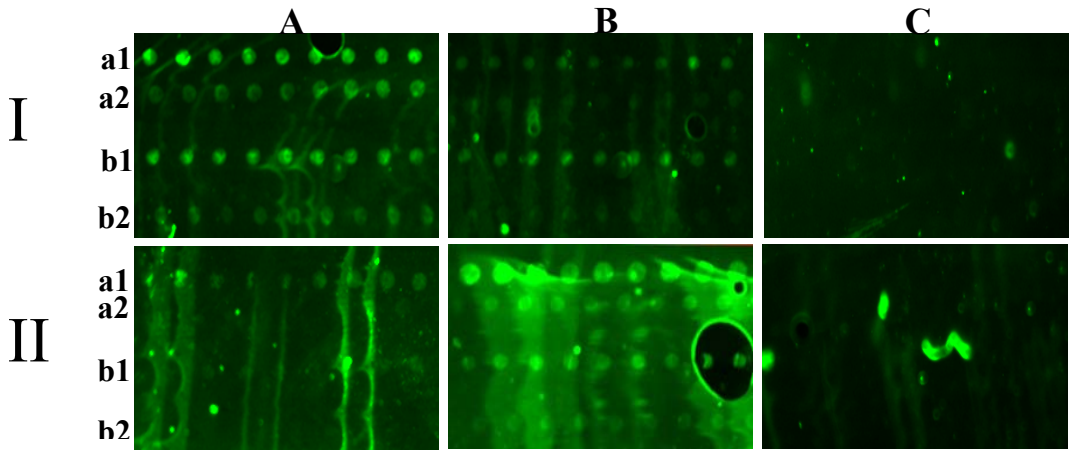

Figure 12. Effect of aging of silylated slides on hybridization. Fresh (I) and 4-month old (II) Telechem slides were used. Line 1: signals of spots of rRNA p15.111 probe (pefect match); line 2: signals of spots of rRNA p15.112 probe (single mismatch); lines a and b: spots prepared from 50 μM and 25 μM probe solution in 1xTelechem spotting solution.

Arrays of spotted 20-mers rRNA p15.111 (perfect match) and rRNA p15.112 (mismatch) were hybridized with FITC-labelled RNA in UniHyb (column A), SSPE-T (column B) or ACES 2.0 (column C) buffers. The results obtained showed superior performance of UniHyb buffer and the necessity of using freshly bought silylated slides.

Temperature. This was chosen based on melting temperature Tm for the oligonucleotide probes. In the case of 15-mers 42°C, which is 8-11°C lower than Tm for all probes of this length given in table 2, was chosen as an initial point in the optimization process. It was proved to be the optimal on comparison with 38°C and 46°C in different buffers mentioned above. All the hybridizations reported in this text in which 15-mers took part as one of hybridization counterparts were performed at 42°C. 56°C was chosen as an initial point for the same reasons and found to be the optimal for 20-mer probes.

Target concentration. All the oligonucleotide array hybridizations reported in this text were performed at concentrations of end-labelled PCR fragments as targets in the range 30-100 nM. *In vitro* labelled RNA was applied at a standard concentration of 75 nM. Total labelled RNA was used in the range of tens of nanograms. These values were generally comparable to those used in membrane macroarray hybridizations and allowed the obtaining of reliable hybridization signals within 1-3 hours of hybridization time under the conditions used (see below).

Volume. TeleChem's recommended hybridization volume of 2.5 µl per mm^2 of array surface was found to be optimal and thus all hybridizations reported in this text were performed under this condition. Lower volumes led to the drying of the hybridization mixture starting from the edges of cover slip. Higher volumes could lead to the displacement of cover slip from array location.

Time. The high DNA immobilization efficiency of silylated slides, 1-100 µM spotting concentration of oligonucleotide probes, and 30-100 nM concentration of targets in combination with optimized volume, temperature, and buffer, allowed the obtaining of reliable single nucleotide discrimination usually within 1-3 hours.

Washing conditions. TeleChem's recommended washing conditions were found to be the basis for a quick, simple and convenient procedure which led to reliable single nucleotide discrimination upon the use of 15-mer immobilized probes.

The results regarding other aspects of the oligonucleotide array hybridization are shown and explained in figures 13-17 and their legends (see below).

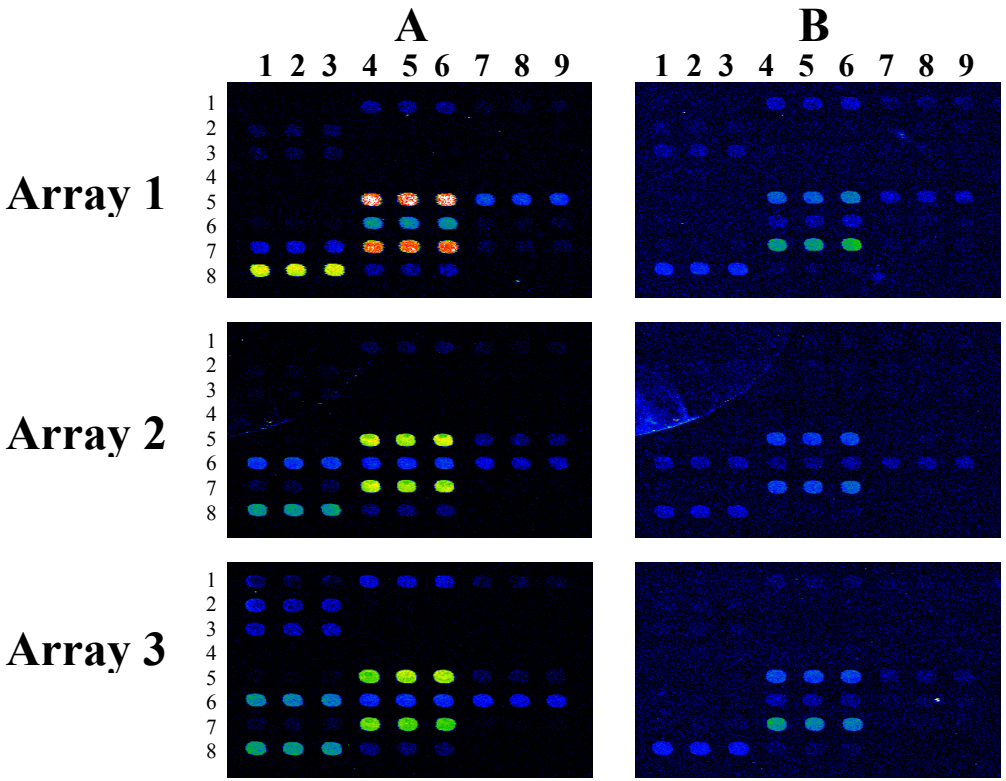

C

	1 2 3	4 5 6	7 8 9
1	rRNA p15.1.2.r	rRNA p15.8.1.r	rRNA p15.12.1.r
2	rRNA p15.1.3.r	rRNA p15.8.2.r	rRNA p15.3.1.r
3	rRNA p15.2.1.r	rRNA p15.13.1.r	rRNA p15.3.2.r
4	rRNA p15.2.2.r	rRNA p15.13.2.r	rRNA p15.3.3.r
5	rRNA p15.1.2	rRNA p15.8.1	rRNA p15.3.1
6	rRNA p15.1.3	rRNA p15.8.2	rRNA p15.3.2
7	rRNA p15.2.1	rRNA p15.9.1	rRNA p15.3.3
8	rRNA p15.2.2	rRNA p15.9.2	

D

A: laser power - 75%

PMT - 85%

B: laser power - 80%

PMT - 85%

Figure 13. Co-hybridizations of two double-stranded DNA target molecules of the same length with array of complementary oligonucleotide probes. 15-mer probes were spotted on silylated slides (Telechem) from 50 µM solutions in 3xSSC as indicated in C. The following hybridization targets were used (* designates Cy3-label at 5'-end of rRNA r2 primer and Cy5 label at 5'-end of rRNA f0 primer): array1: rRNA f0-r2*.7653 and rRNA f0*-r2.7653 PCR fragments hybridized separately at 100 µM final concentration each (A and B, respectively); array 2: rRNA f1-r2*.7653 and rRNA f0*-r2.9550 fragments hybridized in 1:1 mixture at 50 nM final concentration each; array 3: rRNA f0*-r2.7653 and rRNA f0-r2*.9550 fragments hybridized in 1:1 mixture at 50 nM final concentration each. The hybridizations were performed in 5 µl of UniHyb buffer at 42°C for 1 h. Column A and B: results obtained by scanning in the Cy3- and Cy5 channel respectively. Signal detection was performed at the scanning parameters given in panel D. Upon hybridization, the signals obtained from spots of oligonucleotides derived from antisense strand of 16S rRNA gene were much weaker than those derived from the sense strand. Both strands of the targets hybridized to the same DNA spots when single PCR fragment or a mixture of two PCR fragments were used as targets. In the latter case the complementary strands belonging to different PCR fragments used were detected (see hybridization to the probes rRNA p15.2.2, 8.1 and 9.1 (match probes for both targets)). Formed PCR fragment strand: oligonucleotide probe: complementary PCR fragment strand structures resulted in the same hybridization pattern for hybridizations where single PCR fragment was used as a target independently on the strand labelled (compare results on array 1 in both channels). This pattern was altered upon the use of this fragment in mixture with another one: specific signals were recorded at rRNA p15.1.3 probe (perfect match for both PCR fragments used) and rRNA p15. 3.2 probe (perfect match for rRNA f0-r2.9550 PCR fragment). The presence of both fragments could be detected independently on dye/fragment/strand combination but the pattern detected was different: in the case of array 2 the pattern obtained in Cy3 channel was sufficient; in the case of array 3 the overlay of patterns obtained in both channels was necessary.

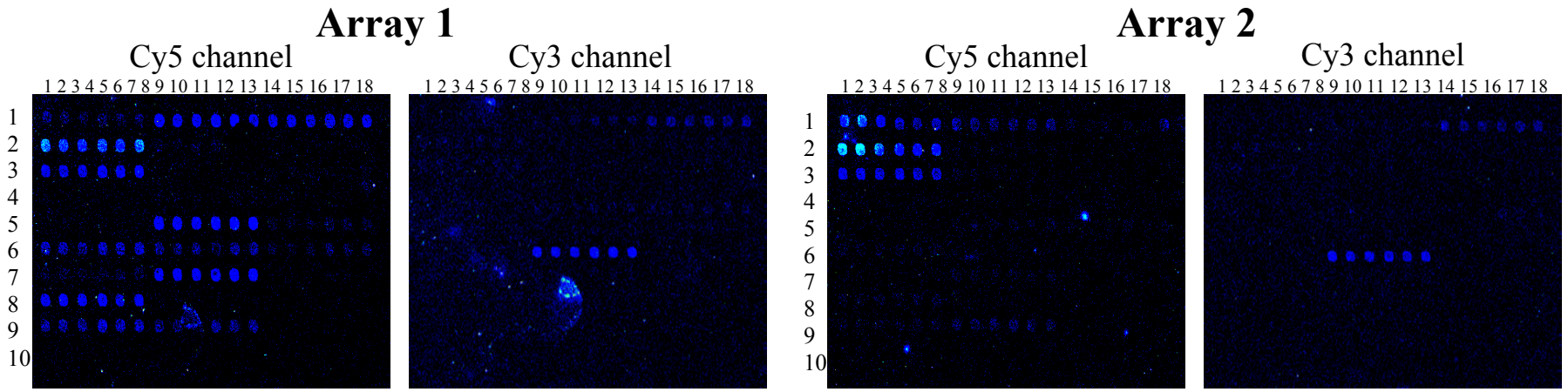

A

	50µM	150µM	50µM	150µM	50µM	150µM
	1 2 3	4 5 6	7 8 9	10 11 12	13 14 15	16 17 18
1	p15.1.2.R	p15.1.2.R	p15.8.1.R	p15.8.1.R	p15.12.1.R	p15.12.1.R
2	p15.1.3.R	p15.1.3.R	p15.8.2.R	p15.8.2.R	p15.3.1.R	p15.3.1.R
3	p15.2.1.R	p15.2.1.R	p15.13.1.R	p15.13.1.R	p15.3.2.R	p15.3.2.R
4	p15.2.2.R	p15.2.2.R	p15.13.2.R	p15.13.2.R	p15.3.3.R	p15.3.3.R
5	p15.1.2	p15.1.2	p15.8.1	p15.8.1	p15.3.1	p15.3.1
6	p15.1.3	p15.1.3	p15.8.2	p15.8.2	p15.3.2	p15.3.2
7	p15.2.1	p15.2.1	p15.9.1	p15.9.1	p15.3.3	p15.3.3
8	p15.2.2	p15.2.2	p15.9.2	p15.9.2		
9	p15.6.1	p15.6.1	p15.7.1	p15.7.1		
10	p15.6.2	p15.6.2	p15.7.4	p15.7.4		

B

Cy5 channel

laser power - 75%

PMT - 85%

Cy3 channel

laser power - 80%

PMT - 85%

Figure 14. Co-hybridizations of two double-stranded DNA target molecules of the different length of the same length with array of complementary oligonucleotide probes. 15-mer probes were spotted on silylated slides (Telechem) from 50 and 150 µM solutions in 3xSSC as indicated in table A and hybridized with the following fragments: rRNA f1-r2 fragment, which is a part of rRNA f0-rRNA r2 fragment (approximately 180 bp), rRNA f0-r1 fragment (approximately 550 bp long 3‘extension of rRNA f0-rRNA r2 fragment) and rRNA f0-r0 fragment (approximately 980 bp long 3‘extension of rRNA f0-r2 fragment) (see table 1). The mixtures of the short former fragment with each of the two long fragments were tested. Array 1: hybridization with the mixtures of rRNA f1-r2*.7653 and rRNA f0*-r1.9550; array 2: hybridization with the mixture of rRNA f1-r2*.7653 and rRNA f0*-r0.9550 (* designates the same labelling scheme as that one described in the legend for the figure 13). The hybridizations were performed at 42°C for 1 h in 5 µl of hybridization mix. The final concentration of the labelled PCR fragment was 100 nM; in the mixture a concentration of each of them accounted 50 nM. Signal detection was performed at the scanning parameters given in panel B. The use of longer targets resulted in increased hybridization signals from sense strand-derived probes rRNA p15.1.X.R and 2.X.R and decreased signals from antisense strand derived probes rRNA p15.1.X, 2.X, 8.X and 9.X when compared with the results shown in figure 15 (see below). The shortest target used, namely Cy3-labelled antisense strand of rRNA f1-rRNA r2 fragment, showed strong hybridization signal only to one sense strand-probe, namely rRNA 15.8.2. This is mismatch probe for the targets used and given result was in full disagreement with hybridization results shown in figure 15. In addition, the hybridization signals from spots of rRNA 15.12.1.R probe were characteristic for this target upon the use in a mixture with both long targets. The longest target (rRNA f0-r0 fragment) did not hybridized to probe sets rRNA p15.1.X, 2.X, 8.X and 9.X in contrast with rRNA f0-r2 and rRNA f0-r1 fragments.

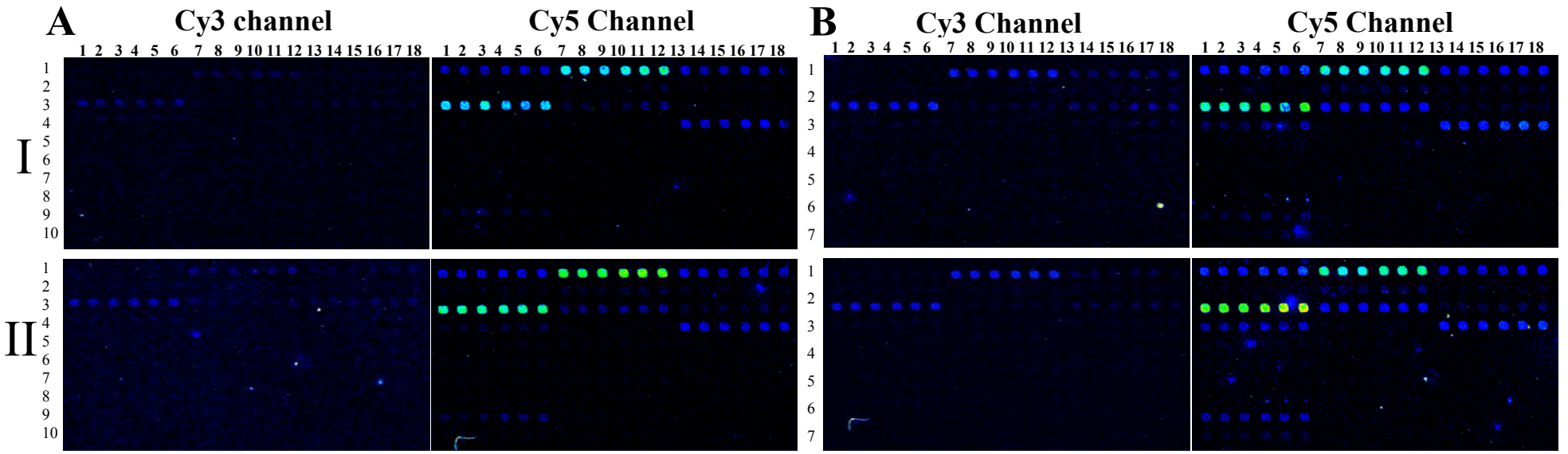

C

	50µM	150µM	50µM	150µM	50µM	150µM
	1 2 3	4 5 6	7 8 9	10 11 12	13 14 15	16 17 18
1	p15.1.2.R	p15.1.2.R	p15.8.1.R	p15.8.1.R	p15.12.1.R	p15.12.1.R
2	p15.1.3.R	p15.1.3.R	p15.8.2.R	p15.8.2.R	p15.3.1.R	p15.3.1.R
3	p15.2.1.R	p15.2.1.R	p15.13.1.R	p15.13.1.R	p15.3.2.R	p15.3.2.R
4	p15.2.2.R	p15.2.2.R	p15.13.2.R	p15.13.2.R	p15.3.3.R	p15.3.3.R
5	p15.1.2	p15.1.2	p15.8.1	p15.8.1	p15.3.1	p15.3.1
6	p15.1.3	p15.1.3	p15.8.2	p15.8.2	p15.3.2	p15.3.2
7	p15.2.1	p15.2.1	p15.9.1	p15.9.1	p15.3.3	p15.3.3
8	p15.2.2	p15.2.2	p15.9.2	p15.9.2		
9	p15.6.1	p15.6.1	p15.7.1	p15.7.1		
10	p15.6.2	p15.6.2	p15.7.4	p15.7.4		

D

Cy3 channel
laser power - 90%
PMT - 90%
Cy5 channel
laser power - 75%
PMT - 85%

Figure 15. Co-hybridization of two RNAs labelled by different dyes. Probes were spotted according to the pattern indicated in the table C. 50 and 150 µM: concentrations of oligonucleotide probes prepared in 3xSSC buffer and used for spotting. Total RNA of *A. madurae* 9585 was labelled by Cy3 and that of *S. hirsuta* 9709 by Cy5. They were used as intact (A) and after fragmentation to the average length of 100 bases (B). When used separately (Lane I) their concentrations were 50 ng/µl (~70 nM) and in the hybridizations of the mixtures (Lane II) they were 25 ng/µl (~35 nM) each. Arrays were hybridized at 42°C for 3 h in 3 µl of UniHyb buffer. Signal detection was performed at the scanning parameters given in panel D. No significant differences between hybridization patterns of both forms of RNA obtained at competitive and non-competitive hybridization conditions were observed. Higher hybridization efficiency of fragmented target molecules was obtained at both conditions when compared with the intact RNA targets. Hybridization to the antisense strand probes was highly reduced with an exception for rRNA p15.6.1 probe which represents full match to the sense strand of 16S rDNA of both organisms. The differential hybridization occurred at rRNA p15.3.X.R probe set in both competitive and non-competitive hybridization. This allowed to recognize the targets participating in the hybridization reaction: *A. madurae*‘s RNA hybridized to rRNA p15.3.2.R probe and *S. hirsuta*‘s RNA did to rRNA p15.3.3.R probe. Given pairs of probes and targets represent perfect complements.

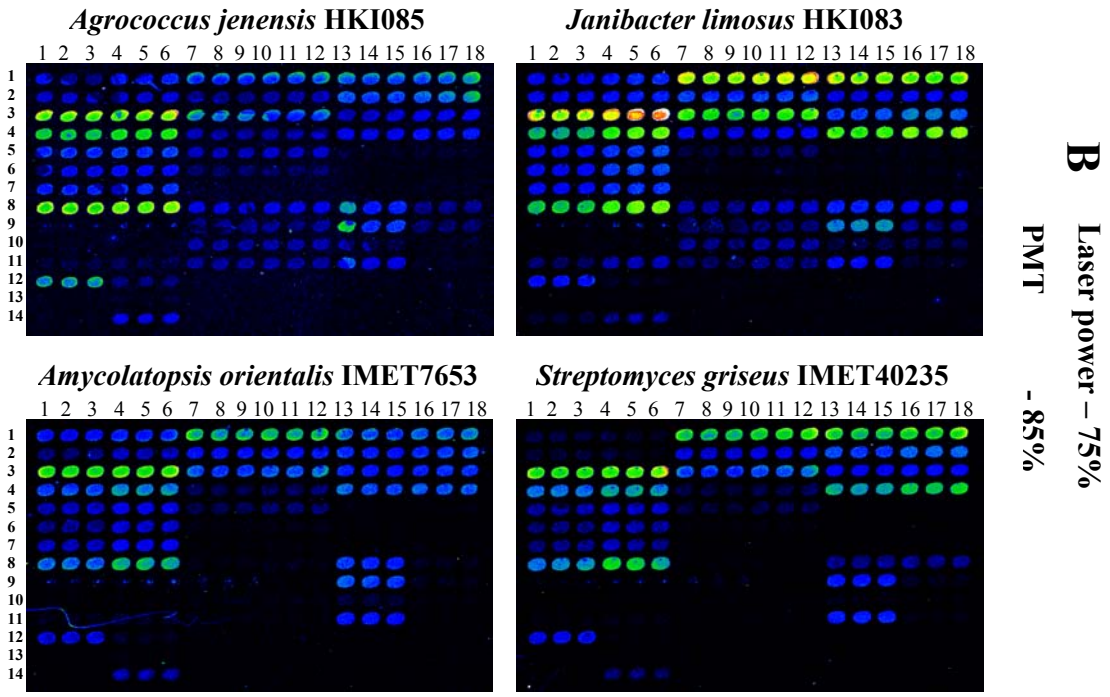

A

	50 µM	200 µM	50 µM	200 µM	50 µM	200 µM
	1 2 3	4 5 6	7 8 9	10 11 12	13 14 15	16 17 18
1	rRNAp15.1.2.r	rRNAp15.1.2.r	rRNAp15.8.1.r	rRNAp15.8.1.r	rRNAp15.12.1.r	rRNAp15.12.1.r
2	rRNAp15.1.3.r	rRNAp15.1.3.r	rRNAp15.8.2.r	rRNAp15.8.2.r	rRNAp15.3.1r	rRNAp15.3.1r
3	rRNAp15.2.1.r	rRNAp15.2.1.r	rRNAp15.13.1.r	rRNAp15.13.1.r	rRNAp15.3.2.r	rRNAp15.3.2.r
4	rRNAp15.2.2.r	rRNAp15.2.2.r	rRNAp15.13.2.r	rRNAp15.13.2.r	rRNAp15.3.3.r	rRNAp15.3.3.r
5	rRNAp15.1.2	rRNAp15.1.2	rRNAp15.8.1	rRNAp15.8.1	rRNAp15.3.1	rRNAp15.3.1
6	rRNAp15.1.3	rRNAp15.1.3	rRNAp15.8.2	rRNAp15.8.2	rRNAp15.3.2	rRNAp15.3.2
7	rRNAp15.1.1	rRNAp15.1.1	rRNAp15.8.3	rRNAp15.8.3	rRNAp15.3.3	rRNAp15.3.3
8	rRNAp15.1.4	rRNAp15.1.4	rRNAp15.9.1	rRNAp15.9.1	rRNAp15.6.1	rRNAp15.6.1
9	rRNAp15.2.1	rRNAp15.2.1	rRNAp15.9.2	rRNAp15.9.2	rRNAp15.6.2	rRNAp15.6.2
10	rRNAp15.2.2	rRNAp15.2.2	rRNAp15.9.3	rRNAp15.9.3	rRNAp15.6.3	rRNAp15.6.3
11	rRNAp15.2.3	rRNAp15.2.3	rRNAp15.9.4	rRNAp15.9.4	rRNAp15.6.4	rRNAp15.6.4
12	rRNAp2.1,100µM	rRNA1.1,100µM				
13	rRNAp2.2,100µM	rRNA2.1,100µM				
14	rRNAp2.3,100µM	rRNA3.1,100µM				

Figure 16. The use of total RNA as a target for the hybridization to oligonucleotide arrays. Oligonucleotide probes and primers were spotted according to the pattern given in table A. 50,100 and 200µM: concentrations of probe spotting samples in TeleChem spotting buffer. Signal detection was performed at the scanning parameters given in panel B.

The total RNAs were isolated from the cells of strains indicated in figure 16, fragmented to the average length of 100 bp, labelled to the average density of one Cy5 molecule per 65 bases of RNA and hybridized at 42°C for 1 h in UniHyb buffer at concentrations 10 ng/µl to array of 15-mer probes derived from both strands of 16S rDNA. Figure 16 and supplementary tables 17-20 show the results of hybridizations between Cy5 fragmented total RNA and immobilized oligonucleotides. The hybridization patterns characteristic for each RNA target were consistently obtained, which allowed performing their differentiation. In regard to probes derived from the antisense strand, significantly higher hybridization signals were obtained from perfect match probes in every case, except the hybridization of *Amycolatopsis orientalis* IMET7653's RNA target to rRNA p15.2.X.R probe set (compare figure 16 and table 10.1 for all antisense-strand derived probes except rRNA p15.12.1.R).

Table 10.1. Sequences of the oligonucleotide probes derived from antisense strand of 16S rDNA and used in array shown in figure 16, as well as corresponding regions of 16S rRNA of the strains under investigation.
The interrogated signature positions are designated as bold, lower-case and by different colours compared with sequence group; additional mismatches are designated as bold, lower-case and by the same colour as used for sequence group. For convenience of comparison, the complementary antisense strand of 16S rRNA is presented.

Probes and strains	Sequence (antisense strand, 5‘-3‘ direction)
rRNA p15.1.2.R	CCAGAGT **g** CAGGGCA
rRNA p15.1.3.R	CCAGAGT **a** CAGGGCA
Agrococcus jenensis HKI085	CCAGAGT **c** **a**AGGGCA
Janibacter limosus HKI083	CCAGAGT **c** **t**GGGGCA
Amycolatopsis orientalis IMET7653	CCAGAGT **g** CAGGGCA
Streptomyces griseus IMET40235	CCAGAGT **g** **a**AGGGCA
rRNA p15.2.1.R	CGTCG **a** CGCCTTGGT
rRNA p15.2.2.R	CGTCG **t** CGCCTTGGT
Agrococcus jenensis HKI085	CGTCG **a** CGCCTTGGT
Janibacter limosus HKI083	CGTCG **a** CGCCTTGGT
Amycolatopsis orientalis IMET7653	CGTCG **a** CGCCTTGGT
Streptomyces griseus IMET40235	CGTCG **a** CGCCTTGGT
rRNA p15.3.1.R	CAGGCTT **g** CGCCCAT
rRNA p15.3.2.R	CAGGCTT **c** CGCCCAT
rRNA p15.3.3.R	CAGGCTT **t** CGCCCAT
Agrococcus jenensis HKI085	CAGGCTT **g** CGCCCAT
Janibacter limosus HKI083	CAGGCTT **t** CGCCCAT
Amycolatopsis orientalis IMET7653	CAGGCTT **g** CGCCCAT
Streptomyces griseus IMET40235	CAGGCTT **t** CGCCCAT
rRNA p15.8.1.R	GGCCGT **g** TCTCAGTC
rRNA p15.8.2.R	GGCCGT **a** TCTCAGTC
Agrococcus jenensis HKI085	GGCCGT **g** TCTCAGTC
Janibacter limosus HKI083	GGCCGT **g** TCTCAGTC
Amycolatopsis orientalis IMET7653	GGCCGT **g** TCTCAGTC
Streptomyces griseus IMET40235	GGCCGT **g** TCTCAGTC
rRNA p15.13.1.R	CACGTAGTT **t** GCCGG
rRNA p15.13.2.R	CACGTAGTT **g** GCCGG
Agrococcus jenensis HKI085	CACGTAGTT **t** GCCGG
Janibacter limosus HKI083	CACGTAGTT **t** GCCGG
Amycolatopsis orientalis IMET7653	CACGTAGTT **t** GCCGG
Streptomyces griseus IMET40235	CACGTAGTT **t** GCCGG

Prominent results concerned the hybridization patterns obtained by the rRNAp15.1.X.r probe set. Only *Amycolatopsis orientalis* IMET7653’s RNA, which is the only one that represents a perfect

complement to one of the probes, rRNAp15.1.2.r, gave a respective discriminatory pattern. Other tree RNAs showed both hampered signals and non-detectable discrimination, due to the presence of mismatches at signature position and neighbouring ones.

The results regarding the hybridizations of arrays composed of aminomodified PCR fragments spotted on silylated slides were as follows:

Hybridization with labelled oligonucleotides as targets. The typical experiment and its results are shown in figure 17. The arrays of rRNAfo-r2 fragments of 13 test strains were spotted from 3 µM solutions in triplicate and iteratively hybridized with rRNA 1.3 (twice, columns A and C) and rRNA 1.1 (column B) 5'-end Cy5-labelled oligonucleotides at 42°C in UniHyb buffer for 0.5 (Lane I) and 1.5 (Lane II) hours.

Table 11.1. Sequences of the oligonucleotide targets rRNA 1.1 and rRNA 1.3 and corresponding region of 16S rDNA of the strains under investigation. The interrogated signature positions are designated as red-coloured upper-case; additional mismatches with target sequences are designated as red-coloured lower-case.

Targets and strains	Sequence (sense strand, 5'-3' direction)
rRNA 1.1	T G C C C T G G A C T C T G G
rRNA 1.3	T G C C C T G T A C T C T G G
A. mediolanus HKI108	T c C C C T G G A C T C T G G
A. madurae IMET9585	T G C C C c t G A C T C T G G
A. jenensis HKI085	T G C C C T t G A C T C T G G
A. orientalis IMET7653	T G C C C T G C A C T C T G G
B. caseilytica HKI088	T G C C C c t G A C T t c G G
D. terragena HKI089	T G t C C T t G A C T C T G G
G. amarae IMET7518	T G C C C c t G A C T t T G G
J. limosus HKI083	T G C C C c a G A C T C T G G
N. albus IMET7807	T G C C C T t C A C T C T G G
N. dassonvilei IMET9605	T G C C C c t G A C T C T G G
S. griseus IMET40235	T G C C C T t C A C T C T G G
S. hirsuta IMET9709	T G C C C T G C A C T C T G G
S. viridis IMET9550	T G C C C T G T A C T C T G G

The hybridization pattern of the first hybridization showed an overall decrease in signal strength upon the extension of hybridization time from 0.5 h to 1.5 h. The PCR fragments obtained from *B. caseilytica* HKI088, *G. amarae* IMET7518 and *D. terragena* HKI089 did not show any hybridization signal after the first hybridization, due to several mismatches (3-5) of their sequences to the sequence of rRNA 1.3 (table 11.1). Signals from *S. viridis* IMET 9550 (perfectly matched fragment) gave the highest signal after 0.5 h hybridization and became

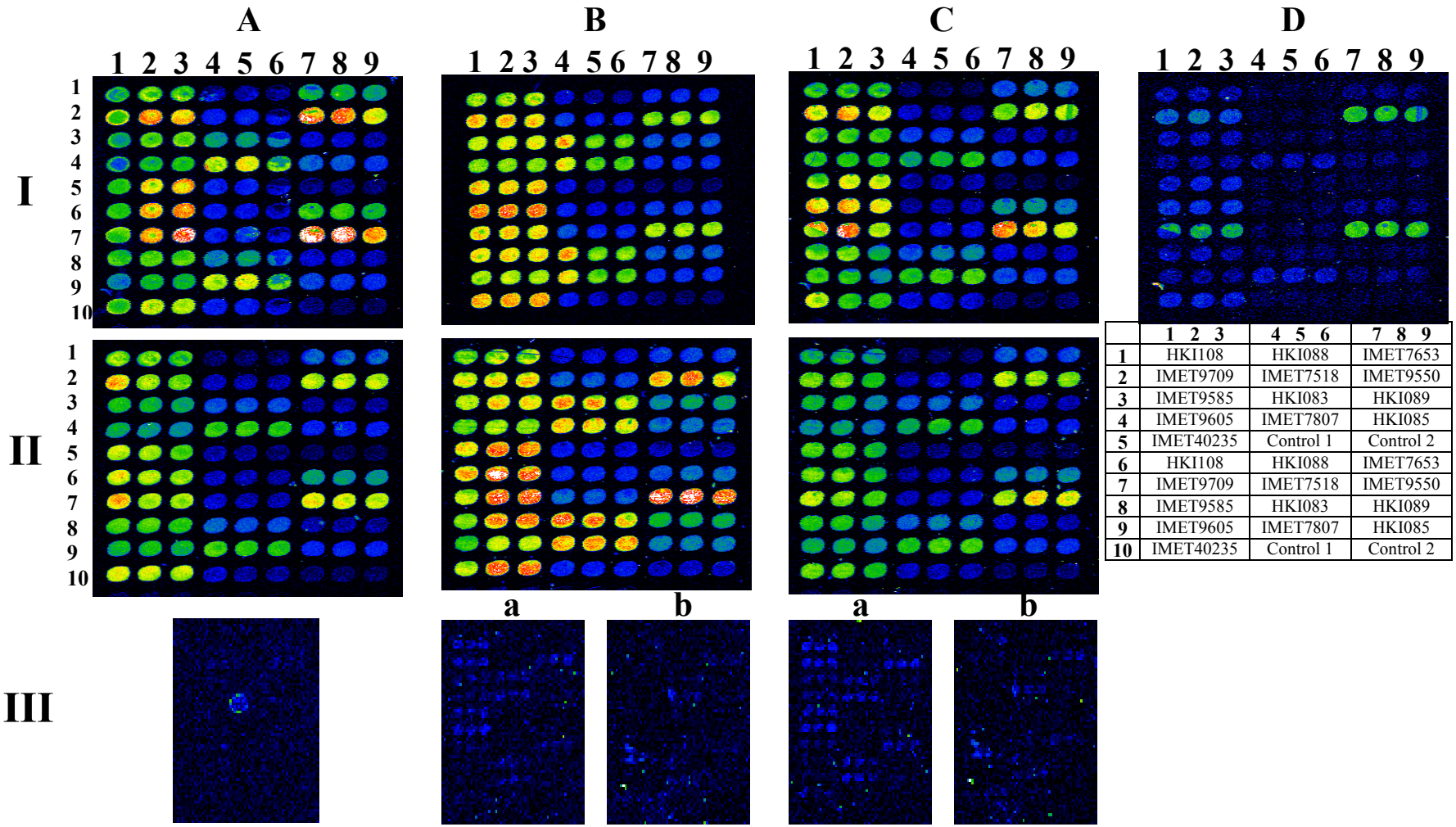

	1 2 3	4 5 6	7 8 9
1	HKI108	HKI088	IMET7653
2	IMET9709	IMET7518	IMET9550
3	IMET9585	HKI083	HKI089
4	IMET9605	IMET7807	HKI085
5	IMET40235	Control 1	Control 2
6	HKI108	HKI088	IMET7653
7	IMET9709	IMET7518	IMET9550
8	IMET9585	HKI083	HKI089
9	IMET9605	IMET7807	HKI085
10	IMET40235	Control 1	Control 2

Figure 17. Iterative hybridization of array of rRNA f0-r2 PCR fragments of 13 *Actinomycetales* strains with Cy5-end labelled oligonucleotides rRNA 1.1 and rRNA 1.3. Spots were made from 3 µM solution in 1xTelechem spotting solution according to the pattern shown in the table. Control 1: *S.cerevisiae* 1.1 kb genomic fragment amplified with the use of primers rRNA f0 and rRNA r2; control 2: rRNA f1-r2.9550 PCR fragment. A detailed experimental description is given in the text.

comparable to the signals from a broad range of fragments after 1.5 h hybridization: for example, those of *S. griseus* IMET40235 (T/G signature mismatch plus additional adjacent G/A mismatch (at this point and later in text, mismatched bases are given for target oligonucleotide sequence/complementary strand of the PCR fragment)) and *S. hirsuta* IMET 9709 (T/G signature mismatch). After successful array stripping (Lane III), its re-hybridization was made with the Cy5-end labelled rRNA 1.1 oligonucleotide (column B), which had no perfect complement among the spotted fragments but, in turn, the majority of them carried matched base at the centrally located signature position (table 11.1). The results showed striking differences to those of preceding hybridization. Firstly, the overall kinetics gave a reversed picture, where signals from all spots increased upon time extension, including the background signals from negative control spots; in this way *S. viridis* IMET 9550 spots again showed the highest signals over the array, despite G/A signature mismatch, but this time after 1.5 h hybridization. Secondly, most prominent differences concerned the highly increased signals for *D. terragena* HKI089 and *J. limosus* HKI083 compared with the results of the first hybridization. Both belong to the group of matched signatures with rRNA 1.1 but nevertheless have one and two additional mismatches adjacent to signature position respectively. Regarding the fragments with decreased signals after the second hybridization, those of *A. orientalis* IMET7653 have to be mentioned; this fragment had just one mismatched base to either of the target oligonucleotides used: G/T in case of rRNA 1.3 and G/G in case of rRNA 1.1. After successful stripping of the array, which had to be performed twice this time (Lane III, column B, a, b), and re-hybridization with rRNA 1.3 oligonucleotide, the same pattern to the one observed after the first hybridization was obtained (I C, II C). Washing at the higher stringency conditions (1xSSC, 0.2%SDS at 37°C for 30 min; 1xSSC for 5 min with shaking at 180 rpm) resulted in strong specific signals from the spots of *S. viridis* IMET9550 PCR fragments. Signals from all other spots except those of *S. hirsuta* IMET9709 were reduced to the level of background (Lane I, D).

Thus, the results obtained within the experimental set-up of spotted PCR fragments hybridized with end-labelled oligonucleotides led to the following conclusions:

- different hybridization kinetics of perfect match/mismatch sequences compared with those obtained with the reversed format of spotted oligonucleotides hybridized with PCR fragments; in this case it was impossible to achieve reliable discrimination between related sequences within the time used for oligonucleotide hybridizations, unless the case of probes with at least three mismatched bases or the use of much stronger washing conditions;
- the arrays could be successfully stripped and re-hybridized with the same or different target oligonucleotides.

The optimized experimental microarray formats for single nucleotide differences detection within domain I of bacterial 16S rRNA are summarized in the following table

Solid support	Microscopic glass
Activation coating	Aldehyde groups, with innert fluorescence in Cy3 channel of at least 2000 units
Probes	1. 15-mer oligonucleotides 2. PCR fragments
Probe modifications	1. aminolink for both oligonucleotides and PCR fragments 2. 15-dT spacer for oligonucleotides
Probe concentrations	1. 50 μM for oligonucleotides 2. 1-3 μM for PCR fragments
Spotting solution	TeleChem spotting solution or 3xSSC
Targets	1. end-labelled PCR fragments or fragmented total RNA labelled by dye chemical coupling for oligonucleotide arrays 2. end-labelled 15-mer oligonucleotides
Target concentrations	1. 30-100 nM for PCR fragments or 5-25 ng for total RNA 2. 10-100 nM for oligonucleotides
Hybridization buffer	UniHyb from TeleChem
Hybridization temperature	Average value from Tm-10°C differences for all oligonucleotides present on array
Hybridization time	1-3 hours
Washing conditions	1. Recommended by TeleChem for oligonucleotide arrays 2. Temperature increased to 37°C and time increased to 30 min for wash I with detergent; wash II at stronger stirring or shaking

The results obtained upon the optimization of arrays composed of unmodified PCR fragments spotted on polylysine slides were used for differential gene expression monitoring:

A shotgun genomic library of *Saccharopolyspora erythraea* DSM 40512 (erythromycin producer) was made by S. Kushnir. Frequently cutting endonuclease *Bsp*1431 was used to obtain as a major fraction genomic fragments of the average length of 0.5 – 1.0 kb. *Bam*HI-digested pUC 118 was used as a cloning vector. The library was prepared in *E.coli* TOP10 cells. Another set of fragments used for investigation represented gene coding sequences sub-cloned from *S. erythraea ery* cluster (erythromycin biosynthesis). DNA was kindly provided by C.R. Hutchinson (University of Wisconsin, Madison, USA). The sub-cloning was performed into the same site of pUC118. Approximately 3820 clones of constructed library were amplified from vector primers (M13/pUC 24-mer sequencing primer and reverse sequencing primer), purified and immobilized on polylysine-activated Borofloat 33 slides. A fraction of them, 240 clones, were additionally spotted and immobilized on nylon membranes. The aims were, firstly, to generally show a proof-of-principle of the use of shotgun library of high G+C content coding sequences for genome-wide expression

monitoring in microarray format, and secondly, in case of a positive outcome at the preliminary stage above, to monitor growth dynamics, erythromycin production and gene expression patterns of *S. erythraea* DSM 40512 cells grown at varying conditions, in order to elucidate possible regulatory mechanisms responsible for coupling of vegetative growth and antibiotic production of this producer. After a series of manipulations with growth media content, the choice was made for SSM (semi-synthetic medium) and modified minimal Czapek media (see Materials), as these supposed to assure a growth rate shift with concomitant onset of antibiotic production. The aforementioned parameters for cells grown in rich M79 and both minimal media were monitored and compared. Membrane arrays were used at the preliminary stage. The total cellular RNA from both types of cells was isolated, radioactively labelled through reverse transcription into cDNA in a presence of [^{32}P]-dATP, and hybridized to two membranes. The preliminary results obtained were evaluated as positive in regard to observed specificity of hybridization, as there were spots found with significantly different hybridization signals within roughly equally distributed total signals over both membranes and, in particular, between positive control spots of 16S rDNA and gyrase B. Thus, gene expression was next monitored with the use of middle-density arrays, prepared on glass and cyanine dyes as labels. For the first hybridization Cy3- and Cy5 labelled cDNAs were prepared from RNA, isolated from bacteria grown in rich and minimal Czapek medium respectively. For the second hybridization a swapped labelling scheme was used. The raw hybridization pictures obtained in experiment 1 are shown in supplementary figures 18 and 19 (page 177 and 178). The evaluation of the data was performed as described in Methods. The resultant data concerning the amount of cDNA applied, its labelling efficiency, overall hybridization results, and the effects of normalization procedure, are given in Tables 12.1 and 13.1. In experiments 1 and 2, 42 and 100 spots respectively could not be evaluated, due to non-uniform high background areas covering those spots completely or partially, or residing in their immediate vicinity. The numbers of array spots where differential gene expression was detected are listed in table 14.1.

Table 12.1. Amount of cDNA, labelling efficiency and numbers of clones with undetectable specific hybridization signals.

No.	Labelling scheme		Labelling efficiency		cDNA amount used for hybridization [µg]		No. of clones which showed no specific hybridization signals (within one standard deviation of background signal)		
	Cy3	Cy5	Cy3 incorporation	Cy5 incorporation	Cy3 labelled	Cy5 labelled	Hybridization of Cy3-labelled cDNA	Hybridization of Cy5-labelled cDNA	Common clones
1	Rich medium	Semi-synthetic medium	4.0	2.9	6.4	7.3	253	349	182
2	Semi-synthetic medium	Rich medium	3.8	2.3	6.0	6.0	661	1037	549

Table 13.1. Background and hybridization signals, signal-to-noise ratios and effects of normalization.

No	cDNA hybridized	Background level			Background corrected overall hybridization signals		Overall signal-to-noise ratios			Normalized hybridization signals		
		Mean	SD	Total	Mean	Total	Mean	SD	Total	Mean	SD	Total
1	Cy3 labelled	8.0×10^{-4}	4.9×10^{-4}	3.00	2.6×10^{-4}	0.98	1.02	1.75	3813.1	1.15	2.00	4319.3
	Cy5 labelled	8.4×10^{-4}	4.9×10^{-4}	3.17	3.1×10^{-4}	1.19	1.97	3.29	7383.4	1.12	1.88	4206.1
2	Cy3 labelled	4.8×10^{-4}	2.7×10^{-4}	1.82	2.9×10^{-4}	1.11	0.99	2.43	3698.2	1.11	3.20	4173.7
	Cy5 labelled	5.9×10^{-4}	3.4×10^{-4}	2.23	3.0×10^{-4}	1.14	1.05	2.66	3970.7	1.19	3.20	4508.1

Table 14.1. Clones which showed differential gene expression surpassing applied threshold values: difference scores 1.0; 3.0; 9.0; ratio scores 1.5, 3.0; 4.5; distribution scores 1.0; 2.0; 4.0.

No.	Amounts of clones detected in the given elemental displays (potencial hits)					
	Difference scores	Ratio scores	Distribution scores	Combined		
				total	Up-regulated in M79 medium	Up-regulated in Czapek medium
1	149	1272	266	134	82	52
2	400	1658	128	116	87	29

When applied to the signals from experiment 2, the distribution scores resulted in a 3-fold decrease of the number of potential hits; in the case of experiment 1, where an almost 3 times lower number of potential hits from the difference elemental display was obtained, the same procedure resulted in twice as many, when compared with experiment 2. The results of the statistical segmentation of data was straightforward: in the combined displays there were almost the same amounts of potential hits. Their average value accounted for 3.3% of the total amount of library clones present on the array. Moreover, the given equalization also affected the amount of the genome entities which were expressed at higher levels in rich medium. This was not the case in regard to those whose transcription rate was higher in semi-synthetic medium: their number in experiment 1 was 2 times higher than in experiment 2. But as a general result, higher numbers of clones with up-regulation in rich medium were noted: in the experiment 1 they constituted 61% of the selected potential hits, and in the experiment 2 this value accounted for 75%.

Four artifacts concerning the hybridization results of the control array elements should be mentioned. Firstly, in the experiment 1 the spot of pBlueScript KS+ showed the signal ratio 0.067 (15-fold difference) and the difference magnitude –1.81; these values were sufficient for the element to be selected into the summary elemental display (see below). Secondly, the spot of *N. tobaccum* chelatase D fragment DNA (one of negative controls used) showed very high signal-to-noise ratios and absolute intensity values compared with the majority of array elements: 2.88 (Cy3)

and 7.92 (Cy5), 2.99 (Cy3) and 3.80 (Cy5), in experiments 1 and 2 respectively. Thirdly, four 16S rDNA spots (1:5 dilution steps) showed consistent, approximately 2 fold, over-expression in the M79 medium, in comparison with the semi-synthetic one in experiment 1 over dilution range; the results of experiment 2 showed the same hybridization pattern in these spots, indicating a significantly (1.5-fold) higher level of expression in semi-synthetic medium, thus showing dye-impacted bias in hybridization data. The last, most pronounced, result concerned one of the mock hybridizations (spot location: row 30, column 57), where a consistent pattern of the relative fluorescence signal intensities across two hybridization experiments was obtained and the resulting values surpassed the threshold values for the hits selection (see above).

1.2.4 Final hit selection and reliability

The results of final hit selection are shown in table 15.1. A number of 33 differentially expressed elements were selected. This consisted of 16 elements which surpassed the stringent selection conditions (table 14.1) and additional 17 elements which passed less stringent ones (table 15.1). These additional 17 elements were 2, 7, 9, 10, 13, 14, 15, 16, 17, 18, 19, 24, 25, 29, 30, 32, 33. The basis for the hit selection at less strict conditions were statistically relevant results in one of the experiments reflected in the high magnitude values of ratio and/or difference scores, the latter being less prone to the measurement and analysis uncertainties. In this way the threshold values above were lowered, distribution scores were excluded from analysis, and resulting combined elementary displays were overlaid with the corresponding displays of the second experiment made under original thresholds. Plasmid clones corresponding to all the differentially expressed elements found were fully sequenced and checked *in silico* for sequence identities. Fragments longer than 700 bp were sequenced from both sides. Two more artifacts were observed: clones 25 and 28 had no inserts. The other 31 contained inserts ranging between approximately 100 and 2500 bp. 53%, i.e. 17 clones, showed fragments within the range 500-1000 bp, which in fact the main fraction of fragments had to lie within. The inserts of 13 clones (41%), the lengths of which were greater than 800 bp, contained sequences of different ORFs.

The reliability of the hit selection above, as well as another parameter allowing an approximate evaluation of sensitivity of the described approach, namely the *S. erythraea* DSM 40512 genome representation on the array, could be primarily accessed based on the results obtained from spots carrying DNA fragments of the same genes. A double representation of three ORFs was found: elements 1 and 6 carried the sequence of putative deoR family transcription regulator of *S. coelicolor* A3(2); elements 9 and 33 - sugar transporter homolog ydjK of *Bacillus subtilis*; elements 15 and 29 - putative NLP/P60-family secreted protein of *S. coelicolor* A3(2). These findings demonstrated a plausibility of the obtained results regarding the technological aspects, given that

the transcriptional changes recorded were concordant within each pair of elements. If it is supposed that this ratio of uniquely represented fragments holds for the whole array (85%, 28 out of 33), then given that the average size of the shotgun library inserts spotted was 750 bp, and that the approximate size of the *S. erythrea* genome is estimated to be 8 Mb, approximately 2.85 Mb coverage, or 36% genome representation on the array, was achieved.

Table 22: Final list of hits which passed lower stringency threshold values: ratio scores >=1.25, difference scores >=0.845.

No.	Hybridization signal comparison				Sequence analysis			
	Exp. No. 1		Exp. No. 2		Length of cloned fragment	Positions of different ORF sequences within cloned fragments	BLAST identity	Accession number
	ratio	Δ	ratio	Δ	Base pairs	proximity to the sequencing primers		
1	2.99	8.64	0.11	-26.45	800		Putative deoR family transcription regulator [*S. coelicolor* A3(2)]	AL355832
2	0.15	-4.16	1.43	4.22	1200	Universal	Hypothetical protein SCJ12.32 [*S. coelicolor* A3(2)]	AL109989
						Reverse	3-oxoacyl-[acyl-carrier-protein] synthase II [*Aquifex aeolyticus*]	AE000752
3	3.35	2.76	0.036	-112.87	1200	Universal	GTP binding protein (*Chlamydophila pneumonia*) (*Mycobacterium leprae*)	AB035954 AL049491
						Reverse	Transcription regulator related to AraC family (*Salmonella enterica*)	AF026270
4	1.71	1.87	0.15	-4.75	1500		Putative bi-domain oxidoreductase [*S. coelicolor* A3(2)]	AL121855
5	2.93	6.75	0.12	-28.91	2000		SanE gene, nikkomycin biosynthesis [*S. ansochromodenes*]	AF228524
6	2.49	2.37	0.44	-4.52	1200	Universal	Putative deoR family transcription regulator [*S. coelicolor* A3(2)]	AL355832
						Reverse	unknown	
7	2.56	0.91	0.00	-1.03	900	Universal	Glutamine synthetase [*Frankia sp*. ACN14a]	AF121818
						Reverse	Iron-sulfur protein (qcrA) [*S. antibioticus* Rieske]	AF184600
8	3.04	1.41	0.10	-6.29	700		Polyketide synthase [*S. coelicolor* A3(2)]	AL138668
9	2.12	14.19	1.13	0.29	118		Sugar transporter homolog ydjK [*Bacillus subtilis*]	AB007638
10	1.77	0.85	0.06	-6.36	1200	Universal	Chitinase precursor [*S. thermoviolaceus*]	D14536
						Reverse	Unknown	
11	2.71	9.05	0.07	-65.22	700		Unknown	
12	1.80	3.49	0.46	-4.08	1300	Universal	Ectoine synthase [*Vibrio cholerae*]	AE004410

No.	Hybridization signal comparison				Sequence analysis			
	Exp. No. 1		Exp. No. 2		Length of cloned fragment	Positions of different ORF sequences within cloned fragments	BLAST identity	Accession number
	ratio	Δ	ratio	Δ	Base pairs	proximity to the sequencing primers		
						Reverse	Trehalose-6-phosphate phosphatase [*E.coli* K12 MG1655]	AE000283
13	0.62	-1.62	1.99	4.69	500		Unknown	
14	0.60	3.11	2.50	9.76	1500	Universal	Glycine cleavage system protein P2 [*Pseudomonas aeruginosa*]	AE004672
						Reverse	Putative transmembrane transport protein [*S. coelicolor* A3(2)]	AL132644
15	0.74	-3.33	4.31	25.33	500		Putative NLP/P60-family secreted protein [*S. coelicolor* A3(2)]	AL391406
16	0.79	-2.36	6.27	38.37	107		Unknown	
17	0.62	-1.96	5.16	15.24	500		Phenylacetyl-CoA-ligase [*Pseudomonas sp.*]	AJ000330
18	0.63	-2.62	4.89	18.48	1600		Putative oxidoreductase [*S. coelicolor* A3(2)]	AL353872
19	0.61	-1.69	2.14	10.94	1000		Homolog to *S. erythraea* beta-ketoacyl synthase [*S. coriofaciens*]	L20249
20	0.80	-2.31	10.74	4.21	800		Unknown	
21	0.30	-8.51	-3.65	40.60	1700	Universal	Putative transcriptional regulator [*S. coelicolor* A3(2)]	AL031031
						Reverse	Putative arabinosyl transferase [*Mycobacterium smegmatis*]	U46844
22	0.45	-2.44	3.11	4.34	2500	Universal	unknown	
						Reverse	Probable integral membrane transport protein [*S. coelicolor* A3(2)]	AL096811
23	0.60	-2.34	2.030	4.86	2500		Putative secreted protein [*S. coelicolor* A3(2)]	AL159178
24	0.57	-5.55	4.113	11.49	no insert			
25	0.50	-2.01	1.46	2.53	900	Universal	NADH dehydrogenase sub-unit [*S. coelicolor* A3(2)]	AL078618
						Reverse	Hypothetical protein [*Chlamydia muridarum*]	AE002280
26	0.39	-2.24	4.18	2.532	180		Hypothetical protein SCL2.32 [*S. coelicolor* A3(2)]	AL137778
27	0.17	-12.72	8.18	3.724	no insert			
28	0.43	-2.750	3.18	17.80	600		Hydroxylacyl-coA dehydrogenase [*S. coelicolor* A3(2)]	X62373
29	0.52	-1.665	1.13	3.71	700		Putative NLP/P60-family secreted protein [*S. coelicolor* A3(2)]	AL391406
30	1.38	1.354	0.45	-5.762	900		ATPase component of putative ABC transporter [*S. roseofulvus*]	AF058302

No.	Hybridization signal comparison				Sequence analysis			
	Exp. No. 1		Exp. No. 2		Length of cloned fragment	Positions of different ORF sequences within cloned fragments	BLAST identity	Accession number
	ratio	Δ	ratio	Δ	Base pairs	proximity to the sequencing primers		
31	0.32	-1.790	3.99	3.59	800	Universal	Conserved hypothetical protein [*S. coelicolor* A3(2)]	AL391515
						Reverse	Hypothetical protein SCF51A.19 [*S. coelicolor* A3(2)]	AL121596
32	0.64	-1.35	4.61	4.32	800	Universal	Glycolate oxidase sub-unit GLcD [*Synechocystis sp.*]	D64001
						Reverse	*Rhodobacter spheroides* ORF277 gene, partial cds	U35443
33	1.73	1.11	0.61	-3.79	800	Universal	unknown	
						Reverse	Sugar transporter homolog ydjK [*Bacillus subtilis*]	AB007638

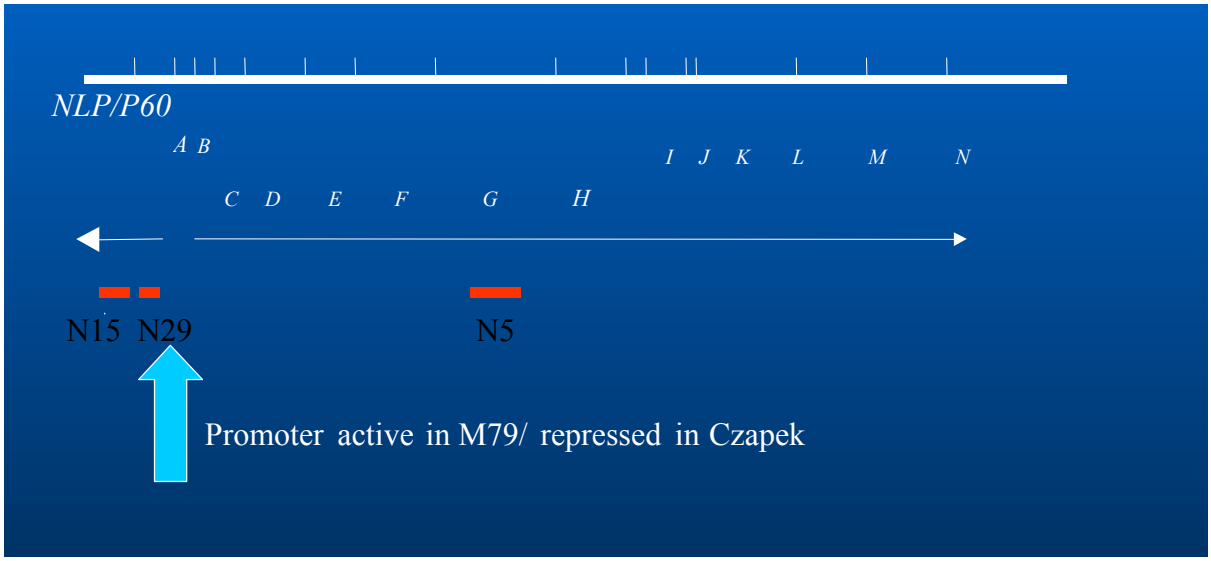

Figure 20. The results of BLAST search for sequences of elements N5, 16 and 30. The transcriptional units are shown by thin white arrows.

When sequences of one pair of doubled representatives belonging to putative NLP/P60-family secreted protein, N15 and N29, were assigned to their chromosomal location, it became evident that they are juxtaposed to their own promoter. The latter, in turn, is adjacent to the neighbouring promoter of the NADH ubiquinone oxidoreductese cluster. The polycystronic mRNA, read from this promoter in the opposite direction relative to the transcript, carrying sequences of N16 and N30, includes sequence of element N5 representing a functional unit G. Despite such tight clustering of sequences of the elements above and their cognate transcriptional units, they were

clearly shown to respond differently to altered growth conditions: N16 and N30 were down-regulated and N5 was up-regulated in Czapek medium relative to rich medium.

None of the erythromycin biosynthesis cluster functional units used for the array construction showed a perturbed transcriptional rate. This was also proved by the detection of erythromycin in both culture media, showing linkage between vegetative growth and secondary metabolism, particularly erythromycin production under both condition set-ups used.

The results obtained clearly showed a great potential and suitability of the application of shotgun-library fragment arrays of G+C high content un-sequenced genomes of actinomycete bacteria for preliminary transcriptional screening experiments on a genome scale.

Discussion

The work was focused on the development of a suitable molecular technology to investigate bacterial systematics and the production of secondary metabolites. As a model system, representatives of the order *Actinomycetales* were chosen. They represent the richest source of bacterial secondary metabolites, e.g. antibiotics, known at present. For the study of this task the 16S-rRNA gene sequence was chosen. The 16S-rRNA consists of both taxonomically highly conserved and variable sequences. Many such sequences are stored in public databases (Ribosomal Database Project, Maidak *et al*., 1999) and are used by taxonomists in their research regarding bacterial systematic ordering. In addition, many prokaryotic and eukaryotic genomes have been analyzed. The gigantic amount of data which resulted from these endeavours provides a completely new insight into the genetic information which is ideally suited for the structural and functional study of genes or combinations of genes, e.g. biochemical pathways. One of our interests concerned the question of whether this information can be used to delineate eubacterial strains and predict the biosynthesis of secondary metabolites.

However, to investigate the genomic puzzle above, a highly advanced technology had to be developed. Although a broad variety of approaches were available for the analysis above (Saluz *et al*., 2002), I focused on DNA arrays because they offer the high-throughput capacity and cost-effectiveness crucial for the large-scale analysis of genomic data. DNA probes from the defined genomic entities or from hundreds to thousands of genes are positioned and immobilized on an active surface of a solid support. The hybridization reactions between immobilized molecular arrays and labelled nucleic acid samples isolated from cells or tissues allow the elucidation of sequence-specific signal patterns, as well as patterns of gene expression. The most important aspects concerning the elements of DNA microarrays (solid support, probes and targets) and the establishment of the conditions for their concerted functioning, as developed during my thesis, are discussed below.

Oligonucleotides to investigate the 16S-rRNA gene sequence.

All the designed primers were selected within highly conserved stretches of the bacterial 16S-rRNA gene sequences. It was not surprising that 3 out of the 7 primer sequences found (rRNA f1, r1, r2; tables 1 and 16) were already used by taxonomists as primers for PCR reactions, sequencing 16S rDNA, and as hybridization probes for the detection of the corresponding organisms in biological

samples (table 16). Three of the primer sequences were novel (rRNA f0, rRNA f2 and rRNA r0; table 1), and the sequences of rRNA f3 (Alm *et al*., 1996) had to be modified.

Table 16: Highly conserved rRNA stretches overlapping selected primers and examples of their applications.

Primer	**Overlapping conserved stretches, 5'-3' direction**	Position	**Application**	Designation	**References**
rRNA f1	AGACTCCTACGGGAGGCAGCAGT	336-358	PCR primer	358f	Weidner *et al*., 1996
	GCTGCCTCCCGTAGGAGT	336-353	Domain *Bacteria* specific hybridization probe	EUB338	Amann *et al*., 1990
				340	Lee *et al*., 1996
rRNA r1	CACGAGCTGACGACAGCCAT	1045-1064	Domain *Bacteria* specific hybridization probe	1060	Lee *et al*., 1996
	ACATTTCACAACACGAGCTG	1066-1085		U2	Weidner *et al*., 1996
rRNA r2	TGCCAGC(A/C)GCCGCGGTAAT(A/T)C	515-536	Sequencing primer	Universal C	Lane *et al*., 1988
	G(A/T)ATTACCGCGGCGGCTG	519-536	PCR primer	K2R	Clement *et al*., 1998
			Universal hybridization probe	520	Lee *et al*., 1996

The use of the primers allowed the amplification of DNA fragments with high efficiency and specificity. The genomic DNA of selected type bacterial strains and strains isolated from an environmental soil sample (Creta island) belonging to the order *Actinomycetales* gave comparable results.

The results presented showed that specific sequences within the first 500 basepairs of the 5'-end of the 16S rRNA sequence (domain I) were sufficient to elucidate the tasks of my work. Combination of 6 chosen signature positions allowed following taxonomic assignment of type strains *A. mediolanum* HKI108, *A. jenensis* HKI085, *J. limosus* HKI083, *A. orientalis* IMET7653, *S. griseus* IMET40235, *A. madurae* IMET9585, *S. hirsuta* IMET 9709 and *S. viridis* IMET 9550 (figures 7, 13, 15, 16, 17): order *Actinomycetales* (signature 239), sub-orders *Streptosporangineae, Micrococcineae, Pseudonocardineae, Streptomycineae* (signature 415) and families *Thermomonosporaceae, Microbacteriaceae, Pseudonocardiaceae, Intrasporangiaceae, Streptomycetaceae* (signatures 139, 280, 328, 370, 381) (Stackebrandt *et al*., 1997). High sequence variability around signature position 139 (rRNA p15.1.X set) allowed deeper insight, till the genera and species level. When the PCR fragment array containing probes for 14 type strains was hybridized with labelled oligonucleotide, designed to interrogate signature position 139, the correct identification of *S. viridis* IMET9550 fragment was achieved. One false positive signal (*S. hirsuta* IMET 9709) was misidentified, which, however, is characterized by most stable G/T mismatch pair compared with the other possible combinations. Based on the range of strains interrogated, this points to the assay specificity of approximately 92%. A further improvement is feasible through the broadening of the signatures to be interrogated.

Concerning the newly isolated strains, after characterization via the whole set of chemotaxonomical analyses, their genomic DNA proved to be an effective template for amplification using primer pairs rRNA fo-r2 and rRNA f1-r2. These fragments will next be spotted and tested in hybridizations with labelled oligonucleotides, interrogating signatures located between these primers and, inversely, be labelled and hybridized to the oligonucleotide arrays designed. This will demonstrate the experimental performance of optimized assays and the correctness of the preliminary assignment of these isolates.

The aspects concerning solid supports, surface treatment, probe structure, immobilization procedure, hybridization parameters, e.g. buffers, temperature, time, target structures, and washing parameters, are discussed in the following sections.

Activation of surfaces

A wide range of commercially available glass slides and others supports (see Materials) were tested in order to evaluate an optimal substrate. It was realized that the quality of nucleic acid arrays is highly dependent on the substrate material. In addition, a poor quality of coated substrate surface led to partial problems with spot uniformity and morphology. Furthermore, the overall background fluorescence (autofluorescence of the substrate, etc.), the spot size, shape, and DNA retention, was varying, thus leading to a loss in sensitivity and resulting in generally poor data.

Primary aminogroups

We investigated Corning GAPS™ slides functionalized by primary aminogroups via gamma aminopropyl silane coating. Our experiments confirmed a high uniformity of amine density and thus a high consistency of surface energy across the surface of these slides. Corning also developed a special packaging to maintain the appropriate storage environment. However, when the packaging was opened the quality of slides dropped rapidly, and after one week they hardly could be used anymore. This low stability of Corning GAPS coated slides after opening the packaging could be attributed to a very high sensitivity of aminosilanes to the light and to humidity, which lead to the photodecomposition and polymerization of their molecules respectively (Chrisey *et al*., 1996). These results were in striking contrast to Borofloat-33 glass slides, coated in our laboratory with polylysine. Once prepared, the polylysine slides had to be incubated for the recommended 2 weeks before use in order to get the proper final assembly of the polylysine layer optimal for DNA spotting and its covalent binding (Eisen *et al*., 1999). This required a preparation of the slides in advance. Long polylysine chains, consisting of approximately 400 lysine residues, used for slide coating and bound to the surface at multiple sites, assured the stability of high DNA binding capacity for a duration of at least 4 months. On the other hand, the same factors led to the compromised uniformity of surface properties over the slide. Given the size of polylysine chains

and the distance between silanol groups on glass (~0.5 nm) the coating proceeds in and the final assemblage of polylysine on slide surface is characterized by unordered manner. This does not happen upon aminosilane coating, where its molecules interact with silanol groups on surface at 1:1 stoihiometry. For these reasons the aminoactivated Borofloat 33 slides were used for shotgun library array production and two-dye hybridization experiments only, as uniformity of DNA content of each spot play a secondary role in this case. Sigma slides, Esco pre-cleaned slides and commercial polylysine slides (Sigma) showed worse characteristics upon hybridization compared with Borofloat-33 slides. A lower background recorded on the latter glass could be attributed to such properties as low content of metal ions. This factor, in combination with the above-mentioned higher durability of the glass. obviously led to a reduced ion migration into the coating. Most probably, under experimental conditions (pH and ionic strength), these ions developed an electrochemical environment in the vicinity of Sigma and Esco glass surfaces, which favoured increased target attachment to the support (Allemand *et al*., 1997).

Aldehyde groups

A wide range of suitable chemistries for the covalent immobilization of DNA molecules via their extremities on activated solid supports were reported (Joos *et al*., 1997; Rasmussen S.R. *et al*., 1991; Ghosh S.S. *et al*., 1987; Guo Z. *et al*., 1994; Schena M. *et al*., 1996; Lamture J.B. *et al*., 1994; Chrisey L.A. *et al*., 1996; Rogers Y.-H. *et al*., 1999). They include a binding of carboxylated or phosphorylated DNA to the aminated supports; a coupling of end-aminomodified DNA to carboxymodified supports, and to glass surfaces activated by isothiocyanate, aldehyde and epoxide; a coupling of thiol-modified or disulfide-modified DNA to aminosilane via a heterobifunktional linker and to 3-mercaptopropylsilane. Finally, a binding strategy which allows modulating the binding capacity of an activated support, its hydrophobisity, and charge, was reported (Beier *et al*., 1999). The simplest chemistry among them, immobilization of aminomodified DNA to the aldehyde-activated glass support, which nevertheless assures high-quality hybridization data, was investigated. Its simplicity is devoted to the absence of any coupling agent or a heterofunctional crosslinker, which are necessary for all other binding reactions described above.

Final surface properties of the activated glass could be varied by modifications of an aldehyde-coupling protocol at the different steps (cleaning process, concentration of silane or aldehyde, their preparation and age, and treatment durations). Those variations led to correspondingly varied hybridization results (figure 7). Therefore, a structure of formed silane-aldehyde DNA binding layer was hypothesized as responsible for the effects observed. Further investigation showed that this layer had fluorescent properties. Moreover, these properties were acquired at the last step of slide preparation (glutaraldehyde coupling). The fluorescent signal recorded from glass surface could be modified by treatment with a reducing agent, sodium borohydride. $NaBH_4$ reduces unreacted

aldehyde groups and Shiff's bases, formed during the immobilization procedure between aminogroups of DNA and aldehyde groups of surface. Thus, these observations led to the assignment of the acquired fluorescence of the activated glass surface to the known process of formation of a system of conjugated Schiff's bases (Cheung *et al*., 1982; Collins *et al*., 1981; Southern *et al*., 2000; Kikugawa *et al*., 1989, Monsan *et al*., 1975). Upon formation in the process of glutaraldehyde fixation of tissues or gelatine, these structures were reported to produce fluorescent signal at 560 nm, being maximally excited at 540 nm (Collins *et al*., 1981). This explains why this fluorescence could be observed in the Cy3 channel. The results of the experiments presented in figures 7, 13-15 showed that the fluorescence level of the top layer of silylated slides could be used as an approximate measure of the density of immobilized aldehyde molecules and thus aldehyde groups available for DNA binding. The optimal density of active aldehyde groups for oligonucleotide immobilization which ensured the highest hybridization signals upon hybridization with long target molecules corresponded to the 2000 greyscale units. A signal saturation obtained on the slides with higher aldehyde group densities could have following explanations: 1) a crowding effect of the immobilized probes, which prevented an effective target access to the probes or caused an interprobe partial hybridization or a hybridization of one target molecule to a few probe molecules (Forman *et al*., 1998; Shchepinov *et al*., 1997); or 2) a glutardyaldehyde dimer formation, which resulted in a decrease of the fraction of aldehyde groups available for DNA binding (Collins *et al*., 1981). Regarding arrays of PCR fragments, their approximately 30 times greater size compared with oligonucleotides points to a lower value for the optimal density of active aldehyde groups in order to prevent the crowding effect. This was confirmed by the results presented in table 7.1, reflecting the kinetics of their hybridization with labelled oligonucleotides. After aminoblocking treatment of arrays, a non-specific background signal decreased and hybridization signals increased, indicating that some amino groups obviously did not take part in the aldehyde coupling reaction. This hypothesis was supported by the results obtained upon the use of aminosilane solutions of different concentrations for the glass treatment (figure 7:arrays 3 and 4). This led to the conclusion that both silane and aldehyde concentrations for the slide treatment have to be adjusted to the relevant amounts which could assure the optimal density of active aldehyde groups and sufficient titration of the silane amino groups. The effect of primary aminogroups can be explained by their protonation under experimental conditions. In this case, it results in electrostatic attraction between the positively charged glass surface and the negatively charged DNA chains (Allemand *et al*., 1997).

The aging of silylated slides caused a worse signal to background ratio (figure 14), indicating a loss of aldehyde groups, due to the above-described effect of the reversal of Schiff's base formation, and

oxidation by air into carboxylic groups (Zammatteo *et al*., 2000). The best results were obtained using Telechem slides or wave-guides, due to a uniform distribution of active groups on the surface.

Immobilization of probe molecules

The results described by Schena's group, that 3xSSC spotting buffers are optimal for both polylysine and silylated slides (Schena *et al*., 1995; Schena *et al*., 1996; Heller *et al*., 1997), could be confirmed in the cases of polylysine slides with immobilized PCR products and aldehyde slides with immobilized oligonucleotides. However, using aldehyde slides with immobilized PCR products, optimal results were obtained using Telechem spotting solution. Unfortunately, the composition of the latter buffer is not available. However, the Telechem buffer most probably contains less salt than the 3xSSC buffer does. This could be explained based on results obtained upon the hybridization between double-stranded PCR targets and immobilized oligonucleotides (figure 10). The cognate TeleChem protocol recommends 5-50 μM oligonucleotide concentrations for spotting. The results showed a linear response between the final hybridization signals and concentrations of spotted oligonucleotides within range above (table 6.1). Interestingly, this was also the case for 3xSSC spotting buffer, when used with another protocol (Shena *et al*., 1996) originally established for the immobilization of PCR fragments. The fact that the same hybridization signals were obtained from the spots prepared from both spotting buffers after the adjustment of the DNA binding time in 3xSSC to that used for the Telechem buffer indicates the same kinetics of Schiff's base formation reaction in the conditions provided by these solutions. Using oligonucleotide concentrations greater than 50 μM, the hybridization signals were still increasing using Schena's protocol only (figure 10, table 6.1). This linear increase could be explained by process of DNA-triplex structure formation. These structures resulted from the hybridization of both complementary strands of a target with the immobilized oligonucleotide strand, either sequentially or in the form of renatured double-stranded fragment. This was observed in experiments on the hybridization of PCR fragments carrying different labels on the opposite strands with immobilized oligonucleotides derived from the same sites of both strands of the fragments above (figure 13). Such a reaction was favoured at spots prepared from 100 μM and higher concentrations. The signal increase mentioned could result from the increase of a complexity of triplex structures with a formation of higher-order structures, namely DNA dendrimers, under the specific hybridization conditions attainable in hybridization on glass arrays (high density of oligonucleotide molecules immobilized on solid support, extremely small hybridization volume, 2-dimentional component of target diffusion) (Chan V. *et al*., 1995). The results of post-hybridization washing at stringent conditions support this hypothesis, because target molecules participating in dendrimer structures obviously had less contact with the activated glass surface and were removed. This decreased the signals to the level of those obtained from spots prepared using 50 μM solution.

Another confirmation of this hypothesis was obtained in the experiments mentioned on the hybridization of PCR fragments carrying different labels on the opposite strands, in a set up where PCR fragments of the same 16S rRNA gene region from two bacteria differing at signature positions were co-hybridized (figure 13). For example, the appearance of a strong Cy3 signal from rRNA p15.3.2 probe spot (perfect match to rRNA f0-r2.9550 PCR fragment) upon hybridization, where rRNA f0-r2.7653 PCR fragment only carried this label at the antisense strand complementary to the probe above, could only be explained as due to the formation of the dendrimer structures above, given a high hybridization specificity of that fragment to its perfect match rRNA p15.3.1 probe (figure 13, arrays 1 and 2). The last proof came from experiments where RNA was used as a target. Its single-stranded structure did not support the process above, and spots prepared from 200 μM solution showed a non-significant signal increase compared with 50 μM solution (figure 16, tables 16-19). Using the protocol of Telechem showed a non-linear increase of the hybridization signals in response to increasing oligonucleotide concentration under the same experimental conditions, i.e. a saturation effect. Moreover, a DNA strand exchange between two different PCR fragments occurred as complementary strands from those fragments carrying different labels, and applied into the hybridization mixture in non-denatured form, could be detected on the same spot. The latter was true for the 500 bp long PCR fragments. When, compared with this length, 2 or 3 times longer fragments (approximately 1050 bp long rRNAf0-r1 and 1500 bp long rRNAf0-r0 fragments respectively) were hybridized with 2.5 times shorter fragments (180 bp long rRNAf1-r2), complementary to immobilized oligonucleotide, the effect described was not observed (figure 14). This can point to a defined minimum length of hybridized DNA molecules necessary to overcome sterical hindrance and the adsorption effects of the glass surface.

For the immobilization of PCR fragments, 3xSSC buffer was required. The negative effect of higher salt concentrations on DNA attachment to aminomodified glass surface was previously known (Southern *et al*., 1999). Regarding a DNA concentration suitable for a microarray preparation, 0.5 kb long PCR fragment showed an increase of the resulting hybridization signals within the 1-3 μM concentration range used for spotting. Corresponding concentrations for the 0.2-1.2 kb long PCR fragments were reported to ensure high-quality hybridization data upon immobilization on polylysine slides (Schena *et al*., 1995, Heller *et al*., 1997).

Target molecules

The results obtained from the various labelling strategies (PCR, *in vitro* transcription, and reverse transcription) revealed a variable acceptance of fluorescence-labelled nucleotides by DNA/RNA polymerases. A similar observation concerning cyanine-labelled deoxnucleotides was already described by Zhu *et al*., 1997. A good incorporation rate was obtained by SuperScript II reverse

transcriptase and cyanine dyes. The incorporation rate was approximately 4.0% for Cy3-labelled and 2,9% for Cy5-labelled deoxynucleotides. This shows a relatively high tolerance of the enzyme above. Other enzymes, such as Taq DNA polymerase and T7-RNA polymerase, showed less acceptance. Taq polymerase and FITC-labelled deoxynucleotides showed an incorporation rate of 1.2% under the experimental conditions described in Methods, and in the case of FITC dye-labelled ribonucleotides and T7-RNA polymerase, the incorporation rate was only 0.8%. These results could mainly be explained by sterical hindrance (Walsh C. 1986). Due to the above observations, other labelling strategies were applied. An excellent experience was had in end-labelled oligonucleotide primers. An additional procedure concerned the chemical labelling by amino-modified cyanine dyes to nucleic acids (see Methods). This procedure led to an equal labelling rate of approximately 1,5% for both Cy3 and Cy5 dyes, which is a great advantage for differential gene expression studies, where both labels have to be measured at the same time (Schena *et al*., 1998). Thus, these two types of the labelled targets could be successfully applied for the hybridization reactions with oligonucleotide arrays for the taxonomical investigations, based on the sequences of genes encoding ribosomal RNAs. End-labelled PCR fragments flanked by conservative regions could be easily obtained from the wide range of genomic DNA. PCR fragment of 5‘ located 500 bp of 16S-rRNA gene sequence showed its suitability upon hybridization with a broad range of oligonucleotide probes interrogating different positions within the region mentioned. In all hybridization reactions, the resulting patterns were characterized by the highest signals from perfectly matched probes. Secondly, total cellular RNA with prevailing rRNA fraction was shown to give satisfactory results upon direct the chemical coupling of dyes (figure 16). The comparison of hybridization efficiency of both targets showed that RNA hybridized with oligonucleotide spots prepared within concentration range 6.125-50 μM gave a 2-fold increase of a signal upon 2-fold increase of oligonucleotide concentration (figure 8, table 4.1). In turn, a 4-fold increase of oligonucleotide concentration was necessary to achieve the same signal increase in the case of PCR fragment hybridizations under the same conditions (figure 10, table 6.1). This was in accordance with the classic kinetics rules regarding the differences between single-stranded and double-stranded hybridization drivers. The size of both targets could be varied, i.e. PCR reactions using primers from differentially spaced regions of the 16S-rDNA could be performed; in the case of RNA, a controlled chemical fragmentation could be made to achieve the desired average size of the main fraction of RNA molecules. The decrease of a target size resulted in increased hybridization efficiency and lower background level due to the higher solution and surface diffusion rates (Chan *et al*., 1995). Both targets showed their suitability for the nucleic acid analysis at single base accuracy. Regarding the multiplexing set up of these kind of assays, the maximum number of analytes investigated in the same experiment was two for both types of targets, according to the

number of different fluorescent labels which could be simultaneously detected on confocal scanner. In the case of PCR fragments, the main advantages are the theoretical possibility of using oligonucleotide probes derived from both strands of 16S-rDNA, as well as no confinement in which strand should carry the label independently on the polarity of the immobilized probes. Indeed, the most important factor in this set up is the fact of the triplex and higher order dendrimer structures formation as discussed above. The foreseeable problem seemed to be the formation of heteroduplexes composed of complementary strands from different but related PCR fragments characterized by a small number of mismatches. They could arise either in the renaturation process occurring in the hybridization solution, with subsequent hybridization to the attached oligonucleotides due to local melting (DNA breathing), or in hybridization of formed oligonucleotide-target strand duplexes, with the strand complementary to the hybridized one and representing a different PCR fragment. But nevertheless, this problem could not preclude the proper detection of the presence of either fragment based on the hybridization patterns, given that basic hybridization event between immobilized oligonucleotides and the complementary target strand was specific and sensitive enough. As the main goal was to detect the specific signal from defined perfect match spots for subsequent reliable assignment to the PCR fragment, it did not matter what the label was detected and which source it came from after proper completion of the basic step above as it was shown in figure 13. In the case of RNA targets, the single-stranded structure and increased stability of RNA-DNA duplexes, compared with DNA-DNA ones, assured approximately 2-fold faster hybridization kinetics, as it was described above. The simultaneous detection of two RNAs labelled by different fluorophores was also successful (figure 15).

Hybridization factors

Buffer

A comparison of 5 different hybridization buffers showed the best data quality upon the use of Telechem and SSPE-T buffers. The former buffer was shown to be optimal for applying to hybridizations on silylated slides. This was not surprising, as both products were developed and adjusted at TeleChem and thus well suited to each other. This buffer resulted in a lower background, which led to an approximately 2 fold increase of the dynamic range of data compared with the SSPE-T buffer. For this reason, the given buffer was subsequently used for the hybridizations involving oligonucleotides (probes or targets). In the cases where both hybridization counterparts were represented by polynucleotides (cDNA, PCR fragments, and *in vitro* made RNA), a buffer composition known from classical and established protocols for nylon membrane hybridizations was used (Maniatis *et al*., 1982, Church *et al*., 1984). In most cases the difference regarding glass microarrays was due to the omitting surface blocking and volume exclusion agents.

This could be explained by microvolumes where hybridization had to take place, and unproportionally decreased volume-to-surface ratio compared with macroarray system. Thus, only using the high salt component (4xSSC or 5xSSC) and detergent (0.1%SDS) in the final composition allowed a reliable diffusion rate of analyzed nucleic acids. In addition, a planar, two-dimentional structure of the glass array surface led to efficient blocking of the sites of possible unspecific attachment of target molecules. Therefore, a full composition buffer was used for pre-hybridization only.

Temperature and probe positioning effects

The hybridization temperatures were selected 10°C below the Tm of the oligonucleotide duplex. Tm was calculated according to the equation of Wallace *et al*.: T= [2xn(A+T)+4xn(C+G)] (Wallace *et al*., 1979), where n indicates the number of bases. The hybridizations were reliable for both 15- and 20-mer immobilized probes showing correct match/mismatch discrimination. The discrimination ratios and hybridization efficiencies varied, owing to the effects of probe sequence context and its position within a target sequence (Uhlenbeck *et al*., 1970, Lima *et al*., 1992). G+C content played a minor role. It did not differ significantly across the probe sequences; most of them had 60-67% G+C content (table 2). It was not surprising that the highest discrimination value was achieved upon hybridization to the spotted probes comprising of rRNA p15.1.X set, due to the presence of 3-5 mismatched nucleotides with the targets used (tables 2, 11.1). The highest hybridization efficiency was achieved upon hybridization to the spotted probes comprising of rRNA p15.8.X and rRNA p15.9.X sets. Their positions in the context of 16S rRNA secondary structure, characterized by a long stretch of 5‘ end (more than 7 nucleotides) within RNA bulges and 3‘ end within a RNA helix, could be the reason for the given outcome (Kim *et al*., 1999). This data is supported by the published results concerning an investigation of the hybridization efficiencies of the probes derived from all regions of *E. coli* 16S rRNA sequence (Fuchs *et al*., 1998). Strong unspecific hybridization signals obtained at probes rRNA p15.1.4, 6.2 and 6.4 upon hybridization with cellular RNAs (figure 16) could be explained by the fact that 11 bases of both probes participate in the formation of helixes in 16S rRNA secondary structure.

Hybridization time

In comparison with macroarrays, the microarray hybridization reaction proceeds in extremely small volume and thus at much higher target concentration. In addition, the probe molecules are immobilized at very high densities within spots and are additionally more accessible for target, due to 2-dimentional configuration of glass support (Southern *et al*., 1999). This leads to very fast kinetics of hybridization obeying pseudo-first order mechanism at the initial stage of reaction after

the very short lag-phase, which is far from thermodynamic equilibrium. At such conditions, hybridization is highly specific and sensitive to single base mismatches (Maskos *et al*., 1992). Therefore, arrays containing a limited number of probes/spots were usually hybridized for short time periods (1-3 h). On the other hand, the hybridization between a highly complex target representing a cellular transcriptome and probe set representing an organismal genome library were allowed to proceed for 24 h, in order to achieve a state of thermodynamic equilibrium. The reason was recognized evidence (Bhanot *et al*., 2003) suggesting that the performance of DNA chips, as measured by a number of false positives, is best at the thermodynamic equilibrium. Thus, the hybridization patterns obtained under such conditions are considered to provide a reliable evaluation of the relative abundances of different target molecules simultaneously hybridized to the high-density cognate probe arrays. The period of 24 h was a trade-off between various published results (Stillman *et al*., 2001, Franssen-van Hal *et al*., 2002, Sartor *et al*., 2004) considering the surface chemistry as well as the structure and concentration of both probes and targets. However, it should be noted that the equilibration time depends on the bulk target composition, particularly the concentration of perfect match and mismatched probes, the number of mismatches, the ionic strength, and the grafting density of the probes. Thus, the equilibration time in one experimental situation is not necessarily the same under different conditions. Accordingly, the equilibration rates for the different spots within the same array may well differ (Halperin *et al*., 2004).

Washing conditions

In the case of the hybridization of PCR fragments with immobilized oligonucleotides, the increase of washing temperature from 25°C to 37°C and the extension of a washing time from 20 min to 3 hours, performed with a shaking instead of a stirring, most probably resulted in the disruption of DNA dendrimers formed during hybridization; this led to a more precise estimation of the amount of hybridized target (see above). However, these adjustments were not necessary for the correct assignment of the hybridized PCR fragments. The reasons were low density of the corresponding arrays and low complexity of the hybridized targets; in addition, obviously, sufficient specificity of signals was already obtained at hybridization step, due to the adjusted conditions regarding a combination of time, temperature, and buffer (see above). In turn, the stringent conditions above (shortened to 30 min) were absolutely necessary for reversed format of immobilized PCR fragments hybridized with oligonucleotides. The reasons were, obviously, different hybridization kinetics, as well as physico-chemical environment at surface-solution interface, and thus the stability of formed duplexes. However, the basic features of hybridization thermodynamics held in these reactions as well: for example, the highest stability of G/T mismatches compared with other mismatched combinations and most destabilizing effect of centrally positioned mismatches were confirmed.

Data retrieval and analysis

The first stage of the analysis process was a spot finding procedure, i.e. overlaying a grid template over the numerical array image retrieved. Usually it is necessary at this stage to carefully prove the locations of each grid element and their diameters. Dust autofluorescent particles or pieces of target clamped material often had diameters approximately equal to those of spots and were characterized by strong signals. In these cases, they were recognized by software as real DNA spots. Those of them located in the vicinity of spots and thus overlapping with area used for background subtraction led to correspondingly decreased specific signals and poor data quality; such spots had to be excluded from subsequent analysis. When too small a spot diameter was defined, this could lead to the inclusion of peripheral spot pixels into the background calculation. On the other hand, too large a defined diameter could lead to a correspondingly decreased specific signal obtained after integration and averaging over spot area; in combination with high background signal, such spots could be unrecognized. Local background subtraction, whereby the area surrounding each spot is used for background signal calculation, showed its out-performance in comparison with when a single background value is calculated for the group of spots. There are approaches which consider the actual background signal as that obtained from area passed through the same chemical treatment as the area of DNA spots (Wu *et al*., 2001). These can be areas where deposition reagents (such as salt buffer) have been spotted without DNA or with non-homologous DNA. In the latter case, the background signal resulting from cross-hybridization can be determined.

The next step in array data analysis is represented by normalization procedure. The aim of this step is a removal of the systemic and random experimental variations unavoidable in this kind of experiments, due to their down-scaling (miniaturization), multi-step proceeding and co-hybridization of two differentially-labelled targets (see below). Every experimental factor can actually contribute to the final cumulative errors: probe DNA preparation and deposition, pin geometry, slide heterogeneity, RNA preparation, reverse transcription into cDNA, fluorescent labelling, hybridization conditions, scanning, and image analysis. Therefore, in order to obtain good quality hybridization data, the first step is to improve the experimental reproducibility; for example, by rigorous quality control through the whole process and optimization of experimental conditions (Wildsmith *et al*., 2001, Wrobel *et al*., 2003). Next, following a standardization of the control measures above is the way to achieve an interchangeability and cross-interpretability of microarray data obtained with different platforms and/or in different labs (Brazma *et al*., 2001). Normalization or data pre-treatment deals with the mathematical operations which are applied to transform data before further data mining. Suitable pre-treatment can greatly improve results, since it removes or minimizes the cumulative error described. Current normalization methods are based on the assumption that that some signals between arrays are consistent. Usually, either of the following

three types of signals is considered in this regard: constitutively expressed “housekeeping” genes, spiked nucleic acids, and the signals calculated from all genes (such as sum, mean or median signal). The latter method was used throughout this work. In the case of oligonucleotide hybridizations with one target analyte, this was useful because the focus was on the relative contribution of match and mismatch probe signals to the total signal obtained from the array. Due to relatively high amount of spots and, in turn, the relatively low amount of those with differential, perturbed expression signals, it was also a reliable method for dual-dye experiments on bacterial differential expression analysis. Both experimental RNAs were labelled by different dyes and the resulting cDNAs were mixed and co-hybridized to the same array, giving by this means the internal standards regarding the quality of each spot for comparative assessments of the relative transcripts abundance levels in the cells under investigation. In addition, both (reverse) combinations of RNA-dye pairs were used, in order to eliminate the error caused by the impacts of their chemical/physical properties on labelling efficiency, the diffusion rate of labelled molecules during hybridization, as well as the correlation between the number of dyes present within a hybridized spots and the resultant signals (Ramdas *et al*., 2001) (table 14.1). An additional level of statistical reliability of the data on the RNA abundance levels comparison was provided by their statistical segmentation, as described in Methods and Results. z-scores reflected a high sensitivity of the ratio calculations to systemic errors: the residual systemic errors still present after the background correction and normalization exerted their impacts on the elements of low signal intensity range, and were removed by combining with two other scores attributable to the Cy5-Cy3 signal differences.

The last step in the experiments on bacterial gene expression monitoring was sampling the elements present in both combined displays of experiments 1 and 2 with corresponding reversed hybridization patterns. These were considered as real hits, with significantly different relative RNA abundance levels in the *S. erythraea* DSM 40512 cells under the experimental conditions described. Their selection, proved by supporting data of technological plausibility, points to the suitability of the approach for the similar tasks on genome-wide expression monitoring in actinomycete bacteria without the available genome sequences, even though the main experimental factors guided to low sensitivity and specificity of the experimental system used. These were: shotgun library fragments served as probes; and total RNA was used as a target and was in addition labelled in the presence of random primers. The latter drawback could be partially alleviated by diluting random primers with those characterized by high G+C content and thus homology to restriction sites found in actinomycete’s ORFs. The shotgun fragments did not necessarily carry the sequences from unique ORFs, given the relatively short intergenic spacers in the bacterial genome and the usual operonic organization of bacterial genomic functional units characterized by their tight clustering. The former cases obviously pose a great problem as genes, which different ORF fragments within the

same clone insert belong to, may respond differently to the conditions analyzed (via up- and down-regulation). In the latter case, this problem would be less pronounced, as polycystronic mRNA is usually transcribed from operon. Nevertheless, the bias could be introduced due to such transcription regulation mechanisms as attenuation, or distal effect on polycystronic mRNA transcription due to the gradient of transcriptional efficiency from proximally to distally located sequences relative to the promoter. Moreover, the library used was not normalized and thus over-representation of clones with rRNA sequences was foreseeable. Regarding the latter problem, the random priming of the total RNA led to the same over-representation of rRNA sequences in the labelled target material. The artifacts obtained and described in Results highlighted other important problems while dealing with an array fabrication of comparable density, namely problems of accurate clone handling at all stages preceding array printing (plate culturing, plasmid DNA isolation, PCR, PCR fragment purification, and mixing with spotting buffer) and carryover of probe DNA during it. The above-mentioned over-representation of rRNA sequences could be the reason for the strong signals detected in negative control spots, as a result of these kinds of processes.

In summary, these kinds of results have to be treated as a preliminary screening and be proved by independent methods for transcriptional analysis, such as real-time PCR or Northern blots. The differentially expressed clones found represent the focus of further research, in order to make the next step in elucidating possible mechanisms of erythromycin production by *S. erythraea*. It concerns, primarily, putative transcriptional regulators and homology hits to those genes which are involved in antibiotic biosynthesis in other actinomycetes (N2, 6, 9, 18, 20, 22, 29).

Biological applications

Based on the results obtained in this work, the following application formats could be proposed. The reliable identification of the members of the defined eubacterial range whose 16S rRNA sequences are known could be realized within oligonucleotide array format. At first, previously selected target sequence(s) with a characteristic level of sequence variability should be determined. At the latter stage, a fabrication of microarrays comprising of probe sequences suitable for detection of above variations could be done. In its easiest format, the prepared arrays could then be hybridized with reference targets prepared from the nucleic acids of the pure culture cells of each of the bacterial representatives above. Depending on the affordability of these targets, PCR amplification of the corresponding genomic fragment(s) or bulk total cellular RNA could be used. The resulting data could be compared with the patterns obtained in subsequent hybridizations with the target material obtained from the newly isolated pure cultures representing the same range of bacteria. Depending on the array density and its probe complexity, the analysis program could give an identification result for the bacterial strain as well as its phylogenetic position (Gingeras *et al*.,

1998). The possibility of broadening the range of selected chronometers/markers in a fast and affordable way represents another great advantage of spotted arrays. The corresponding additional oligonucleotide probes should just be evaluated and included into the array design. The format of immobilized PCR fragments hybridized with oligonucleotide targets could be used for the parallel interrogation of thousands of immobilized PCR fragments representing members of microbial community(ies). The arrays could be reused at least three times. In addition, this format allows simultaneous use of multiple oligonucleotides labelled by different dyes, speeding up the time of analysis. Thus, oligonucleotides which are highly specific for the different ranking levels, could be used in descending order, starting from the oligonucleotides of more general specificity and using probes of narrower specificity at every next step (Amann *et al*, 1995).

The shotgun library arrays construction represents a method of choice for preliminary genome-wide expression monitoring in actinomycete bacteria with un-sequenced genomes, due to requirements needed and its relative simplicity. The sensitivity of these kinds of experiments will be significantly increased upon the availability of the whole genome sequences of the biotechnologically important representatives of this group. But the trade off will be a rather tedious process of primer pair search for each annotated ORF or, even more challengingly, 50-70 mer probe optimization for each of them. The latter probe type is nowadays considered to be the best choice, conbining the advantages of initial cDNA and short oligonucleotide probes.

Given the increasing affordability of the technology at the moment (DNA purchase, activated slide purchase, possibilities for customized spotting, optimized labelling, and hybridization protocols, as well as improved and available data analysis tools), the DNA microarray format soon will take its place in methodological arsenal of polyphasic taxonomy.

Zusammenfassung

Die Aufgabe prospektiver Mikrobiologie besteht in der Erforschung der realen Diversität prokaryotischer Lebensformen sowie in der Erforschung ihrer neuartigen biochemischen und biosynthetischen Eigenschaften. Da jede phänotypische und taxonomische Besonderheit lebender Organismen durch ihre genomische Sequenz und deren Expression bestimmt ist, bestand die Ziele der vorliegenden Arbeit darin, zweckmäßige Formate für DNA-Microarrays zu entwickeln. Diese Arrays sollten sowohl für die Sequenzanalyse mit Einzelnukleotidpräzision geeignet sein als auch für die Analyse der Genexpression auf RNA-Ebene; als Modellorganismus wurde die eubakterielle Gruppe der Aktinomyceten ausgesucht. Beide Ansätze wurden im Rahmen der Arbeit durch die Optimierung folgender Parameter etabliert: Array-Hardware (Slide, Oberfläche etc.), Chemie der Aktivierung, Struktur und Konzentration der Hybridisierungssonden und Zielmoleküle, Zusammensetzung des Hybridisierungspuffers, Volumina, Zeit, Waschbedingungen, Signaldetektion und Datenanalyse. Als taxonomische Marker wurde Domäne I der eubakteriellen 16S rRNS und ihre Sequenzauthentifikatoren, welche für die taxonomische Abgrenzung der Aktinomyceten auf Genusebene und höher verantwortlich sind, gewählt. PCR-Primer, deren Sequenzen innerhalb der konservierten Bereiche ausgewählt wurden, und Oligonukleotidsonden die innerhalb variabler Bereiche entsprechend der taxonomischen Bedeutung gewählt wurden, erlaubten sensible und spezifische Nachweise verwandter bakterieller Sequenzen mit Detektion von Einzelnbasenunterschieden. Eine prinzipielle Austauschbarkeit der beiden Molekültypen, gewonnene PCR-Produkte und Oligonukleotide als immobilisierte Sonden bzw. hybridisierbare Zielmoleküle, wurde gezeigt. Für diesen Zweck, sollten auch DNA-Moleküle mit ihrem 5'-Ende an der Oberfläche immobilisiert werden. Eine Kombination von am 5'-Ende amino-modifizierter DNS, handelsüblichen aldehyd-aktivierten Slides und 100 µM Oligonukleotid-Konzentration sowie 3 µM PCR-Produkt-Konzentrationen in verwandten Spottingpuffer, zeigte optimale Ergebnisse. Darüber hinaus wurde eine verbesserte und schnelle Methode zur direkten Markierung von total-RNS durch chemische Kopplung von Zyaninfluoreszenzfarben mit nachfolgender Fragmentierung gewonnener RNS und deren Hybridisierung etabliert. Unter Anwendung optimierter Bedingungen konnte die vollständige Identifizierung einer Auswahl kultivierbarer Aktinomyces-Repräsentanten innerhalb von acht Stunden realisiert werden. Auf die andere Seite, wurden DNS-Arrays, die aus Tausenden Spots nicht-modifizierter PCR-Produkte zusammengesetzt sind, mit selbst hergestellten Polylysin-Slides erstellt. Diese nicht-modifizierter PCR-Produkte, welche das nicht-annotierte (nicht-sequenzierte) bakterielle Genom mit hohem G+C-Inhalt abdecken, konnten aus den Fragmenten einer Shotgun-Bibliothek hergestellt werden. Beispielhaft wurde ein Array hergestellt, welcher 3820 Spots aus Bibliothekfragmenten enthält, die ca. 36% des Genoms des

Erythromycinproduzenten *S. erythrea* DSM40517 entsprechen. Die Hybridisierung mit zwei RNS-Proben, die aus Zellen isoliert wurden, welche in Komplettmedium und in halbsynthetischen Nährböden gewachsen waren, ergab plausible Ergebnisse. Damit konnten genomische Bereiche, die mit veränderter RNS-Expression bei Wachstum auf oben genannten Kulturmedien reagiert hatten, empfindlich und spezifisch nachgewiesen werden.

References

Adamczyk J., Hesselsoe M., Iversen N., Horn M., Lehner A., Nielsen P.H., Schloter M., Roslev P., Wagner M. (2003) The isotope array, a new tool that employs substrate-mediated labeling of rRNA for determination of microbial community structure and function. Appl. Environ. Microbiol. 69(11):6875-87.

Alm, E.W., Oerther, D.B., Larsen, N., Stahl, D.A., Raskin, L. (1996) The oligonucleotide probe database. Appl. Environ. Microbiol. 62(10):3557-9.

Alemand, J.F., Bensimon, D., Jullien, L., Bensimon, A. and Croquette, V. (1997) pH-dependent specific binding and combining of DNA. Biophys. J. 73:2064-2070.

Amann, R.I., Ludwig, W., Schleifer, K.H. (1995) Phylogenetic identification and *in situ* detection of individual microbial cells without cultivation. Microbiol Rev. 59(1):143-69.

Anthony, R.M., Brown, T.J. and French, G.L. (2000) Rapid diagnosis of bacteremia by universal amplification of 23S ribosomal RNA followed by hybridization to an oligonucleotide array. J. Clin. Microbiol. 38: 781-788.

Barry, T., Colleran, G., Glennon, M., Dunican, L.K., and Gannon, F. The 16S-23S ribosomal spacer region as a target for DNA probes to identify eubacteria. In: PCR methods and applications. 1991 by Cold Spring Harbor Laboratory Press, 1:51-56.

Bate N., Butler A.R., Gandecha A.R., Cundliffe E. (1999) Multiple regulatory genes in the tylosin biosynthetic cluster of *Streptomyces fradiae*. Chem. Biol. 6(9):617-24.

Beattie, K.L., Beattie, W.G., Meng, L., Turner, S.L., Coral-Vasquez, R., Smith, D.D., McIntyre, P.M., Dao, D.D. (1995) Advances in Genosensor Research . Clin. Chem. 41:700-706.

Bertucci, F., Bernerd, K., Loriod, B., Chang, Y.-C., Granjeaud, S., Birnbaum, D., Nguyen, C., Peck, K. and Jordan, B.R. (1999) Sensitivity issues in DNA-array based expression measurements and performance of nylon microarrays for small samples. Hum. Mol. Genet. 8:1715-1722.

Bhanot G., Louzoun Y., Zhu J., DeLisi C. (2003) The importance of thermodynamic equilibrium for high throughput gene expression arrays. Biophys. J. 84(1):124-35.

Bjorkholm B., Lundin A., Sillen A., Guillemin K., Salama N., Rubio C., Gordon J.I., Falk P., Engstrand L. (2001) Comparison of genetic divergence and fitness between two subclones of *Helicobacter pylori*. Infect. Immun. 69(12):7832-8.

Bodrossy L., Stralis-Pavese N., Murrell J.C., Radajewski S., Weilharter A., Sessitsch A. (2003) Development and validation of a diagnostic microbial microarray for methanotrophs. Environ. Microbiol. 5(7):566-82.

Boucherie, H., Dujardin, G., Kermorgant, M., Monribot, C., Slonimski, P., Perrot, M. (1995) Two-dimensional protein mapof *Saccharomyces cerevisiea*: construction of a gene-protein index. Yeast 11:601-613.

Brakenhoff, R.H., Schoenmakers, J.G.G., and Lubsen, N.H. (1991) Chimeric cDNA clones: a novel PCR artifact. Nucleic Acids Res. 19:1949.

Brazma A., Hingamp P., Quackenbush J., Sherlock G., Spellman P., Stoeckert C., Aach J., Ansorge W., Ball C.A., Causton H.C., Gaasterland T., Glenisson P., Holstege F.C., Kim I.F., Markowitz V., Matese J.C., Parkinson H., Robinson A., Sarkans U., Schulze-Kremer S., Stewart J., Taylor R., Vilo J., Vingron M. (2001) Minimum information about a microarray experiment (MIAME)-toward standards for microarray data. Nat. Genet. 29(4):365-71.

Brikun I.A., Reeves A.R., Cernota W.H., Luu M.B., Weber J.M. (2004) The erythromycin biosynthetic gene cluster of *Aeromicrobium erythreum*. J. Ind. Microbiol. Biotechnol. 31(7):335-44. Epub 2004 Jul 15.

Brosius, J., Palmer, M.L., Kennedy, J.P., and H.P. Noller. (1978) Complete nucleotide sequence of a 16S ribosomal RNA gene from *Escherichia coli*. Proc. Natl. Acad. Sci. USA 75:4801-4805.

Burns, N., Grimwade, B., Ross-Macdonald, P.B., Choi, E.Y., Finberg, K., Roeder, G.S., Snyder, M. (1994) Large-scale analysis of gene exression, protein localisation and gene disruption in *Saccharomyces cerevisiae*. Genes Dev. 8:1087-1105.

Call D.R., Borucki M.K., Loge F.J. (2003) Detection of bacterial pathogens in environmental samples using DNA microarrays. J. Microbiol. Methods. 53(2):235-43.

Chan, V., Graves, D.J., McKenzie, S.E. (1995) The biophysics of DNA hybridization with immobilized oligonucleotide probes. Biophys. J. 69(6):2243-2255.

Charlebois R.L., Beiko R.G., Ragan M.A. (2003) Microbial phylogenomics: Branching out. Nature. 16; 421(6920):217.

Chater K.F. (1993) Genetics of differentiation in Streptomyces. Annu. Rev. Microbiol. 47:685-713.

Cheung, D.T, Nimni M.E. (1982) Mechanism of crosslinking of proteins by glutaraldehyde I: reaction with model compounds. Connect. Tissue Res. 10(2):187-199.

Cheung, V.G., Morley, M., Aguilar, F., Massimi, A., Kucherlapati R., and Childs, G. (1999) Making and reading microarrays. Nat. Genet. 21: 15-19.

Chrisey, L.A., Lee, G.U., O'Ferrall, C.E. (1996) Covalent attachment of synthetic DNA to self-assembled monolayer films. Nucleic Acids Res. 1996 24(15):3031-9.

Church, G.M. and Gilbert, W. (1984) Genomic sequencing. Proc. Natl. Acad. Sci. USA 81:1991-5.

Clayton, R.A., Sutton, G., Hinkle, Jr., P.S., Bult, C., and Fields, C. (1995) Intraspecific variation in small-subunit rRNA sequences in GenBank: why single sequences may not adequately represent prokaryotic taxa. Int. J. Syst. Bacteriol. 45:595-599.

Clement, B.G., Kehl, L.E., DeBord, K.L., Kitts, C.L. (1998) Terminal restriction fragment patterns (TRFPs), a rapid, PCR-based method for the comparison of complex bacterial communities. J. Microbiol. Methods. 31:135-142.

Collins, J.S., Goldsmith, T.H. (1981) Spectral properties of fluorescence induced by glutaraldehyde fixation. J Histochem Cytochem 29(3):411-414.

Cook K L , Layton A C , Dionisi H M , Fleming J T , Sayler G S. (2004) Evaluation of a plasmid-based 16S-23S rDNA intergenic spacer region array for analysis of microbial diversity in industrial wastewater. J. Microbiol. Methods. 57(1):79-93.

Cummings, C.A. and Relman, D.A. (2000) Using DNA microarrays to study host-microbe interactions. Emerg. Infect. Dis. 6:513-525.

DeGraaf, A.A., Eggeling, L., Sahm, H. (2001) Metabolic engineering for L-lysine production by *Corynebacterium glutamicum*. Adv Biochem Eng Biotechnol. 73:9-29.

Denef V.J., Park J., Rodrigues J.L., Tsoi T.V., Hashsham S.A., Tiedje J.M. (2003) Validation of a more sensitive method for using spotted oligonucleotide DNA microarrays for functional genomics studies on bacterial communities. Environ. Microbiol. 5(10):933-43.

Dennis P., Edwards E.A., Liss S.N., Fulthorpe R. (2003) Monitoring gene expression in mixed microbial communities by using DNA microarrays. Appl. Environ. Microbiol. 2003 Feb;69(2):769-78.

DeRisi, J.L., Iyer, V.R. and Brown, P.O. (1997) Exploring the metabolic and genetic control of gene expression on a genomic scale. Science 278(24):680-686.

DeSaizieu, A., Certa, U., Warrington, J., Gray, C., Keck, W. and Mous, J. (1998) Bacterial transcript imaging by hybridization of total RNA to oligonucleotide arrays. Nat. Biotechnol. 16:45-48.

Diehn, M., Eisen, M.B., Botstein, D., Brown, P.O. (2000) Large-scale identification of secreted and membrane associated gene products using DNA microarrays. Nature Genet. 25:58-62.

Distler J., Ebert A., Mansouri K., Pissowotzki K., Stockmann M., Piepersberg W. (1987) Gene cluster for streptomycin biosynthesis in Streptomyces griseus: nucleotide sequence of three genes and analysis of transcriptional activity. Nucleic Acids Res. 12;15(19):8041-56.

Drmanac, S., Kita, D., Labat, I., Hauser, B., Schmidt, C., Burczak, J.D., Drmanac, R. (1998) Accurate sequencing by hybridization for DNA diagnostics and individual genomics. Nature Biotechnol. 16(1):54-58.

Drobyshev, A., Mologina, N., Shik, V., Pobedimskaja, D., Yershov, G. and Mirzabekov, A. (1997) Sequence analysis by hybridization with oligonucleotide microchip: identification of B-thalassemia mutations. Gene 188:45-52.

Edman, C.F., Raymond, D.E., Wu, D.J., Tu, E., Sosnowski, R.G., Butler, W.F., Nerenberg, M., Heller, M.J. Electric field directed nucleic acid hybridization on microchips. Nucleic Acid Res. 1997; 25:4907-4914.

Ferguson, J.A., Boles, T.C., Adams, C.P., Walt, D.R. (1996) A fiber-optic DNA biosensor microarray for the analysis of gene expression. Nat Biotechnol. 14:1681-1684.

Fodor, S.P., Read, J.L., Pirrung, M.C., Stryer, L., Lu, A.T., Solas, D. (1991) Light-directed, spatially adressable parallel chemical synthesis. Science 251:767-773.

Fox, G.E., Wisotzkey, J.D., and Jurtshuk, P.Jr. (1992) How close is close: 16S rRNA sequence identity may not be sufficient to quarantee species identity. Int J Syst Bacteriol. 42:166-170.

Forman, J.E.,Walton, I.D.,Stern, D.,Rava, R.P.,Trulson, M.O. (1998) Thermodynamics of duplex formation and mismatch discrimination on photolithographically synthesized oligonucleotide arrays. Acs. Symposium Series 682:206-228.

Franssen-van Hal N.L., Vorst O., Kramer E., Hall R.D., Keijer J. (2002) Factors influencing cDNA microarray hybridization on silylated glass slides. Anal. Biochem. 308(1):5-17.

Fuchs BM, Wallner G, Beisker W, Schwippl I, Ludwig W, Amann R. (1998) Flow cytometric analysis of the in situ accessibility of *Escherichia coli* 16S rRNA for fluorescently labeled oligonucleotide probes. Appl. Environ. Microbiol. 64(12):4973-82.

Geistlich M., Losick R., Turner J.R., Rao R.N. (1992) Characterization of a novel regulatory gene governing the expression of a polyketide synthase gene in *Streptomyces ambofaciens*. Mol. Microbiol. 6(14):2019-29.

Ghosh, S.S., Musso, G.F. (1987) Covalent attachment of oligonucleotides to solid supports. Nucleic Acids Res. 15(13):5353-5372.

Gill, R.T., DeLisa, M.P., Valdes, J.J., Bentley, W.E. (2001) Genomic analysis of high-cell density recombinant *Escherichia coli* fermenattion and "cell conditioning" for improved recombiannt protein yield. Biotechnol. Bioeng. 72:85-95.

Gingeras, T.R., Ghandour, G., Wang, E., Berno, A., Small, P.M., Drobniewski, F., Alland, D., Desmond, E., Holodnij, M. and Drenkow, J. (1998) Simultaneous genotyping and species identification using hybridization pettern recognition analysis of generic mycobacterium DNA arrays. Genome Res. 8:435-448.

Gramajo H.C., Takano E., Bibb M.J. (1993) Stationary-phase production of the antibiotic actinorhodin in *Streptomyces coelicolor* A3(2) is transcriptionally regulated. Mol. Microbiol. 7(6):837-45.

Granjeaud, S., Bertucci, F. and Jordan, B.R. (1999) Expression profiling: DNA arrays in many guises. BioEssays 21:781-790.

Graves, D.J. (1999) Powerful tools for genetic analysis come of age. TIBTECH 17:127-134.

Gray, D.E., Case-Green, S.C., Fell, T.S., Dobson, P.J. and Southern, E.M. (1997) Ellipsometric and interferometric characterization of DNA probes immobilised on a combinatorial array. Langmuir 13:2833-2842.

Groth I., Schumann P., Weiss N., Martin K., Rainey F.A. (1996) Agrococcus jenensis gen. nov., sp. nov., a new genus of actinomycetes with diaminobutyric acid in the cell wall. Int. J. Syst. Bacteriol. 46(1):234-9.

Groth, I., Schumann, P., Rainey, F.A., Martin, K., Schuetze, B., and Augsten, K. (1997) Bogoriella caseilytica gen. Nov., sp. Nov., a new alcaliphilic actinomycete from a soda lake in Africa. Internat. J. Syst. Bacteriol. 47 (3):788-794.

Gruber, T.M., Bryant, D.A. (1997) Molecular systematic studies of eubacteria, using sigma70-type sigma factors of group 1 and group 2. J. Bacteriol. 179(5):1734-47.

Guertler, V., Stanisich, V.A. (1996) New approaches to typing and identification of bacteria using the 16S-23S rDNA spacer region. Microbiology 142:3-16.

Guo, Z., Guilfoyle, R.A., Thiel, A.J., Wang, R. and Smith, R. (1994) Direct fluorescence analysis of genetic polymorphisms by hybridizazion with oligonucleotide arrays on glass supports. Nucleic Acids Res. 22(24):5456-5465.

Gutell, R.R., Larsen, N., and Woese, C.R. (1994) Lessons from evolving rRNA: 16S and 23S rRNA structures from a comparative perspective. Microbiol. Rev. 58:10-26.

Gygi, S.P., Rist, B., Gerber, S.A., Turecek, F., Gelb, M.H., Aebersold, R. (1999) Quantitative analysis of complex protein mixtures using isotope coded affinity tags. Nature Biotechnol. 17:994-999.

Hacia, J.G., Brody, L.C., Chee, M.S., Fodor, S.P.A., Collins, F.S. (1996) Detection of heterozygous mutations in BRCA 1 using high density oligonucleotide arrays and two-color fluorescence analysis. Nature Genet. 14:441-447.

Halperin A, Buhot A, Zhulina EB. (2004) Sensitivity, specificity, and the hybridization isotherms of DNA chips. Biophys. J. 86(2):718-30.

Hanel F., Schumann G., Fiedler G. and Krugel H. (1993) Stimulation of erythromycin A yield by integration of a chromosomal DNA fragment including the eryC1 gene into the chromosome of *Saccharopolyspora erythraea*. Biotechnol. Lett. 15 (2): 105-110.

Hayward, R.E., DeRisi, J.L., Alfadhli, S., Kaslow, D.C., Brown, P.O. and Rathod, P.K. (2000) Shotgun DNA microarrays and stage-specific gene expression in *Plasmodium falciparum* malaria. Mol. Microbiol. 35:6-14.

Heller, R.A., Schena, M., Chai, A., Shalon, D., Bedilion, T., Gilmore, J., Woolley, D.E., Davi,s R.W. (1997) Discovery and analysis of inflammatory disease-related genes using cDNA microarrays. Proc. Natl. Acad. Sci. U S A 94(6):2150-5.

Hopwood, D.A., Bibb, M.J., Chater, K.F., Kieser, T., Bruton, C.J., Kieser, H.M., Lydiate, D.J., Smith, C.P., Ward, J.M. and Schrempf, H.(1985) Genetic manipulation of Streptomyces: a laboratory manual. John Innes Foundation, Norwich, United Kingdom.

Hopwood D.A., Chater K.F., Bibb M.J. (1995) Genetics of antibiotic production in *Streptomyces coelicolor* A3(2), a model streptomycete. Biotechnology 28:65-102.

Hopwood DA. (1999) Forty years of genetics with *Streptomyces*: from in vivo through in vitro to in silico. Microbiology. 145 (Pt 9):2183-202.

Huang J., Lih C.J., Pan K.H., Cohen S.N. (2001) Global analysis of growth phase responsive gene expression and regulation of antibiotic biosynthetic pathways in *Streptomyces coelicolor* using DNA microarrays. Genes Dev. 15(23):3183-92.

Ideker, T., Thorsson, V., Ranish, J.A., Christmas, R., Buhler, J., Eng, J.K., Bumgarner, R., Goodlett, D.R., Aebersold, R., Hood, L. (2001) Integrated genomic and proteomic analyses of a systematically perturbed metabolic network. Science 292(5518):929-34.

Jensen, M.A., Webster, J.A., and Straus, N. (1993) Rapid identification of bacteria on the basis of polymerase chain reaction-amplified ribosomal DNA spacer polymorphisms. Appl. Environ. Microbiol. 59:945-952.

Joos, B., Kuster, H., Cone, R. (1997) Covalent attachment of hybridizable oligonucleotides to glass supports. Anal. Biochem. 247(1):96-101.

Kato-Maeda M., Rhee J.T., Gingeras T.R., Salamon H., Drenkow J., Smittipat N., Small P.M. (2001) Comparing genomes within the species *Mycobacterium tuberculosis*. Genome Res. 11(4):547-54.

Kennedy J., Murli S., Kealey J.T. (2003) 6-Deoxyerythronolide B analogue production in Escherichia coli through metabolic pathway engineering. Biochemistry 9;42(48):14342-8.

Keramas G., Bang D.D., Lund M., Madsen M., Rasmussen S.E., Bunkenborg H., Telleman P., Christensen C.B. (2003) Development of a sensitive DNA microarray suitable for rapid detection of *Campylobacter* spp. Mol. Cell. Probes. 17(4):187-96.

Khrapko KR, Lysov YuP, Khorlyn AA, Shick VV, Florentiev VL, Mirzabekov AD. (1989) An oligonucleotide hybridization approach to DNA sequencing. FEBS Lett. 9;256(1-2):118-22.

Kieser T., Bibb M.J., Chater K.F., Hopwood D.A. (2000) Practical *Streptomyces* genetics. John Innes Foundation, Norwich, United Kingdom.

Kikugawa K, Kato T, Beppu M, Hayasaka A. (1989) Fluorescent and cross-linked proteins formed by free radical and aldehyde species generated during lipid oxidation. Adv. Exp. Med. Biol. 266: 345-56; discussion 357.

Klatte S., Rainey F.A., Kroppenstedt R.M. (1994) Transfer of *Rhodococcus aichiensis* Tsukamura 1982 and Nocardia amarae Lechevalier and Lechevalier 1974 to the genus *Gordona* as *Gordona aichiensis* comb. nov. and *Gordona amarae* comb. nov. Int. J. Syst. Bacteriol. 44(4):769-73.

Kleespies M., Kroppenstedt R.M., Rainey F.A., Webb L.E., Stackebrandt E. (1996) Mycobacterium hodleri sp. nov., a new member of the fast-growing mycobacteria capable of degrading polycyclic aromatic hydrocarbons. Int. J. Syst. Bacteriol. 46(3):683-7.

Koizumi Y., Kelly J.J., Nakagawa T., Urakawa H., El-Fantroussi S., Al-Muzaini S., Fukui M., Urushigawa Y., Stahl D.A. (2002) Parallel characterization of anaerobic toluene- and ethylbenzene-degrading microbial consortia by PCR-denaturing gradient gel electrophoresis, RNA-DNA membrane hybridization, and DNA microarray technology. Appl. Environ. Microbiol. 68(7):3215-25.

Korycka-Machala, M., Rumijowska-Galewicz, A., Lisowska, K., Ziolkowskit, A., Sedlacze, L. (2001) Enhancement of beta-sitosterol transformation in *Mycobacterium vaccae* with increased cell wall permeability. Acta Microbiol. Pol. 50(2):107-15.

Kopczynski, E.D., Bateson, M.M., and Ward, D.M. (1994) Recognition of chimeric small-subunit ribosomal DNAs composed of genes from uncultivated microorganisms. Appl. Environ. Microbiol. 60:746-748.

Lamture, J.B., Beattie, K.L., Burke, B.E., Eggers, M.D., Ehrlich, D.J., Fowler, R., Hollis, M.A., Kosicki, B.B., Reich, R.K., Smith, S.R., Varma, R.S., Hogan, M.E. (1994) Direct detection of

nucleic acid hybridization on the surface of a charged couple device. Nucleic Acid Res. 22:2121-2125.

Lane, D.J., Field, K.G., Olsen, G.J., and Pace, N.R. (1988) Reverse transcriptase sequencing of ribosomal RNA for phylogenetic analysis. Methods Enzymol. 167:138-144.

Lee, S.Y., Bollinger, J., Bezdicek, D., Ogram, A. (1996) Estimation of the abundance of an uncultured soil bacterial strain by a competitive quantitative PCR method. Appl. Environ. Microbiol. 62(10):3787-93.

Liesack, W., Weyland, H., and Stackebrandt, E. (1991) Potential risks of gene amplification by PCR as determined by 16S rDNA analysis of a mixed-culture of strict barophilic bacteria. Microb. Ecol. 21:191-198.

Lima, W.F., Monia, B.P., Ecker, D.J., Freier, S.M. (1992) Implication of RNA structure on antisense oligonucleotide hybridization kinetics. Biochemistry 31(48):12055-2061.

Lemieux, B., Aharoni, A. and Schena, M. (1998) Overview of DNA chip technology. Mol. Breeding 4, 277-289.

Lipshutz, R. J., Morris, D., Chee, M., Hubbel, E., Kozal, M. J., Shah, N., Shen, N., Yang, R. and Fodor, S.P.A. (1995) Using oligonucleotide probe array to access genetic diversity. BioTechniques 19, 442-447.

Lockhart, D. J.,Dong, H., Byrne, M.C., Follettie, M.T., Chee, M.S., Mittmann, M., Wang, C., Kobayashi, M., Horton, H., Brown, E.L. (1996) Expression monitoring by hybridization to high-density oligonucleotide arrays. Nat. Biotechnol. 14:1675-1680.

Lockhart D.J. and Winzeler E. A. Genomics, gene expression and DNA arrays. Nature 2000; 405:827-836.

Long, P.F., Wilkinson, C.J., Bisang, C.P., Cortes, J., Dunster, N., Oliynyk, M., McCormick, E., McArthur, H., Mendez, C., Salas, J.A., Staunton, J., Leadlay, P.F. (2002) Engineering specificity of starter unit selection by the erythromycin-producing polyketide synthase. Mol. Microbiol. 43(5):1215-25.

Ludwig, W., Schleifer, K.H. (1999) Phylogeny of bacteria beyond the 16S rRNA standard. ASM News 65:752-757.

Lum AM, Huang J, Hutchinson CR, Kao CM. (2004) Reverse engineering of industrial pharmaceutical-producing actinomycete strains using DNA microarrays. Metab. Eng. 2004 Jul;6(3):186-96.

Maidak, B.L., Cole, J.R., Parker, C.T. Jr, Garrity, G.M., Larsen, N., Li, B., Lilburn, T.G., McCaughey, M.J., Olsen, G.J., Overbeek, R., Pramanik, S., Schmidt, T.M., Tiedje, J.M., Woese, C.R. (1999) A new version of the RDP (Ribosomal Database Project). Nucleic Acids Res. 27(1):171-3.

Maniatis, T., Fritsch, E.F., Sambrook, J. (1982) Molecular cloning: a laboratory manual. Cold Spring Harbor: Cold Spring Harbor Laboratory Press.

Mann M. (1999) Quantitative proteomics? Nature Biotechnol. 17:954-955.

Manz, W., Amann, R., Ludwig, W., Wagner, M., and Schleifer, K.-H. (1992) Phylogenetic oligonucleotide probes for the major subclasses of proteobacteria: problems and solutions. System. Appl. Microbiol. 15:593-600.

Marin-Sanguino, A., Torres, N.V. (2000) Optimization of tryptophan production in bacteria. Design of a strategy for genetic manipulation of the tryptophan operon for tryptophan flux maximization. Biotechnol. Prog. 16(2):133-45.

Matson, R.S., Rampal, J., Pentoney, S.L.J., Anderson, P.D., Coassin, P. (1995) Biopolymer synthesis on polypropylene supports: Oligonucleotide arrays. Anal. Biochem 224:110-116.

Maxam A.M., Gilbert W. (1977) A new method for sequencing DNA. Proc. Natl. Acad. Sci U S A. 74(2):560-4.

Meyerhans, A., Yartanian, J., and Wain-Hobson, S. (1990) DNA recombination during PCR. Nucleic Acids Res. 18:1687-1691.

Michael, K.L., Taylor, L.C., Schultz, S.L., Walt, D.R. (1998) Randomly ordered adressable high-density optical sensor arrays. Anal. Chem. 70:1242-1248.

Mir, K.U., Southern, E.M. (1999) Determining the influence of structure on hybridization using oligonucleotide arrays. Nat. Biotechnol. 17:788-792.

Mirzabekov, A. (1994) DNA sequencing by hybridization: a megasequencing method and a diagnostic tool? Trends Biotechnol. 12: 27-32.

Mollet, C., Drancourt, M., Raoult, D. (1997) *rpoB* sequence analysis as a novel basis for bacterial identification. Mol Microbiol. 26(5):1005-11.

Monsan, P., Puzo, G., Mazarguil, H. (1975) Mechanism of glutaraldehyde-protein bond formation. Biochimie. 57(11-12):1281-92.

Moore, B.S., Piel, J. (2000) Engineering biodiversity with type II polyketide synthase genes. Antonie Van Leeuwenhoek 78(3-4):391-8.

Nakamura K., Hiraishi A., Yoshimi Y., Kawaharasaki M., Masuda K., Kamagata Y. Microlunatus phosphovorus gen. nov., sp. nov., a new gram-positive polyphosphate-accumulating bacterium isolated from activated sludge. Int. J. Syst. Bacteriol. 1995 Jan;45(1):17-22.

Narva K.E., Feitelson J.S. (1990) Nucleotide sequence and transcriptional analysis of the redD locus of *Streptomyces coelicolor* A3(2). J. Bacteriol. 172(1):326-33.

Ogawa-Miyata, Y., Kojima, H., Sano, K. (2001) Mutation analysis of the feedback inhibition site of aspartokinase III of *Escherichia coli* K-12 and its use in L-threonine production. Biosci. Biotechnol. Biochem. 65(5):1149-54.

Oh, M.K., Liao, J.C. (2000) Gene expression profiling by DNA microarrays and metabolic fluxes in *Escherichia coli*. Biotechnol. Prog. 16:278-286.

Paradkar, A.S., Mosher, R.H., Anders, C., Griffin, A., Griffin, J., Hughes, C., Greaves, P., Barton, B., Jensen, S.E. Applications of gene replacement technology to *Streptomyces clavuligerus* strain development for clavulanic acid production. Appl. Environ. Microbiol. 67(5):2292-7.

Pease, A.C., Solas, D., Sullivan, E.J., Cronin, M.T., Holmes, C.P., Fodor, S.P. (1994) Light-generated oligonucleotide arrays for rapid DNA sequence analysis. Proc. Natl. Acad. Sci. USA 91:5022-5026.

Raibaud A., Zalacain M., Holt T.G., Tizard R., Thompson C.J. (1991) Nucleotide sequence analysis reveals linked N-acetyl hydrolase, thioesterase, transport, and regulatory genes encoded by the bialaphos biosynthetic gene cluster of *Streptomyces hygroscopicus*. J. Bacteriol. 173(14):4454-63.

Rainey F.A., Klatte S., Kroppenstedt R.M., Stackebrandt E. (1995) *Dietzia*, a new genus including *Dietzia maris* comb. nov., formerly Rhodococcus maris. Int. J. Syst. Bacteriol. 1995 Jan;45(1):32-6.

Ramdas, L., Coombes, K.R., Baggerly, K., Abruzzo, L., Highsmith, W.E., Krogmann, T., Hamilton, S.R., Zhang, W. (2001) Sources of nonlinearity in cDNA microarray expression measurements. Genome Biol. 2(11):RESEARCH0047.

Rasmussen, S.R., Larsen, M.R., Rasmussen, S.E. (1991) Covalent immobilization of DNA onto polystyrene microwells: the molecules are only bound at the 5' end. Anal. Biochem. 198(1):138-42.

Reeves A.R., English R.S., Lampel J.S., Post D.A., Vanden Boom T.J. (1999) Transcriptional organization of the erythromycin biosynthetic gene cluster of *Saccharopolyspora erythraea*. J. Bacteriol. 181(22):7098-106.

Reeves A.R., Weber G., Cernota W.H., Weber J.M. (2002) Analysis of an 8.1-kb DNA fragment contiguous with the erythromycin gene cluster of *Saccharopolyspora erythraea* in the eryCI-flanking region. Antimicrob. Agents Chemother. 2002 Dec;46(12):3892-9.

Richmond, C.S., Glasner, J.D., Mau, R., Jin, H. and Blattner, F.R. (1999) Genome-wide expression profiling in *Escherichia coli* K-12. Nucleic Acids Res. 27(19):3821-3835.

Rogers, Y.H., Jiang-Baucom, P., Huang, Z.J., Bogdanov, V., Anderson, S., Boyce-Jacino, M.T. (1999) Immobilization of oligonucleotides onto a glass support via disulfide bonds: A method for preparation of DNA microarrays. Anal. Biochem. 266(1):23-30.

Roller, C., Ludwig, W., Schleifer, K.H. (1992) Gram-positive bacteria with a high DNA G+C content are characterized by a common insertion within their 23S rRNA genes. J. Gen. Microbiol. 138 (Pt 6):1167-75.

Ross, D.T., Scherf, U., Eisen, M.B., Perou, C.M., Rees, C., Spellman, P., Iyer, V., Jeffrey, S.S., Van den Rijn, M., Waltham, M., Pergamenschikov, A., Lee, J.C.F., Lashkari, D., Shalon, D., Myers, T.G., Weinstein, J.N., Botstein, D. and Brown, P.O. (2000) Systematic variation in gene expression patterns in human cancer cell lines. Nat. Genet. 24:227-235.

Ross-Macdonald, P., Sheehan, A., Roeder, G.S., Snyder, M. (1997) A multipurpose transposon system for analyzing protein production, localization and function in *Saccharomyces cerevisiae*. Proc. Natl. Acad. Sci. USA 94:190-195.

Ross-Macdonald, P., Coelho, P.S., Roemer, T., Agarwal, S., Kumar, A., Jansen, R., Cheung, K.H., Sheehan, A., Symoniatis, D., Umansky, L., Heidtman, M., Nelson, F.K., Iwasaki, H., Hager, K., Gerstein, M., Miller, P., Roeder, G.S., Snyder, M. (1999) Large-scale analysis of the yeast genome by transposon tagging and gene disruption. Nature 402:413-418.

Rudi K., Nogva H.K., Moen B., Nissen H., Bredholt S., Moretro T., Naterstad K., Holck A. (2002) Development and application of new nucleic acid-based technologies for microbial community analyses in foods. Int. J. Food Microbiol. 78(1-2):171-80.

Salazar, N.M., Caetano-Annoles, G. (1996) Nucleic acid scanning-by-hybridization of enterohemorrhagic *Escherichia coli* isolates using oligodeoxynucleotide arrays. Nucleic Acid Res. 24:5056-5057.

Saluz, H.P., and Jost, J-P., A laboratory guide for *in vivo* studies of DNA methylation and protein/DNA interactions, BioMethods, volume 3, (Birkhauser, Boston, 1990).

Saluz H.P., Iqbal J., Limmon G.V., Ruryk A. and Wu Z. (2002) Fundamentals of DNA-chip/array technology for comparative gene expression analysis. Current Science 83: 829-833.

Sambrook, J., Fritsch, E.F., and Maniatis, T. (1989) Molecular cloning: a laboratory manual. Cold Spring Harbor: Cold Spring Harbor Laboratory Press.

Sanger F, Nicklen S, Coulson AR. (1977) DNA sequencing with chain-terminating inhibitors. Proc. Natl. Acad. Sci. U S A. 74(12):5463-7.

Sartor M., Schwanekamp J., Halbleib D., Mohamed I., Karyala S., Medvedovic M., Tomlinson C.R. (2004) Microarray results improve significantly as hybridization approaches equilibrium. Biotechniques 36(5):790-6.

Schena, M., Shalon, D., Davis, R.W., Brown, P.O. (1995) Quantitative monitoring of gene expression patterns with a complementary DNA microarray. Science 270(5235):467-70.

Schena, M., Shalon, D., Heller, R., Chai, A., Brown, P.O., Davis, R.W. (1996) Parallel human genome analysis: microarray-based expression monitoring of 1000 genes. Proc. Natl. Acad. Sci. U S A 93(20):10614-9.

Schena, M., Heller, R.A., Theriault, T.P., Konrad, K., Lachenmeier, E., Davis, R.W. (1998) Microarrays: biotechnology's discovery platform for functional genomics. Trends Biotechnol. 16(7):301-6.

Shchepinov, M.S., Case-Green, S.C. and Southern, E.M. (1997) Steric factors influencing hybridization of nucleic acids to oligonucleotide arrays. Nucleic Acids Res. 25(6):1155-1161.

Small J., Call D.R., Brockman F.J., Straub T.M., Chandler D.P. (2001) Direct detection of 16S rRNA in soil extracts by using oligonucleotide microarrays. Appl. Environ. Microbiol. 67(10):4708-16.

Snyder L.A., Davies J.K., Saunders N.J. (2004) Microarray genomotyping of key experimental strains of *Neisseria gonorrhoeae* reveals gene complement diversity and five new neisserial genes associated with Minimal Mobile Elements. BMC Genomics 5(1):23.

Sohn, Y.S., Nam, D.H., Ryu, D.D. (2001) Biosynthetic pathway of cephabacins in *Lysobacter lactamgenus*: molecular and biochemical characterization of the upstream region of the gene clusters for engineering of novel antibiotics. Metab. Eng. 3(4):380-92.

Southern, E.M. (1974) An improved method for transferring nucleotides from electrophoresis strips to thin layers of ion-exchange cellulose. Anal. Biochem. 62(1):317-8.

Southern, E.M., Mir, K., and Shchepinov, M. (1999) Molecular interactions on microarrays**.** Nat. Genet. 21:5-9.

Southern L.J, Hughes H, Lawford P.V, Clench M.R, Manning N.J. (2000) Glutaraldehyde-induced cross-links: a study of model compounds and commercial bioprosthetic valves. J. Heart Valve Dis. 9(2): 241-8; discussion 248-249.

Stackebrandt, E., Witt, D., Kemmerling, C., Kroppenstedt, R., and Liesack, W. (1991) Designation of *Streptomycete* 16S and 23S rRNA-based target regions for oligonucleotide probes. Appl. Environ. Microbiol. 57:1468-1477.

Stackebrandt, E., Rainey, F.A., and Ward-Rainey, N.L. (1997) Proposal for a new hierarhic classification system, *Actinobacteria* classis nov. Int. J. Syst. Bacteriol. 47:479-491.

Stassi D., Donadio S., Staver M.J., Katz L. (1993) Identification of a *Saccharopolyspora erythraea* gene required for the final hydroxylation step in erythromycin biosynthesis. J. Bacteriol. 175(1):182-9.

Stillman B.A., Tonkinson J.L. (2001) Expression microarray hybridization kinetics depend on length of the immobilized DNA but are independent of immobilization substrate. Anal. Biochem. 295(2):149-57.

Stin O.C., Carnahan A., Singh R., Powell J., Furuno J.P., Dorsey A., Silbergeld E., Williams H.N., Morris J.G. (2003) Characterization of microbial communities from coastal waters using microarrays. Environ. Monit. Assess. 81(1-3):327-36.

Summers R.G., Donadio S., Staver M.J., Wendt-Pienkowski E., Hutchinson C.R., Katz L. (1997) Sequencing and mutagenesis of genes from the erythromycin biosynthetic gene cluster of *Saccharopolyspora erythraea* that are involved in L-mycarose and D-desosamine production. Microbiology 1997 Oct;143 (Pt 10):3251-62.

Suzuki, M.T., and Giovannoni, S.J: (1996) Bias caused by template annealing in the amplification of mixtures of 16S rRNA genes by PCR. Appl. Environ. Microbiol. 62:625-630.

Tao, H., Gonzalez, R., Martinez, A., Rodriguez, A., Ingram, L.O., Preston, J.F., Shanmugam, K.T. (2001) Engineering a homoethanol pathway in *Escherichia coli*: increased glycolytic glux and levels of expression of glycolytic genes during xylose fermenattion. J. Bacteriol.183:2979-2988.

Taroncher-Oldenburg G., Griner E.M., Francis C.A., Ward B.B. (2003) Oligonucleotide microarray for the study of functional gene diversity in the nitrogen cycle in the environment. Appl. Environ. Microbiol. 69(2):1159-71.

Trebesius, K., Amann, R., Ludwig, W., Muehlegger, K., and Schleifer, K.-H. (1994) Identification of whole fixed bacterial cells with nonradioactive 23S rRNA-targeted polynucleotide probes. Appl. Environ. Microbiol. 60:3228-3235.

Troesch, A., Nguyen, H., Miyada, C.G., Desvarenne, S., Gingeras, T.R., Kaplan, P.M., Cros, P. and Mabilat, C. (1999) *Mycobacterium* species identification and rifampin resistance testing with high-density DNA probe arrays. J. Clin. Microbiol. 37:49-55.

Trombly R., Tappel A. (1975) Fractionation and analysis of fluorescent products of lipid peroxydation. Lipids 10(8):441-447.

Uhlenbeck, O.C., Baller, J., Doty, P. (1970) Complementary oligonucleotide binding to the anticodon loop of fMet-transfer RNA. Nature 225(232):508-10.

Vandamme, P., Pot, B., Gillis, M., de Vos, P., Kersters, K., Swings, J. (1996) Polyphasic taxonomy, a consensus approach to bacterial systematics. Microbiol. Rev. 60(2):407-38.

Vara J., Lewandowska-Skarbek M., Wang Y.G., Donadio S., Hutchinson C.R. (1989) Cloning of genes governing the deoxysugar portion of the erythromycin biosynthesis pathway in *Saccharopolyspora erythraea* (*Streptomyces erythreus*). J. Bacteriol. 171(11):5872-81.

Waddell, W.H., Schaffer, A.M., Becker, R.S. (1973) Visual pigments. III. Determination and interpretation of the fluorescence quantum yields of retinals, Schiff bases and protonated Schiff bases. J. Am. Chem. Soc. 95(25):8223-8227.

Wallace, R.B., Shaffer, J., Murphy, R.F., Bonner, J., Hirose, T., Itakura, K. (1979) Hybridization of synthetic oligodeoxyribonucleotides to phi chi 174 DNA: the effect of single base pair mismatch. Nucleic Acids Res. 6(11):3543-57.

Walsh, C. Enzymatic reaction mechanisms. Freeman, San Francisco, 1986.

Walt, D.R. (2000) Bead-based fiber-optic arrays. Science 287:451.

Wang, G.C.-Y., Wang, Y. (1997) Frequency of formation of chimeric molecules as a consequence of PCR coamplification of 16S rRNA genes from mixed bacterial genomes. Appl. Environ. Microbiol. 63:4645-4650.

Wang R.F., Beggs M.L., Robertson L.H., Cerniglia C.E. (2002) Design and evaluation of oligonucleotide-microarray method for the detection of human intestinal bacteria in fecal samples. FEMS Microbiol. Lett. 213(2):175-82.

Watanabe T., Murata Y., Oka S., Iwahashi H. (2004) A new approach to species determination for yeast strains: DNA microarray-based comparative genomic hybridization using a yeast DNA microarray with 6000 genes. Yeast 21(4):351-65.

Weidner, S., Arnold, W., Puhler, A. (1996) Diversity of uncultured microorganisms associated with the seagrass *Halophila stipulacea* estimated by restriction fragment length polymorphism analysis of PCR-amplified 16S rRNA genes. Appl. Environ. Microbiol. 62(3):766-71.

Wildsmith S.E., Archer G.E., Winkley A.J., Lane P.W., Bugelski P.J. (2001) Maximization of signal derived from cDNA microarrays. Biotechniques 30(1):202-6, 208.

Willse A., Straub T.M., Wunschel S.C., Small J.A., Call D.R., Daly D.S., Chandler D.P. (2004) Quantitative oligonucleotide microarray fingerprinting of *Salmonella enterica* isolates. Nucleic Acids Res. 32(5):1848-56. Print 2004.

Wilson D.J., Xue Y., Reynolds K.A., Sherman D.H. (2001) Characterization and analysis of the PikD regulatory factor in the pikromycin biosynthetic pathway of *Streptomyces venezuelae.* J Bacteriol. 183(11):3468-75.

Wilson K.H., Wilson W.J., Radosevich J.L., DeSantis T.Z., Viswanathan V.S., Kuczmarski T.A., Andersen G.L. (2002) High-density microarray of small-subunit ribosomal DNA probes. Appl. Environ. Microbiol. 68(5):2535-41.

Wilson, M., DeRisi, J., Kristensen, H.-H., Imboden, P., Rane, S., Brown, P.O. and Schoolnik, G.K. (1999) Exploring drug-induced alterations in gene expression in *Mycobacterium tuberculosis* by microarray hybridization. Proc. Natl. Acad. Sci. USA 96:12833-12838.

Woese, C.R. (1987) Bacterial evolution. Microbiol. Rev. 51:221-271.

Wrobel G, Schlingemann J, Hummerich L, Kramer H, Lichter P, Hahn M. (2003) Optimization of high-density cDNA-microarray protocols by 'design of experiments'. Nucleic Acids Res. 31(12):e67.

Wu L., Thompson D.K., Li G., Hurt R.A., Tiedje J.M., Zhou J. (2001) Development and evaluation of functional gene arrays for detection of selected genes in the environment. Appl. Environ. Microbiol. 67(12):5780-90.

Yamamoto, S., Harayama, S. (1998) Phylogenetic relationships of *Pseudomonas putida* strains deduced from the nucleotide sequences of *gyrB*, *rpoD* and 16S rRNA genes. Int. J. Syst. Bacteriol. 48:813-819.

Yassin A.F., Rainey F.A., Brzezinka H., Burghardt J., Rifai M., Seifert P., Feldmann K., Schaal K.P. (1996) *Tsukamurella pulmonis* sp. nov. Int. J. Syst. Bacteriol. 46(2):429-36.

Yoon, J.-H., Lee, S.T., and Park, Y.-H. (1998) Genetic analyses of the genus *Nocardioides* and related taxa based on 16S-23S rDNA internally transcribed spacer sequences. Int. J. Syst. Bacteriol. 48:641-650.

Zabarovsky E.R., Petrenko L., Protopopov A., Vorontsova O., Kutsenko A.S., Zhao Y., Kilosanidze G., Zabarovska V., Rakhmanaliev E., Pettersson B., Kashuba V.I., Ljungqvist O., Norin E., Midtvedt T., Mollby R., Winberg G., Ernberg I. (2003) Restriction site tagged (RST) microarrays: a novel technique to study the species composition of complex microbial systems. Nucleic Acids Res. 31(16):e95.

Zammatteo, N., Jeanmart, L., Hamels, S., Courtois, S., Louette, P., Hevesi, L. and Remacle, J. (2000) Comparison between different strategies of covalent attachment of DNA to glass surfaces to build DNA microarrays. Anal. Biochem. 280:143-150.

Zhou J., Thompson D.: Microarrays: applications in environmental microbiology. In Encyclopedia of Environmental Microbiology, vol 4. Ed. by Bitton G. New York: John Wiley & Sons; 2002: 1968-1979.

Zhu Z, Waggoner AS. (1997) Molecular mechanism controlling the incorporation of fluorescent nucleotides into DNA by PCR. Cytometry 28(3):206-11.

Acknowledgements

At this place I would like to express my deep acknowledgements to all people who helped and supported me during preparation of this work.

My special thanks go to my supervisor, **Prof. Hans Peter Saluz**, the head of the Department of Cell and Molecular Biology, HKI, Jena, where this work was carried out. I thank him for his constant help, "solid support" and for lessons in nonstandard management of scientific problems and scientific writing.

I am very grateful to **Dr. Hans Krügel** for his help, constant and great interest in this work, its organization, proceeding and preparation as well as insights and lessons in different aspects of molecular biology.

I am highly indebted to **Dr. Alexander Tretyakov** for our long, interesting and productive discussions which gave me so much for the understanding of underlying aspects of microsystem technology.

I express my gratitude to **Grit Mrotzek** for her constant help, support and friendly atmosphere in the lab. I give my sincere thanks to **Vera Hanemann** for the first insights in performing microarray experiments.

I am thankful to **Vera Klujeva** for providing a broad spectrum of activated slides.

I express my gratitude to **Dr. Karin Martin** and her colleagues **Dr. Ingrid Groth** and **Dr. Peter Schumann** for the insights into actinomycete taxonomy and bacterial chemotaxonomical characterization.

I give my sincere thanks to **Susana Kushnir** and **Katrin Hänsch** for construction and maintenance of a genomic library of *S. erythreae* DSM 40517 and for the sequencing experiments.

I am grateful to **Gino V. Limmon**, **Javeed Iqball** and **Zghaohi Wu** for their constant help and stimulative suggestions. I am much obliged to **Torsten Kroll** for his help in management and maintenance of microarray data.

I express my gratitude to **Dr. Victor O. Fedorenko and Dr. Nadija V. Kyrychenko,** heads of the Chair of Genetics and Biotechnology, Lviv's State University, Ukraine, and its research lab, respectively, for their kind supervision and providing the possibility to perform this work.

I also express my special thanks to whole **SIRS-Lab team** for full understanding and great support during final preparation of this text.

Selbständigkeitserklärung

Hiermit erkläre ich, dass ich die vorliegende Arbeit selbständig und nur unter Verwendung der angegebenen Literatur und Hilfsmittel angefertigt habe.

Jena, den 25.08.2004 Andriy Ruryk

Curriculum Vitae

Personal data

Name	Andriy Ruryk
Date & place of birth	08.03.1971, Lviv, Ukraine
Sex and marital status	Male, single
Nationality	Ukrainian

Education

1978-1988	Lviv's secondary school, Ukraine
1988	Baccalaureate (Abitur): Lviv's secondary school, Ukraine
1988-1993	Lviv's State University, Chair of Microbiology, Ukraine
1993	Diploma in biology and teacher of biology and chemistry

Experience

1993-1996	Staff scientist in the project "Molecular cloning of the alpha-amylase gene from *Bacillus amyloliquefaciens* into *Zymomonas mobilis* cells", Chair of Microbiology, Lviv's State University, Ukraine
1996-1997	Staff scientist in the project "Construction of *Streptomyces peucetius* strains with an increased capacity for production of antitumor antibiotic rubromycin", Chair of Genetics and Biotechnology, Lviv's State University, Ukraine
1997-2001	Ph.D. student at the Department of Cell and Molecular Biology, Hans-Knöll-Insititute, Jena, Germany; Supervisor: Prof. Dr. Hans-Peter Saluz.
2001-current time	Staff scientist at SIRS-Lab GmbH, Jena, Germany

Jena, den 25.08.2004 Andriy Ruryk

Publications

1. Goodz S.P., Zakal'skyj A.J., Ruryk A. (1997) Development of the transformation system for *Zymomonas mobilis* cells. In: Kovalyshyn B.J. (ed.) Actual problems of medicine, biology, veterinary and agriculture, Lviv, Ukraine, pp.73-74.

2. M. Berdichevskaya, A. Ruryk, H.P. Saluz and H. Kruegel. Identification of genetic diversity in Streptomycetes by representational difference analysis. 11th International Symposium on the biology of Actinomycetes. Sissi-Heraklion, Greece, October 24-28, 1999.

3. A. Ruryk, S. Kushnir, J. Demydchuk, M. Demydchuk, A. Tretiakov, K. Haensch, H.P. Saluz and H. Kruegel. Genomic DNA microarray for differential gene expression and metabolic engineering of *Saccharopolyspora erythraea*. 12th International Symposium on the biology of Actinomycetes. Vancouver, Canada, August 5-9, 2001.

4. Saluz H.P., Iqbal J., Limmon G.V., Ruryk A. and Wu Z. (2002) Fundamentals of DNA-chip/array technology for comparative gene expression analysis. Current Science, 83: 829-833.

5. Iqbal J., Ruryk A., Limmon G.V., Schwarz S., Tretiakov A., Duerst M., Hanel F., Saluz H.P. Sensitivity issues of HPV genotyping with oligonucleotide micro-chips (2004), in press.

Date: July 12, 2004 Andriy Ruryk

Supplement

Table 3. Results obtained on in-house prepared silylated slides upon hybridization with Cy3-end labelled rRNAf0-r2.108 PCR fragment. In element column capital letters designate spot rows and numbers designate spots from left to right. ROD, relative optical density (an Imaging Research Inc. proprietary density scale which represents an inverse logarithmic function of grey-level values).

Element	D x A - ROD x mm2	SD - ROD	Area - mm2	Bkgd	sRef	nDxA	S/N
A - 1	7.53E-06	0.0025	0.004	1.01E-06	1.44E-05	0.454	2.314
A - 2	1.50E-05	0.0049	0.004	1.20E-06	1.44E-05	0.956	4.636
A - 3	1.63E-05	0.0055	0.004	1.40E-06	1.44E-05	1.039	3.354
A - 4	3.24E-05	0.0093	0.004	6.23E-06	1.44E-05	1.821	1.333
A - 5	3.70E-05	0.0081	0.004	1.41E-06	1.44E-05	2.477	6.201
A - 6	3.94E-05	0.008	0.004	1.20E-06	1.44E-05	2.66	12.897
B - 1	2.58E-06	0.0018	0.004	0	1.44E-05	0.151	1.401
B - 2	1.05E-06	0.0009	0.004	1.40E-06	1.44E-05	0	0
B - 3	7.04E-07	0.0005	0.004	0	1.44E-05	0.02	0.185
B - 4	1.73E-06	0.0012	0.004	1.60E-06	1.44E-05	0.009	0.033
B - 5	2.58E-06	0.0013	0.004	0	1.44E-05	0.137	0.799
B - 6	3.09E-06	0.0014	0.004	0	1.44E-05	0.186	1.199
C - 1	1.95E-07	0.0003	0.004	0	1.44E-05	0	0
C - 2	7.04E-07	0.0005	0.004	0	1.44E-05	0.034	0.435
C - 3	3.43E-06	0.0014	0.004	0	1.44E-05	0.196	1.511
C - 4	2.92E-06	0.0015	0.004	1.80E-06	1.44E-05	0.078	0.244
C - 5	3.60E-06	0.0016	0.004	2.98E-06	1.44E-05	0.043	0.088
C - 6	4.97E-06	0.0022	0.004	1.79E-06	1.44E-05	0.221	0.966
D - 1	3.64E-07	0.0004	0.004	1.60E-06	1.44E-05	0	0
D - 2	1.40E-06	0.002	0.004	0	1.44E-05	0.041	0.221
D - 3	3.64E-07	0.0004	0.004	0	1.44E-05	0	0
D - 4	4.80E-06	0.0022	0.004	2.59E-06	1.44E-05	0.154	0.385
D - 5	5.47E-06	0.0016	0.004	2.59E-06	1.44E-05	0.201	0.523
D - 6	6.85E-06	0.0025	0.004	1.60E-06	1.44E-05	0.365	1.468
E - 1	4.97E-06	0.0023	0.004	2.59E-06	1.44E-05	0.166	0.415
E - 2	6.33E-06	0.0022	0.004	1.01E-06	1.44E-05	0.37	2.296
E - 3	3.77E-06	0.0017	0.004	1.99E-06	1.44E-05	0.124	0.408
E - 4	6.68E-06	0.0024	0.004	1.40E-06	1.44E-05	0.367	1.516
E - 5	8.22E-06	0.0028	0.004	1.40E-06	1.44E-05	0.474	1.64
E - 6	8.93E-06	0.0038	0.004	5.17E-06	1.44E-05	0.261	0.324
F - 1	1.22E-06	0.0011	0.004	1.99E-06	1.44E-05	0	0
F - 2	2.41E-06	0.0012	0.004	1.99E-06	1.44E-05	0.029	0.089

F - 3	1.22E-06	0.0009	0.004	0	1.44E-05	0.028	0.152
F - 4	1.22E-06	0.0008	0.004	0	1.44E-05	0.069	0.894
F - 5	1.39E-06	0.0014	0.004	0	1.44E-05	0.081	1.052
F - 6	2.25E-06	0.0018	0.004	0	1.44E-05	0.1	0.54
G - 1	1.56E-06	0.0009	0.004	0	1.44E-05	0.052	0.353
G - 2	1.39E-06	0.0011	0.004	1.21E-06	1.44E-05	0.012	0.038
G - 3	1.05E-06	0.0009	0.004	0	1.44E-05	0.071	2.76E+96
G - 4	2.41E-06	0.0015	0.004	0	1.44E-05	0.139	0.894
G - 5	0	0	0.004	1.20E-06	1.44E-05	0	0
G - 6	1.21E-06	0.0007	0.004	1.01E-06	1.44E-05	0.014	0.063
H - 1	1.56E-06	0.0008	0.004	1.21E-06	1.44E-05	0.024	0.074
H - 2	3.78E-06	0.0019	0.004	0	1.44E-05	0.206	0.662
H - 3	3.09E-06	0.0018	0.004	0	1.44E-05	0.2	2.584
H - 4	1.22E-06	0.0012	0.004	0	1.44E-05	0.069	0.897
H - 5	2.92E-06	0.0017	0.004	1.20E-06	1.44E-05	0.12	0.58
H - 6	2.24E-06	0.0015	0.004	1.21E-06	1.44E-05	0.072	0.307
I - 1	1.22E-06	0.0011	0.004	0	1.44E-05	0.069	0.896
I - 2	8.76E-07	0.0008	0.004	0	1.44E-05	0.059	2.30E+96
I - 3	3.64E-07	0.0004	0.004	0	1.44E-05	0	0
I - 4	0.0001	0.0119	0.004	6.23E-05	1.44E-05	4.709	1.092
I - 5	0.0003	0.0228	0.004	9.58E-05	1.44E-05	11.164	2.277
I - 6	0.0003	0.0291	0.004	1.28E-04	1.44E-05	10.299	1.415
J - 1	1.22E-06	0.0008	0.004	0	1.44E-05	0.042	0.323
J - 2	3.65E-07	0.0006	0.004	0	1.44E-05	0	0
J - 3	7.04E-07	0.0005	0.004	0	1.44E-05	0.006	0.048
J - 4	5.56E-05	0.0091	0.004	2.57E-05	1.44E-05	2.078	1.213
J - 5	0.0001	0.0123	0.004	4.80E-05	1.44E-05	4.31	1.684
J - 6	0.0001	0.0117	0.004	6.37E-05	1.44E-05	3.327	1.002
K - 1	4.28E-06	0.0017	0.004	3.38E-06	1.44E-05	0.063	0.114
K - 2	4.63E-06	0.0018	0.004	1.01E-06	1.44E-05	0.252	1.283
K - 3	4.12E-06	0.0019	0.004	3.98E-06	1.44E-05	0.009	0.014
K - 4	0.0002	0.0106	0.004	6.08E-05	1.44E-05	6.272	1.679
K - 5	0.0002	0.0112	0.004	6.34E-05	1.44E-05	7.441	1.884
K - 6	0.0002	0.0133	0.004	7.42E-05	1.44E-05	6.847	1.585
L - 1	6.23E-05	0.0075	0.004	2.01E-05	1.44E-05	2.939	2.079
L - 2	6.36E-05	0.0079	0.004	1.99E-05	1.44E-05	3.037	1.81
L - 3	5.61E-05	0.0067	0.004	2.87E-05	1.44E-05	1.906	1.011
L - 4	8.40E-06	0.0031	0.004	0	1.44E-05	0.528	2.171
L - 5	6.68E-06	0.0023	0.004	2.78E-06	1.44E-05	0.271	1
L - 6	1.35E-05	0.0031	0.004	3.38E-06	1.44E-05	0.705	1.188
M - 1	1.90E-06	0.0011	0.004	1.80E-06	1.44E-05	0.007	0.023
M - 2	3.62E-06	0.0025	0.004	1.01E-06	1.44E-05	0.181	0.925
M - 3	2.92E-06	0.0016	0.004	1.21E-06	1.44E-05	0.119	0.509
M - 4	1.44E-05	0.0031	0.004	2.00E-06	1.44E-05	0.861	2.391
M - 5	1.47E-05	0.0036	0.004	8.12E-06	1.44E-05	0.46	0.649

M - 6	1.37E-05	0.0036	0.004	5.75E-06	1.44E-05	0.554	0.931
N - 1	1.95E-07	0.0003	0.004	0	1.44E-05	0.012	4.59E+95
N - 2	7.05E-07	0.0007	0.004	0	1.44E-05	0	0
N - 3	3.65E-07	0.0006	0.004	1.01E-06	1.44E-05	0	0
N - 4	9.76E-06	0.0031	0.004	2.19E-06	1.44E-05	0.527	1.841
N - 5	1.15E-05	0.0028	0.004	6.54E-06	1.44E-05	0.342	0.464
N - 6	1.47E-05	0.0031	0.004	4.96E-06	1.44E-05	0.679	1.114
A. n	84	84	84	84	84	84	84
A. Mean	2.40E-05	0.0035	0.004	9.63E-06	1.44E-05	1.004	6.57E+94
A. SD	5.35E-05	0.0048	0	2.30E-05	0	2.162	3.92E+95
A. CV	222.8182	135.8573	3.69E-06	239.176	3.87E-06	215.309	596.661
A. Total	0.002	0.2963	0.311	8.09E-04	0.001	84.367	5.52E+96

Table 4. Results obtained on commercial silylated slides (array 2) upon hybridization with Cy3-end labelled rRNAf0-r2.108 PCR fragment. In element column capital letters designate spot rows and numbers designate spots from left to right. ROD, relative optical density (an Imaging Research Inc. proprietary density scale which represents an inverse logarithmic function of grey-level values).

Element	D x A - ROD x mm2	SD - ROD	Area - mm2	Bkgd	sRef	nDxA	S/N
A - 1	0.0004	0.0627	0.004	1.72E-05	8.98E-04	0.427	13.19
A - 2	0.0005	0.0725	0.004	2.11E-05	8.98E-04	0.56	23.388
A - 3	0.0006	0.0779	0.004	2.28E-05	8.98E-04	0.612	18.412
A - 4	0.0007	0.1005	0.004	2.72E-05	8.98E-04	0.706	15.346
A - 5	0.0007	0.1048	0.004	2.46E-05	8.98E-04	0.789	16.899
A - 6	0.0008	0.1195	0.004	2.03E-05	8.98E-04	0.874	23.381
B - 1	3.60E-05	0.0054	0.004	2.42E-05	8.98E-04	0.013	0.718
B - 2	4.23E-05	0.0055	0.004	2.58E-05	8.98E-04	0.018	1.028
B - 3	4.34E-05	0.007	0.004	2.52E-05	8.98E-04	0.02	1.082
B - 4	0.0001	0.0117	0.004	2.67E-05	8.98E-04	0.109	4.069
B - 5	0.0001	0.0156	0.004	3.33E-05	8.98E-04	0.113	3.922
B - 6	0.0001	0.0148	0.004	2.72E-05	8.98E-04	0.128	3.738
C - 1	5.70E-05	0.0063	0.004	3.22E-05	8.98E-04	0.028	1.214
C - 2	6.05E-05	0.0083	0.004	2.68E-05	8.98E-04	0.038	2.266
C - 3	7.75E-05	0.0106	0.004	2.29E-05	8.98E-04	0.061	2.419
C - 4	0.0002	0.0118	0.004	3.78E-05	8.98E-04	0.148	4.421
C - 5	0.0002	0.0117	0.004	5.52E-05	8.98E-04	0.138	2.048
C - 6	0.0002	0.0151	0.004	5.63E-05	8.98E-04	0.181	3.566
D - 1	4.56E-05	0.0063	0.004	3.76E-05	8.98E-04	0.009	0.44
D - 2	4.59E-05	0.005	0.004	2.10E-05	8.98E-04	0.028	1.693
D - 3	4.84E-05	0.0059	0.004	2.52E-05	8.98E-04	0.026	1.408
D - 4	0.0002	0.0159	0.004	4.12E-05	8.98E-04	0.16	4.967
D - 5	0.0002	0.014	0.004	4.96E-05	8.98E-04	0.16	3.319
D - 6	0.0002	0.0245	0.004	4.17E-05	8.98E-04	0.23	4.971
E - 1	0.0001	0.0123	0.004	5.48E-05	8.98E-04	0.085	1.883
E - 2	0.0001	0.011	0.004	3.74E-05	8.98E-04	0.103	3.026
E - 3	0.0001	0.012	0.004	3.03E-05	8.98E-04	0.131	4.744
E - 4	0.0002	0.0132	0.004	5.71E-05	8.98E-04	0.205	3.17
E - 5	0.0003	0.0199	0.004	4.75E-05	8.98E-04	0.266	5.954
E - 6	0.0004	0.0578	0.004	4.00E-05	8.98E-04	0.421	9.648
F - 1	8.02E-05	0.0094	0.004	3.88E-05	8.98E-04	0.046	1.322
F - 2	8.36E-05	0.0073	0.004	3.81E-05	8.98E-04	0.051	2.084
F - 3	9.76E-05	0.0092	0.004	3.73E-05	8.98E-04	0.067	2.456
F - 4	8.32E-05	0.0084	0.004	3.67E-05	8.98E-04	0.052	2.205
F - 5	7.86E-05	0.0089	0.004	4.15E-05	8.98E-04	0.041	1.837
F - 6	9.82E-05	0.0084	0.004	4.60E-05	8.98E-04	0.058	2.168

G - 1	5.18E-05	0.0067	0.004	2.69E-05	8.98E-04	0.028	1.067
G - 2	5.69E-05	0.0077	0.004	3.52E-05	8.98E-04	0.024	1.218
G - 3	5.57E-05	0.0054	0.004	3.41E-05	8.98E-04	0.024	1.018
G - 4	6.76E-05	0.007	0.004	3.51E-05	8.98E-04	0.036	1.409
G - 5	7.28E-05	0.0051	0.004	4.88E-05	8.98E-04	0.027	0.893
G - 6	8.08E-05	0.0076	0.004	5.68E-05	8.98E-04	0.027	0.759
H - 1	0.0001	0.0132	0.004	3.14E-05	8.98E-04	0.096	4.296
H - 2	0.0001	0.0123	0.004	4.97E-05	8.98E-04	0.085	2.537
H - 3	0.0001	0.0127	0.004	5.00E-05	8.98E-04	0.102	2.509
H - 4	0.0003	0.0472	0.004	1.79E-04	8.98E-04	0.104	0.314
H - 5	0.0002	0.067	0.004	1.09E-04	8.98E-04	0.146	0.761
H - 6	0.0003	0.0214	0.004	6.84E-05	8.98E-04	0.256	4.115
I - 1	6.14E-05	0.007	0.004	2.58E-05	8.98E-04	0.04	2.025
I - 2	7.22E-05	0.0069	0.004	4.18E-05	8.98E-04	0.034	1.182
I - 3	6.97E-05	0.0067	0.004	5.15E-05	8.98E-04	0.02	0.625
I - 4	0.0089	0	0.004	0.002	8.98E-04	8.207	2.494
I - 5	0.0089	0	0.004	0.001	8.98E-04	8.37	2.751
I - 6	0.0089	0	0.004	0.002	8.98E-04	7.686	2
J - 1	5.55E-05	0.0083	0.004	2.15E-05	8.98E-04	0.038	1.808
J - 2	5.60E-05	0.0068	0.004	2.49E-05	8.98E-04	0.035	1.27
J - 3	8.37E-05	0.0088	0.004	4.57E-05	8.98E-04	0.042	2.097
J - 4	0.0074	0.5487	0.004	4.00E-04	8.98E-04	7.831	10.588
J - 5	0.0079	0.4835	0.004	6.21E-04	8.98E-04	8.126	5.593
J - 6	0.0086	0.2521	0.004	4.42E-04	8.98E-04	9.067	12.909
K - 1	0.0002	0.0193	0.004	6.16E-05	8.98E-04	0.189	2.455
K - 2	0.0003	0.0196	0.004	7.26E-05	8.98E-04	0.244	2.965
K - 3	0.0002	0.014	0.004	8.88E-05	8.98E-04	0.177	2.382
K - 4	0.006	0.6584	0.004	2.76E-04	8.98E-04	6.35	13.008
K - 5	0.0056	0.6577	0.004	4.73E-04	8.98E-04	5.66	5.438
K - 6	0.0045	0.5745	0.004	2.75E-04	8.98E-04	4.717	10.731
L - 1	0.0014	0.0777	0.004	2.59E-04	8.98E-04	1.274	2.889
L - 2	0.0016	0.107	0.004	2.69E-04	8.98E-04	1.451	3.776
L - 3	0.0014	0.0907	0.004	2.94E-04	8.98E-04	1.247	2.758
L - 4	0.0004	0.0236	0.004	8.27E-05	8.98E-04	0.407	3.692
L - 5	0.0004	0.032	0.004	9.26E-05	8.98E-04	0.371	1.975
L - 6	0.0004	0.0366	0.004	7.20E-05	8.98E-04	0.396	3.357
M - 1	0.0002	0.015	0.004	6.38E-05	8.98E-04	0.152	2.179
M - 2	0.0002	0.0122	0.004	6.41E-05	8.98E-04	0.111	2.065
M - 3	0.0002	0.0145	0.004	6.65E-05	8.98E-04	0.155	2.334
M - 4	0.0007	0.0372	0.004	1.79E-04	8.98E-04	0.573	2.303
M - 5	0.0007	0.0393	0.004	1.43E-04	8.98E-04	0.636	3.257
M - 6	0.0007	0.0498	0.004	1.10E-04	8.98E-04	0.644	4.079
N - 1	3.16E-05	0.0046	0.004	2.92E-05	8.98E-04	0.003	0.15
N - 2	4.17E-05	0.0056	0.004	4.00E-05	8.98E-04	0.002	0.095
N - 3	3.27E-05	0.0057	0.004	3.65E-05	8.98E-04	0	0

N - 4	0.0007	0.058	0.004	1.24E-04	8.98E-04	0.599	3.276
N - 5	0.0006	0.0558	0.004	1.21E-04	8.98E-04	0.53	3.395
N - 6	0.0006	0.0522	0.004	1.14E-04	8.98E-04	0.564	3.161
A. n	84	84	84	84	84	84	84
A. Mean	0.001	0.0609	0.004	1.43E-04	8.98E-04	1	4.123
A. SD	0.0023	0.1386	0	3.17E-04	0	2.271	4.826
A. CV	221.0439	227.6318	3.69E-06	221.519	0	227.113	117.038
A. Total	0.0874	5.1145	0.311	0.012	0.075	84.004	346.362

Table 5. Results obtained on commercial silylated slides (array 3) upon hybridization with Cy3-end labelled rRNAf0-r2.108 PCR fragment. In element column capital letters designate spot rows and numbers designate spots from left to right. ROD, relative optical density (an Imaging Research Inc. proprietary density scale which represents an inverse logarithmic function of grey-level values).

Element	D x A - ROD x mm2	SD - ROD	Area - mm2	Bkgd	sRef	nDxA	S/N
A - 1	0.0006	0.0759	0.004	7.03E-05	7.79E-04	0.635	16.097
A - 2	0.0006	0.0753	0.004	7.33E-05	7.79E-04	0.643	17.851
A - 3	0.0006	0.0836	0.004	6.97E-05	7.79E-04	0.683	12.214
A - 4	0.0008	0.127	0.004	6.83E-05	7.79E-04	0.997	17.614
A - 5	0.0008	0.1201	0.004	6.60E-05	7.79E-04	0.997	24.611
A - 6	0.0008	0.1243	0.004	7.14E-05	7.79E-04	0.978	17.022
B - 1	9.86E-05	0.0077	0.004	6.66E-05	7.79E-04	0.041	0.96
B - 2	0.0001	0.0086	0.004	6.96E-05	7.79E-04	0.04	0.833
B - 3	0.0001	0.0113	0.004	6.31E-05	7.79E-04	0.056	1.482
B - 4	0.0002	0.0158	0.004	7.21E-05	7.79E-04	0.11	2.261
B - 5	0.0002	0.0178	0.004	6.41E-05	7.79E-04	0.164	4.778
B - 6	0.0002	0.0191	0.004	6.98E-05	7.79E-04	0.146	2.462
C - 1	0.0001	0.0121	0.004	6.92E-05	7.79E-04	0.04	0.995
C - 2	0.0001	0.0106	0.004	6.69E-05	7.79E-04	0.053	1.475
C - 3	0.0001	0.0114	0.004	7.11E-05	7.79E-04	0.072	1.718
C - 4	0.0002	0.0128	0.004	7.62E-05	7.79E-04	0.145	2.464
C - 5	0.0002	0.0173	0.004	8.17E-05	7.79E-04	0.142	3.016
C - 6	0.0002	0.0139	0.004	8.86E-05	7.79E-04	0.142	2.238
D - 1	0.0001	0.0108	0.004	7.52E-05	7.79E-04	0.041	0.665
D - 2	8.85E-05	0.008	0.004	8.24E-05	7.79E-04	0.008	0.147
D - 3	9.66E-05	0.0082	0.004	6.55E-05	7.79E-04	0.04	1.09
D - 4	0.0002	0.015	0.004	7.69E-05	7.79E-04	0.142	2.688
D - 5	0.0002	0.0148	0.004	7.07E-05	7.79E-04	0.142	2.186
D - 6	0.0002	0.0164	0.004	7.51E-05	7.79E-04	0.169	3.486
E - 1	0.0002	0.0127	0.004	8.66E-05	7.79E-04	0.107	1.631
E - 2	0.0001	0.014	0.004	9.16E-05	7.79E-04	0.064	0.953
E - 3	0.0002	0.0142	0.004	9.32E-05	7.79E-04	0.114	2.124
E - 4	0.0003	0.0174	0.004	8.71E-05	7.79E-04	0.219	2.925
E - 5	0.0002	0.0186	0.004	8.91E-05	7.79E-04	0.154	1.903
E - 6	0.0002	0.0157	0.004	8.07E-05	7.79E-04	0.186	3.107
F - 1	0.0001	0.012	0.004	7.99E-05	7.79E-04	0.059	1.203
F - 2	0.0001	0.0136	0.004	8.41E-05	7.79E-04	0.051	0.971
F - 3	0.0001	0.0115	0.004	8.27E-05	7.79E-04	0.07	1.634
F - 4	0.0001	0.0097	0.004	7.30E-05	7.79E-04	0.044	1.077

F - 5	0.0001	0.0112	0.004	6.13E-05	7.79E-04	0.057	1.486
F - 6	0.0001	0.01	0.004	7.06E-05	7.79E-04	0.051	1.552
G - 1	9.44E-05	0.0101	0.004	7.60E-05	7.79E-04	0.024	0.617
G - 2	9.03E-05	0.008	0.004	6.58E-05	7.79E-04	0.031	0.733
G - 3	8.74E-05	0.0094	0.004	7.57E-05	7.79E-04	0.015	0.325
G - 4	9.98E-05	0.0079	0.004	7.40E-05	7.79E-04	0.033	0.825
G - 5	9.99E-05	0.0094	0.004	6.52E-05	7.79E-04	0.045	1.561
G - 6	9.14E-05	0.0082	0.004	8.32E-05	7.79E-04	0.011	0.216
H - 1	0.0001	0.0124	0.004	7.88E-05	7.79E-04	0.073	1.289
H - 2	0.0002	0.012	0.004	6.69E-05	7.79E-04	0.124	3.665
H - 3	0.0002	0.0198	0.004	8.49E-05	7.79E-04	0.111	2.09
H - 4	0.0002	0.0162	0.004	8.28E-05	7.79E-04	0.143	2.326
H - 5	0.0002	0.0174	0.004	8.97E-05	7.79E-04	0.148	3.489
H - 6	0.0002	0.0149	0.004	7.59E-05	7.79E-04	0.2	3.539
I - 1	9.47E-05	0.0088	0.004	7.14E-05	7.79E-04	0.03	0.673
I - 2	9.41E-05	0.0076	0.004	6.76E-05	7.79E-04	0.034	0.694
I - 3	0.0001	0.0103	0.004	7.23E-05	7.79E-04	0.04	0.976
I - 4	0.0089	0	0.004	6.49E-04	7.79E-04	10.612	4.902
I - 5	0.0089	0	0.004	8.00E-04	7.79E-04	10.418	3.717
I - 6	0.0089	0	0.004	9.87E-04	7.79E-04	10.178	3.583
J - 1	8.06E-05	0.0079	0.004	6.00E-05	7.79E-04	0.026	0.76
J - 2	8.53E-05	0.0082	0.004	6.63E-05	7.79E-04	0.024	0.697
J - 3	0.0001	0.0112	0.004	5.19E-05	7.79E-04	0.073	3.818
J - 4	0.0049	0.7496	0.004	3.06E-04	7.79E-04	5.881	7.561
J - 5	0.0056	0.7404	0.004	3.35E-04	7.79E-04	6.747	7.693
J - 6	0.006	0.7135	0.004	1.66E-04	7.79E-04	7.511	25.905
K - 1	0.0001	0.0126	0.004	7.75E-05	7.79E-04	0.091	2.276
K - 2	0.0002	0.0141	0.004	8.58E-05	7.79E-04	0.104	1.806
K - 3	0.0002	0.0149	0.004	8.73E-05	7.79E-04	0.111	1.612
K - 4	0.0039	0.4643	0.004	2.53E-04	7.79E-04	4.715	9.576
K - 5	0.0055	0.671	0.004	4.60E-04	7.79E-04	6.411	4.764
K - 6	0.0045	0.5877	0.004	2.46E-04	7.79E-04	5.451	9.127
L - 1	0.0008	0.044	0.004	1.57E-04	7.79E-04	0.788	3.467
L - 2	0.0009	0.051	0.004	1.42E-04	7.79E-04	0.916	5.095
L - 3	0.0009	0.0744	0.004	2.57E-04	7.79E-04	0.889	1.933
L - 4	0.0003	0.0195	0.004	7.43E-05	7.79E-04	0.332	6.613
L - 5	0.0004	0.0225	0.004	8.22E-05	7.79E-04	0.348	6.928
L - 6	0.0004	0.0223	0.004	9.74E-05	7.79E-04	0.349	2.967
M - 1	0.0001	0.0129	0.004	7.53E-05	7.79E-04	0.073	1.33
M - 2	0.0001	0.0088	0.004	7.12E-05	7.79E-04	0.078	2.776
M - 3	0.0002	0.0127	0.004	8.28E-05	7.79E-04	0.108	2.628
M - 4	0.0005	0.0424	0.004	9.73E-05	7.79E-04	0.493	5.013

M - 5	0.0006	0.0486	0.004	1.18E-04	7.79E-04	0.567	3.175
M - 6	0.0006	0.0456	0.004	1.34E-04	7.79E-04	0.559	3.363
N - 1	5.10E-05	0.0052	0.004	5.99E-05	7.79E-04	0	0
N - 2	6.44E-05	0.0067	0.004	6.81E-05	7.79E-04	0	0
N - 3	6.21E-05	0.0072	0.004	6.12E-05	7.79E-04	0.001	0.035
N - 4	0.0004	0.0241	0.004	8.45E-05	7.79E-04	0.347	3.929
N - 5	0.0005	0.0329	0.004	8.81E-05	7.79E-04	0.47	5.716
N - 6	0.0005	0.0314	0.004	1.11E-04	7.79E-04	0.483	3.577
A. n	84	84	84	84	84	84	84
A. Mean	0.0009	0.0676	0.004	1.23E-04	7.79E-04	1	3.932
A. SD	0.002	0.1679	0	1.51E-04	0	2.403	5.088
A. CV	222.8219	248.3763	3.69E-06	122.768	5.45E-06	240.213	129.409
A. Total	0.0758	5.6788	0.311	0.01	0.065	84.016	330.277

Table 6. Comparison between wave-guide wafer and Borofloat-33 slides. Results obtained using Borofloat slides. Only spots without overlapping with or disturbance from the regions of high background signal were evaluated.

Element	D x A - ROD x mm2	SD - ROD	Area - mm2	Bkgd	sRef	nDxA	S/N
B - 1	1.0925	0.0114	17.05	0.328	0.252	3.04	6.181
B - 4	1.342	0.0252	17.05	0.424	0.252	3.649	5.719
B - 8	1.4036	0.0131	17.05	0.538	0.252	3.44	6.857
C - 1	0.3038	0.004	17.05	0.222	0.252	0.324	1.087
C - 2	0.3255	0.0055	17.05	0.228	0.252	0.388	1.548
C - 6	0.342	0.004	17.05	0.293	0.252	0.193	0.426
C - 8	0.4006	0.0039	17.05	0.3	0.252	0.402	3.244
D - 2	0.626	0.008	17.05	0.274	0.252	1.399	1.807
D - 3	0.7302	0.0091	17.05	0.324	0.252	1.616	3.29
D - 4	0.8323	0.0084	17.05	0.368	0.252	1.846	3.751
D - 5	0.7304	0.0068	17.05	0.308	0.252	1.678	6.478
D - 6	0.832	0.009	17.05	0.324	0.252	2.021	5.726
D - 7	0.9692	0.0127	17.05	0.416	0.252	2.2	4.571
D - 8	1.0908	0.013	17.05	0.403	0.252	2.733	5.336
E - 2	0.186	0.0027	17.05	0.114	0.252	0.288	2.712
E - 3	0.211	0.0031	17.05	0.15	0.252	0.243	1.86
E - 5	0.3572	0.0032	17.05	0.279	0.252	0.309	1.174
E - 6	0.3321	0.0029	17.05	0.255	0.252	0.306	2.497
E - 7	0.3518	0.0045	17.05	0.256	0.252	0.38	2.872
F - 4	0.3748	0.004	17.05	0.18	0.252	0.776	3.354
F - 5	0.4316	0.0039	17.05	0.209	0.252	0.886	5.46
F - 6	0.5066	0.0056	17.05	0.235	0.252	1.08	5.057
F - 7	0.479	0.0061	17.05	0.233	0.252	0.977	5.822
F - 8	0.516	0.0049	17.05	0.273	0.252	0.964	3.77
G - 4	0.2027	0.0026	17.05	0.134	0.252	0.273	2.455
G - 5	0.2345	0.0027	17.05	0.199	0.252	0.143	1.015
G - 8	0.2888	0.0034	17.05	0.234	0.252	0.219	1.008
H - 2	0.2374	0.0046	17.05	0.12	0.252	0.467	3.059
H - 4	0.2813	0.0044	17.05	0.138	0.252	0.568	4.606
H - 7	0.3067	0.0037	17.05	0.172	0.252	0.535	5.187
H - 8	0.3073	0.0035	17.05	0.199	0.252	0.43	2.916
A. n	34	34	34	34	34	34	34
A. Mean	0.5049	0.0061	17.05	0.253	0.252	1.001	3.325
A. SD	0.3425	0.0047	0	0.099	0	1.016	1.971
A. CV	67.8369	77.5117	0	38.994	0	101.558	59.277
A. Total	17.1674	0.2058	579.717	8.615	8.552	34.029	113.039

Table 7. Comparison between wave-guide wafer and Borofloat-33 slides. Results obtained using wave-guide wafer.

Element	D x A - ROD x mm2	SD - ROD	Area - mm2	Bkgd	sRef	nDxA	S/N
A - 1	2.3621	0.0517	28.003	0.066	2.305	0.996	43.063
A - 2	3.1103	0.0681	28.003	0.266	2.305	1.234	43.047
A - 3	4.3073	0.0878	28.003	0.112	2.305	1.82	71.27
A - 4	5.3354	0.1015	28.003	0.12	2.305	2.263	89.185
A - 5	4.0042	0.0763	28.003	0.086	2.305	1.7	32.18
A - 6	3.7378	0.0565	28.003	0.108	2.305	1.575	34.604
A - 7	4.7634	0.0894	28.003	0.108	2.305	2.02	44.381
B - 1	2.3069	0.016	28.003	0.086	2.305	0.964	37.86
B - 2	1.8624	0.0133	28.003	0.266	2.305	0.693	24.161
B - 3	1.7551	0.0148	28.003	0.266	2.305	0.646	22.537
B - 4	1.5959	0.0154	28.003	0.12	2.305	0.64	25.235
B - 5	1.6678	0.0183	28.003	0.12	2.305	0.672	26.466
B - 6	1.8618	0.0104	28.003	0.161	2.305	0.738	19.406
B - 7	1.9624	0.0189	28.003	0.161	2.305	0.782	20.553
C - 1	6.7347	0.0888	28.003	0.185	2.305	2.842	119.961
C - 2	6.4243	0.0647	28.003	0.266	2.305	2.672	93.207
C - 3	5.4408	0.0681	28.003	0.453	2.305	2.164	82.786
C - 4	4.9266	0.0716	28.003	0.12	2.305	2.086	82.196
C - 5	4.9367	0.0827	28.003	0.12	2.305	2.09	82.367
C - 6	4.0375	0.0586	28.003	0.161	2.305	1.682	44.224
C - 7	4.8783	0.1041	28.003	0.161	2.305	2.047	53.815
D - 1	3.9123	0.0635	28.003	0.618	2.305	1.429	18.02
D - 2	3.6608	0.048	28.003	0.453	2.305	1.392	53.245
D - 3	2.6351	0.0408	28.003	0.453	2.305	0.947	36.222
D - 4	2.0647	0.0268	28.003	0.242	2.305	0.791	26.332
D - 5	1.9796	0.0236	28.003	0.242	2.305	0.754	25.102
D - 6	1.7667	0.0216	28.003	0.2	2.305	0.68	28.529
D - 7	2.5053	0.0406	28.003	0.2	2.305	1	41.976
E - 1	3.9947	0.0517	28.003	0.618	2.305	1.465	18.471
E - 2	3.247	0.0435	28.003	0.453	2.305	1.212	46.376
E - 3	2.5398	0.0257	28.003	0.453	2.305	0.906	34.64
E - 4	2.6549	0.0318	28.003	0.242	2.305	1.047	34.86
E - 5	2.1284	0.0228	28.003	0.242	2.305	0.818	27.253
E - 6	2.4803	0.0367	28.003	0.2	2.305	0.99	41.52
E - 7	2.6449	0.0421	28.003	0.2	2.305	1.061	44.518
F - 1	0.9305	0.0116	28.003	0.161	2.305	0.334	14.289
F - 2	1.0799	0.0129	28.003	0.161	2.305	0.399	17.062
F - 3	1.1789	0.0125	28.003	0.453	2.305	0.315	12.053

F - 4	1.3092	0.0159	28.003	0.242	2.305	0.463	15.414
F - 5	1.2086	0.0148	28.003	0.242	2.305	0.419	13.961
F - 6	1.3419	0.0244	28.003	0.2	2.305	0.496	20.794
F - 7	1.248	0.0351	28.003	0.158	2.305	0.473	22.805
G - 1	0.6639	0.0088	28.003	0.075	2.305	0.256	20.712
G - 2	0.785	0.0108	28.003	0.075	2.305	0.308	24.972
G - 3	0.9566	0.0111	28.003	0.059	2.305	0.389	11.627
G - 4	1.1251	0.0126	28.003	0.059	2.305	0.462	13.811
G - 5	1.4788	0.0185	28.003	0.014	2.305	0.636	51.854
G - 6	1.9157	0.0264	28.003	0.014	2.305	0.825	67.32
G - 7	2.1615	0.0389	28.003	0.158	2.305	0.869	41.918
H - 1	0.2377	0.0036	28.003	0.059	2.305	0.077	2.31
H - 2	0.3716	0.004	28.003	0.059	2.305	0.135	4.045
H - 3	0.5101	0.0059	28.003	0.059	2.305	0.196	5.84
H - 4	0.5419	0.0072	28.003	0.014	2.305	0.229	18.685
H - 6	0.7562	0.0118	28.003	0.014	2.305	0.322	26.272
H - 7	1.4931	0.0208	28.003	0.158	2.305	0.579	27.933
A. n	55	55	55	55	55	55	55
A. Mean	2.5004	0.0364	28.003	0.196	2.305	1	36.423
A. SD	1.6031	0.0278	1.22E-06	0.145	0	0.679	24.702
A. CV	64.116	76.293	4.34E-06	74.334	1.29E-06	67.868	67.82
A. Total	137.5204	2.0034	1540.145	10.764	126.757	55	2003.245

Table 8. Results obtained upon the use of TeleChem immobilization protocol and standard washing conditions. In element column capital letters designate spot rows and numbers designate spots from left to right. ROD, relative optical density (an Imaging Research Inc. proprietary density scale which represents an inverse logarithmic function of grey-level values).

Element	D x A - ROD x mm2	SD - ROD	Area - mm2	Bkgd	sRef	nDxA	S/N
A - 1	9.41E-05	0.0058	0.016	6.15E-05	6.36E-04	0.051	0.552
A - 2	8.61E-05	0.0048	0.016	6.64E-05	6.36E-04	0.031	0.311
A - 3	0.0002	0.0445	0.016	8.04E-05	6.36E-04	0.138	1.153
A - 4	9.05E-05	0.0048	0.016	6.28E-05	6.36E-04	0.044	0.472
A - 5	7.79E-05	0.0045	0.016	5.88E-05	6.36E-04	0.03	0.332
A - 6	8.43E-05	0.0048	0.016	6.73E-05	6.36E-04	0.027	0.274
A - 7	8.54E-05	0.0051	0.016	7.30E-05	6.36E-04	0.02	0.134
A - 8	7.59E-05	0.0047	0.016	7.88E-05	6.36E-04	0	0
A - 9	9.07E-05	0.0046	0.016	6.42E-05	6.36E-04	0.042	0.459
A - 10	0.0001	0.0056	0.016	7.40E-05	6.36E-04	0.044	0.446
A - 11	8.48E-05	0.0048	0.016	8.17E-05	6.36E-04	0.005	0.04
A - 12	9.98E-05	0.0055	0.016	6.55E-05	6.36E-04	0.054	0.658
A - 13	0.0001	0.0057	0.016	7.18E-05	6.36E-04	0.051	0.545
A - 14	9.74E-05	0.005	0.016	7.86E-05	6.36E-04	0.03	0.262
A - 15	9.41E-05	0.0046	0.016	8.13E-05	6.36E-04	0.02	0.157
B - 1	7.72E-05	0.0041	0.016	7.05E-05	6.36E-04	0.011	0.098
B - 2	9.24E-05	0.005	0.016	7.19E-05	6.36E-04	0.032	0.276
B - 3	0.0001	0.0062	0.016	8.21E-05	6.36E-04	0.032	0.299
B - 4	9.19E-05	0.0049	0.016	8.11E-05	6.36E-04	0.017	0.173
B - 5	9.07E-05	0.005	0.016	7.67E-05	6.36E-04	0.022	0.217
B - 6	8.99E-05	0.005	0.016	8.17E-05	6.36E-04	0.013	0.112
B - 7	9.56E-05	0.0053	0.016	8.48E-05	6.36E-04	0.017	0.156
B - 8	8.99E-05	0.0043	0.016	7.40E-05	6.36E-04	0.025	0.244
B - 9	0.0001	0.0229	0.016	6.91E-05	6.36E-04	0.08	0.826
B - 10	7.44E-05	0.0039	0.016	6.60E-05	6.36E-04	0.013	0.139
B - 11	7.68E-05	0.0057	0.016	6.65E-05	6.36E-04	0.016	0.15
B - 12	0.0001	0.0053	0.016	7.95E-05	6.36E-04	0.036	0.286
B - 13	8.23E-05	0.006	0.016	6.96E-05	6.36E-04	0.02	0.198
B - 14	0.0135	0.3916	0.016	0.004	6.36E-04	15.538	1.976
B - 15	0.0168	0.5297	0.016	0.003	6.36E-04	21.808	3.019
C - 1	0.0002	0.0127	0.016	1.20E-04	6.36E-04	0.152	0.77
C - 2	0.0002	0.0106	0.016	1.26E-04	6.36E-04	0.166	0.756
C - 3	0.0003	0.0126	0.016	1.38E-04	6.36E-04	0.197	0.872
C - 4	0.0003	0.0122	0.016	2.29E-04	6.36E-04	0.117	0.288
C - 5	0.0003	0.011	0.016	1.85E-04	6.36E-04	0.104	0.325
C - 6	0.0003	0.0139	0.016	1.63E-04	6.36E-04	0.224	0.915
C - 7	0.0003	0.0133	0.016	1.95E-04	6.36E-04	0.093	0.264
C - 8	0.0003	0.0114	0.016	2.14E-04	6.36E-04	0.137	0.356

C - 9	0.0003	0.0121	0.016	1.21E-04	6.36E-04	0.277	1.153
C - 10	0.0003	0.0147	0.016	2.48E-04	6.36E-04	0.137	0.338
C - 11	0.0003	0.0142	0.016	2.99E-04	6.36E-04	0.01	0.02
C - 12	0.0003	0.0132	0.016	2.72E-04	6.36E-04	0.069	0.149
C - 13	0.0002	0.0117	0.016	2.04E-04	6.36E-04	0.059	0.16
C - 14	0.0004	0.0229	0.016	2.30E-04	6.36E-04	0.238	0.565
C - 15	0.0003	0.0105	0.016	2.11E-04	6.36E-04	0.154	0.368
D - 1	0.0002	0.0126	0.016	1.36E-04	6.36E-04	0.135	0.573
D - 2	0.0002	0.0113	0.016	1.38E-04	6.36E-04	0.166	0.869
D - 3	0.0002	0.0112	0.016	1.73E-04	6.36E-04	0.081	0.242
D - 4	0.0003	0.0112	0.016	2.51E-04	6.36E-04	0.054	0.143
D - 5	0.0003	0.0094	0.016	2.03E-04	6.36E-04	0.096	0.252
D - 6	0.0003	0.0126	0.016	2.11E-04	6.36E-04	0.168	0.454
D - 7	0.0003	0.0132	0.016	1.94E-04	6.36E-04	0.152	0.423
D - 8	0.0003	0.0108	0.016	1.90E-04	6.36E-04	0.105	0.297
D - 9	0.0003	0.0122	0.016	1.46E-04	6.36E-04	0.256	1.097
D - 10	0.0002	0.0107	0.016	1.41E-04	6.36E-04	0.128	0.45
D - 11	0.0005	0.1922	0.016	1.43E-04	6.36E-04	0.517	1.903
D - 12	0.0003	0.0115	0.016	1.76E-04	6.36E-04	0.175	0.499
D - 13	0.0067	0.0829	0.016	0.001	6.36E-04	8.614	2.936
D - 14	0.0071	0.0997	0.016	0.001	6.36E-04	9.279	3.042
D - 15	0.0083	0.2546	0.016	0.001	6.36E-04	10.89	2.312
E - 1	0.0007	0.0176	0.016	2.63E-04	6.36E-04	0.74	1.219
E - 2	0.0005	0.0156	0.016	1.63E-04	6.36E-04	0.597	1.853
E - 3	0.0007	0.0228	0.016	1.61E-04	6.36E-04	0.784	2.008
E - 4	0.0005	0.014	0.016	3.39E-04	6.36E-04	0.233	0.467
E - 5	0.0006	0.0196	0.016	3.23E-04	6.36E-04	0.415	0.834
E - 6	0.0006	0.0174	0.016	2.97E-04	6.36E-04	0.416	0.76
E - 7	0.0006	0.0209	0.016	2.55E-04	6.36E-04	0.468	0.905
E - 8	0.0006	0.0215	0.016	2.46E-04	6.36E-04	0.609	1.275
E - 9	0.0004	0.0158	0.016	1.71E-04	6.36E-04	0.419	1.264
E - 10	0.0007	0.0233	0.016	1.97E-04	6.36E-04	0.754	1.454
E - 11	0.0008	0.0248	0.016	1.98E-04	6.36E-04	0.884	1.96
E - 12	0.0007	0.0207	0.016	8.27E-04	6.36E-04	0	0
E - 13	0.0008	0.0171	0.016	1.12E-04	6.36E-04	1.048	3.95
E - 14	0.0008	0.0175	0.016	1.13E-04	6.36E-04	1.08	5.225
E - 15	0.0008	0.0224	0.016	1.23E-04	6.36E-04	1.02	3.231
F - 1	0.0005	0.0187	0.016	1.84E-04	6.36E-04	0.573	1.429
F - 2	0.0007	0.0183	0.016	1.36E-04	6.36E-04	0.91	2.941
F - 3	0.0007	0.0178	0.016	1.46E-04	6.36E-04	0.941	2.802
F - 4	0.0008	0.0213	0.016	2.26E-04	6.36E-04	0.963	1.967
F - 5	0.0008	0.0205	0.016	1.89E-04	6.36E-04	1.01	2.675
F - 6	0.0008	0.0203	0.016	1.48E-04	6.36E-04	1.052	2.645
F - 7	0.0007	0.0214	0.016	2.49E-04	6.36E-04	0.724	1.342
F - 8	0.0007	0.0225	0.016	2.18E-04	6.36E-04	0.729	1.529

F - 9	0.0007	0.0197	0.016	1.74E-04	6.36E-04	0.879	2.048
F - 10	0.0008	0.0217	0.016	2.01E-04	6.36E-04	0.95	2.003
F - 11	0.0009	0.0211	0.016	1.59E-04	6.36E-04	1.114	3.167
F - 12	0.0008	0.0192	0.016	1.66E-04	6.36E-04	1.04	2.26
F - 13	0.0027	0.0419	0.016	4.65E-04	6.36E-04	3.584	2.621
F - 14	0.0025	0.0441	0.016	4.19E-04	6.36E-04	3.3	2.917
F - 15	0.0027	0.046	0.016	3.61E-04	6.36E-04	3.648	2.938
G - 1	0.001	0.0231	0.016	1.65E-04	6.36E-04	1.346	3.199
G - 2	0.001	0.0204	0.016	1.64E-04	6.36E-04	1.314	3.44
G - 3	0.0009	0.0192	0.016	1.70E-04	6.36E-04	1.205	3.178
G - 4	0.0009	0.022	0.016	2.16E-04	6.36E-04	1.093	2.126
G - 5	0.0009	0.0227	0.016	2.02E-04	6.36E-04	1.103	2.388
G - 6	0.0008	0.0248	0.016	2.10E-04	6.36E-04	0.973	2.258
G - 7	0.0009	0.0242	0.016	1.33E-04	6.36E-04	1.166	4.214
G - 8	0.0009	0.0433	0.016	1.58E-04	6.36E-04	1.224	3.632
G - 9	0.001	0.0232	0.016	1.48E-04	6.36E-04	1.415	4.217
G - 10	0.0011	0.0245	0.016	1.96E-04	6.36E-04	1.418	2.83
G - 11	0.0011	0.0258	0.016	1.97E-04	6.36E-04	1.371	2.959
G - 12	0.0011	0.0231	0.016	1.53E-04	6.36E-04	1.442	4.892
G - 13	0.001	0.032	0.016	2.33E-04	6.36E-04	1.257	2.312
G - 14	0.001	0.0223	0.016	1.06E-04	6.36E-04	1.345	6.267
G - 15	0.001	0.0199	0.016	1.47E-04	6.36E-04	1.274	3.595
H - 1	0.001	0.0213	0.016	1.77E-04	6.36E-04	1.255	2.962
H - 2	0.001	0.0205	0.016	1.37E-04	6.36E-04	1.387	4.098
H - 3	0.0009	0.0221	0.016	1.24E-04	6.36E-04	1.288	4.061
H - 4	0.0008	0.0295	0.016	4.06E-04	6.36E-04	0.691	0.858
H - 5	0.001	0.0202	0.016	1.54E-04	6.36E-04	1.373	3.494
H - 6	0.001	0.0226	0.016	1.47E-04	6.36E-04	1.4	4.788
H - 7	0.001	0.0232	0.016	1.59E-04	6.36E-04	1.337	3.037
H - 8	0.0011	0.0213	0.016	1.48E-04	6.36E-04	1.461	4.536
H - 9	0.0011	0.0238	0.016	1.66E-04	6.36E-04	1.391	3.579
H - 10	0.001	0.0246	0.016	1.65E-04	6.36E-04	1.291	2.857
H - 11	0.001	0.0264	0.016	1.69E-04	6.36E-04	1.317	3.901
H - 12	0.0011	0.024	0.016	1.77E-04	6.36E-04	1.382	3.422
H - 13	0.0013	0.0269	0.016	2.23E-04	6.36E-04	1.703	3.283
H - 14	0.0013	0.0307	0.016	3.12E-04	6.36E-04	1.622	1.904
H - 15	0.0014	0.0293	0.016	1.63E-04	6.36E-04	1.944	4.038
I - 1	0.0011	0.0233	0.016	1.25E-04	6.36E-04	1.516	5.013
I - 2	0.001	0.0246	0.016	1.42E-04	6.36E-04	1.304	4.363
I - 3	0.001	0.0232	0.016	1.56E-04	6.36E-04	1.403	3.451
I - 4	0.0011	0.0226	0.016	1.78E-04	6.36E-04	1.444	3.493
I - 5	0.0011	0.0251	0.016	2.46E-04	6.36E-04	1.354	2.11
I - 6	0.001	0.0252	0.016	1.61E-04	6.36E-04	1.387	3.289
I - 7	0.0011	0.0264	0.016	1.72E-04	6.36E-04	1.425	2.929
I - 8	0.0011	0.0251	0.016	1.75E-04	6.36E-04	1.385	2.857

I - 9	0.0012	0.0231	0.016	1.31E-04	6.36E-04	1.654	5.736
I - 10	0.0011	0.0232	0.016	1.72E-04	6.36E-04	1.506	3.794
I - 11	0.0011	0.0246	0.016	2.63E-04	6.36E-04	1.269	2.156
I - 12	0.001	0.0283	0.016	1.65E-04	6.36E-04	1.366	2.71
I - 13	0.001	0.0335	0.016	2.45E-04	6.36E-04	1.239	2.12
I - 14	0.0011	0.0262	0.016	1.46E-04	6.36E-04	1.55	4.591
I - 15	0.0012	0.0241	0.016	1.51E-04	6.36E-04	1.627	4.514
J - 1	0.001	0.0246	0.016	1.66E-04	6.36E-04	1.28	2.366
J - 2	0.0009	0.0238	0.016	1.67E-04	6.36E-04	1.222	3.011
J - 3	0.001	0.0245	0.016	1.98E-04	6.36E-04	1.316	3.094
J - 4	0.001	0.0214	0.016	1.45E-04	6.36E-04	1.333	3.769
J - 5	0.001	0.0232	0.016	1.45E-04	6.36E-04	1.413	4.149
J - 6	0.001	0.0259	0.016	1.48E-04	6.36E-04	1.318	3.561
J - 7	0.001	0.0249	0.016	1.49E-04	6.36E-04	1.401	3.07
J - 8	0.0011	0.021	0.016	1.87E-04	6.36E-04	1.475	2.548
J - 9	0.001	0.0239	0.016	1.37E-04	6.36E-04	1.376	3.667
J - 10	0.0015	0.2659	0.016	1.45E-04	6.36E-04	2.159	5.731
J - 11	0.0011	0.0237	0.016	1.82E-04	6.36E-04	1.468	2.66
J - 12	0.0012	0.0249	0.016	1.75E-04	6.36E-04	1.606	3.922
J - 13	0.0013	0.0245	0.016	1.22E-04	6.36E-04	1.794	5.927
J - 14	0.0012	0.0244	0.016	1.29E-04	6.36E-04	1.758	7.176
J - 15	0.0011	0.0232	0.016	1.06E-04	6.36E-04	1.604	8.709
K - 1	0.0011	0.025	0.016	1.31E-04	6.36E-04	1.576	3.381
K - 2	0.0011	0.0243	0.016	1.79E-04	6.36E-04	1.37	2.784
K - 3	0.001	0.0225	0.016	1.18E-04	6.36E-04	1.432	5.092
K - 4	6.59E-05	0.0041	0.016	7.09E-05	6.36E-04	0	0
K - 5	6.98E-05	0.0041	0.016	5.92E-05	6.36E-04	0.017	0.191
K - 6	6.99E-05	0.0044	0.016	5.22E-05	6.36E-04	0.028	0.298
K - 7	6.41E-05	0.0037	0.016	5.48E-05	6.36E-04	0.015	0.182
K - 8	6.31E-05	0.0037	0.016	5.88E-05	6.36E-04	0.007	0.081
K - 9	6.52E-05	0.0043	0.016	5.36E-05	6.36E-04	0.018	0.176
K - 10	7.45E-05	0.0044	0.016	6.19E-05	6.36E-04	0.02	0.229
K - 11	7.15E-05	0.005	0.016	1.02E-04	6.36E-04	0	0
K - 12	7.00E-05	0.0043	0.016	6.71E-05	6.36E-04	0.005	0.037
K - 13	7.08E-05	0.005	0.016	6.55E-05	6.36E-04	0.008	0.093
K - 14	5.32E-05	0.0038	0.016	5.17E-05	6.36E-04	0.002	0.025
K - 15	6.83E-05	0.0043	0.016	7.00E-05	6.36E-04	0	0
L - 1	8.26E-05	0.0049	0.016	7.16E-05	6.36E-04	0.017	0.124
L - 2	8.08E-05	0.0052	0.016	6.37E-05	6.36E-04	0.027	0.315
L - 3	8.20E-05	0.005	0.016	7.00E-05	6.36E-04	0.019	0.195
L - 4	8.19E-05	0.0045	0.016	6.60E-05	6.36E-04	0.025	0.258
L - 5	7.69E-05	0.0046	0.016	6.28E-05	6.36E-04	0.022	0.258
L - 6	7.17E-05	0.0044	0.016	8.32E-05	6.36E-04	0	0
L - 7	7.70E-05	0.0043	0.016	7.27E-05	6.36E-04	0.007	0.067
L - 8	7.72E-05	0.0043	0.016	7.99E-05	6.36E-04	0	0

L - 9	8.38E-05	0.0048	0.016	8.11E-05	6.36E-04	0.004	0.047
L - 10	0.0001	0.0049	0.016	7.18E-05	6.36E-04	0.058	0.586
L - 11	0.0001	0.0056	0.016	6.46E-05	6.36E-04	0.061	0.635
L - 12	0.0001	0.0049	0.016	7.44E-05	6.36E-04	0.048	0.496
L - 13	9.02E-05	0.0049	0.016	6.10E-05	6.36E-04	0.046	0.528
L - 14	7.98E-05	0.0042	0.016	6.90E-05	6.36E-04	0.017	0.192
L - 15	8.71E-05	0.0049	0.016	7.76E-05	6.36E-04	0.015	0.152
M - 1	5.90E-05	0.0037	0.016	5.39E-05	6.36E-04	0.008	0.085
M - 2	8.39E-05	0.0053	0.016	7.49E-05	6.36E-04	0.014	0.135
M - 3	6.54E-05	0.0041	0.016	5.89E-05	6.36E-04	0.01	0.102
M - 4	8.63E-05	0.0051	0.016	7.45E-05	6.36E-04	0.018	0.168
M - 5	8.60E-05	0.0045	0.016	6.60E-05	6.36E-04	0.031	0.329
M - 6	8.08E-05	0.0043	0.016	6.02E-05	6.36E-04	0.033	0.36
M - 7	7.85E-05	0.004	0.016	6.43E-05	6.36E-04	0.022	0.202
M - 8	7.09E-05	0.0044	0.016	5.61E-05	6.36E-04	0.023	0.264
M - 9	8.60E-05	0.0048	0.016	7.09E-05	6.36E-04	0.024	0.232
M - 10	7.99E-05	0.0041	0.016	9.97E-05	6.36E-04	0	0
M - 11	0.0001	0.0056	0.016	8.25E-05	6.36E-04	0.061	0.572
M - 12	7.62E-05	0.0045	0.016	6.50E-05	6.36E-04	0.018	0.221
M - 13	0.0243	0.7163	0.016	0.007	6.36E-04	27.07	1.529
M - 14	0.0176	0.5591	0.016	0.005	6.36E-04	19.192	1.421
M - 15	0.0259	0.7347	0.016	0.004	6.36E-04	34.193	2.782
N - 1	7.12E-05	0.0042	0.016	4.18E-05	6.36E-04	0.046	0.674
N - 2	8.37E-05	0.0049	0.016	7.00E-05	6.36E-04	0.021	0.131
N - 3	8.59E-05	0.0041	0.016	6.92E-05	6.36E-04	0.026	0.243
N - 4	8.19E-05	0.0045	0.016	5.97E-05	6.36E-04	0.035	0.441
N - 5	8.00E-05	0.0044	0.016	5.66E-05	6.36E-04	0.037	0.407
N - 6	8.30E-05	0.0054	0.016	5.34E-05	6.36E-04	0.047	0.595
N - 7	8.72E-05	0.0047	0.016	7.10E-04	6.36E-04	0	0
N - 8	7.26E-05	0.0042	0.016	6.68E-05	6.36E-04	0.009	0.099
N - 9	7.26E-05	0.0043	0.016	5.97E-05	6.36E-04	0.02	0.214
N - 10	7.97E-05	0.0046	0.016	7.01E-05	6.36E-04	0.015	0.138
N - 11	0.0001	0.0055	0.016	8.35E-05	6.36E-04	0.039	0.345
N - 12	7.74E-05	0.0044	0.016	6.73E-05	6.36E-04	0.016	0.17
N - 13	0.0001	0.0175	0.016	6.24E-05	6.36E-04	0.101	1.107
N - 14	6.91E-05	0.0041	0.016	3.74E-05	6.36E-04	0.05	0.703
N - 15	7.33E-05	0.0047	0.016	5.79E-05	6.36E-04	0.024	0.264
O - 1	6.38E-05	0.004	0.016	5.97E-05	6.36E-04	0.006	0.067
O - 2	7.74E-05	0.0042	0.016	7.50E-05	6.36E-04	0.004	0.03
O - 3	7.16E-05	0.0044	0.016	5.39E-05	6.36E-04	0.028	0.338
O - 4	7.60E-05	0.0042	0.016	6.28E-05	6.36E-04	0.021	0.244
O - 5	7.02E-05	0.0044	0.016	6.64E-05	6.36E-04	0.006	0.064
O - 6	6.94E-05	0.0037	0.016	7.01E-05	6.36E-04	0	0
O - 7	6.74E-05	0.0041	0.016	1.69E-04	6.36E-04	0	0
O - 8	6.86E-05	0.0042	0.016	6.64E-05	6.36E-04	0.003	0.037

O - 9	6.64E-05	0.0041	0.016	5.66E-05	6.36E-04	0.015	0.169
O - 10	7.37E-05	0.0039	0.016	6.20E-05	6.36E-04	0.018	0.192
O - 11	7.57E-05	0.0043	0.016	7.67E-05	6.36E-04	0	0
O - 12	6.27E-05	0.0047	0.016	5.93E-05	6.36E-04	0.005	0.06
O - 13	0.0061	0.2466	0.016	0.004	6.36E-04	3.098	0.226
O - 14	0.0077	0.4581	0.016	0.001	6.36E-04	9.71	2.158
O - 15	0.0109	0.4571	0.016	0.003	6.36E-04	13.063	1.323
P - 1	8.55E-05	0.0046	0.016	5.35E-05	6.36E-04	0.05	0.581
P - 2	9.03E-05	0.0053	0.016	7.29E-05	6.36E-04	0.027	0.211
P - 3	8.19E-05	0.0045	0.016	6.19E-05	6.36E-04	0.031	0.34
P - 4	8.24E-05	0.0045	0.016	7.24E-05	6.36E-04	0.016	0.121
P - 5	6.88E-05	0.0043	0.016	6.37E-05	6.36E-04	0.008	0.09
P - 6	7.38E-05	0.0043	0.016	6.74E-05	6.36E-04	0.01	0.097
P - 7	8.03E-05	0.0042	0.016	7.46E-05	6.36E-04	0.009	0.069
P - 8	7.81E-05	0.0046	0.016	5.08E-05	6.36E-04	0.043	0.554
P - 9	7.01E-05	0.0038	0.016	6.11E-05	6.36E-04	0.014	0.147
P - 10	6.84E-05	0.0051	0.016	5.07E-05	6.36E-04	0.028	0.377
P - 11	6.80E-05	0.0038	0.016	6.60E-05	6.36E-04	0.003	0.03
P - 12	0.0001	0.0058	0.016	7.63E-05	6.36E-04	0.042	0.395
P - 13	7.12E-05	0.0044	0.016	5.57E-05	6.36E-04	0.024	0.266
P - 14	6.89E-05	0.0051	0.016	5.80E-05	6.36E-04	0.017	0.174
P - 15	7.60E-05	0.0044	0.016	6.96E-05	6.36E-04	0.01	0.096
Q - 1	7.37E-05	0.0041	0.016	4.85E-05	6.36E-04	0.04	0.523
Q - 2	7.00E-05	0.0054	0.016	6.20E-05	6.36E-04	0.013	0.129
Q - 3	6.07E-05	0.0042	0.016	5.52E-05	6.36E-04	0.009	0.105
Q - 4	6.19E-05	0.0039	0.016	5.34E-05	6.36E-04	0.013	0.173
Q - 5	7.67E-05	0.0042	0.016	4.95E-05	6.36E-04	0.043	0.444
Q - 6	6.16E-05	0.0044	0.016	5.88E-05	6.36E-04	0.004	0.051
Q - 7	7.32E-05	0.0039	0.016	6.11E-05	6.36E-04	0.019	0.194
Q - 8	5.28E-05	0.0035	0.016	5.80E-05	6.36E-04	0	0
Q - 9	7.11E-05	0.0048	0.016	6.78E-05	6.36E-04	0.005	0.053
Q - 10	6.55E-05	0.004	0.016	7.15E-05	6.36E-04	0	0
Q - 11	6.00E-05	0.0039	0.016	6.11E-05	6.36E-04	0	0
Q - 12	6.92E-05	0.0046	0.016	5.66E-05	6.36E-04	0.02	0.208
Q - 13	0.0037	0.0983	0.016	0.001	6.36E-04	3.981	1.133
Q - 14	0.0037	0.091	0.016	6.35E-04	6.36E-04	4.868	2.464
Q - 15	0.0041	0.1012	0.016	5.05E-04	6.36E-04	5.7	3.619
R - 1	7.01E-05	0.0041	0.016	6.78E-05	6.36E-04	0.004	0.035
R - 2	7.95E-05	0.0047	0.016	5.83E-05	6.36E-04	0.033	0.388
R - 3	7.91E-05	0.0044	0.016	7.14E-05	6.36E-04	0.012	0.113
R - 4	8.09E-05	0.0048	0.016	6.42E-05	6.36E-04	0.026	0.25
R - 5	6.25E-05	0.0043	0.016	6.06E-05	6.36E-04	0.003	0.035
R - 6	7.33E-05	0.0045	0.016	6.56E-05	6.36E-04	0.012	0.121
R - 7	0.0002	0.1249	0.016	4.32E-05	6.36E-04	0.301	4.232
R - 8	5.69E-05	0.0036	0.016	5.79E-05	6.36E-04	0	0

R - 9	6.76E-05	0.0043	0.016	6.37E-05	6.36E-04	0.006	0.067
R - 10	6.44E-05	0.0038	0.016	6.43E-05	6.36E-04	1.92E-04	0.002
R - 11	6.88E-05	0.0041	0.016	3.38E-05	6.36E-04	0.055	0.89
R - 12	7.01E-05	0.004	0.016	5.13E-05	6.36E-04	0.03	0.314
R - 13	7.65E-05	0.0041	0.016	5.22E-05	6.36E-04	0.038	0.398
R - 14	7.00E-05	0.0041	0.016	5.61E-05	6.36E-04	0.022	0.266
R - 15	6.29E-05	0.0038	0.016	5.80E-05	6.36E-04	0.008	0.08
S - 1	8.33E-05	0.0048	0.016	9.81E-05	6.36E-04	0	0
S - 2	7.13E-05	0.0048	0.016	6.24E-05	6.36E-04	0.014	0.142
S - 3	6.22E-05	0.0038	0.016	4.58E-05	6.36E-04	0.026	0.349
S - 4	7.57E-05	0.0043	0.016	6.96E-05	6.36E-04	0.01	0.092
S - 5	5.79E-05	0.0038	0.016	5.75E-05	6.36E-04	7.45E-04	0.008
S - 6	6.28E-05	0.004	0.016	4.67E-05	6.36E-04	0.025	0.356
S - 7	6.93E-05	0.0041	0.016	5.30E-05	6.36E-04	0.026	0.3
S - 8	6.19E-05	0.004	0.016	4.95E-05	6.36E-04	0.02	0.229
S - 9	6.32E-05	0.0037	0.016	6.47E-05	6.36E-04	0	0
S - 10	6.44E-05	0.0038	0.016	6.84E-05	6.36E-04	0	0
S - 11	5.86E-05	0.0034	0.016	7.14E-05	6.36E-04	0	0
S - 12	0.0001	0.006	0.016	9.03E-05	6.36E-04	0.076	0.601
S - 13	0.0032	0.0775	0.016	0.003	6.36E-04	0.798	0.4
S - 14	0.0032	0.0662	0.016	0.002	6.36E-04	1.401	0.997
S - 15	0.0024	0.0545	0.016	0.003	6.36E-04	0	0
T - 1	8.58E-05	0.0043	0.016	8.13E-05	6.36E-04	0.007	0.059
T - 2	9.10E-05	0.0047	0.016	8.39E-05	6.36E-04	0.011	0.096
T - 3	7.56E-05	0.0051	0.016	6.78E-05	6.36E-04	0.012	0.114
T - 4	7.72E-05	0.0041	0.016	5.21E-05	6.36E-04	0.039	0.511
T - 5	6.33E-05	0.0042	0.016	6.32E-05	6.36E-04	1.07E-04	0.001
T - 6	6.17E-05	0.0037	0.016	5.66E-05	6.36E-04	0.008	0.081
T - 7	5.88E-05	0.004	0.016	4.67E-05	6.36E-04	0.019	0.259
T - 8	6.79E-05	0.0039	0.016	5.93E-05	6.36E-04	0.014	0.148
T - 9	5.96E-05	0.0036	0.016	5.43E-05	6.36E-04	0.008	0.099
T - 10	7.03E-05	0.0042	0.016	6.91E-05	6.36E-04	0.002	0.019
T - 11	6.10E-05	0.0037	0.016	6.24E-05	6.36E-04	0	0
T - 12	7.70E-05	0.0042	0.016	6.91E-05	6.36E-04	0.013	0.137
T - 13	5.57E-05	0.0036	0.016	4.41E-05	6.36E-04	0.018	0.224
T - 14	6.78E-05	0.0042	0.016	6.02E-05	6.36E-04	0.012	0.124
T - 15	6.76E-05	0.004	0.016	4.99E-05	6.36E-04	0.028	0.304
U - 1	6.30E-05	0.0043	0.016	6.39E-05	6.36E-04	0	0
U - 2	0.0001	0.0572	0.016	7.01E-05	6.36E-04	0.124	1.053
U - 3	8.51E-05	0.0045	0.016	7.54E-05	6.36E-04	0.015	0.141
U - 4	6.19E-05	0.0038	0.016	4.95E-05	6.36E-04	0.02	0.214
U - 5	6.41E-05	0.004	0.016	5.44E-05	6.36E-04	0.015	0.178
U - 6	5.56E-05	0.0039	0.016	6.60E-05	6.36E-04	0	0
U - 7	5.90E-05	0.0038	0.016	5.04E-05	6.36E-04	0.014	0.151
U - 8	7.04E-05	0.0057	0.016	4.82E-05	6.36E-04	0.035	0.346

U - 9	6.16E-05	0.0042	0.016	4.63E-05	6.36E-04	0.024	0.322
U - 10	6.02E-05	0.0041	0.016	6.06E-05	6.36E-04	0	0
U - 11	6.44E-05	0.0046	0.016	4.72E-05	6.36E-04	0.027	0.324
U - 12	9.48E-05	0.0048	0.016	6.69E-05	6.36E-04	0.044	0.45
U - 13	0.0002	0.0115	0.016	1.55E-04	6.36E-04	0.118	0.424
U - 14	0.0002	0.0127	0.016	1.40E-04	6.36E-04	0.159	0.511
U - 15	0.0003	0.0147	0.016	9.82E-05	6.36E-04	0.387	3.421
A. n	315	315	315	315	315	315	315
A. Mean	0.0009	0.0287	0.016	2.57E-04	6.36E-04	1.007	1.224
A. SD	0.0027	0.0862	0	7.10E-04	0	3.328	1.569
A. CV	306.3019	299.9392	0	276.545	0	330.662	128.161
A. Total	0.2812	9.0547	4.914	0.081	0.2	317.057	385.538

Table 9. Results obtained upon the use of Schena's immobilization protocol and standard washing conditions. In element column capital letters designate spot rows and numbers designate spots from left to right. ROD, relative optical density (an Imaging Research Inc. proprietary density scale which represents an inverse logarithmic function of grey-level values).

Element	D x A - ROD x mm2	SD - ROD	Area - mm2	Bkgd	sRef	nDxA	S/N
A - 1	1.65E-05	0.0021	0.016	1.38E-05	1.51E-04	0.018	0.101
A - 2	1.39E-05	0.0018	0.016	1.61E-05	1.51E-04	0	0
A - 3	1.22E-05	0.0015	0.016	6.74E-06	1.51E-04	0.036	0.36
A - 4	1.84E-05	0.0024	0.016	1.07E-05	1.51E-04	0.051	0.293
A - 5	1.22E-05	0.0018	0.016	9.86E-06	1.51E-04	0.016	0.096
A - 6	9.99E-06	0.0015	0.016	7.63E-06	1.51E-04	0.016	0.12
A - 7	1.31E-05	0.0017	0.016	8.51E-06	1.51E-04	0.03	0.275
A - 8	1.43E-05	0.002	0.016	1.47E-05	1.51E-04	0	0
A - 9	1.68E-05	0.0022	0.016	2.06E-05	1.51E-04	0	0
A - 10	1.27E-05	0.0018	0.016	1.03E-05	1.51E-04	0.016	0.108
A - 11	5.87E-05	0.0303	0.016	9.85E-06	1.51E-04	0.323	2.353
A - 12	1.31E-05	0.0018	0.016	8.97E-06	1.51E-04	0.027	0.172
A - 13	1.29E-05	0.0017	0.016	1.16E-05	1.51E-04	0.008	0.046
A - 14	1.78E-05	0.002	0.016	1.61E-05	1.51E-04	0.012	0.048
A - 15	2.13E-05	0.0024	0.016	1.56E-05	1.51E-04	0.037	0.172
B - 1	1.87E-05	0.0041	0.016	1.39E-05	1.51E-04	0.032	0.158
B - 2	1.16E-05	0.0022	0.016	8.08E-06	1.51E-04	0.023	0.166
B - 3	8.97E-06	0.0014	0.016	7.63E-06	1.51E-04	0.009	0.079
B - 4	8.11E-06	0.0013	0.016	7.63E-06	1.51E-04	0.003	0.025
B - 5	1.19E-05	0.0017	0.016	8.11E-06	1.51E-04	0.025	0.123
B - 6	1.20E-05	0.0016	0.016	5.42E-06	1.51E-04	0.044	0.432
B - 7	2.53E-05	0.0058	0.016	7.18E-06	1.51E-04	0.12	1.182
B - 8	1.63E-05	0.0021	0.016	1.35E-05	1.51E-04	0.019	0.077
B - 9	1.31E-05	0.0017	0.016	1.52E-05	1.51E-04	0	0
B - 10	2.08E-05	0.0027	0.016	1.43E-05	1.51E-04	0.043	0.203
B - 11	4.53E-05	0.0157	0.016	8.97E-06	1.51E-04	0.241	1.554
B - 12	2.37E-05	0.0042	0.016	1.12E-05	1.51E-04	0.083	0.478
B - 13	0.0027	0.0446	0.016	3.38E-04	1.51E-04	15.557	2.883
B - 14	0.0025	0.0275	0.016	2.75E-04	1.51E-04	14.838	3.527
B - 15	0.0022	0.0371	0.016	3.92E-04	1.51E-04	11.993	2.083
C - 1	6.21E-05	0.005	0.016	2.24E-05	1.51E-04	0.263	0.816
C - 2	5.63E-05	0.0045	0.016	2.95E-05	1.51E-04	0.178	0.523
C - 3	6.22E-05	0.005	0.016	3.62E-05	1.51E-04	0.172	0.413
C - 4	7.84E-05	0.0044	0.016	1.79E-05	1.51E-04	0.401	1.751
C - 5	8.14E-05	0.0066	0.016	1.43E-05	1.51E-04	0.445	2.075
C - 6	8.55E-05	0.0055	0.016	2.06E-05	1.51E-04	0.43	1.49
C - 7	7.64E-05	0.0049	0.016	4.39E-05	1.51E-04	0.216	0.414
C - 8	7.85E-05	0.0057	0.016	2.64E-05	1.51E-04	0.345	1.039

C - 9	8.46E-05	0.0055	0.016	7.38E-05	1.51E-04	0.072	0.093
C - 10	9.72E-05	0.0055	0.016	1.70E-05	1.51E-04	0.531	2.049
C - 11	0.0001	0.0095	0.016	3.27E-05	1.51E-04	0.686	1.658
C - 12	0.0001	0.009	0.016	2.24E-05	1.51E-04	0.77	2.258
C - 13	0.0001	0.0067	0.016	3.09E-05	1.51E-04	0.608	1.435
C - 14	0.0001	0.0056	0.016	2.10E-05	1.51E-04	0.603	2.39
C - 15	0.0001	0.0057	0.016	1.57E-05	1.51E-04	0.56	2.347
D - 1	5.13E-05	0.0037	0.016	1.25E-05	1.51E-04	0.257	1.456
D - 2	5.27E-05	0.0039	0.016	1.88E-05	1.51E-04	0.224	0.826
D - 3	4.15E-05	0.0035	0.016	4.02E-05	1.51E-04	0.008	0.019
D - 4	7.94E-05	0.005	0.016	2.47E-05	1.51E-04	0.363	0.927
D - 5	7.39E-05	0.0051	0.016	4.49E-05	1.51E-04	0.192	0.333
D - 6	8.76E-05	0.0059	0.016	3.73E-05	1.51E-04	0.333	0.598
D - 7	8.03E-05	0.0046	0.016	5.35E-05	1.51E-04	0.178	0.08
D - 8	8.18E-05	0.005	0.016	3.31E-05	1.51E-04	0.323	0.826
D - 9	7.70E-05	0.0049	0.016	3.99E-05	1.51E-04	0.246	0.485
D - 10	7.98E-05	0.0053	0.016	1.61E-05	1.51E-04	0.422	1.588
D - 11	0.0001	0.0056	0.016	3.09E-05	1.51E-04	0.535	1.201
D - 12	9.25E-05	0.0061	0.016	2.54E-05	1.51E-04	0.444	1.437
D - 13	0.0016	0.0256	0.016	6.79E-05	1.51E-04	10.465	11.716
D - 14	0.0017	0.0323	0.016	1.24E-04	1.51E-04	10.599	6.622
D - 15	0.0017	0.0285	0.016	1.91E-04	1.51E-04	9.93	4.131
E - 1	0.0001	0.007	0.016	4.62E-05	1.51E-04	0.679	1.223
E - 2	0.0002	0.0072	0.016	1.61E-05	1.51E-04	1.066	4.527
E - 3	0.0001	0.0058	0.016	2.41E-05	1.51E-04	0.787	2.666
E - 4	0.0002	0.0067	0.016	3.20E-05	1.51E-04	0.886	1.624
E - 5	0.0002	0.0075	0.016	3.43E-05	1.51E-04	1.086	1.802
E - 6	0.0002	0.0073	0.016	2.75E-05	1.51E-04	1.015	1.95
E - 7	0.0002	0.007	0.016	2.42E-05	1.51E-04	0.896	2.654
E - 8	0.0002	0.0073	0.016	2.20E-05	1.51E-04	1.132	2.781
E - 9	0.0002	0.0079	0.016	2.73E-05	1.51E-04	1.147	1.826
E - 10	0.0002	0.0114	0.016	3.89E-05	1.51E-04	1.213	2.578
E - 11	0.0002	0.012	0.016	2.19E-05	1.51E-04	1.418	5.468
E - 12	0.0002	0.01	0.016	4.66E-05	1.51E-04	1.331	1.013
E - 13	0.0002	0.0078	0.016	2.65E-05	1.51E-04	1.204	2.654
E - 14	0.0002	0.0081	0.016	4.08E-05	1.51E-04	1.138	2.107
E - 15	0.0002	0.0072	0.016	2.59E-05	1.51E-04	1.144	3.167
F - 1	0.0001	0.0066	0.016	2.28E-05	1.51E-04	0.782	2.849
F - 2	0.0002	0.0065	0.016	1.83E-05	1.51E-04	0.933	3.559
F - 3	0.0001	0.0061	0.016	2.20E-05	1.51E-04	0.753	2.138
F - 4	0.0001	0.0058	0.016	2.68E-05	1.51E-04	0.752	2.046
F - 5	0.0001	0.0067	0.016	3.42E-05	1.51E-04	0.711	1.262
F - 6	0.0002	0.0078	0.016	3.15E-05	1.51E-04	0.785	1.505
F - 7	0.0002	0.0078	0.016	1.88E-05	1.51E-04	1.079	3.724
F - 8	0.0002	0.0076	0.016	1.80E-05	1.51E-04	1.117	3.326

F - 9	0.0002	0.0128	0.016	2.77E-05	1.51E-04	1.098	2.868
F - 10	0.0002	0.0127	0.016	3.60E-05	1.51E-04	1.128	1.997
F - 11	0.0002	0.0085	0.016	1.61E-05	1.51E-04	1.547	6.632
F - 12	0.0002	0.0075	0.016	3.08E-05	1.51E-04	1.17	1.839
F - 13	0.0008	0.0169	0.016	4.78E-05	1.51E-04	5.196	6.048
F - 14	0.0007	0.0183	0.016	5.50E-05	1.51E-04	4.153	3.979
F - 15	0.0007	0.0179	0.016	2.90E-05	1.51E-04	4.386	7.187
G - 1	0.0002	0.0067	0.016	1.21E-05	1.51E-04	1.114	7.601
G - 2	0.0002	0.0065	0.016	2.28E-05	1.51E-04	1.074	3.036
G - 3	0.0002	0.0078	0.016	4.44E-05	1.51E-04	0.907	1.685
G - 4	0.0002	0.0075	0.016	1.66E-05	1.51E-04	0.942	3.066
G - 5	0.0002	0.0069	0.016	2.82E-05	1.51E-04	0.875	2.213
G - 6	0.0002	0.0076	0.016	2.23E-05	1.51E-04	1.059	3.967
G - 7	0.0002	0.0074	0.016	1.66E-05	1.51E-04	1.039	3.534
G - 8	0.0002	0.0079	0.016	2.92E-05	1.51E-04	1.122	2.432
G - 9	0.0002	0.0201	0.016	2.11E-05	1.51E-04	1.476	4.274
G - 10	0.0002	0.011	0.016	2.91E-05	1.51E-04	1.339	3.071
G - 11	0.0003	0.0084	0.016	1.34E-05	1.51E-04	1.718	7.564
G - 12	0.0003	0.0101	0.016	1.39E-05	1.51E-04	1.745	7.945
G - 13	0.0002	0.0095	0.016	5.67E-05	1.51E-04	1.238	1.442
G - 14	0.0003	0.0095	0.016	2.95E-05	1.51E-04	1.617	4.213
G - 15	0.0003	0.0457	0.016	4.79E-05	1.51E-04	1.675	3.429
H - 1	0.0002	0.0068	0.016	3.00E-05	1.51E-04	0.833	1.975
H - 2	0.0002	0.0075	0.016	2.37E-05	1.51E-04	1.125	3.585
H - 3	0.0002	0.0068	0.016	1.43E-05	1.51E-04	1.175	5.287
H - 4	0.0002	0.0074	0.016	2.64E-05	1.51E-04	1.075	2.751
H - 5	0.0002	0.0072	0.016	2.55E-05	1.51E-04	1.166	3.145
H - 6	0.0002	0.0076	0.016	3.12E-05	1.51E-04	1.204	2.061
H - 7	0.0002	0.0097	0.016	1.94E-05	1.51E-04	1.172	2.649
H - 8	0.0002	0.0077	0.016	1.57E-05	1.51E-04	1.403	5.547
H - 9	0.0002	0.009	0.016	2.77E-05	1.51E-04	1.454	2.378
H - 10	0.0002	0.007	0.016	1.52E-05	1.51E-04	1.03	5.187
H - 11	0.0002	0.0084	0.016	5.75E-05	1.51E-04	1.069	1.286
H - 12	0.0002	0.0082	0.016	1.43E-04	1.51E-04	0.397	0.07
H - 13	0.0004	0.0117	0.016	2.37E-05	1.51E-04	2.207	6.284
H - 14	0.0004	0.0102	0.016	1.88E-05	1.51E-04	2.27	6.939
H - 15	0.0003	0.009	0.016	3.05E-05	1.51E-04	1.574	3.495
I - 1	0.0002	0.0068	0.016	3.00E-05	1.51E-04	0.966	2.221
I - 2	0.0002	0.0078	0.016	2.42E-05	1.51E-04	1.124	3.099
I - 3	0.0002	0.0068	0.016	2.29E-05	1.51E-04	1.109	2.91
I - 4	0.0002	0.0071	0.016	1.43E-05	1.51E-04	1.152	7.182
I - 5	0.0002	0.0074	0.016	1.30E-05	1.51E-04	1.12	4.883
I - 6	0.0002	0.0085	0.016	2.42E-05	1.51E-04	1.024	2.774
I - 7	0.0002	0.008	0.016	2.94E-05	1.51E-04	1.309	2.286
I - 8	0.0002	0.0076	0.016	3.29E-05	1.51E-04	1.168	2.151

I - 9	0.0002	0.0092	0.016	1.56E-05	1.51E-04	1.453	7.128
I - 10	0.0002	0.0142	0.016	1.79E-05	1.51E-04	1.466	6.668
I - 11	0.0003	0.0405	0.016	2.05E-05	1.51E-04	1.867	7.258
I - 12	0.0002	0.0089	0.016	6.43E-05	1.51E-04	0.985	1.414
I - 13	0.0002	0.0088	0.016	1.80E-05	1.51E-04	1.474	3.561
I - 14	0.0002	0.0088	0.016	3.18E-05	1.51E-04	1.395	3.12
I - 15	0.0002	0.0091	0.016	1.97E-05	1.51E-04	1.314	4.345
J - 1	0.0002	0.007	0.016	2.41E-05	1.51E-04	1.042	3.254
J - 2	0.0002	0.0076	0.016	1.53E-05	1.51E-04	1.14	4.008
J - 3	0.0002	0.0068	0.016	1.83E-05	1.51E-04	1.029	3.923
J - 4	0.0002	0.0073	0.016	1.65E-05	1.51E-04	1.159	4.975
J - 5	0.0002	0.0073	0.016	2.77E-05	1.51E-04	1.043	2.95
J - 6	0.0002	0.0088	0.016	2.60E-05	1.51E-04	1.235	3.17
J - 7	0.0002	0.0083	0.016	2.15E-05	1.51E-04	1.367	3.969
J - 8	0.0002	0.0081	0.016	3.03E-05	1.51E-04	1.402	2.278
J - 9	0.0002	0.009	0.016	1.43E-05	1.51E-04	1.475	8.093
J - 10	0.0003	0.021	0.016	2.32E-05	1.51E-04	1.627	5.738
J - 11	0.0005	0.1919	0.016	7.46E-05	1.51E-04	2.778	1.478
J - 12	0.0002	0.0075	0.016	2.86E-05	1.51E-04	1.22	1.996
J - 13	0.0002	0.0077	0.016	2.06E-05	1.51E-04	1.418	4.813
J - 14	0.0002	0.0072	0.016	9.87E-06	1.51E-04	1.111	6.031
J - 15	0.0002	0.0076	0.016	3.18E-05	1.51E-04	1.123	2.524
K - 1	0.0002	0.0071	0.016	2.46E-05	1.51E-04	1.127	3.059
K - 2	0.0002	0.0067	0.016	1.48E-05	1.51E-04	1.145	4.439
K - 3	0.0002	0.008	0.016	1.43E-05	1.51E-04	1.217	6.786
K - 4	7.26E-06	0.0012	0.016	6.75E-06	1.51E-04	0.003	0.026
K - 5	7.94E-06	0.0012	0.016	7.21E-06	1.51E-04	0.005	0.03
K - 6	9.32E-06	0.0016	0.016	6.74E-06	1.51E-04	0.017	0.154
K - 7	4.87E-06	0.001	0.016	6.31E-06	1.51E-04	0	0
K - 8	2.64E-05	0.0059	0.016	7.63E-06	1.51E-04	0.124	1.059
K - 9	7.94E-06	0.0014	0.016	6.31E-06	1.51E-04	0.011	0.085
K - 10	1.42E-05	0.0042	0.016	5.42E-06	1.51E-04	0.058	0.571
K - 11	9.70E-06	0.0023	0.016	1.84E-05	1.51E-04	0	0
K - 12	6.92E-06	0.0012	0.016	7.20E-06	1.51E-04	0	0
K - 13	1.00E-05	0.002	0.016	9.86E-06	1.51E-04	0.001	0.007
K - 14	1.33E-05	0.002	0.016	6.75E-06	1.51E-04	0.043	0.335
K - 15	1.07E-05	0.0014	0.016	1.07E-05	1.51E-04	0	0
L - 1	1.79E-05	0.0022	0.016	1.34E-05	1.51E-04	0.029	0.164
L - 2	1.55E-05	0.002	0.016	1.39E-05	1.51E-04	0.011	0.05
L - 3	1.68E-05	0.0023	0.016	1.34E-05	1.51E-04	0.023	0.149
L - 4	9.14E-06	0.0015	0.016	6.31E-06	1.51E-04	0.019	0.139
L - 5	1.17E-05	0.0017	0.016	1.03E-05	1.51E-04	0.009	0.061
L - 6	1.14E-05	0.0017	0.016	5.87E-06	1.51E-04	0.036	0.263
L - 7	1.09E-05	0.0018	0.016	8.96E-06	1.51E-04	0.013	0.089
L - 8	1.02E-05	0.0017	0.016	4.98E-06	1.51E-04	0.034	0.328

L - 9	1.80E-05	0.0022	0.016	8.55E-06	1.51E-04	0.063	0.338
L - 10	2.21E-05	0.0024	0.016	1.75E-05	1.51E-04	0.031	0.112
L - 11	1.66E-05	0.002	0.016	7.64E-06	1.51E-04	0.06	0.4
L - 12	2.07E-05	0.0021	0.016	1.21E-05	1.51E-04	0.057	0.344
L - 13	2.37E-05	0.0025	0.016	8.52E-06	1.51E-04	0.1	0.682
L - 14	1.27E-05	0.0017	0.016	1.43E-05	1.51E-04	0	0
L - 15	1.58E-05	0.0021	0.016	8.52E-06	1.51E-04	0.048	0.346
M - 1	1.20E-05	0.0016	0.016	9.86E-06	1.51E-04	0.014	0.085
M - 2	1.08E-05	0.0014	0.016	7.20E-06	1.51E-04	0.024	0.162
M - 3	1.13E-05	0.0014	0.016	8.51E-06	1.51E-04	0.019	0.164
M - 4	1.02E-05	0.0016	0.016	3.20E-06	1.51E-04	0.046	0.812
M - 5	8.12E-06	0.0015	0.016	7.64E-06	1.51E-04	0.003	0.023
M - 6	8.62E-06	0.0013	0.016	7.19E-06	1.51E-04	0.009	0.073
M - 7	1.22E-05	0.0015	0.016	7.19E-06	1.51E-04	0.033	0.265
M - 8	1.41E-05	0.0017	0.016	8.96E-06	1.51E-04	0.034	0.256
M - 9	1.91E-05	0.0024	0.016	1.12E-05	1.51E-04	0.052	0.349
M - 10	7.78E-06	0.0014	0.016	1.25E-05	1.51E-04	0	0
M - 11	1.80E-05	0.002	0.016	1.03E-05	1.51E-04	0.051	0.302
M - 12	2.54E-05	0.007	0.016	1.03E-05	1.51E-04	0.1	0.688
M - 13	0.0032	0.0457	0.016	4.03E-04	1.51E-04	18.271	3.372
M - 14	0.0029	0.043	0.016	5.43E-04	1.51E-04	15.45	2.201
M - 15	0.0033	0.0446	0.016	4.20E-04	1.51E-04	19.168	3.895
N - 1	8.45E-06	0.0013	0.016	1.21E-05	1.51E-04	0	0
N - 2	1.12E-05	0.0016	0.016	4.98E-06	1.51E-04	0.041	0.391
N - 3	1.08E-05	0.0015	0.016	1.39E-05	1.51E-04	0	0
N - 4	1.14E-05	0.0017	0.016	1.39E-05	1.51E-04	0	0
N - 5	9.82E-06	0.0015	0.016	9.87E-06	1.51E-04	0	0
N - 6	1.37E-05	0.0018	0.016	1.12E-05	1.51E-04	0.017	0.114
N - 7	9.83E-06	0.0016	0.016	1.12E-05	1.51E-04	0	0
N - 8	1.20E-05	0.0017	0.016	1.25E-05	1.51E-04	0	0
N - 9	9.26E-05	0.0284	0.016	7.63E-06	1.51E-04	0.563	4.462
N - 10	8.96E-06	0.0013	0.016	1.88E-05	1.51E-04	0	0
N - 11	1.77E-05	0.0025	0.016	9.84E-06	1.51E-04	0.052	0.39
N - 12	1.22E-05	0.002	0.016	1.12E-05	1.51E-04	0.007	0.039
N - 13	1.12E-05	0.0015	0.016	8.09E-06	1.51E-04	0.02	0.127
N - 14	1.20E-05	0.0016	0.016	1.21E-05	1.51E-04	0	0
N - 15	1.34E-05	0.0018	0.016	8.54E-06	1.51E-04	0.032	0.186
O - 1	1.10E-05	0.0017	0.016	1.52E-05	1.51E-04	0	0
O - 2	1.20E-05	0.0015	0.016	4.09E-06	1.51E-04	0.053	0.622
O - 3	1.15E-05	0.0017	0.016	6.30E-06	1.51E-04	0.035	0.304
O - 4	1.89E-05	0.0051	0.016	1.03E-05	1.51E-04	0.057	0.308
O - 5	5.90E-06	0.0011	0.016	3.20E-06	1.51E-04	0.018	0.244
O - 6	6.58E-06	0.0012	0.016	1.17E-05	1.51E-04	0	0
O - 7	1.08E-05	0.0016	0.016	8.52E-06	1.51E-04	0.015	0.107
O - 8	8.79E-06	0.0013	0.016	4.98E-06	1.51E-04	0.025	0.22

O - 9	8.27E-06	0.0011	0.016	1.38E-05	1.51E-04	0	0
O - 10	3.37E-05	0.0109	0.016	8.97E-06	1.51E-04	0.164	1.11
O - 11	2.42E-05	0.0039	0.016	9.85E-06	1.51E-04	0.095	0.623
O - 12	1.42E-05	0.0029	0.016	1.21E-05	1.51E-04	0.014	0.07
O - 13	0.0024	0.0589	0.016	9.02E-04	1.51E-04	9.808	0.945
O - 14	0.0025	0.0562	0.016	8.19E-04	1.51E-04	11.46	1.181
O - 15	0.0019	0.0406	0.016	2.44E-04	1.51E-04	10.683	2.72
P - 1	1.00E-05	0.0017	0.016	6.31E-06	1.51E-04	0.024	0.186
P - 2	1.10E-05	0.0016	0.016	9.85E-06	1.51E-04	0.008	0.052
P - 3	1.43E-05	0.0026	0.016	8.08E-06	1.51E-04	0.041	0.306
P - 4	1.02E-05	0.0016	0.016	8.10E-06	1.51E-04	0.014	0.081
P - 5	1.05E-05	0.0016	0.016	6.74E-06	1.51E-04	0.025	0.216
P - 6	7.60E-06	0.0013	0.016	4.97E-06	1.51E-04	0.017	0.184
P - 7	1.00E-05	0.0016	0.016	8.54E-06	1.51E-04	0.01	0.058
P - 8	1.17E-05	0.0018	0.016	9.44E-06	1.51E-04	0.015	0.074
P - 9	7.09E-06	0.0012	0.016	7.20E-06	1.51E-04	0	0
P - 10	1.10E-05	0.0017	0.016	1.56E-05	1.51E-04	0	0
P - 11	1.14E-05	0.0019	0.016	1.12E-05	1.51E-04	0.001	0.005
P - 12	1.10E-05	0.0015	0.016	5.41E-06	1.51E-04	0.037	0.386
P - 13	1.15E-05	0.0017	0.016	8.95E-06	1.51E-04	0.017	0.148
P - 14	1.14E-05	0.0017	0.016	9.86E-06	1.51E-04	0.01	0.061
P - 15	1.76E-05	0.0026	0.016	1.61E-05	1.51E-04	0.01	0.054
Q - 1	9.99E-06	0.0015	0.016	8.53E-06	1.51E-04	0.01	0.063
Q - 2	1.24E-05	0.0023	0.016	8.98E-06	1.51E-04	0.023	0.133
Q - 3	8.45E-06	0.0013	0.016	6.31E-06	1.51E-04	0.014	0.111
Q - 4	7.43E-06	0.0012	0.016	4.09E-06	1.51E-04	0.022	0.244
Q - 5	4.70E-06	0.0009	0.016	1.35E-05	1.51E-04	0	0
Q - 6	1.03E-05	0.0015	0.016	8.08E-06	1.51E-04	0.015	0.11
Q - 7	6.40E-06	0.0011	0.016	5.42E-06	1.51E-04	0.007	0.059
Q - 8	7.10E-06	0.0015	0.016	1.16E-05	1.51E-04	0	0
Q - 9	9.49E-06	0.0016	0.016	8.97E-06	1.51E-04	0.003	0.022
Q - 10	0.0002	0.1182	0.016	6.65E-05	1.51E-04	0.807	0.278
Q - 11	1.17E-05	0.002	0.016	8.51E-06	1.51E-04	0.021	0.186
Q - 12	1.58E-05	0.0056	0.016	1.53E-05	1.51E-04	0.003	0.011
Q - 13	0.0009	0.0256	0.016	1.14E-04	1.51E-04	5.313	2.447
Q - 14	0.001	0.0275	0.016	1.54E-04	1.51E-04	5.43	2.348
Q - 15	0.0008	0.0278	0.016	1.38E-04	1.51E-04	4.145	1.8
R - 1	1.27E-05	0.0031	0.016	1.12E-05	1.51E-04	0.01	0.054
R - 2	7.95E-06	0.0015	0.016	1.07E-05	1.51E-04	0	0
R - 3	5.04E-06	0.0009	0.016	8.08E-06	1.51E-04	0	0
R - 4	6.58E-06	0.0012	0.016	9.41E-06	1.51E-04	0	0
R - 5	7.26E-06	0.0013	0.016	7.63E-06	1.51E-04	0	0
R - 6	7.43E-06	0.0012	0.016	1.12E-05	1.51E-04	0	0
R - 7	8.62E-06	0.0014	0.016	1.21E-05	1.51E-04	0	0
R - 8	1.20E-05	0.0017	0.016	1.12E-05	1.51E-04	0.006	0.037

R - 9	6.94E-06	0.0015	0.016	8.07E-06	1.51E-04	0	0
R - 10	1.08E-05	0.0015	0.016	1.65E-05	1.51E-04	0	0
R - 11	7.94E-06	0.0012	0.016	5.41E-05	1.51E-04	0	0
R - 12	4.98E-05	0.0149	0.016	7.20E-06	1.51E-04	0.282	1.902
R - 13	9.83E-06	0.0016	0.016	7.64E-06	1.51E-04	0.015	0.108
R - 14	2.64E-05	0.0029	0.016	2.95E-05	1.51E-04	0	0
R - 15	5.56E-06	0.0011	0.016	9.42E-06	1.51E-04	0	0
S - 1	1.38E-05	0.0022	0.016	1.08E-05	1.51E-04	0.02	0.11
S - 2	9.32E-06	0.0017	0.016	5.86E-06	1.51E-04	0.023	0.223
S - 3	1.57E-05	0.006	0.016	1.16E-05	1.51E-04	0.027	0.133
S - 4	9.65E-06	0.0015	0.016	6.30E-06	1.51E-04	0.022	0.224
S - 5	1.24E-05	0.0016	0.016	1.79E-05	1.51E-04	0	0
S - 6	1.48E-05	0.0022	0.016	2.28E-05	1.51E-04	0	0
S - 7	4.53E-06	0.001	0.016	5.42E-06	1.51E-04	0	0
S - 8	1.23E-05	0.0024	0.016	3.20E-06	1.51E-04	0.06	0.917
S - 9	7.60E-06	0.0012	0.016	1.45E-05	1.51E-04	0	0
S - 10	1.22E-05	0.0017	0.016	3.45E-04	1.51E-04	0	0
S - 11	1.13E-05	0.0033	0.016	1.07E-05	1.51E-04	0.004	0.023
S - 12	7.60E-06	0.0013	0.016	1.25E-05	1.51E-04	0	0
S - 13	0.0005	0.0243	0.016	7.90E-05	1.51E-04	2.519	1.71
S - 14	0.0004	0.0237	0.016	4.56E-05	1.51E-04	2.403	3.391
S - 15	0.0004	0.0195	0.016	6.47E-05	1.51E-04	1.921	1.669
T - 1	7.10E-06	0.0014	0.016	8.08E-06	1.51E-04	0	0
T - 2	9.82E-06	0.0014	0.016	4.97E-06	1.51E-04	0.032	0.321
T - 3	1.02E-05	0.0017	0.016	5.41E-06	1.51E-04	0.032	0.328
T - 4	7.78E-06	0.0014	0.016	1.53E-05	1.51E-04	0	0
T - 5	5.56E-06	0.0012	0.016	6.32E-06	1.51E-04	0	0
T - 6	6.23E-06	0.001	0.016	9.41E-06	1.51E-04	0	0
T - 7	7.26E-06	0.0012	0.016	8.53E-06	1.51E-04	0	0
T - 8	6.57E-06	0.0011	0.016	1.16E-05	1.51E-04	0	0
T - 9	8.11E-06	0.0013	0.016	1.43E-05	1.51E-04	0	0
T - 10	0.0003	0.193	0.016	4.82E-05	1.51E-04	1.444	0.744
T - 11	1.03E-05	0.0018	0.016	1.15E-04	1.51E-04	0	0
T - 12	1.69E-05	0.0064	0.016	8.08E-06	1.51E-04	0.059	0.422
T - 13	1.02E-05	0.0015	0.016	9.85E-06	1.51E-04	0.002	0.013
T - 14	9.31E-06	0.0015	0.016	1.03E-05	1.51E-04	0	0
T - 15	9.31E-06	0.0014	0.016	6.74E-06	1.51E-04	0.017	0.161
U - 1	8.28E-06	0.0013	0.016	7.19E-06	1.51E-04	0.007	0.056
U - 2	6.58E-06	0.0013	0.016	1.47E-05	1.51E-04	0	0
U - 3	1.14E-05	0.002	0.016	8.53E-06	1.51E-04	0.019	0.125
U - 4	7.78E-06	0.0015	0.016	7.19E-06	1.51E-04	0.004	0.035
U - 5	9.82E-06	0.0014	0.016	7.64E-06	1.51E-04	0.014	0.102
U - 6	8.30E-06	0.0016	0.016	1.03E-05	1.51E-04	0	0
U - 7	6.75E-06	0.0013	0.016	7.64E-06	1.51E-04	0	0
U - 8	8.97E-06	0.0015	0.016	8.96E-06	1.51E-04	4.64E-05	3.41E-04

U - 9	1.27E-05	0.0058	0.016	9.85E-06	1.51E-04	0.019	0.123
U - 10	1.30E-05	0.003	0.016	1.04E-05	1.51E-04	0.017	0.069
U - 11	1.22E-05	0.002	0.016	2.82E-05	1.51E-04	0	0
U - 12	6.58E-06	0.0012	0.016	9.85E-06	1.51E-04	0	0
U - 13	2.90E-05	0.0026	0.016	2.92E-05	1.51E-04	0	0
U - 14	3.96E-05	0.0034	0.016	9.08E-06	1.51E-04	0.202	0.66
U - 15	4.06E-05	0.003	0.016	1.16E-05	1.51E-04	0.192	1.054
A. n	315	315	315	315	315	315	315
A. Mean	0.0002	0.0082	0.016	3.53E-05	1.51E-04	1.014	1.469
A. SD	0.0005	0.0184	0	9.00E-05	0	2.64	1.99
A. CV	253.4647	224.3534	0	255.383	0	260.279	135.532
A. Total	0.0587	2.5881	4.914	0.011	0.048	319.472	462.585

Table 10. Results obtained upon the use of TeleChem immobilization protocol and higher stringency washing conditions. In element column capital letters designate spot rows and numbers designate spots from left to right. ROD, relative optical density (an Imaging Research Inc. proprietary density scale which represents an inverse logarithmic function of grey-level values).

Element	D x A - ROD x mm2	SD - ROD	Area - mm2	Bkgd	sRef	nDxA	S/N
A - 1	1.84E-05	0.0023	0.016	1.74E-05	1.22E-04	0.008	0.031
A - 2	3.79E-05	0.0032	0.016	3.39E-05	1.22E-04	0.033	0.09
A - 3	4.13E-05	0.0036	0.016	8.07E-05	1.22E-04	0	0
A - 4	3.53E-05	0.003	0.016	1.92E-05	1.22E-04	0.132	0.507
A - 5	1.29E-05	0.002	0.016	2.41E-05	1.22E-04	0	0
A - 6	3.99E-05	0.0212	0.016	3.81E-05	1.22E-04	0.015	0.012
A - 7	2.01E-05	0.0023	0.016	1.16E-05	1.22E-04	0.069	0.383
A - 8	1.68E-05	0.002	0.016	5.43E-06	1.22E-04	0.093	0.567
A - 9	2.59E-05	0.0026	0.016	1.21E-05	1.22E-04	0.113	0.511
A - 10	2.62E-05	0.0024	0.016	1.25E-05	1.22E-04	0.112	0.554
A - 11	2.16E-05	0.0022	0.016	1.70E-05	1.22E-04	0.038	0.142
A - 12	6.10E-05	0.0133	0.016	8.97E-06	1.22E-04	0.425	2.33
A - 13	3.67E-05	0.0035	0.016	1.70E-05	1.22E-04	0.162	0.58
A - 14	1.82E-05	0.0022	0.016	1.87E-05	1.22E-04	0	0
A - 15	1.63E-05	0.0021	0.016	1.47E-05	1.22E-04	0.013	0.052
B - 1	1.75E-05	0.0019	0.016	1.79E-05	1.22E-04	0	0
B - 2	2.66E-05	0.0027	0.016	2.05E-05	1.22E-04	0.05	0.162
B - 3	2.52E-05	0.0027	0.016	2.27E-05	1.22E-04	0.02	0.07
B - 4	2.62E-05	0.0023	0.016	1.61E-05	1.22E-04	0.083	0.3
B - 5	2.59E-05	0.0028	0.016	1.83E-05	1.22E-04	0.063	0.282
B - 6	1.81E-05	0.0028	0.016	1.21E-05	1.22E-04	0.049	0.238
B - 7	1.77E-05	0.0019	0.016	1.30E-05	1.22E-04	0.038	0.142
B - 8	2.60E-05	0.0024	0.016	1.30E-05	1.22E-04	0.107	0.398
B - 9	2.52E-05	0.0044	0.016	9.87E-06	1.22E-04	0.126	0.561
B - 10	7.42E-06	0.0011	0.016	8.95E-06	1.22E-04	0	0
B - 11	7.43E-06	0.0013	0.016	1.07E-05	1.22E-04	0	0
B - 12	2.11E-05	0.0021	0.016	9.87E-06	1.22E-04	0.092	0.41
B - 13	9.48E-06	0.0015	0.016	8.52E-06	1.22E-04	0.008	0.047
B - 14	0.0019	0.0286	0.016	8.01E-04	1.22E-04	9.16	1.303
B - 15	0.0022	0.0353	0.016	6.16E-04	1.22E-04	12.646	1.643
C - 1	4.26E-05	0.0039	0.016	3.12E-05	1.22E-04	0.093	0.254
C - 2	5.37E-05	0.0049	0.016	2.77E-05	1.22E-04	0.213	0.547
C - 3	5.20E-05	0.004	0.016	2.73E-05	1.22E-04	0.202	0.463
C - 4	6.63E-05	0.0045	0.016	5.00E-05	1.22E-04	0.133	0.257
C - 5	5.05E-05	0.0041	0.016	3.13E-05	1.22E-04	0.157	0.332
C - 6	5.01E-05	0.0038	0.016	3.00E-05	1.22E-04	0.164	0.321
C - 7	3.45E-05	0.0033	0.016	4.22E-05	1.22E-04	0	0
C - 8	4.99E-05	0.004	0.016	3.31E-05	1.22E-04	0.138	0.298

C - 9	4.20E-05	0.0036	0.016	2.81E-05	1.22E-04	0.114	0.312
C - 10	7.98E-05	0.0044	0.016	4.58E-05	1.22E-04	0.278	0.381
C - 11	5.94E-05	0.0041	0.016	3.85E-05	1.22E-04	0.17	0.283
C - 12	6.25E-05	0.0044	0.016	3.45E-05	1.22E-04	0.229	0.404
C - 13	3.77E-05	0.0034	0.016	3.58E-05	1.22E-04	0.016	0.028
C - 14	7.14E-05	0.0047	0.016	4.20E-05	1.22E-04	0.24	0.422
C - 15	6.04E-05	0.0042	0.016	3.45E-05	1.22E-04	0.212	0.39
D - 1	4.84E-05	0.0042	0.016	3.39E-05	1.22E-04	0.119	0.305
D - 2	5.11E-05	0.0051	0.016	3.30E-05	1.22E-04	0.148	0.348
D - 3	4.85E-05	0.0046	0.016	4.79E-05	1.22E-04	0.005	0.008
D - 4	6.61E-05	0.0044	0.016	3.66E-05	1.22E-04	0.241	0.574
D - 5	4.58E-05	0.0036	0.016	5.41E-05	1.22E-04	0	0
D - 6	5.27E-05	0.0045	0.016	3.71E-05	1.22E-04	0.128	0.254
D - 7	5.50E-05	0.0048	0.016	4.22E-05	1.22E-04	0.105	0.147
D - 8	3.81E-05	0.0038	0.016	2.82E-05	1.22E-04	0.081	0.17
D - 9	4.74E-05	0.0043	0.016	2.45E-05	1.22E-04	0.187	0.6
D - 10	4.17E-05	0.0038	0.016	2.87E-05	1.22E-04	0.106	0.192
D - 11	8.62E-05	0.04	0.016	3.72E-05	1.22E-04	0.401	0.673
D - 12	5.00E-05	0.0044	0.016	3.85E-05	1.22E-04	0.094	0.165
D - 13	0.0015	0.0239	0.016	3.86E-04	1.22E-04	9.132	1.791
D - 14	0.0016	0.0231	0.016	3.73E-04	1.22E-04	10.054	2.2
D - 15	0.0016	0.0224	0.016	3.15E-04	1.22E-04	10.61	2.481
E - 1	0.0001	0.0066	0.016	7.60E-05	1.22E-04	0.504	0.443
E - 2	9.86E-05	0.0056	0.016	4.11E-05	1.22E-04	0.47	0.843
E - 3	0.0001	0.0063	0.016	4.11E-05	1.22E-04	0.669	1.254
E - 4	9.50E-05	0.0047	0.016	7.72E-05	1.22E-04	0.145	0.165
E - 5	0.0001	0.0056	0.016	5.14E-05	1.22E-04	0.411	0.687
E - 6	0.0001	0.0132	0.016	8.12E-05	1.22E-04	0.517	0.611
E - 7	0.0001	0.0066	0.016	3.35E-05	1.22E-04	0.835	1.836
E - 8	0.0001	0.0064	0.016	5.21E-05	1.22E-04	0.653	0.844
E - 9	7.90E-05	0.0056	0.016	2.58E-05	1.22E-04	0.435	1.34
E - 10	0.0001	0.0065	0.016	3.32E-05	1.22E-04	0.813	1.413
E - 11	0.0001	0.0066	0.016	3.24E-05	1.22E-04	0.812	1.187
E - 12	0.0002	0.0079	0.016	3.80E-05	1.22E-04	0.918	1.622
E - 13	0.0001	0.0064	0.016	2.50E-05	1.22E-04	0.884	2.14
E - 14	0.0001	0.0063	0.016	3.49E-05	1.22E-04	0.847	1.56
E - 15	0.0001	0.0066	0.016	1.61E-05	1.22E-04	1.003	3.352
F - 1	0.0001	0.0061	0.016	1.61E-05	1.22E-04	0.896	3.315
F - 2	0.0001	0.0073	0.016	2.23E-05	1.22E-04	0.918	2.51
F - 3	0.0001	0.006	0.016	4.07E-05	1.22E-04	0.599	1.02
F - 4	0.0001	0.0072	0.016	6.49E-05	1.22E-04	0.531	0.734
F - 5	0.0006	0.2221	0.016	3.86E-05	1.22E-04	4.593	7.228
F - 6	0.0002	0.0074	0.016	4.16E-05	1.22E-04	0.943	1.634
F - 7	0.0002	0.0078	0.016	7.69E-05	1.22E-04	0.637	0.679
F - 8	0.0001	0.0067	0.016	6.16E-05	1.22E-04	0.681	1.134

F - 9	0.0001	0.0058	0.016	4.63E-05	1.22E-04	0.589	0.796
F - 10	0.0001	0.0068	0.016	4.89E-05	1.22E-04	0.825	1.207
F - 11	0.0002	0.0076	0.016	3.38E-05	1.22E-04	1.174	1.67
F - 12	0.0002	0.0082	0.016	4.71E-05	1.22E-04	0.89	1.269
F - 13	0.0007	0.0165	0.016	1.26E-04	1.22E-04	4.956	2.531
F - 14	0.0007	0.0157	0.016	1.26E-04	1.22E-04	4.628	2.486
F - 15	0.0007	0.0149	0.016	6.02E-05	1.22E-04	4.934	4.621
G - 1	0.0002	0.0081	0.016	6.71E-05	1.22E-04	1.44	1.269
G - 2	0.0002	0.0076	0.016	4.24E-05	1.22E-04	1.282	1.586
G - 3	0.0002	0.0071	0.016	4.13E-05	1.22E-04	0.957	1.474
G - 4	0.0002	0.008	0.016	4.56E-05	1.22E-04	0.91	1.527
G - 5	0.0001	0.0075	0.016	5.92E-05	1.22E-04	0.687	0.877
G - 6	0.0002	0.0075	0.016	3.63E-05	1.22E-04	1.069	1.806
G - 7	0.0001	0.0076	0.016	5.93E-05	1.22E-04	0.617	0.758
G - 8	0.0002	0.0078	0.016	7.24E-05	1.22E-04	0.823	0.919
G - 9	0.0002	0.0089	0.016	4.57E-05	1.22E-04	1.348	1.984
G - 10	0.0002	0.0089	0.016	4.82E-05	1.22E-04	1.375	1.706
G - 11	0.0002	0.0082	0.016	5.26E-05	1.22E-04	1.252	1.606
G - 12	0.0002	0.0076	0.016	2.46E-05	1.22E-04	1.651	3.846
G - 13	0.0002	0.0081	0.016	4.72E-05	1.22E-04	1.378	1.78
G - 14	0.0002	0.0078	0.016	1.61E-05	1.22E-04	1.293	4.206
G - 15	0.0002	0.0075	0.016	3.42E-05	1.22E-04	1.432	2.228
H - 1	0.0002	0.0075	0.016	2.95E-05	1.22E-04	1.452	3.352
H - 2	0.0002	0.0071	0.016	3.53E-05	1.22E-04	1.267	2.578
H - 3	0.0002	0.0078	0.016	4.61E-05	1.22E-04	1.08	1.855
H - 4	0.0002	0.0071	0.016	7.03E-05	1.22E-04	0.838	0.846
H - 5	0.0002	0.0074	0.016	3.89E-05	1.22E-04	0.996	1.746
H - 6	0.0002	0.0077	0.016	1.34E-05	1.22E-04	1.481	6.099
H - 7	0.0002	0.0074	0.016	5.65E-05	1.22E-04	1.026	1.4
H - 8	0.0002	0.0082	0.016	7.58E-05	1.22E-04	1.255	1.507
H - 9	0.0002	0.0076	0.016	4.26E-05	1.22E-04	1.173	1.839
H - 10	0.0002	0.0086	0.016	3.83E-05	1.22E-04	1.132	1.519
H - 11	0.0002	0.0075	0.016	4.44E-05	1.22E-04	1.127	1.684
H - 12	0.0003	0.0087	0.016	3.10E-05	1.22E-04	1.801	3.098
H - 13	0.0003	0.0103	0.016	6.14E-05	1.22E-04	2.05	2.117
H - 14	0.0003	0.0107	0.016	4.65E-05	1.22E-04	2.258	2.521
H - 15	0.0003	0.0105	0.016	1.97E-05	1.22E-04	2.614	7.106
I - 1	0.0002	0.0087	0.016	6.90E-05	1.22E-04	1.307	1.681
I - 2	0.0002	0.0075	0.016	4.04E-05	1.22E-04	1.231	1.942
I - 3	0.0002	0.0081	0.016	5.12E-05	1.22E-04	1.233	1.648
I - 4	0.0002	0.0078	0.016	4.35E-05	1.22E-04	1.32	1.957
I - 5	0.0002	0.0082	0.016	2.41E-05	1.22E-04	1.523	3.698
I - 6	0.0002	0.0075	0.016	2.45E-05	1.22E-04	1.624	5.206
I - 7	0.0002	0.0084	0.016	3.65E-05	1.22E-04	1.491	2.114
I - 8	0.0002	0.0078	0.016	6.36E-05	1.22E-04	1.046	1.422

I - 9	0.0002	0.0083	0.016	6.07E-05	1.22E-04	1.215	2.19
I - 10	0.0002	0.0084	0.016	1.74E-05	1.22E-04	1.828	7.212
I - 11	0.0002	0.0096	0.016	5.69E-05	1.22E-04	1.557	1.653
I - 12	0.0002	0.0091	0.016	3.05E-05	1.22E-04	1.747	2.934
I - 13	0.0002	0.0094	0.016	8.59E-05	1.22E-04	1.001	0.866
I - 14	0.0003	0.0092	0.016	2.90E-05	1.22E-04	1.862	4.782
I - 15	0.0002	0.0092	0.016	6.39E-05	1.22E-04	1.441	1.601
J - 1	0.0002	0.0094	0.016	2.10E-05	1.22E-04	1.832	4.445
J - 2	0.0002	0.0086	0.016	6.01E-05	1.22E-04	1.07	1.084
J - 3	0.0002	0.0085	0.016	5.33E-05	1.22E-04	1.423	2.131
J - 4	0.0002	0.0085	0.016	5.89E-05	1.22E-04	1.212	1.45
J - 5	0.0002	0.0077	0.016	3.77E-05	1.22E-04	1.483	2.435
J - 6	0.0002	0.0098	0.016	5.20E-05	1.22E-04	1.434	2.006
J - 7	0.0002	0.009	0.016	4.39E-05	1.22E-04	1.298	1.961
J - 8	0.0002	0.0101	0.016	7.55E-05	1.22E-04	1.244	1.412
J - 9	0.0002	0.0076	0.016	1.96E-05	1.22E-04	1.243	3.889
J - 10	0.0002	0.0117	0.016	4.43E-05	1.22E-04	1.381	2.352
J - 11	0.0002	0.009	0.016	2.74E-05	1.22E-04	1.814	3.446
J - 12	0.0003	0.0091	0.016	4.28E-05	1.22E-04	1.856	2.421
J - 13	0.0003	0.0099	0.016	7.13E-05	1.22E-04	1.464	1.403
J - 14	0.0002	0.0095	0.016	8.78E-05	1.22E-04	1.256	0.912
J - 15	0.0002	0.0094	0.016	4.68E-05	1.22E-04	1.534	1.888
K - 1	0.0003	0.0089	0.016	3.27E-05	1.22E-04	1.811	3.273
K - 2	0.0002	0.0082	0.016	1.16E-05	1.22E-04	1.817	9.184
K - 3	0.0002	0.0082	0.016	3.78E-05	1.22E-04	1.384	1.902
K - 4	9.99E-06	0.0016	0.016	1.34E-05	1.22E-04	0	0
K - 5	1.05E-05	0.0018	0.016	7.63E-06	1.22E-04	0.024	0.157
K - 6	6.23E-06	0.001	0.016	1.25E-05	1.22E-04	0	0
K - 7	9.98E-06	0.0014	0.016	6.30E-06	1.22E-04	0.03	0.214
K - 8	1.48E-05	0.0037	0.016	1.12E-05	1.22E-04	0.029	0.138
K - 9	9.99E-06	0.0016	0.016	1.16E-05	1.22E-04	0	0
K - 10	1.46E-05	0.002	0.016	1.39E-05	1.22E-04	0.006	0.026
K - 11	1.03E-05	0.0017	0.016	1.43E-05	1.22E-04	0	0
K - 12	1.32E-05	0.0019	0.016	1.03E-05	1.22E-04	0.024	0.12
K - 13	2.73E-05	0.003	0.016	1.47E-05	1.22E-04	0.103	0.443
K - 14	8.62E-06	0.0012	0.016	7.63E-06	1.22E-04	0.008	0.052
K - 15	1.03E-05	0.0016	0.016	6.75E-06	1.22E-04	0.029	0.179
L - 1	2.35E-05	0.0025	0.016	1.12E-05	1.22E-04	0.101	0.5
L - 2	2.21E-05	0.0025	0.016	1.92E-05	1.22E-04	0.024	0.088
L - 3	2.33E-05	0.0025	0.016	2.72E-05	1.22E-04	0	0
L - 4	2.19E-05	0.0021	0.016	1.70E-05	1.22E-04	0.041	0.137
L - 5	1.12E-05	0.0017	0.016	1.25E-05	1.22E-04	0	0
L - 6	2.74E-05	0.0028	0.016	2.09E-05	1.22E-04	0.053	0.2
L - 7	1.24E-05	0.0018	0.016	9.85E-06	1.22E-04	0.021	0.119
L - 8	1.87E-05	0.0019	0.016	1.52E-05	1.22E-04	0.029	0.12

L - 9	2.13E-05	0.0027	0.016	1.07E-05	1.22E-04	0.086	0.397
L - 10	5.25E-05	0.0041	0.016	3.12E-05	1.22E-04	0.175	0.534
L - 11	1.82E-05	0.0021	0.016	1.56E-05	1.22E-04	0.021	0.088
L - 12	1.48E-05	0.0022	0.016	1.52E-05	1.22E-04	0	0
L - 13	2.21E-05	0.0024	0.016	1.56E-05	1.22E-04	0.053	0.224
L - 14	2.25E-05	0.0023	0.016	1.12E-05	1.22E-04	0.092	0.488
L - 15	1.97E-05	0.0021	0.016	4.18E-05	1.22E-04	0	0
M - 1	1.07E-05	0.0018	0.016	9.45E-06	1.22E-04	0.01	0.039
M - 2	2.01E-05	0.0023	0.016	1.12E-05	1.22E-04	0.073	0.347
M - 3	2.76E-05	0.0029	0.016	9.85E-06	1.22E-04	0.145	0.756
M - 4	1.24E-05	0.0017	0.016	7.63E-06	1.22E-04	0.039	0.25
M - 5	1.22E-05	0.0015	0.016	1.38E-05	1.22E-04	0	0
M - 6	8.45E-06	0.0014	0.016	1.12E-05	1.22E-04	0	0
M - 7	3.30E-05	0.0034	0.016	1.61E-05	1.22E-04	0.138	0.517
M - 8	2.18E-05	0.0029	0.016	1.83E-05	1.22E-04	0.029	0.1
M - 9	3.19E-05	0.0031	0.016	1.65E-05	1.22E-04	0.126	0.446
M - 10	2.45E-05	0.0025	0.016	1.78E-05	1.22E-04	0.055	0.216
M - 11	1.90E-05	0.0022	0.016	8.98E-06	1.22E-04	0.082	0.405
M - 12	2.13E-05	0.0026	0.016	1.70E-05	1.22E-04	0.035	0.119
M - 13	0.0036	0.0442	0.016	0.002	1.22E-04	16.514	1.158
M - 14	0.0035	0.049	0.016	0.001	1.22E-04	17.116	1.316
M - 15	0.0033	0.044	0.016	8.61E-04	1.22E-04	20.356	2.028
N - 1	9.83E-06	0.0016	0.016	6.75E-06	1.22E-04	0.025	0.164
N - 2	1.81E-05	0.003	0.016	1.25E-05	1.22E-04	0.046	0.185
N - 3	1.55E-05	0.002	0.016	1.12E-05	1.22E-04	0.035	0.194
N - 4	1.99E-05	0.0023	0.016	1.92E-05	1.22E-04	0.006	0.022
N - 5	1.77E-05	0.002	0.016	7.64E-06	1.22E-04	0.082	0.495
N - 6	6.91E-06	0.001	0.016	1.30E-05	1.22E-04	0	0
N - 7	1.61E-05	0.0019	0.016	1.52E-05	1.22E-04	0.008	0.031
N - 8	1.48E-05	0.002	0.016	1.47E-05	1.22E-04	3.58E-04	0.002
N - 9	1.31E-05	0.0017	0.016	1.61E-05	1.22E-04	0	0
N - 10	1.82E-05	0.0022	0.016	1.87E-05	1.22E-04	0	0
N - 11	1.80E-05	0.0019	0.016	1.16E-05	1.22E-04	0.052	0.232
N - 12	1.36E-05	0.0017	0.016	1.16E-05	1.22E-04	0.016	0.084
N - 13	4.34E-05	0.0046	0.016	1.70E-05	1.22E-04	0.216	0.886
N - 14	1.92E-05	0.0021	0.016	1.03E-05	1.22E-04	0.073	0.417
N - 15	1.34E-05	0.0021	0.016	8.53E-06	1.22E-04	0.04	0.201
O - 1	9.31E-06	0.0015	0.016	8.54E-06	1.22E-04	0.006	0.03
O - 2	1.32E-05	0.0019	0.016	4.97E-06	1.22E-04	0.068	0.618
O - 3	1.70E-05	0.0022	0.016	1.88E-05	1.22E-04	0	0
O - 4	1.36E-05	0.0017	0.016	7.62E-06	1.22E-04	0.049	0.383
O - 5	9.98E-06	0.0014	0.016	1.25E-05	1.22E-04	0	0
O - 6	9.30E-06	0.0013	0.016	6.30E-06	1.22E-04	0.025	0.167
O - 7	1.27E-05	0.0015	0.016	1.12E-05	1.22E-04	0.012	0.057
O - 8	1.32E-05	0.0015	0.016	1.12E-05	1.22E-04	0.017	0.086

O - 9	1.19E-05	0.0015	0.016	2.06E-05	1.22E-04	0	0
O - 10	1.50E-05	0.0026	0.016	1.52E-05	1.22E-04	0	0
O - 11	1.39E-05	0.0018	0.016	9.87E-06	1.22E-04	0.033	0.15
O - 12	1.34E-05	0.0017	0.016	1.97E-05	1.22E-04	0	0
O - 13	0.0025	0.0704	0.016	8.37E-04	1.22E-04	13.692	1.158
O - 14	0.0025	0.066	0.016	6.40E-04	1.22E-04	15.061	1.614
O - 15	0.003	0.0718	0.016	7.18E-04	1.22E-04	18.964	1.7
P - 1	1.07E-05	0.0017	0.016	1.38E-05	1.22E-04	0	0
P - 2	1.22E-05	0.0019	0.016	1.21E-05	1.22E-04	0.001	0.006
P - 3	1.02E-05	0.0015	0.016	1.47E-05	1.22E-04	0	0
P - 4	1.79E-05	0.0024	0.016	6.30E-06	1.22E-04	0.095	0.701
P - 5	1.48E-05	0.002	0.016	1.43E-05	1.22E-04	0.004	0.017
P - 6	1.55E-05	0.0022	0.016	9.85E-06	1.22E-04	0.046	0.257
P - 7	1.05E-05	0.0017	0.016	9.84E-06	1.22E-04	0.005	0.033
P - 8	2.13E-05	0.0025	0.016	8.53E-06	1.22E-04	0.104	0.536
P - 9	2.01E-05	0.0022	0.016	2.05E-05	1.22E-04	0	0
P - 10	7.26E-06	0.0013	0.016	5.86E-06	1.22E-04	0.011	0.09
P - 11	1.38E-05	0.0021	0.016	8.07E-06	1.22E-04	0.047	0.319
P - 12	1.84E-05	0.0023	0.016	1.25E-05	1.22E-04	0.048	0.237
P - 13	8.11E-06	0.0012	0.016	6.74E-06	1.22E-04	0.011	0.086
P - 14	1.19E-05	0.0019	0.016	1.39E-05	1.22E-04	0	0
P - 15	1.39E-05	0.002	0.016	1.08E-05	1.22E-04	0.026	0.088
Q - 1	1.15E-05	0.0018	0.016	1.16E-05	1.22E-04	0	0
Q - 2	1.17E-05	0.0015	0.016	1.34E-05	1.22E-04	0	0
Q - 3	1.14E-05	0.0017	0.016	1.21E-05	1.22E-04	0	0
Q - 4	1.03E-05	0.0017	0.016	1.12E-05	1.22E-04	0	0
Q - 5	1.07E-05	0.0016	0.016	1.52E-05	1.22E-04	0	0
Q - 6	1.46E-05	0.0021	0.016	1.65E-05	1.22E-04	0	0
Q - 7	1.10E-05	0.0015	0.016	9.85E-06	1.22E-04	0.009	0.05
Q - 8	1.26E-05	0.0017	0.016	7.19E-06	1.22E-04	0.044	0.275
Q - 9	3.91E-05	0.0031	0.016	1.56E-05	1.22E-04	0.192	0.734
Q - 10	1.20E-05	0.0032	0.016	8.07E-06	1.22E-04	0.032	0.205
Q - 11	1.10E-05	0.0015	0.016	9.41E-06	1.22E-04	0.013	0.07
Q - 12	9.14E-06	0.0015	0.016	4.97E-06	1.22E-04	0.034	0.335
Q - 13	0.0015	0.0409	0.016	2.11E-04	1.22E-04	10.445	2.973
Q - 14	0.0013	0.0335	0.016	5.13E-04	1.22E-04	6.734	0.895
Q - 15	0.0016	0.0427	0.016	3.23E-04	1.22E-04	10.276	1.519
R - 1	1.36E-05	0.0019	0.016	6.30E-06	1.22E-04	0.06	0.487
R - 2	1.12E-05	0.0017	0.016	1.30E-05	1.22E-04	0	0
R - 3	9.31E-06	0.0015	0.016	1.47E-05	1.22E-04	0	0
R - 4	8.45E-06	0.0014	0.016	7.63E-06	1.22E-04	0.007	0.049
R - 5	1.14E-05	0.0017	0.016	1.16E-05	1.22E-04	0	0
R - 6	8.12E-06	0.0015	0.016	8.07E-06	1.22E-04	3.75E-04	0.002
R - 7	8.96E-06	0.0013	0.016	8.97E-06	1.22E-04	0	0
R - 8	9.47E-06	0.0013	0.016	8.96E-06	1.22E-04	0.004	0.026

R - 9	2.61E-05	0.0025	0.016	9.26E-05	1.22E-04	0	0
R - 10	1.08E-05	0.0015	0.016	1.08E-05	1.22E-04	7.06E-04	0.003
R - 11	1.19E-05	0.0016	0.016	1.61E-05	1.22E-04	0	0
R - 12	1.14E-05	0.0019	0.016	9.43E-06	1.22E-04	0.016	0.067
R - 13	1.24E-05	0.0018	0.016	4.97E-06	1.22E-04	0.061	0.554
R - 14	1.19E-05	0.002	0.016	8.51E-06	1.22E-04	0.028	0.181
R - 15	9.32E-06	0.0017	0.016	1.61E-05	1.22E-04	0	0
S - 1	2.39E-05	0.0031	0.016	2.05E-05	1.22E-04	0.027	0.082
S - 2	2.03E-05	0.0024	0.016	9.86E-06	1.22E-04	0.085	0.4
S - 3	1.58E-05	0.002	0.016	2.10E-05	1.22E-04	0	0
S - 4	8.62E-06	0.0013	0.016	9.85E-06	1.22E-04	0	0
S - 5	5.90E-06	0.0011	0.016	1.21E-05	1.22E-04	0	0
S - 6	7.77E-06	0.0013	0.016	9.41E-06	1.22E-04	0	0
S - 7	8.97E-06	0.0015	0.016	7.65E-06	1.22E-04	0.011	0.053
S - 8	9.31E-06	0.0015	0.016	8.95E-06	1.22E-04	0.003	0.02
S - 9	2.45E-05	0.0026	0.016	2.14E-05	1.22E-04	0.026	0.091
S - 10	9.49E-06	0.0016	0.016	8.96E-06	1.22E-04	0.004	0.027
S - 11	1.77E-05	0.0021	0.016	1.16E-05	1.22E-04	0.049	0.201
S - 12	1.87E-05	0.0022	0.016	1.47E-05	1.22E-04	0.033	0.162
S - 13	0.001	0.0219	0.016	9.18E-04	1.22E-04	1.009	0.334
S - 14	0.001	0.024	0.016	8.50E-04	1.22E-04	1.293	0.376
S - 15	0.0008	0.019	0.016	9.37E-04	1.22E-04	0	0
T - 1	1.41E-05	0.0016	0.016	7.19E-06	1.22E-04	0.056	0.393
T - 2	1.39E-05	0.0018	0.016	1.69E-05	1.22E-04	0	0
T - 3	1.27E-05	0.0018	0.016	1.12E-05	1.22E-04	0.013	0.067
T - 4	1.03E-05	0.0015	0.016	1.25E-05	1.22E-04	0	0
T - 5	1.41E-05	0.0021	0.016	7.66E-06	1.22E-04	0.053	0.231
T - 6	1.29E-05	0.0016	0.016	6.75E-06	1.22E-04	0.05	0.327
T - 7	1.32E-05	0.0019	0.016	7.64E-06	1.22E-04	0.046	0.269
T - 8	7.77E-06	0.0012	0.016	7.19E-06	1.22E-04	0.005	0.028
T - 9	3.02E-05	0.0028	0.016	2.15E-05	1.22E-04	0.071	0.17
T - 10	1.02E-05	0.0016	0.016	1.65E-05	1.22E-04	0	0
T - 11	1.08E-05	0.0016	0.016	6.30E-06	1.22E-04	0.037	0.254
T - 12	1.39E-05	0.0018	0.016	6.74E-06	1.22E-04	0.059	0.45
T - 13	1.38E-05	0.002	0.016	1.07E-05	1.22E-04	0.025	0.137
T - 14	2.23E-05	0.0053	0.016	1.16E-05	1.22E-04	0.088	0.442
T - 15	9.99E-06	0.0015	0.016	8.98E-06	1.22E-04	0.008	0.041
U - 1	1.07E-05	0.0015	0.016	1.21E-05	1.22E-04	0	0
U - 2	1.36E-05	0.0018	0.016	1.34E-05	1.22E-04	0.002	0.008
U - 3	7.77E-06	0.0011	0.016	8.09E-06	1.22E-04	0	0
U - 4	1.08E-05	0.0016	0.016	8.97E-06	1.22E-04	0.015	0.079
U - 5	7.43E-06	0.0012	0.016	1.52E-05	1.22E-04	0	0
U - 6	5.90E-06	0.0011	0.016	8.55E-06	1.22E-04	0	0
U - 7	1.24E-05	0.0018	0.016	8.97E-06	1.22E-04	0.028	0.15
U - 8	9.48E-06	0.0014	0.016	6.30E-06	1.22E-04	0.026	0.212

U - 9	2.85E-05	0.003	0.016	2.55E-05	1.22E-04	0.025	0.063
U - 10	5.04E-06	0.0011	0.016	5.86E-06	1.22E-04	0	0
U - 11	9.83E-06	0.0016	0.016	6.30E-06	1.22E-04	0.029	0.236
U - 12	1.22E-05	0.0019	0.016	1.43E-05	1.22E-04	0	0
U - 13	6.41E-05	0.0046	0.016	4.01E-05	1.22E-04	0.196	0.476
U - 14	7.05E-05	0.0055	0.016	2.67E-05	1.22E-04	0.358	1.082
U - 15	6.77E-05	0.005	0.016	4.24E-05	1.22E-04	0.207	0.397
A. n	315	315	315	315	315	315	315
A. Mean	0.0002	0.007	0.016	6.37E-05	1.22E-04	1.012	0.864
A. SD	0.0005	0.0154	0	1.78E-04	0	2.805	1.302
A. CV	266.4751	221.8536	0	279.425	0	277.312	150.624
A. Total	0.0586	2.1897	4.914	0.02	0.039	318.664	272.227

Table 11. Results obtained upon the use of Schena's immobilization protocol and higher stringency washing conditions. In element column capital letters designate spot rows and numbers designate spots from left to right. ROD, relative optical density (an Imaging Research Inc. proprietary density scale which represents an inverse logarithmic function of grey-level values).

Element	D x A - ROD x mm2	SD - ROD	Area - mm2	Bkgd	sRef	nDxA	S/N
A - 1	2.77E-05	0.0073	0.002	9.03E-06	1.21E-04	0.155	0.265
A - 2	3.28E-05	0.0065	0.002	9.03E-06	1.21E-04	0.197	0.337
A - 3	3.45E-05	0.0075	0.002	9.03E-06	1.21E-04	0.212	0.362
A - 4	6.67E-05	0.0087	0.002	9.03E-06	1.21E-04	0.478	0.819
A - 5	6.22E-05	0.0065	0.002	9.03E-06	1.21E-04	0.441	0.756
A - 6	6.02E-05	0.0093	0.002	9.03E-06	1.21E-04	0.424	0.726
A - 7	6.50E-05	0.0073	0.002	9.03E-06	1.21E-04	0.464	0.795
A - 8	7.02E-05	0.0104	0.002	9.03E-06	1.21E-04	0.508	0.869
A - 9	6.77E-05	0.0079	0.002	9.03E-06	1.21E-04	0.487	0.834
A - 10	3.98E-05	0.0073	0.002	9.03E-06	1.21E-04	0.256	0.438
A - 11	3.26E-05	0.0066	0.002	9.03E-06	1.21E-04	0.195	0.334
A - 12	5.14E-05	0.0115	0.002	9.03E-06	1.21E-04	0.352	0.602
B - 1	6.31E-05	0.0102	0.002	9.03E-06	1.21E-04	0.449	0.768
B - 2	9.89E-05	0.0106	0.002	9.03E-06	1.21E-04	0.746	1.277
B - 3	0.0001	0.0146	0.002	9.03E-06	1.21E-04	0.876	1.499
B - 4	0.0003	0.0265	0.002	9.03E-06	1.21E-04	2.21	3.784
B - 5	0.0003	0.0326	0.002	9.03E-06	1.21E-04	2.194	3.756
B - 6	0.0002	0.0291	0.002	9.03E-06	1.21E-04	1.839	3.148
B - 7	3.98E-05	0.0059	0.002	9.03E-06	1.21E-04	0.255	0.437
B - 8	2.97E-05	0.0055	0.002	9.03E-06	1.21E-04	0.172	0.294
B - 9	2.36E-05	0.0059	0.002	9.03E-06	1.21E-04	0.121	0.207
B - 10	2.12E-05	0.0035	0.002	9.03E-06	1.21E-04	0.101	0.172
B - 11	1.86E-05	0.0051	0.002	9.03E-06	1.21E-04	0.079	0.136
B - 12	3.32E-05	0.0084	0.002	9.03E-06	1.21E-04	0.2	0.343
C - 1	4.68E-05	0.0069	0.002	9.03E-06	1.21E-04	0.313	0.536
C - 2	5.01E-05	0.0057	0.002	9.03E-06	1.21E-04	0.341	0.584
C - 3	3.24E-05	0.0057	0.002	9.03E-06	1.21E-04	0.194	0.332
C - 4	3.05E-05	0.008	0.002	9.03E-06	1.21E-04	0.178	0.305
C - 5	2.86E-05	0.0069	0.002	9.03E-06	1.21E-04	0.162	0.277
C - 6	2.96E-05	0.0052	0.002	9.03E-06	1.21E-04	0.17	0.292
C - 7	2.21E-05	0.005	0.002	9.03E-06	1.21E-04	0.108	0.185
C - 8	1.92E-05	0.0038	0.002	9.03E-06	1.21E-04	0.085	0.145
C - 9	2.03E-05	0.0055	0.002	9.03E-06	1.21E-04	0.094	0.16
C - 10	1.53E-05	0.0059	0.002	9.03E-06	1.21E-04	0.052	0.089
C - 11	1.81E-05	0.0049	0.002	9.03E-06	1.21E-04	0.075	0.128
C - 12	1.89E-05	0.005	0.002	9.03E-06	1.21E-04	0.082	0.141
D - 1	0.0002	0.0594	0.002	9.03E-06	1.21E-04	1.936	3.315
D - 2	0.0002	0.0339	0.002	9.03E-06	1.21E-04	1.405	2.406

D - 3	0.0003	0.027	0.002	9.03E-06	1.21E-04	2.062	3.53
D - 4	0.0002	0.0326	0.002	9.03E-06	1.21E-04	1.601	2.741
D - 5	0.0002	0.0284	0.002	9.03E-06	1.21E-04	1.61	2.756
D - 6	0.0002	0.037	0.002	9.03E-06	1.21E-04	1.614	2.764
D - 7	2.30E-05	0.0062	0.002	9.03E-06	1.21E-04	0.115	0.198
D - 8	2.17E-05	0.0033	0.002	9.03E-06	1.21E-04	0.105	0.18
D - 9	2.31E-05	0.0045	0.002	9.03E-06	1.21E-04	0.117	0.2
D - 10	1.20E-05	0.0033	0.002	9.03E-06	1.21E-04	0.025	0.042
D - 11	1.77E-05	0.0055	0.002	9.03E-06	1.21E-04	0.072	0.123
D - 12	1.81E-05	0.0046	0.002	9.03E-06	1.21E-04	0.075	0.128
E - 1	8.30E-05	0.017	0.002	9.03E-06	1.21E-04	0.614	1.051
E - 2	8.62E-05	0.015	0.002	9.03E-06	1.21E-04	0.64	1.096
E - 3	8.16E-05	0.0195	0.002	9.03E-06	1.21E-04	0.602	1.03
E - 4	8.56E-05	0.0149	0.002	9.03E-06	1.21E-04	0.636	1.088
E - 5	7.89E-05	0.0161	0.002	9.03E-06	1.21E-04	0.579	0.992
E - 6	7.84E-05	0.0191	0.002	9.03E-06	1.21E-04	0.575	0.985
E - 7	0.0001	0.0123	0.002	9.03E-06	1.21E-04	0.868	1.486
E - 8	9.81E-05	0.0102	0.002	9.03E-06	1.21E-04	0.739	1.266
E - 9	8.57E-05	0.0198	0.002	9.03E-06	1.21E-04	0.636	1.089
E - 10	9.45E-05	0.0126	0.002	9.03E-06	1.21E-04	0.709	1.214
E - 11	0.0001	0.0138	0.002	9.03E-06	1.21E-04	0.793	1.357
E - 12	9.20E-05	0.0144	0.002	9.03E-06	1.21E-04	0.688	1.178
F - 1	0.0001	0.0369	0.002	9.03E-06	1.21E-04	1.082	1.852
F - 2	0.0001	0.0183	0.002	9.03E-06	1.21E-04	1.043	1.785
F - 3	0.0004	0.5127	0.002	9.03E-06	1.21E-04	3.014	5.16
F - 4	0.0002	0.0346	0.002	9.03E-06	1.21E-04	1.95	3.338
F - 5	0.0002	0.0378	0.002	9.03E-06	1.21E-04	1.993	3.412
F - 6	0.0003	0.0564	0.002	9.03E-06	1.21E-04	2.129	3.645
F - 7	6.36E-05	0.0119	0.002	9.03E-06	1.21E-04	0.452	0.775
F - 8	4.31E-05	0.0086	0.002	9.03E-06	1.21E-04	0.283	0.484
F - 9	4.52E-05	0.0127	0.002	9.03E-06	1.21E-04	0.3	0.514
F - 10	4.67E-05	0.0187	0.002	9.03E-06	1.21E-04	0.313	0.535
F - 11	3.14E-05	0.0077	0.002	9.03E-06	1.21E-04	0.185	0.318
F - 12	3.17E-05	0.0067	0.002	9.03E-06	1.21E-04	0.188	0.322
G - 1	0.0001	0.0243	0.002	9.03E-06	1.21E-04	0.8	1.37
G - 2	8.94E-05	0.0214	0.002	9.03E-06	1.21E-04	0.667	1.141
G - 3	9.49E-05	0.018	0.002	9.03E-06	1.21E-04	0.712	1.219
G - 4	1.40E-05	0.0075	0.002	9.03E-06	1.21E-04	0.041	0.07
G - 5	9.08E-06	0.0036	0.002	9.03E-06	1.21E-04	3.82E-04	6.53E-04
G - 6	8.74E-06	0.0039	0.002	9.03E-06	1.21E-04	0	0
G - 7	5.55E-05	0.0101	0.002	9.03E-06	1.21E-04	0.386	0.66
G - 8	6.02E-05	0.0104	0.002	9.03E-06	1.21E-04	0.425	0.727
G - 9	3.62E-05	0.0085	0.002	9.03E-06	1.21E-04	0.225	0.385
G - 10	3.85E-05	0.0092	0.002	9.03E-06	1.21E-04	0.244	0.418
G - 11	4.50E-05	0.0201	0.002	9.03E-06	1.21E-04	0.299	0.512

G - 12	4.12E-05	0.0095	0.002	9.03E-06	1.21E-04	0.267	0.456
H - 1	0.0003	0.0559	0.002	9.03E-06	1.21E-04	2.599	4.45
H - 2	0.0003	0.073	0.002	9.03E-06	1.21E-04	2.409	4.124
H - 3	0.0004	0.0511	0.002	9.03E-06	1.21E-04	3.06	5.238
H - 4	0.0002	0.0389	0.002	9.03E-06	1.21E-04	1.832	3.137
H - 5	0.0002	0.0387	0.002	9.03E-06	1.21E-04	1.551	2.655
H - 6	0.0003	0.0393	0.002	9.03E-06	1.21E-04	2.098	3.591
H - 7	2.72E-05	0.0126	0.002	9.03E-06	1.21E-04	0.151	0.258
H - 8	6.21E-05	0.0118	0.002	9.03E-06	1.21E-04	0.44	0.754
H - 9	5.41E-05	0.0112	0.002	9.03E-06	1.21E-04	0.374	0.64
H - 10	4.30E-05	0.0105	0.002	9.03E-06	1.21E-04	0.282	0.482
H - 11	4.45E-05	0.0091	0.002	9.03E-06	1.21E-04	0.295	0.504
H - 12	4.29E-05	0.0077	0.002	9.03E-06	1.21E-04	0.281	0.481
I - 1	0.0001	0.0297	0.002	9.03E-06	1.21E-04	1.045	1.789
I - 2	0.0001	0.0264	0.002	9.03E-06	1.21E-04	0.901	1.543
I - 3	0.0001	0.0333	0.002	9.03E-06	1.21E-04	1.036	1.774
I - 4	9.63E-05	0.0152	0.002	9.03E-06	1.21E-04	0.725	1.24
I - 5	8.86E-05	0.023	0.002	9.03E-06	1.21E-04	0.66	1.13
I - 6	0.0002	0.0843	0.002	9.03E-06	1.21E-04	1.215	2.08
I - 7	0.0001	0.0217	0.002	9.03E-06	1.21E-04	0.831	1.423
I - 8	0.0001	0.0198	0.002	9.03E-06	1.21E-04	1.088	1.862
I - 9	0.0001	0.0197	0.002	9.03E-06	1.21E-04	1.086	1.859
I - 10	0.0002	0.0255	0.002	9.03E-06	1.21E-04	1.257	2.152
I - 11	0.0001	0.0197	0.002	9.03E-06	1.21E-04	1.165	1.995
I - 12	0.0002	0.0163	0.002	9.03E-06	1.21E-04	1.253	2.145
J - 1	0.0002	0.0365	0.002	9.03E-06	1.21E-04	1.655	2.833
J - 2	0.0002	0.0457	0.002	9.03E-06	1.21E-04	1.322	2.263
J - 3	0.0002	0.0353	0.002	9.03E-06	1.21E-04	1.511	2.587
J - 4	0.0003	0.0534	0.002	9.03E-06	1.21E-04	2.301	3.939
J - 5	0.0003	0.0557	0.002	9.03E-06	1.21E-04	2.509	4.296
J - 6	0.0004	0.0649	0.002	9.03E-06	1.21E-04	2.917	4.993
J - 7	0.0001	0.0242	0.002	9.03E-06	1.21E-04	0.843	1.444
J - 8	0.0002	0.0627	0.002	9.03E-06	1.21E-04	1.375	2.354
J - 9	0.0001	0.0174	0.002	9.03E-06	1.21E-04	0.943	1.615
J - 10	0.0001	0.018	0.002	9.03E-06	1.21E-04	0.9	1.541
J - 11	0.0001	0.0169	0.002	9.03E-06	1.21E-04	1.047	1.792
J - 12	0.0001	0.0208	0.002	9.03E-06	1.21E-04	0.989	1.694
K - 1	0.0002	0.0187	0.002	9.03E-06	1.21E-04	1.3	2.225
K - 2	0.0002	0.0353	0.002	9.03E-06	1.21E-04	1.22	2.089
K - 3	0.0002	0.026	0.002	9.03E-06	1.21E-04	1.212	2.075
K - 4	9.35E-05	0.0145	0.002	9.03E-06	1.21E-04	0.701	1.199
K - 5	0.0001	0.0262	0.002	9.03E-06	1.21E-04	0.836	1.43
K - 6	0.0001	0.0198	0.002	9.03E-06	1.21E-04	0.938	1.607
K - 7	9.46E-05	0.0139	0.002	9.03E-06	1.21E-04	0.71	1.215
K - 8	0.0001	0.0174	0.002	9.03E-06	1.21E-04	0.806	1.38

K - 9	0.0001	0.0174	0.002	9.03E-06	1.21E-04	0.828	1.418
K - 10	9.65E-05	0.0174	0.002	9.03E-06	1.21E-04	0.726	1.243
K - 11	0.0001	0.0108	0.002	9.03E-06	1.21E-04	0.807	1.382
K - 12	8.65E-05	0.0163	0.002	9.03E-06	1.21E-04	0.643	1.1
L - 1	0.0002	0.0469	0.002	9.03E-06	1.21E-04	1.686	2.885
L - 2	0.0003	0.0852	0.002	9.03E-06	1.21E-04	2.437	4.172
L - 3	0.0004	0.0455	0.002	9.03E-06	1.21E-04	3.276	5.609
L - 4	0.0003	0.0498	0.002	9.03E-06	1.21E-04	2.41	4.126
L - 5	0.0003	0.068	0.002	9.03E-06	1.21E-04	2.21	3.784
L - 6	0.0004	0.0493	0.002	9.03E-06	1.21E-04	2.838	4.859
L - 7	6.66E-05	0.0146	0.002	9.03E-06	1.21E-04	0.478	0.818
L - 8	4.23E-05	0.0116	0.002	9.03E-06	1.21E-04	0.276	0.473
L - 9	6.64E-05	0.0139	0.002	9.03E-06	1.21E-04	0.476	0.815
L - 10	0.0001	0.0196	0.002	9.03E-06	1.21E-04	0.876	1.499
L - 11	0.0001	0.0193	0.002	9.03E-06	1.21E-04	0.906	1.551
L - 12	0.0001	0.0204	0.002	9.03E-06	1.21E-04	0.827	1.416
M - 1	0.0002	0.0242	0.002	9.03E-06	1.21E-04	1.266	2.167
M - 2	0.0002	0.0359	0.002	9.03E-06	1.21E-04	1.41	2.414
M - 3	0.0002	0.0261	0.002	9.03E-06	1.21E-04	1.298	2.222
M - 4	0.0002	0.0259	0.002	9.03E-06	1.21E-04	1.379	2.361
M - 5	0.0002	0.0346	0.002	9.03E-06	1.21E-04	1.623	2.778
M - 6	0.0002	0.0638	0.002	9.03E-06	1.21E-04	1.387	2.375
M - 7	0.0002	0.049	0.002	9.03E-06	1.21E-04	1.287	2.203
M - 8	0.0001	0.0401	0.002	9.03E-06	1.21E-04	1.149	1.967
M - 9	0.0001	0.0293	0.002	9.03E-06	1.21E-04	1.123	1.923
M - 10	9.46E-05	0.0284	0.002	9.03E-06	1.21E-04	0.71	1.216
M - 11	0.0002	0.051	0.002	9.03E-06	1.21E-04	1.732	2.964
M - 12	0.0002	0.04	0.002	9.03E-06	1.21E-04	1.782	3.051
N - 1	0.0001	0.0392	0.002	9.03E-06	1.21E-04	1.139	1.95
N - 2	0.0002	0.0384	0.002	9.03E-06	1.21E-04	1.236	2.116
N - 3	0.0001	0.0209	0.002	9.03E-06	1.21E-04	1.146	1.963
N - 4	0.0002	0.0556	0.002	9.03E-06	1.21E-04	1.374	2.353
N - 5	0.0002	0.0697	0.002	9.03E-06	1.21E-04	1.536	2.63
N - 6	0.0002	0.071	0.002	9.03E-06	1.21E-04	1.654	2.831
N - 7	0.0002	0.0421	0.002	9.03E-06	1.21E-04	1.654	2.831
N - 8	0.0002	0.0353	0.002	9.03E-06	1.21E-04	1.38	2.363
N - 9	0.0001	0.0238	0.002	9.03E-06	1.21E-04	0.854	1.462
N - 10	0.0002	0.036	0.002	9.03E-06	1.21E-04	1.466	2.51
N - 11	0.0002	0.0256	0.002	9.03E-06	1.21E-04	1.294	2.215
N - 12	0.0002	0.0423	0.002	9.03E-06	1.21E-04	1.203	2.06
O - 1	0.0002	0.0336	0.002	9.03E-06	1.21E-04	1.263	2.162
O - 2	0.0002	0.034	0.002	9.03E-06	1.21E-04	1.699	2.909
O - 3	0.0002	0.0247	0.002	9.03E-06	1.21E-04	1.671	2.861
O - 4	0.0002	0.0361	0.002	9.03E-06	1.21E-04	1.268	2.17
O - 5	0.0001	0.0256	0.002	9.03E-06	1.21E-04	0.966	1.653

O - 6	0.0002	0.044	0.002	9.03E-06	1.21E-04	1.482	2.538
O - 7	0.0002	0.0556	0.002	9.03E-06	1.21E-04	1.629	2.789
O - 8	0.0002	0.0371	0.002	9.03E-06	1.21E-04	1.406	2.408
O - 9	0.0001	0.0283	0.002	9.03E-06	1.21E-04	1.17	2.003
O - 10	0.0002	0.037	0.002	9.03E-06	1.21E-04	1.671	2.861
O - 11	0.0001	0.0447	0.002	9.03E-06	1.21E-04	1.071	1.834
O - 12	0.0001	0.0216	0.002	9.03E-06	1.21E-04	0.977	1.672
P - 1	0.0001	0.0299	0.002	9.03E-06	1.21E-04	1.131	1.936
P - 2	0.0002	0.0225	0.002	9.03E-06	1.21E-04	1.708	2.924
P - 3	0.0002	0.0279	0.002	9.03E-06	1.21E-04	1.668	2.855
P - 4	0.0002	0.0456	0.002	9.03E-06	1.21E-04	1.483	2.539
P - 5	0.0002	0.0348	0.002	9.03E-06	1.21E-04	1.869	3.2
P - 6	0.0002	0.0452	0.002	9.03E-06	1.21E-04	1.796	3.074
P - 7	0.0002	0.0373	0.002	9.03E-06	1.21E-04	1.312	2.246
P - 8	7.84E-05	0.0175	0.002	9.03E-06	1.21E-04	0.576	0.986
P - 9	0.0002	0.0291	0.002	9.03E-06	1.21E-04	1.281	2.193
P - 10	0.0002	0.0298	0.002	9.03E-06	1.21E-04	1.564	2.678
P - 11	0.0002	0.0379	0.002	9.03E-06	1.21E-04	1.326	2.271
P - 12	0.0002	0.0304	0.002	9.03E-06	1.21E-04	1.478	2.531
A. n	192	192	192	192	192	192	192
A. Mean	0.0001	0.0273	0.002	9.03E-06	1.21E-04	1	1.712
A. SD	8.63E-05	0.0393	0	0	0	0.716	1.226
A. CV	66.6137	144.0257	9.80E-06	6.89E-06	8.61E-06	71.605	71.605
A. Total	0.0249	5.2452	0.403	0.002	0.023	192.002	328.688

Table 12. Results obtained on testing TeleChem immobilization protocol for PCR fragments upon their hybridization with 0.1 µM of Cy3-end labelled rRNA f1-r2.9550 fragment. In element column capital letters designate spot rows and numbers designate spots from left to right. ROD, relative optical density (an Imaging Research Inc. proprietary density scale which represents an inverse logarithmic function of grey-level values).

	D x A - ROD						
Element	x mm2	SD - ROD	Area - mm2	Bkgd	sRef	nDxA	S/N
A - 1	9.43E-05	0.0034	0.038	4.78E-05	1.99E-04	0.233	0.449
A - 2	0.0001	0.004	0.038	3.34E-05	1.99E-04	0.379	0.855
A - 3	7.64E-05	0.0032	0.038	3.03E-05	1.99E-04	0.231	0.589
A - 4	0.0002	0.0062	0.038	5.43E-05	1.99E-04	0.726	1.308
A - 5	0.0002	0.0055	0.038	7.04E-05	1.99E-04	0.534	0.39
A - 6	0.0001	0.0049	0.038	4.02E-05	1.99E-04	0.515	1.387
B - 1	0.0001	0.0048	0.038	6.23E-05	1.99E-04	0.405	0.387
B - 2	0.0002	0.0052	0.038	5.87E-05	1.99E-04	0.545	1
B - 3	0.0002	0.0066	0.038	7.71E-05	1.99E-04	0.519	0.674
B - 4	0.0002	0.0064	0.038	4.55E-05	1.99E-04	0.612	1.083
B - 5	0.0004	0.126	0.038	5.77E-05	1.99E-04	1.91	3.492
B - 6	0.0001	0.005	0.038	7.26E-05	1.99E-04	0.366	0.35
C - 1	0.0001	0.0044	0.038	7.44E-05	1.99E-04	0.175	0.094
C - 2	0.0001	0.0038	0.038	4.57E-05	1.99E-04	0.367	0.774
C - 3	0.0001	0.0063	0.038	4.43E-05	1.99E-04	0.526	1.153
C - 4	0.0002	0.0127	0.038	9.30E-05	1.99E-04	0.537	0.617
C - 5	0.0002	0.0064	0.038	5.36E-05	1.99E-04	0.754	1.347
C - 6	0.0002	0.008	0.038	5.05E-05	1.99E-04	0.993	2.164
D - 1	0.0002	0.0047	0.038	5.40E-05	1.99E-04	0.553	0.976
D - 2	0.0002	0.0049	0.038	7.14E-05	1.99E-04	0.433	0.289
D - 3	0.0002	0.0055	0.038	5.39E-05	1.99E-04	0.687	1.413
D - 4	0.0002	0.0056	0.038	6.05E-05	1.99E-04	0.68	1.125
D - 5	0.0003	0.0267	0.038	4.64E-05	1.99E-04	1.217	2.498
D - 6	0.0002	0.0069	0.038	5.84E-05	1.99E-04	0.752	0.779
E - 1	0.0002	0.0057	0.038	5.36E-05	1.99E-04	0.636	1.266
E - 2	0.0002	0.0077	0.038	7.01E-05	1.99E-04	0.898	1.35
E - 3	0.0002	0.0047	0.038	6.32E-05	1.99E-04	0.472	0.864
E - 4	0.0002	0.0059	0.038	8.14E-05	1.99E-04	0.702	1.034
E - 5	0.0002	0.0054	0.038	1.03E-04	1.99E-04	0.574	0.676
E - 6	0.0002	0.006	0.038	1.17E-04	1.99E-04	0.488	0.265
F - 1	0.0003	0.015	0.038	5.91E-05	1.99E-04	0.958	1.759
F - 2	0.0001	0.0048	0.038	6.59E-05	1.99E-04	0.418	0.759
F - 3	0.0002	0.0051	0.038	1.09E-04	1.99E-04	0.358	0.21
F - 4	0.0004	0.009	0.038	8.24E-05	1.99E-04	1.396	2.022
F - 5	0.0004	0.0091	0.038	1.22E-04	1.99E-04	1.379	1.78
F - 6	0.0004	0.0105	0.038	7.15E-05	1.99E-04	1.529	2.282

G - 1	0.0002	0.0065	0.038	8.35E-05	1.99E-04	0.704	0.49
G - 2	0.0003	0.0114	0.038	8.41E-05	1.99E-04	1.173	1.839
G - 3	0.0004	0.0092	0.038	1.31E-04	1.99E-04	1.33	1.577
G - 4	0.0006	0.0149	0.038	9.18E-05	1.99E-04	2.772	3.595
G - 5	0.0005	0.0119	0.038	1.03E-04	1.99E-04	1.977	1.824
G - 6	0.0004	0.0115	0.038	9.33E-05	1.99E-04	1.704	1.976
H - 1	0.0003	0.007	0.038	5.95E-05	1.99E-04	0.967	1.565
H - 2	0.0003	0.0079	0.038	1.20E-04	1.99E-04	1.006	0.878
H - 3	0.0004	0.0098	0.038	1.05E-04	1.99E-04	1.569	2.205
H - 4	0.0007	0.0147	0.038	1.60E-04	1.99E-04	2.519	1.15
H - 5	0.0005	0.0111	0.038	1.03E-04	1.99E-04	2.061	2.328
H - 6	0.0005	0.0114	0.038	1.04E-04	1.99E-04	1.787	1.264
I - 1	0.0002	0.0063	0.038	6.04E-05	1.99E-04	0.807	1.083
I - 2	0.0004	0.0083	0.038	1.00E-04	1.99E-04	1.32	1.635
I - 3	0.0003	0.0081	0.038	1.05E-04	1.99E-04	1.098	1.689
I - 4	0.0005	0.0115	0.038	1.24E-04	1.99E-04	2.104	2.721
I - 5	0.0004	0.0103	0.038	6.78E-04	1.99E-04	0	0
I - 6	0.0004	0.0092	0.038	1.11E-04	1.99E-04	1.374	0.797
J - 1	0.0004	0.0105	0.038	1.09E-04	1.99E-04	1.572	0.884
J - 2	0.0005	0.0097	0.038	1.09E-04	1.99E-04	1.816	2.337
J - 3	0.001	0.1736	0.038	1.04E-04	1.99E-04	4.491	6.364
J - 4	0.0004	0.0094	0.038	1.83E-04	1.99E-04	0.962	0.313
J - 5	0.0003	0.0079	0.038	1.10E-04	1.99E-04	0.986	1.177
J - 6	0.0002	0.0063	0.038	6.57E-05	1.99E-04	0.721	1.127
A. n	60	60	60	60	60	60	60
A. Mean	0.0003	0.0127	0.038	9.09E-05	1.99E-04	1.021	1.338
A. SD	0.0002	0.0263	0	8.31E-05	0	0.758	1.022
A. CV	57.4346	206.6803	0	91.428	0	74.216	76.358
A. Total	0.0174	0.764	2.304	0.005	0.012	61.281	80.278

Table 13. Results obtained on testing TeleChem immobilization protocol for PCR fragments upon their hybridization with 1 µM of Cy3-end labelled rRNA f1-r2.9550 fragment. In element column capital letters designate spot rows and numbers designate spots from left to right. ROD, relative optical density (an Imaging Research Inc. proprietary density scale which represents an inverse logarithmic function of grey-level values).

	D x A - ROD						
Element	x mm2	SD - ROD	Area - mm2	Bkgd	sRef	nDxA	S/N
A - 1	0.0004	0.0091	0.038	9.78E-05	5.41E-04	0.597	2.285
A - 2	0.0004	0.0089	0.038	8.21E-05	5.41E-04	0.601	2.332
A - 3	0.0004	0.0085	0.038	7.25E-05	5.41E-04	0.552	2.367
A - 4	0.0007	0.0134	0.038	6.65E-05	5.41E-04	1.137	5.748
A - 5	0.0006	0.012	0.038	4.29E-05	5.41E-04	0.989	6.595
A - 6	0.0006	0.0115	0.038	5.50E-05	5.41E-04	0.976	5.066
B - 1	0.0005	0.0106	0.038	7.79E-05	5.41E-04	0.801	3.493
B - 2	0.0006	0.0107	0.038	8.31E-05	5.41E-04	0.868	3.6
B - 3	0.0005	0.0109	0.038	9.86E-05	5.41E-04	0.797	2.824
B - 4	0.0007	0.0133	0.038	7.38E-05	5.41E-04	1.184	5.37
B - 5	0.0006	0.0136	0.038	6.25E-05	5.41E-04	1.06	5.275
B - 6	0.0006	0.0122	0.038	6.17E-05	5.41E-04	0.946	5.013
C - 1	0.0004	0.0089	0.038	6.85E-05	5.41E-04	0.623	3.442
C - 2	0.0004	0.0094	0.038	7.63E-05	5.41E-04	0.646	2.649
C - 3	0.0004	0.0094	0.038	8.29E-05	5.41E-04	0.619	3.037
C - 4	0.0008	0.015	0.038	6.27E-05	5.41E-04	1.273	7.009
C - 5	0.0008	0.0143	0.038	6.63E-05	5.41E-04	1.291	5.933
C - 6	0.0007	0.0141	0.038	6.79E-05	5.41E-04	1.167	5.92
D - 1	0.0005	0.0109	0.038	7.17E-05	5.41E-04	0.872	4.035
D - 2	0.0005	0.0111	0.038	1.27E-04	5.41E-04	0.721	0.579
D - 3	0.0005	0.0107	0.038	6.79E-05	5.41E-04	0.771	3.8
D - 4	0.0006	0.0124	0.038	7.10E-05	5.41E-04	0.958	4.587
D - 5	0.0006	0.0121	0.038	5.53E-05	5.41E-04	0.939	4.672
D - 6	0.0006	0.013	0.038	4.16E-05	5.41E-04	1.045	6.527
E - 1	0.0006	0.0128	0.038	7.07E-05	5.41E-04	0.951	4.336
E - 2	0.0005	0.0125	0.038	7.94E-05	5.41E-04	0.86	3.377
E - 3	0.0005	0.0102	0.038	7.93E-05	5.41E-04	0.707	2.876
E - 4	0.0006	0.0091	0.038	7.97E-05	5.41E-04	0.983	3.127
E - 5	0.0006	0.0096	0.038	9.43E-05	5.41E-04	0.998	3.252
E - 6	0.0012	0.1738	0.038	7.59E-05	5.41E-04	2.014	8.753
F - 1	0.0005	0.01	0.038	7.80E-05	5.41E-04	0.832	3.453
F - 2	0.0005	0.0101	0.038	7.59E-05	5.41E-04	0.811	3.451
F - 3	0.0005	0.01	0.038	7.66E-05	5.41E-04	0.786	3.265
F - 4	0.0009	0.1229	0.038	6.25E-05	5.41E-04	1.471	7.086
F - 5	0.0006	0.0143	0.038	5.36E-05	5.41E-04	0.933	4.566
F - 6	0.0006	0.0147	0.038	1.22E-04	5.41E-04	0.892	0.751

G - 1	0.0006	0.0124	0.038	7.96E-05	5.41E-04	0.931	4.033
G - 2	0.0006	0.0125	0.038	8.98E-05	5.41E-04	1.021	3.577
G - 3	0.0006	0.0107	0.038	1.02E-04	5.41E-04	0.878	2.618
G - 4	0.0007	0.015	0.038	5.77E-05	5.41E-04	1.244	6.332
G - 5	0.0007	0.0146	0.038	4.98E-05	5.41E-04	1.202	6.872
G - 6	0.0009	0.0183	0.038	6.96E-05	5.41E-04	1.521	7.667
H - 1	0.0006	0.0133	0.038	1.05E-04	5.41E-04	0.976	2.41
H - 2	0.0007	0.0156	0.038	1.05E-04	5.41E-04	1.101	2.861
H - 3	0.0014	0.1871	0.038	7.62E-05	5.41E-04	2.426	10.222
H - 4	0.0008	0.0157	0.038	5.81E-05	5.41E-04	1.287	6.217
H - 5	0.0006	0.0139	0.038	5.25E-05	5.41E-04	0.999	5.661
H - 6	0.0008	0.0168	0.038	7.83E-05	5.41E-04	1.248	5.211
I - 1	0.0005	0.0127	0.038	7.93E-05	5.41E-04	0.753	2.474
I - 2	0.0005	0.011	0.038	6.73E-05	5.41E-04	0.742	3.357
I - 3	0.0004	0.01	0.038	4.71E-05	5.41E-04	0.716	3.852
I - 4	0.0006	0.0129	0.038	1.13E-04	5.41E-04	0.918	0.985
I - 5	0.0006	0.0136	0.038	7.04E-05	5.41E-04	1.002	4.595
I - 6	0.0008	0.0189	0.038	9.50E-05	5.41E-04	1.274	4.058
J - 1	0.0007	0.0142	0.038	1.02E-04	5.41E-04	1.056	3.543
J - 2	0.0006	0.0136	0.038	5.33E-05	5.41E-04	1.002	4.861
J - 3	0.0005	0.0126	0.038	8.54E-05	5.41E-04	0.721	1.091
J - 4	0.0009	0.1732	0.038	6.32E-05	5.41E-04	1.545	7.654
J - 5	0.0006	0.0123	0.038	6.99E-05	5.41E-04	0.901	4.859
J - 6	0.0005	0.0108	0.038	5.97E-05	5.41E-04	0.865	4.572
A. n	60	60	60	60	60	60	60
A. Mean	0.0006	0.0225	0.038	7.52E-05	5.41E-04	1	4.334
A. SD	0.0002	0.0388	0	1.84E-05	0	0.324	1.938
A. CV	28.0975	172.8043	0	24.468	0	32.402	44.718
A. Total	0.037	1.3476	2.304	0.005	0.032	60	260.035

Table 14. Data obtained upon the use of SSPE buffer and old TeleChem silylated slides. In element column capital letters designate spot rows and number s designate spots from left to right. ROD, relative optical density (an Imaging Research Inc. proprietary density scale which represents an inverse logarithmic function of grey-level values).

Element	D x A - ROD x mm2	SD - ROD	Area - mm2	Bkgd	sRef	nDxA	S/N
A - 1	2.5781	0.1022	14.476	2.899	0.734	2.855	1.583
A - 2	1.2539	0.0489	14.476	1.473	0.734	1.353	3.513
A - 3	1.3782	0.0582	14.476	1.536	0.734	1.594	2.642
A - 4	2.2666	0.0538	14.476	1.267	0.734	1.584	2.745
A - 6	2.5595	0.0599	14.476	2.053	0.734	1.621	1.833
A - 7	2.3536	0.0499	14.476	1.974	0.734	1.612	3.196
A - 8	3.2036	0.0932	14.476	1.746	0.734	2.293	2.594
B - 1	2.9052	0.0123	14.476	2.423	0.734	0.327	1.385
B - 2	1.1195	0.0214	14.476	1.984	0.734	0.447	1.395
B - 3	1.0194	0.0154	14.476	1.84	0.734	0.426	0.847
B - 4	1.0861	0.0163	14.476	1.598	0.734	0.454	2.382
B - 5	1.7894	0.0399	14.476	2.867	0.734	0.857	1.236
B - 6	2.1232	0.0274	14.476	2.267	0.734	0.982	0.936
B - 7	1.942	0.0306	14.476	1.897	0.734	0.97	1.364
B - 8	2.095	0.0294	14.476	2.04	0.734	1.041	2.936
C - 1	1.1237	0.0548	14.476	1.379	0.734	1.15	2.003
C - 2	1.7947	0.0499	14.476	2.562	0.734	1.088	1.837
C - 3	1.833	0.0474	14.476	1.172	0.734	1.045	3.715
C - 4	2.7366	0.0581	14.476	2.271	0.734	1.361	1.382
C - 5	2.2675	0.0555	14.476	1.948	0.734	1.225	1.023
C - 6	1.7258	0.0381	14.476	1.023	0.734	0.931	0.826
C - 7	2.129	0.0487	14.476	1.876	0.734	1.164	2.735
C - 8	1.6104	0.0294	14.476	1.263	0.734	0.78	2.378
D - 2	1.1777	0.0198	14.476	1.038	0.734	0.501	1.274
D - 3	0.7675	0.0074	14.476	1.616	0.734	0.139	0.927
D - 4	1.3345	0.0078	14.476	1.275	0.734	0.333	1.826
D - 5	1.2415	0.0139	14.476	0.919	0.734	0.392	2.037
D - 6	1.5137	0.0226	14.476	1.399	0.734	0.571	1.225
D - 7	1.1314	0.0122	14.476	1.785	0.734	0.322	0.973
D - 8	1.4995	0.0195	14.476	1.273	0.734	0.582	1.887
A. n	30	30	30	30	30	30	30
A. Mean	0.5284	0.0381	14.476	2.938	0.128	1	2.213
A. SD	0.3173	0.0236	0	0.179	0	0.617	0.354
A. CV	27.4972	61.8565	6.33E-06	42.354	0	61.656	23.472
A. Total	34.3784	1.0159	418.173	61.136	22.007	30	42.467

Table 15. Data obtained upon the use of SSPE buffer and new TeleChem silylated slides. In element column capital letters designate spot rows and number s designate spots from left to right. ROD, relative optical density (an Imaging Research Inc. proprietary density scale which represents an inverse logarithmic function of grey-level values).

Element	D x A - ROD x mm2	SD - ROD	Area - mm2	Bkgd	sRef	nDxA	S/N
A - 1	0.7688	0.0134	17.05	0.492	0.329	0.84	1.682
A - 2	0.8738	0.0157	17.05	0.526	0.329	1.055	2.965
A - 4	0.7109	0.0142	17.05	0.436	0.329	0.837	3.434
A - 5	0.6941	0.0137	17.05	0.421	0.329	0.831	3.616
A - 6	0.9098	0.0169	17.05	0.571	0.329	1.031	2.191
A - 7	1.6255	0.0551	17.05	0.554	0.329	3.257	8.196
A - 8	0.9831	0.0236	17.05	0.513	0.329	1.427	5.257
B - 1	0.8717	0.0065	17.05	0.631	0.329	0.73	2.067
B - 3	0.8171	0.0081	17.05	0.614	0.329	0.618	1.621
B - 4	0.5142	0.0037	17.05	0.432	0.329	0.25	1.618
B - 5	0.6675	0.0094	17.05	0.431	0.329	0.718	3.028
B - 6	0.7485	0.0088	17.05	0.546	0.329	0.617	2.018
B - 7	0.5848	0.0042	17.05	0.459	0.329	0.381	1.491
B - 8	0.724	0.0063	17.05	0.484	0.329	0.729	4.38
C - 1	1.1617	0.0197	17.05	0.601	0.329	1.704	5.621
C - 3	1.7227	0.0415	17.05	0.845	0.329	2.668	5.218
C - 4	1.078	0.0213	17.05	0.527	0.329	1.675	11.717
C - 8	1.011	0.0211	17.05	0.503	0.329	1.545	7.338
D - 2	0.8517	0.0099	17.05	0.723	0.329	0.39	0.78
D - 3	0.9312	0.0115	17.05	0.757	0.329	0.529	1.12
D - 4	0.7997	0.0077	17.05	0.58	0.329	0.668	2.827
D - 7	0.5311	0.0047	17.05	0.452	0.329	0.241	1.149
D - 8	0.5348	0.0033	17.05	0.449	0.329	0.26	1.42
A. n	23	23	23	23	23	23	23
A. Mean	0.8746	0.0148	17.05	0.546	0.329	1	3.511
A. SD	0.3053	0.0123	0	0.111	0	0.759	2.696
A. CV	34.908	83.2187	0	20.384	0	75.929	76.781
A. Total	20.1155	0.3402	392.161	12.547	7.569	23	80.754

Table 16. Data obtained upon the use of UniHyb buffer and new TeleChem silylated slides. In element column capital letters designate spot rows and number s designate spots from left to right. ROD, relative optical density (an Imaging Research Inc. proprietary density scale which represents an inverse logarithmic function of grey-level values).

Element	D x A - ROD x mm2	SD - ROD	Area - mm2	Bkgd	sRef	nDxA	S/N
A - 1	3.9742	0.1022	13.939	0.899	1.077	2.855	5.466
A - 2	2.081	0.0489	13.939	0.623	1.077	1.353	8.828
A - 3	2.2931	0.0582	13.939	0.576	1.077	1.594	10.917
A - 4	2.2666	0.0538	13.939	0.56	1.077	1.584	7.575
A - 6	2.5595	0.0599	13.939	0.814	1.077	1.621	3.13
A - 7	2.3536	0.0499	13.939	0.617	1.077	1.612	17.196
A - 8	3.2036	0.0932	13.939	0.733	1.077	2.293	11.77
B - 1	0.9052	0.0123	13.939	0.553	1.077	0.327	2.26
B - 2	1.1195	0.0214	13.939	0.639	1.077	0.447	2.842
B - 3	1.0194	0.0154	13.939	0.561	1.077	0.426	4.046
B - 4	1.0861	0.0163	13.939	0.598	1.077	0.454	4.108
B - 5	1.7894	0.0399	13.939	0.867	1.077	0.857	2.52
B - 6	2.1232	0.0274	13.939	1.066	1.077	0.982	3.359
B - 7	1.942	0.0306	13.939	0.897	1.077	0.97	3.676
B - 8	2.095	0.0294	13.939	0.974	1.077	1.041	4.477
C - 1	2.0144	0.0548	13.939	0.776	1.077	1.15	5.493
C - 2	1.7947	0.0499	13.939	0.623	1.077	1.088	7.033
C - 3	1.833	0.0474	13.939	0.707	1.077	1.045	6.687
C - 4	2.7366	0.0581	13.939	1.271	1.077	1.361	3.325
C - 5	2.2675	0.0555	13.939	0.948	1.077	1.225	3.02
C - 6	1.7258	0.0381	13.939	0.723	1.077	0.931	3.928
C - 7	2.129	0.0487	13.939	0.876	1.077	1.164	7.296
C - 8	1.6104	0.0294	13.939	0.771	1.077	0.78	4.269
D - 2	1.1777	0.0198	13.939	0.638	1.077	0.501	3.731
D - 3	0.6655	0.0074	13.939	0.516	1.077	0.139	2.016
D - 4	0.9345	0.0078	13.939	0.575	1.077	0.333	4.593
D - 5	1.3413	0.0139	13.939	0.919	1.077	0.392	2.439
D - 6	1.5137	0.0226	13.939	0.899	1.077	0.571	3.589
D - 7	1.1314	0.0122	13.939	0.785	1.077	0.322	3.172
D - 8	1.4995	0.0195	13.939	0.873	1.077	0.582	2.887
A. n	30	30	30	30	30	30	30
A. Mean	1.8396	0.0381	13.939	0.763	1.077	1	5.188
A. SD	0.7243	0.0236	0	0.179	0	0.617	3.354
A. CV	39.3738	61.8565	3.42E-06	23.456	0	61.656	64.642
A. Total	55.1865	1.1439	418.173	22.876	32.311	30	155.646

Table 17. Results obtained upon the hybridization with *Agrococcus jenensis* HKI085's RNA.

Element	D x A - ROD x mm2	SD - ROD	Area - mm2	Bkgd	sRef	nDxA	S/N
A - 1	0.0008	0.0126	0.045	9.31E-05	0.001	0.634	5.895
A - 2	0.0005	0.0109	0.045	8.50E-05	0.001	0.386	4.002
A - 3	0.0003	0.0056	0.045	9.31E-04	0.001	0	0
A - 4	0.0009	0.0144	0.045	6.28E-05	0.001	0.788	9.329
A - 5	0.001	0.0176	0.045	1.93E-04	0.001	0.702	1.691
A - 6	0.0014	0.0176	0.045	9.81E-05	0.001	1.154	9.775
A - 7	0.0022	0.0334	0.045	7.44E-05	0.001	1.99	19.458
A - 8	0.0019	0.028	0.045	8.68E-05	0.001	1.676	9.615
A - 9	0.002	0.0306	0.045	7.41E-05	0.001	1.772	18.85
A - 10	0.0024	0.0383	0.045	7.88E-05	0.001	2.092	16.784
A - 11	0.0024	0.0357	0.045	8.57E-05	0.001	2.169	13.696
A - 12	0.0031	0.0441	0.045	8.21E-05	0.001	2.747	18.162
A - 13	0.0027	0.0365	0.045	1.05E-04	0.001	2.415	17.021
A - 14	0.0022	0.0296	0.045	1.02E-04	0.001	1.954	12.083
A - 15	0.0024	0.0301	0.045	8.36E-05	0.001	2.12	22.15
A - 16	0.0025	0.0319	0.045	8.88E-05	0.001	2.249	21.163
A - 17	0.0029	0.0362	0.045	8.95E-05	0.001	2.542	18.921
A - 18	0.0043	0.0574	0.045	1.22E-04	0.001	3.848	16.003
B - 1	0.0005	0.0075	0.045	9.09E-05	0.001	0.377	3.639
B - 2	0.0005	0.0076	0.045	9.56E-05	0.001	0.381	3.679
B - 3	0.0004	0.0071	0.045	9.52E-05	0.001	0.239	1.645
B - 4	0.0004	0.0075	0.045	6.94E-05	0.001	0.337	3.746
B - 5	0.0005	0.0083	0.045	6.33E-05	0.001	0.441	4.847
B - 6	0.0006	0.0086	0.045	9.87E-05	0.001	0.464	3.403
B - 7	0.0004	0.0079	0.045	7.91E-05	0.001	0.336	3.435
B - 8	0.0004	0.0065	0.045	8.09E-05	0.001	0.278	2.368
B - 9	0.0003	0.0051	0.045	8.53E-05	0.001	0.229	2.04
B - 10	0.0004	0.0058	0.045	9.21E-05	0.001	0.292	2.053
B - 11	0.0005	0.0157	0.045	8.95E-05	0.001	0.345	3.371
B - 12	0.0005	0.0067	0.045	9.54E-05	0.001	0.379	3.538
B - 13	0.0021	0.0211	0.045	9.07E-05	0.001	1.828	12.533
B - 14	0.0018	0.018	0.045	8.95E-05	0.001	1.562	14.465
B - 15	0.0018	0.0186	0.045	7.55E-05	0.001	1.624	17.438
B - 16	0.0022	0.0231	0.045	8.95E-05	0.001	1.962	14.684
B - 17	0.0026	0.0263	0.045	1.05E-04	0.001	2.253	18.065
B - 18	0.0036	0.0383	0.045	1.08E-04	0.001	3.217	25.051
C - 1	0.0103	0.207	0.045	1.02E-04	0.001	9.357	89.642
C - 2	0.0085	0.1545	0.045	1.10E-04	0.001	7.659	65.287
C - 3	0.0085	0.1543	0.045	1.09E-04	0.001	7.694	60.463
C - 4	0.0079	0.1695	0.045	9.09E-05	0.001	7.151	70.982
C - 5	0.0096	0.1999	0.045	8.76E-05	0.001	8.739	83.126
C - 6	0.016	0.4587	0.045	9.80E-05	0.001	14.598	139.324

C - 7	0.0032	0.0542	0.045	8.92E-05	0.001	2.859	28.013
C - 8	0.0023	0.0361	0.045	9.45E-05	0.001	2.044	19.504
C - 9	0.0021	0.03	0.045	1.04E-04	0.001	1.869	17.284
C - 10	0.0019	0.0275	0.045	7.96E-05	0.001	1.666	15.024
C - 11	0.0017	0.0216	0.045	8.60E-05	0.001	1.511	14.53
C - 12	0.0023	0.0279	0.045	6.15E-04	0.001	1.526	0.246
C - 13	0.0005	0.0067	0.045	8.78E-05	0.001	0.366	2.804
C - 14	0.0006	0.0075	0.045	7.48E-05	0.001	0.442	4.729
C - 15	0.0006	0.0073	0.045	9.30E-05	0.001	0.475	4.621
C - 16	0.0007	0.0088	0.045	1.05E-04	0.001	0.584	3.189
C - 17	0.0007	0.0086	0.045	7.32E-05	0.001	0.602	6.787
C - 18	0.0008	0.0097	0.045	8.45E-05	0.001	0.674	6.752
D - 1	0.0044	0.0587	0.045	1.04E-04	0.001	3.935	26.376
D - 2	0.0041	0.0547	0.045	1.08E-04	0.001	3.649	30.45
D - 3	0.004	0.0529	0.045	1.02E-04	0.001	3.573	32.631
D - 4	0.0053	0.0662	0.045	1.03E-04	0.001	4.764	44.483
D - 5	0.0052	0.0646	0.045	9.87E-05	0.001	4.668	15.645
D - 6	0.0061	0.0777	0.045	1.08E-04	0.001	5.467	49.223
D - 7	0.0005	0.0074	0.045	1.07E-04	0.001	0.328	3.098
D - 8	0.0004	0.006	0.045	1.05E-04	0.001	0.273	2.545
D - 9	0.0004	0.0059	0.045	1.01E-04	0.001	0.261	2.695
D - 10	0.0004	0.0058	0.045	1.10E-04	0.001	0.277	2.393
D - 11	0.0004	0.0061	0.045	1.02E-04	0.001	0.272	2.565
D - 12	0.0005	0.0074	0.045	1.29E-04	0.001	0.295	0.521
D - 13	0.0008	0.0087	0.045	6.80E-05	0.001	0.629	6.737
D - 14	0.0008	0.0103	0.045	8.52E-05	0.001	0.628	6.257
D - 15	0.0008	0.0095	0.045	8.11E-05	0.001	0.682	8.032
D - 16	0.0011	0.0119	0.045	8.60E-05	0.001	0.95	9.301
D - 17	0.0011	0.0125	0.045	1.04E-04	0.001	0.958	9.227
D - 18	0.0012	0.014	0.045	8.83E-05	0.001	1.005	10.196
E - 1	0.0012	0.02	0.045	1.31E-04	0.001	1.026	6.854
E - 2	0.0014	0.0209	0.045	1.18E-04	0.001	1.217	10.523
E - 3	0.0014	0.0198	0.045	1.04E-04	0.001	1.182	10.669
E - 4	0.0017	0.0214	0.045	1.03E-04	0.001	1.421	12.443
E - 5	0.0014	0.0187	0.045	8.83E-05	0.001	1.202	11.565
E - 6	0.0017	0.0225	0.045	1.09E-04	0.001	1.418	12.926
E - 7	0.0005	0.0071	0.045	1.26E-04	0.001	0.317	2.484
E - 8	0.0004	0.0064	0.045	1.22E-04	0.001	0.287	2.317
E - 9	0.0005	0.0072	0.045	1.19E-04	0.001	0.306	2.7
E - 10	0.0005	0.0074	0.045	1.29E-04	0.001	0.366	1.26
E - 11	0.0005	0.0072	0.045	1.26E-04	0.001	0.34	1.897
E - 12	0.0005	0.0075	0.045	1.34E-04	0.001	0.38	2.783
E - 13	0.0002	0.0034	0.045	1.21E-04	0.001	0.032	0.223
E - 14	0.0001	0.003	0.045	1.25E-04	0.001	0	0
E - 15	0.0001	0.0033	0.045	8.74E-05	0.001	0.047	0.35

E - 16	0.0002	0.0031	0.045	9.68E-05	0.001	0.052	0.49
E - 17	0.0002	0.0035	0.045	8.76E-05	0.001	0.065	0.629
E - 18	0.0002	0.0029	0.045	1.09E-04	0.001	0.04	0.32
F - 1	0.0005	0.0115	0.045	1.03E-04	0.001	0.369	3.267
F - 2	0.0008	0.0116	0.045	1.09E-04	0.001	0.621	6.003
F - 3	0.0008	0.0116	0.045	1.40E-04	0.001	0.588	0.85
F - 4	0.001	0.012	0.045	1.34E-04	0.001	0.766	2.978
F - 5	0.0009	0.015	0.045	8.36E-05	0.001	0.717	5.074
F - 6	0.001	0.0124	0.045	1.04E-04	0.001	0.794	6.985
F - 7	0.0003	0.0045	0.045	1.22E-04	0.001	0.135	1.172
F - 8	0.0003	0.0041	0.045	1.23E-04	0.001	0.125	1.159
F - 9	0.0003	0.0053	0.045	1.40E-04	0.001	0.127	0.954
F - 10	0.0003	0.0076	0.045	1.24E-04	0.001	0.158	1.124
F - 11	0.0003	0.0045	0.045	1.47E-04	0.001	0.1	0.753
F - 12	0.0003	0.0042	0.045	1.60E-04	0.001	0.115	0.599
F - 13	0.0001	0.0029	0.045	1.06E-04	0.001	0.016	0.15
F - 14	8.18E-05	0.0022	0.045	8.91E-05	0.001	0	0
F - 15	8.99E-05	0.0027	0.045	8.88E-05	0.001	0.001	0.01
F - 16	9.21E-05	0.0026	0.045	8.71E-05	0.001	0.005	0.045
F - 17	8.70E-05	0.0025	0.045	1.01E-04	0.001	0	0
F - 18	0.0001	0.0027	0.045	9.11E-05	0.001	0.014	0.139
G - 1	0.0011	0.0167	0.045	9.59E-05	0.001	0.958	6.941
G - 2	0.0012	0.0178	0.045	1.37E-04	0.001	0.98	4.708
G - 3	0.001	0.0177	0.045	8.77E-05	0.001	0.819	7.334
G - 4	0.0008	0.0148	0.045	1.01E-04	0.001	0.601	4.912
G - 5	0.0014	0.0183	0.045	8.64E-05	0.001	1.164	12.622
G - 6	0.0015	0.0194	0.045	1.05E-04	0.001	1.251	11.615
G - 7	0.0002	0.0056	0.045	1.27E-04	0.001	0.055	0.427
G - 8	0.0002	0.0046	0.045	1.23E-04	0.001	0.04	0.351
G - 9	0.0001	0.0032	0.045	1.23E-04	0.001	0.021	0.175
G - 10	0.0002	0.003	0.045	1.44E-04	0.001	0.007	0.052
G - 11	0.0001	0.0031	0.045	1.53E-04	0.001	0	0
G - 12	0.0002	0.0034	0.045	1.37E-04	0.001	0.027	0.223
G - 13	0.0001	0.0032	0.045	1.33E-04	0.001	0	0
G - 14	9.61E-05	0.0038	0.045	8.74E-05	0.001	0.008	0.077
G - 15	9.41E-05	0.0025	0.045	8.12E-05	0.001	0.012	0.131
G - 16	0.0001	0.0029	0.045	8.97E-05	0.001	0.027	0.259
G - 17	0.0001	0.0028	0.045	9.20E-05	0.001	0.027	0.21
G - 18	0.0001	0.005	0.045	1.02E-04	0.001	0.032	0.279
H - 1	0.0085	0.1376	0.045	1.10E-04	0.001	7.67	67.991
H - 2	0.0081	0.1297	0.045	1.14E-04	0.001	7.354	64.43
H - 3	0.008	0.1354	0.045	1.06E-04	0.001	7.292	64.517
H - 4	0.0096	0.1161	0.045	7.50E-04	0.001	8.144	1.315
H - 5	0.0086	0.1101	0.045	9.00E-05	0.001	7.811	73.703
H - 6	0.0104	0.1323	0.045	1.19E-04	0.001	9.463	82.591

H - 7	0.0007	0.0089	0.045	1.12E-04	0.001	0.503	4.393
H - 8	0.0006	0.0083	0.045	1.42E-04	0.001	0.442	1.923
H - 9	0.0005	0.0077	0.045	1.27E-04	0.001	0.324	2.254
H - 10	0.0007	0.0096	0.045	1.35E-04	0.001	0.54	4.397
H - 11	0.0007	0.0099	0.045	1.55E-04	0.001	0.515	3.49
H - 12	0.0007	0.0091	0.045	1.33E-04	0.001	0.558	4.232
H - 13	0.003	0.0342	0.045	1.24E-04	0.001	2.629	23.092
H - 14	0.0013	0.0119	0.045	1.18E-04	0.001	1.131	7.623
H - 15	0.0015	0.0131	0.045	1.15E-04	0.001	1.279	7.596
H - 16	0.0004	0.0078	0.045	9.26E-05	0.001	0.26	2.376
H - 17	0.0004	0.0054	0.045	9.11E-05	0.001	0.261	2.057
H - 18	0.0004	0.0083	0.045	8.86E-05	0.001	0.286	2.76
I - 1	0.0002	0.0063	0.045	1.11E-04	0.001	0.07	0.67
I - 2	0.0002	0.0081	0.045	1.09E-04	0.001	0.068	0.621
I - 3	0.0002	0.0059	0.045	1.15E-04	0.001	0.049	0.444
I - 4	0.0002	0.0107	0.045	1.27E-04	0.001	0.108	0.826
I - 5	0.0002	0.0082	0.045	7.91E-05	0.001	0.1	1.071
I - 6	0.0003	0.0272	0.045	9.85E-05	0.001	0.152	1.37
I - 7	0.0003	0.005	0.045	1.57E-04	0.001	0.111	0.725
I - 8	0.0003	0.0055	0.045	1.87E-04	0.001	0.108	0.424
I - 9	0.0004	0.0053	0.045	1.67E-04	0.001	0.191	1.161
I - 10	0.0004	0.0062	0.045	1.41E-04	0.001	0.232	1.688
I - 11	0.0005	0.0408	0.045	1.47E-04	0.001	0.321	1.674
I - 12	0.0004	0.0059	0.045	1.85E-04	0.001	0.211	0.295
I - 13	0.004	0.0552	0.045	1.27E-04	0.001	3.564	28.65
I - 14	0.0017	0.0149	0.045	1.12E-04	0.001	1.43	9.714
I - 15	0.0019	0.0163	0.045	1.09E-04	0.001	1.601	9.983
I - 16	0.0003	0.0046	0.045	1.13E-04	0.001	0.187	1.704
I - 17	0.0003	0.0049	0.045	8.97E-05	0.001	0.189	1.843
I - 18	0.0003	0.0049	0.045	9.59E-05	0.001	0.206	1.932
J - 1	0.0001	0.0029	0.045	8.71E-05	0.001	0.032	0.327
J - 2	0.0001	0.0034	0.045	1.09E-04	0.001	0.025	0.2
J - 3	0.0001	0.004	0.045	2.49E-04	0.001	0	0
J - 4	0.0001	0.0033	0.045	2.07E-04	0.001	0	0
J - 5	0.0001	0.0026	0.045	1.02E-04	0.001	0.003	0.025
J - 6	0.0001	0.003	0.045	1.20E-04	0.001	0.012	0.104
J - 7	0.0004	0.0061	0.045	1.40E-04	0.001	0.245	1.806
J - 8	0.0004	0.0061	0.045	1.20E-04	0.001	0.259	2.176
J - 9	0.0004	0.0058	0.045	1.33E-04	0.001	0.232	1.172
J - 10	0.0004	0.0057	0.045	1.55E-04	0.001	0.234	0.608
J - 11	0.0004	0.0063	0.045	1.22E-04	0.001	0.285	2.37
J - 12	0.0005	0.0066	0.045	1.49E-04	0.001	0.295	2.397
J - 13	0.0004	0.0059	0.045	1.25E-04	0.001	0.217	1.587
J - 14	0.0003	0.0055	0.045	1.67E-04	0.001	0.112	0.344
J - 15	0.0002	0.0037	0.045	9.09E-05	0.001	0.119	1.253

J - 16	0.0001	0.0024	0.045	8.10E-05	0.001	0.025	0.252
J - 17	0.0001	0.0028	0.045	9.81E-05	0.001	0.03	0.205
J - 18	0.0002	0.0042	0.045	9.36E-05	0.001	0.055	0.492
K - 1	0.0002	0.0066	0.045	1.00E-04	0.001	0.067	0.607
K - 2	0.0002	0.0039	0.045	1.04E-04	0.001	0.09	0.742
K - 3	0.0002	0.0038	0.045	1.12E-04	0.001	0.076	0.607
K - 4	0.0002	0.0041	0.045	1.16E-04	0.001	0.123	1.025
K - 5	0.0002	0.004	0.045	1.15E-04	0.001	0.094	0.347
K - 6	0.0002	0.0041	0.045	1.14E-04	0.001	0.1	0.921
K - 7	0.0004	0.0059	0.045	1.30E-04	0.001	0.241	1.943
K - 8	0.0004	0.006	0.045	1.38E-04	0.001	0.248	1.338
K - 9	0.0004	0.0062	0.045	1.31E-04	0.001	0.243	2.044
K - 10	0.0004	0.006	0.045	1.15E-04	0.001	0.288	2.506
K - 11	0.0004	0.0062	0.045	1.36E-04	0.001	0.264	1.871
K - 12	0.0004	0.0057	0.045	1.23E-04	0.001	0.263	1.989
K - 13	0.0014	0.0228	0.045	1.29E-04	0.001	1.172	7.805
K - 14	0.0007	0.008	0.045	1.20E-04	0.001	0.54	3.961
K - 15	0.0007	0.0077	0.045	8.70E-05	0.001	0.57	4.586
K - 16	0.0001	0.0029	0.045	1.41E-04	0.001	0	0
K - 17	0.0001	0.0036	0.045	1.09E-04	0.001	0.032	0.284
K - 18	0.0001	0.003	0.045	9.05E-05	0.001	0.042	0.387
L - 1	0.003	0.0534	0.045	9.50E-05	0.001	2.634	24.065
L - 2	0.003	0.0552	0.045	9.92E-05	0.001	2.705	18.313
L - 3	0.0033	0.0582	0.045	1.07E-04	0.001	2.907	26.346
L - 4	0.0003	0.0052	0.045	1.01E-04	0.001	0.193	1.721
L - 5	0.0003	0.0049	0.045	8.87E-05	0.001	0.17	1.797
L - 6	0.0003	0.0049	0.045	1.30E-04	0.001	0.151	1.26
L - 7	0.0001	0.0045	0.045	1.29E-04	0.001	0.015	0.129
L - 8	0.0001	0.0029	0.045	1.46E-04	0.001	0	0
L - 9	0.0001	0.0029	0.045	1.27E-04	0.001	0.012	0.113
L - 10	0.0001	0.0028	0.045	1.99E-04	0.001	0	0
L - 11	0.0004	0.1138	0.045	1.47E-04	0.001	0.244	1.229
L - 12	0.0001	0.0033	0.045	1.42E-04	0.001	0.006	0.037
L - 13	0.0001	0.0028	0.045	1.03E-04	0.001	0.007	0.053
L - 14	0.0001	0.0026	0.045	1.04E-04	0.001	0	0
L - 15	0.0001	0.0039	0.045	1.00E-04	0.001	0.003	0.031
L - 16	8.95E-05	0.0024	0.045	9.98E-05	0.001	0	0
L - 17	0.0001	0.0038	0.045	1.08E-04	0.001	0.021	0.186
L - 18	9.44E-05	0.0029	0.045	1.01E-04	0.001	0	0
M - 1	0.0001	0.0039	0.045	8.59E-05	0.001	0.027	0.282
M - 2	9.40E-05	0.0025	0.045	9.59E-05	0.001	0	0
M - 3	0.0001	0.0027	0.045	8.76E-05	0.001	0.022	0.227
M - 4	0.0001	0.0032	0.045	1.07E-04	0.001	0.024	0.206
M - 5	0.0001	0.0028	0.045	8.50E-05	0.001	0.037	0.392
M - 6	0.0002	0.0034	0.045	1.07E-04	0.001	0.045	0.412

M - 7	0.0001	0.0029	0.045	1.52E-04	0.001	0	0
M - 8	0.0001	0.0044	0.045	1.44E-04	0.001	5.43E-04	0.004
M - 9	0.0001	0.0029	0.045	1.12E-04	0.001	0.006	0.055
M - 10	0.0001	0.0031	0.045	1.35E-04	0.001	0	0
M - 11	0.0001	0.003	0.045	1.49E-04	0.001	0	0
M - 12	0.0002	0.0055	0.045	1.30E-04	0.001	0.025	0.174
M - 13	9.28E-05	0.0024	0.045	8.80E-05	0.001	0.004	0.044
M - 14	8.34E-05	0.0025	0.045	1.07E-04	0.001	0	0
M - 15	9.45E-05	0.0024	0.045	9.87E-05	0.001	0	0
M - 16	0.0001	0.0101	0.045	9.45E-05	0.001	0.018	0.163
M - 17	0.0001	0.0028	0.045	9.07E-05	0.001	0.029	0.275
M - 18	8.95E-05	0.0025	0.045	1.28E-04	0.001	0	0
N - 1	0.0001	0.0031	0.045	9.94E-05	0.001	0.022	0.209
N - 2	0.0001	0.0026	0.045	1.04E-04	0.001	0.004	0.037
N - 3	0.0001	0.0027	0.045	8.88E-05	0.001	0.02	0.2
N - 4	0.0006	0.0091	0.045	1.02E-04	0.001	0.446	3.799
N - 5	0.0005	0.0082	0.045	7.01E-05	0.001	0.4	4.51
N - 6	0.0006	0.0097	0.045	1.01E-04	0.001	0.467	4.236
N - 7	0.0001	0.0029	0.045	1.22E-04	0.001	0	0
N - 8	0.0001	0.0034	0.045	1.07E-04	0.001	0.016	0.14
N - 9	0.0001	0.0034	0.045	1.18E-04	0.001	0.002	0.018
N - 10	0.0001	0.0032	0.045	1.16E-04	0.001	0.007	0.061
N - 11	0.0001	0.0034	0.045	1.44E-04	0.001	0	0
N - 12	0.0001	0.0027	0.045	1.13E-04	0.001	0	0
N - 13	0.0001	0.0029	0.045	1.12E-04	0.001	0	0
N - 14	8.36E-05	0.0024	0.045	9.23E-05	0.001	0	0
N - 15	0.0001	0.0069	0.045	1.01E-04	0.001	0	0
N - 16	0.0001	0.0028	0.045	8.92E-05	0.001	0.015	0.16
N - 17	0.0001	0.0039	0.045	9.61E-05	0.001	0.021	0.211
N - 18	0.0001	0.0038	0.045	4.50E-04	0.001	0	0
A. n	252	252	252	252	252	252	252
A. Mean	0.0012	0.0201	0.045	1.19E-04	0.001	1.005	8.16
A. SD	0.0022	0.0427	0	7.98E-05	0	1.989	17.439
A. CV	179.931	212.6532	0	67.025	5.17E-06	197.899	213.731
A. Total	0.3045	5.0652	11.29	0.03	0.275	253.298	2056.198

Table 18. Results obtained upon the hybridization with *Janibacter limosus* HKI083's RNA.

Element	D x A - ROD x mm2	SD - ROD	Area - mm2	Bkgd	sRef	nDxA	S/N
A - 1	0.0008	0.0098	0.045	3.40E-05	0.002	0.305	9.917
A - 2	0.0007	0.0103	0.045	4.44E-05	0.002	0.261	7.084
A - 3	0.0007	0.0099	0.045	3.61E-05	0.002	0.29	10.697
A - 4	0.0012	0.0137	0.045	4.12E-05	0.002	0.468	11.122
A - 5	0.0015	0.0167	0.045	2.57E-05	0.002	0.605	23.988
A - 6	0.0016	0.029	0.045	7.27E-04	0.002	0.344	0.12
A - 7	0.0153	0.2124	0.045	7.10E-05	0.002	6.24	91.148
A - 8	0.0116	0.1691	0.045	7.68E-05	0.002	4.731	65.617
A - 9	0.0124	0.1801	0.045	7.14E-05	0.002	5.087	99.477
A - 10	0.015	0.245	0.045	8.26E-05	0.002	6.132	111.23
A - 11	0.0165	0.2071	0.045	7.49E-05	0.002	6.769	106.694
A - 12	0.0243	0.4979	0.045	5.01E-04	0.002	9.766	8.929
A - 13	0.0151	0.206	0.045	6.87E-05	0.002	6.165	154.88
A - 14	0.0105	0.1305	0.045	7.39E-05	0.002	4.286	97.145
A - 15	0.0107	0.1181	0.045	7.13E-05	0.002	4.368	101.295
A - 16	0.0111	0.142	0.045	7.79E-05	0.002	4.524	111.07
A - 17	0.0089	0.0928	0.045	7.44E-05	0.002	3.615	43.19
A - 18	0.011	0.1414	0.045	1.23E-04	0.002	4.475	17.905
B - 1	0.0008	0.0102	0.045	3.94E-05	0.002	0.292	9.97
B - 2	0.0008	0.0094	0.045	7.61E-05	0.002	0.283	1.248
B - 3	0.0008	0.0099	0.045	3.26E-05	0.002	0.304	11.055
B - 4	0.0011	0.013	0.045	3.47E-05	0.002	0.426	14.12
B - 5	0.0012	0.0154	0.045	4.45E-05	0.002	0.494	11.595
B - 6	0.0013	0.0155	0.045	5.55E-05	0.002	0.506	14.063
B - 7	0.0017	0.0199	0.045	5.78E-05	0.002	0.694	19.187
B - 8	0.0015	0.0178	0.045	5.64E-05	0.002	0.593	16.195
B - 9	0.0015	0.0183	0.045	4.72E-05	0.002	0.599	18.704
B - 10	0.0016	0.0212	0.045	6.22E-05	0.002	0.65	13.396
B - 11	0.0018	0.0195	0.045	7.47E-05	0.002	0.706	13.628
B - 12	0.002	0.0225	0.045	4.05E-04	0.002	0.652	0.264
B - 13	0.0007	0.0089	0.045	7.47E-05	0.002	0.251	5.375
B - 14	0.0006	0.0087	0.045	6.80E-05	0.002	0.239	5.628
B - 15	0.0007	0.0086	0.045	7.65E-05	0.002	0.244	5.394
B - 16	0.0009	0.0109	0.045	2.84E-04	0.002	0.259	0.202
B - 17	0.0008	0.0104	0.045	7.65E-05	0.002	0.306	7.143
B - 18	0.0008	0.0099	0.045	4.86E-05	0.002	0.304	9.121
C - 1	0.0186	0.4853	0.045	2.74E-04	0.002	7.535	9.976
C - 2	0.0135	0.2216	0.045	4.94E-05	0.002	5.508	68.484
C - 3	0.016	0.3301	0.045	4.85E-05	0.002	6.543	159.491
C - 4	0.0238	0.5004	0.045	6.55E-05	0.002	9.755	156.054
C - 5	0.0456	0.8034	0.045	1.68E-04	0.002	18.694	38.271

C - 6	0.0635	0.9153	0.045	5.03E-04	0.002	25.912	10.371
C - 7	0.0076	0.0825	0.045	6.68E-05	0.002	3.095	71.398
C - 8	0.0058	0.0626	0.045	6.66E-05	0.002	2.361	53.793
C - 9	0.005	0.0609	0.045	6.93E-05	0.002	2.012	29.961
C - 10	0.0069	0.0728	0.045	6.75E-05	0.002	2.819	47.946
C - 11	0.0072	0.068	0.045	6.95E-05	0.002	2.936	61.025
C - 12	0.0081	0.0872	0.045	7.34E-05	0.002	3.299	56.285
C - 13	0.0018	0.0176	0.045	7.09E-05	0.002	0.706	16.132
C - 14	0.0018	0.0194	0.045	6.86E-05	0.002	0.696	12.848
C - 15	0.002	0.02	0.045	7.13E-05	0.002	0.798	19.319
C - 16	0.0027	0.0268	0.045	7.22E-05	0.002	1.071	27.083
C - 17	0.0026	0.0261	0.045	6.04E-05	0.002	1.025	27.19
C - 18	0.0022	0.0218	0.045	6.36E-05	0.002	0.861	17.247
D - 1	0.0041	0.0376	0.045	3.63E-05	0.002	1.671	58.29
D - 2	0.0037	0.0359	0.045	4.44E-05	0.002	1.49	40.127
D - 3	0.004	0.0382	0.045	6.97E-05	0.002	1.617	12.355
D - 4	0.0073	0.0621	0.045	7.87E-05	0.002	2.986	48.254
D - 5	0.0089	0.0835	0.045	8.43E-05	0.002	3.628	25.346
D - 6	0.0097	0.1361	0.045	8.12E-05	0.002	3.956	44.291
D - 7	0.0011	0.1134	0.045	6.92E-05	0.002	0.443	11.176
D - 8	0.0007	0.0088	0.045	5.31E-05	0.002	0.263	7.73
D - 9	0.0006	0.0078	0.045	5.79E-05	0.002	0.236	2.189
D - 10	0.0008	0.0095	0.045	5.45E-05	0.002	0.298	8.975
D - 11	0.0008	0.0094	0.045	5.48E-05	0.002	0.32	8.739
D - 12	0.001	0.0109	0.045	9.13E-05	0.002	0.353	5.128
D - 13	0.0078	0.0809	0.045	6.97E-05	0.002	3.166	66.808
D - 14	0.0071	0.0748	0.045	7.31E-05	0.002	2.893	43.395
D - 15	0.0076	0.0771	0.045	7.20E-05	0.002	3.091	53.594
D - 16	0.0094	0.1005	0.045	6.71E-05	0.002	3.837	91.193
D - 17	0.0093	0.1017	0.045	7.73E-05	0.002	3.783	35.941
D - 18	0.01	0.1019	0.045	5.60E-05	0.002	4.07	105.955
E - 1	0.0009	0.0092	0.045	4.23E-05	0.002	0.338	8.985
E - 2	0.0009	0.0105	0.045	4.25E-05	0.002	0.346	9.474
E - 3	0.001	0.0108	0.045	5.17E-05	0.002	0.389	10.45
E - 4	0.0017	0.0166	0.045	4.53E-05	0.002	0.662	19.731
E - 5	0.0017	0.0182	0.045	6.63E-05	0.002	0.687	12.735
E - 6	0.0019	0.0205	0.045	5.19E-05	0.002	0.778	22.202
E - 7	0.0002	0.0038	0.045	5.81E-05	0.002	0.054	1.33
E - 8	0.0002	0.0037	0.045	7.07E-05	0.002	0.052	1.065
E - 9	0.0002	0.0036	0.045	4.65E-05	0.002	0.057	1.559
E - 10	0.0003	0.0046	0.045	5.60E-05	0.002	0.082	1.819
E - 11	0.0003	0.0045	0.045	6.16E-05	0.002	0.087	2.225
E - 12	0.0003	0.0049	0.045	6.09E-05	0.002	0.091	1.614
E - 13	8.08E-05	0.0024	0.045	4.53E-05	0.002	0.015	0.442
E - 14	8.46E-05	0.0026	0.045	6.04E-05	0.002	0.01	0.268

E - 15	0.0001	0.0029	0.045	6.80E-05	0.002	0.013	0.329
E - 16	0.0001	0.0031	0.045	6.88E-05	0.002	0.013	0.181
E - 17	0.0001	0.0029	0.045	5.59E-05	0.002	0.018	0.35
E - 18	8.25E-05	0.0024	0.045	6.26E-05	0.002	0.008	0.192
F - 1	0.0009	0.01	0.045	4.01E-05	0.002	0.346	11.18
F - 2	0.0009	0.0109	0.045	4.46E-05	0.002	0.346	10.696
F - 3	0.001	0.0104	0.045	7.21E-05	0.002	0.379	3.364
F - 4	0.0018	0.0179	0.045	5.27E-05	0.002	0.701	17.096
F - 5	0.0019	0.0197	0.045	5.54E-05	0.002	0.77	11.96
F - 6	0.002	0.0191	0.045	5.06E-05	0.002	0.788	18.768
F - 7	8.39E-05	0.003	0.045	6.43E-05	0.002	0.008	0.172
F - 8	0.0003	0.0711	0.045	6.28E-05	0.002	0.08	2.093
F - 9	7.50E-05	0.0024	0.045	5.10E-05	0.002	0.01	0.28
F - 10	8.72E-05	0.0025	0.045	5.76E-05	0.002	0.012	0.32
F - 11	0.0001	0.0043	0.045	6.91E-05	0.002	0.025	0.493
F - 12	8.82E-05	0.0026	0.045	5.29E-05	0.002	0.015	0.394
F - 13	8.75E-05	0.0026	0.045	5.67E-05	0.002	0.013	0.296
F - 14	8.80E-05	0.0024	0.045	6.23E-05	0.002	0.011	0.255
F - 15	9.14E-05	0.0024	0.045	5.03E-05	0.002	0.017	0.451
F - 16	9.49E-05	0.0026	0.045	4.32E-05	0.002	0.021	0.668
F - 17	9.26E-05	0.0025	0.045	5.15E-05	0.002	0.017	0.479
F - 18	0.0001	0.0037	0.045	6.16E-05	0.002	0.021	0.553
G - 1	0.0009	0.0109	0.045	4.13E-05	0.002	0.354	10.19
G - 2	0.0009	0.0105	0.045	3.78E-05	0.002	0.35	11.979
G - 3	0.0009	0.0115	0.045	8.62E-05	0.002	0.344	1.557
G - 4	0.0016	0.0171	0.045	4.75E-05	0.002	0.621	15.558
G - 5	0.0017	0.0182	0.045	3.96E-05	0.002	0.663	22.518
G - 6	0.0017	0.0175	0.045	1.55E-04	0.002	0.638	0.825
G - 7	7.57E-05	0.0023	0.045	6.17E-05	0.002	0.006	0.091
G - 8	8.00E-05	0.0025	0.045	4.77E-05	0.002	0.013	0.359
G - 9	5.89E-05	0.002	0.045	3.61E-05	0.002	0.009	0.326
G - 10	7.01E-05	0.0026	0.045	4.72E-05	0.002	0.009	0.28
G - 11	9.45E-05	0.0026	0.045	6.61E-05	0.002	0.012	0.299
G - 12	8.49E-05	0.0024	0.045	5.00E-05	0.002	0.014	0.423
G - 13	5.98E-05	0.0021	0.045	5.34E-05	0.002	0.003	0.071
G - 14	5.64E-05	0.0019	0.045	6.20E-05	0.002	0	0
G - 15	5.99E-05	0.0023	0.045	5.14E-05	0.002	0.003	0.102
G - 16	7.96E-05	0.0024	0.045	6.19E-05	0.002	0.007	0.165
G - 17	7.52E-05	0.0022	0.045	4.74E-05	0.002	0.011	0.345
G - 18	8.61E-05	0.0025	0.045	6.68E-05	0.002	0.008	0.191
H - 1	0.0045	0.043	0.045	1.28E-04	0.002	1.806	6.979
H - 2	0.0049	0.0494	0.045	4.54E-05	0.002	2.005	47.191
H - 3	0.0047	0.0481	0.045	6.44E-05	0.002	1.897	34.666
H - 4	0.0082	0.0669	0.045	1.31E-04	0.002	3.3	12.247
H - 5	0.0098	0.0785	0.045	2.55E-04	0.002	3.904	6.873

H - 6	0.0103	0.0795	0.045	1.31E-04	0.002	4.171	13.349
H - 7	0.0005	0.0059	0.045	6.52E-05	0.002	0.159	1.446
H - 8	0.0004	0.006	0.045	4.72E-05	0.002	0.155	4.563
H - 9	0.0004	0.0058	0.045	5.60E-05	0.002	0.13	2.92
H - 10	0.0007	0.0233	0.045	5.44E-05	0.002	0.253	5.513
H - 11	0.0006	0.0069	0.045	6.76E-05	0.002	0.222	4.84
H - 12	0.0006	0.0073	0.045	5.31E-05	0.002	0.217	6.721
H - 13	0.0014	0.0136	0.045	4.77E-05	0.002	0.574	17.043
H - 14	0.0015	0.0133	0.045	6.00E-05	0.002	0.586	15.52
H - 15	0.0015	0.014	0.045	5.36E-05	0.002	0.609	16.666
H - 16	0.0008	0.0089	0.045	7.25E-05	0.002	0.304	4.384
H - 17	0.0008	0.0086	0.045	6.07E-05	0.002	0.29	7.778
H - 18	0.0008	0.0084	0.045	5.17E-05	0.002	0.307	9.651
I - 1	9.09E-05	0.0048	0.045	3.52E-05	0.002	0.023	0.842
I - 2	0.0001	0.0112	0.045	3.66E-05	0.002	0.028	0.898
I - 3	8.77E-05	0.0038	0.045	5.52E-05	0.002	0.013	0.374
I - 4	0.0002	0.0137	0.045	5.29E-05	0.002	0.069	1.803
I - 5	0.0002	0.0127	0.045	4.58E-05	0.002	0.071	2.123
I - 6	0.0002	0.0104	0.045	5.07E-05	0.002	0.057	1.672
I - 7	0.0004	0.0164	0.045	1.45E-04	0.002	0.092	0.888
I - 8	0.0003	0.0098	0.045	1.46E-04	0.002	0.075	0.629
I - 9	0.0002	0.0041	0.045	1.27E-04	0.002	0.038	0.521
I - 10	0.0003	0.0054	0.045	4.75E-05	0.002	0.109	3.093
I - 11	0.0003	0.0047	0.045	4.53E-05	0.002	0.111	3.471
I - 12	0.0003	0.0053	0.045	6.70E-05	0.002	0.107	1.556
I - 13	0.0028	0.0248	0.045	7.04E-05	0.002	1.102	19.059
I - 14	0.003	0.0262	0.045	6.19E-05	0.002	1.226	28.822
I - 15	0.0032	0.0265	0.045	6.02E-05	0.002	1.305	30.855
I - 16	0.0004	0.0054	0.045	4.84E-05	0.002	0.137	4.197
I - 17	0.0003	0.005	0.045	5.54E-05	0.002	0.113	3.444
I - 18	0.0004	0.005	0.045	5.67E-05	0.002	0.13	3.173
J - 1	4.58E-05	0.0017	0.045	3.31E-05	0.002	0.005	0.182
J - 2	3.64E-05	0.0015	0.045	3.61E-05	0.002	1.30E-04	0.005
J - 3	6.18E-05	0.0027	0.045	5.48E-05	0.002	0.003	0.078
J - 4	7.44E-05	0.0025	0.045	5.10E-05	0.002	0.01	0.266
J - 5	6.50E-05	0.0023	0.045	3.52E-05	0.002	0.012	0.452
J - 6	7.03E-05	0.0045	0.045	5.52E-05	0.002	0.006	0.173
J - 7	0.0004	0.0055	0.045	5.07E-05	0.002	0.139	4.038
J - 8	0.0003	0.0054	0.045	7.89E-05	0.002	0.108	0.874
J - 9	0.0003	0.0058	0.045	4.51E-05	0.002	0.105	3.17
J - 10	0.0005	0.0065	0.045	5.79E-05	0.002	0.165	4.052
J - 11	0.0004	0.006	0.045	5.22E-05	0.002	0.157	4.436
J - 12	0.0004	0.0061	0.045	6.70E-05	0.002	0.144	1.877
J - 13	0.0002	0.0037	0.045	5.91E-05	0.002	0.058	1.379
J - 14	0.0003	0.0287	0.045	6.12E-05	0.002	0.107	1.04

J - 15	0.0002	0.0041	0.045	5.38E-05	0.002	0.071	1.933
J - 16	0.0002	0.0043	0.045	5.52E-05	0.002	0.075	2.175
J - 17	0.0002	0.0043	0.045	6.03E-05	0.002	0.075	1.161
J - 18	0.0002	0.004	0.045	5.50E-05	0.002	0.065	1.988
K - 1	0.0003	0.0047	0.045	2.64E-05	0.002	0.1	4.341
K - 2	0.0003	0.0045	0.045	3.59E-05	0.002	0.089	3.303
K - 3	0.0003	0.0046	0.045	5.29E-05	0.002	0.083	2.245
K - 4	0.0004	0.0059	0.045	5.22E-05	0.002	0.158	4.241
K - 5	0.0005	0.0069	0.045	6.94E-05	0.002	0.177	0.743
K - 6	0.0005	0.0061	0.045	4.30E-05	0.002	0.197	6.133
K - 7	0.0003	0.0043	0.045	5.17E-05	0.002	0.091	2.434
K - 8	0.0003	0.0047	0.045	5.99E-05	0.002	0.087	1.771
K - 9	0.0004	0.012	0.045	4.82E-05	0.002	0.127	3.526
K - 10	0.0004	0.0218	0.045	5.15E-05	0.002	0.156	4.242
K - 11	0.0004	0.0056	0.045	5.78E-05	0.002	0.132	3.374
K - 12	0.0003	0.0054	0.045	6.68E-05	0.002	0.107	1.969
K - 13	0.0011	0.0124	0.045	3.94E-05	0.002	0.416	14.098
K - 14	0.001	0.0114	0.045	4.20E-05	0.002	0.396	12.124
K - 15	0.001	0.0107	0.045	5.97E-05	0.002	0.39	10.35
K - 16	0.0002	0.0034	0.045	5.60E-05	0.002	0.047	1.102
K - 17	0.0001	0.003	0.045	6.09E-05	0.002	0.033	0.818
K - 18	0.0002	0.0184	0.045	5.62E-05	0.002	0.058	1.383
L - 1	0.0011	0.0141	0.045	3.49E-05	0.002	0.419	14.907
L - 2	0.0011	0.0136	0.045	3.68E-05	0.002	0.423	13.339
L - 3	0.0011	0.0158	0.045	2.95E-05	0.002	0.441	17.544
L - 4	0.0001	0.0035	0.045	5.97E-05	0.002	0.022	0.59
L - 5	0.0001	0.0032	0.045	3.82E-05	0.002	0.033	1.054
L - 6	0.0001	0.0029	0.045	5.25E-05	0.002	0.022	0.465
L - 7	5.59E-05	0.0021	0.045	5.08E-05	0.002	0.002	0.055
L - 8	5.01E-05	0.0019	0.045	4.91E-05	0.002	3.98E-04	0.011
L - 9	6.01E-05	0.0024	0.045	5.59E-05	0.002	0.002	0.045
L - 10	6.02E-05	0.0025	0.045	4.58E-05	0.002	0.006	0.178
L - 11	6.05E-05	0.0022	0.045	5.65E-05	0.002	0.002	0.041
L - 12	4.50E-05	0.0018	0.045	5.05E-05	0.002	0	0
L - 13	5.51E-05	0.004	0.045	4.60E-05	0.002	0.004	0.113
L - 14	4.70E-05	0.0025	0.045	6.60E-05	0.002	0	0
L - 15	5.89E-05	0.0024	0.045	5.48E-05	0.002	0.002	0.041
L - 16	4.84E-05	0.0021	0.045	5.43E-05	0.002	0	0
L - 17	5.63E-05	0.0021	0.045	6.32E-05	0.002	0	0
L - 18	5.83E-05	0.0022	0.045	5.56E-05	0.002	0.001	0.025
M - 1	3.64E-05	0.0015	0.045	2.48E-05	0.002	0.005	0.206
M - 2	5.08E-05	0.0027	0.045	4.41E-05	0.002	0.003	0.088
M - 3	4.28E-05	0.0019	0.045	2.93E-05	0.002	0.006	0.222
M - 4	6.92E-05	0.0024	0.045	4.55E-05	0.002	0.01	0.303
M - 5	5.57E-05	0.0028	0.045	3.52E-05	0.002	0.008	0.293

M - 6	5.79E-05	0.0025	0.045	4.60E-05	0.002	0.005	0.153
M - 7	4.86E-05	0.0019	0.045	5.34E-05	0.002	0	0
M - 8	5.08E-05	0.002	0.045	7.06E-05	0.002	0	0
M - 9	4.91E-05	0.0019	0.045	5.85E-05	0.002	0	0
M - 10	5.18E-05	0.0018	0.045	5.73E-05	0.002	0	0
M - 11	4.44E-05	0.0018	0.045	4.86E-05	0.002	0	0
M - 12	5.68E-05	0.0021	0.045	6.31E-05	0.002	0	0
M - 13	5.32E-05	0.002	0.045	5.98E-05	0.002	0	0
M - 14	7.08E-05	0.0031	0.045	5.68E-05	0.002	0.006	0.126
M - 15	5.52E-05	0.0021	0.045	5.70E-05	0.002	0	0
M - 16	5.52E-05	0.0022	0.045	6.34E-05	0.002	0	0
M - 17	0.0002	0.0064	0.045	6.67E-05	0.002	0.037	0.735
M - 18	5.72E-05	0.0024	0.045	5.21E-05	0.002	0.002	0.063
N - 1	0.0001	0.0033	0.045	3.43E-05	0.002	0.045	1.372
N - 2	0.0002	0.0034	0.045	4.72E-05	0.002	0.045	1.282
N - 3	0.0002	0.0033	0.045	2.81E-05	0.002	0.061	2.494
N - 4	0.0003	0.0053	0.045	3.12E-05	0.002	0.104	3.673
N - 5	0.0004	0.0062	0.045	3.47E-05	0.002	0.138	4.76
N - 6	0.0004	0.0065	0.045	5.30E-05	0.002	0.128	2.916
N - 7	5.20E-05	0.002	0.045	4.49E-05	0.002	0.003	0.082
N - 8	5.11E-05	0.002	0.045	5.15E-05	0.002	0	0
N - 9	5.57E-05	0.0021	0.045	5.43E-05	0.002	5.96E-04	0.016
N - 10	5.39E-05	0.0021	0.045	2.49E-04	0.002	0	0
N - 11	3.87E-05	0.0019	0.045	5.22E-05	0.002	0	0
N - 12	5.42E-05	0.0027	0.045	4.60E-05	0.002	0.003	0.1
N - 13	4.82E-05	0.0021	0.045	5.07E-05	0.002	0	0
N - 14	5.09E-05	0.0019	0.045	5.10E-05	0.002	0	0
N - 15	5.08E-05	0.002	0.045	6.13E-05	0.002	0	0
N - 16	4.70E-05	0.0019	0.045	5.98E-05	0.002	0	0
N - 17	6.39E-05	0.0033	0.045	5.45E-05	0.002	0.004	0.101
N - 18	5.09E-05	0.0019	0.045	5.52E-05	0.002	0	0
A. n	252	252	252	252	252	252	252
A. Mean	0.0025	0.0362	0.045	6.95E-05	0.002	1.001	14.05
A. SD	0.0062	0.1009	0	6.92E-05	0	2.55	27.327
A. CV	249.1982	278.3345	0	99.57	0	254.836	194.502
A. Total	0.6306	9.1312	11.29	0.018	0.613	252.143	3540.553

Table 19. Results obtained upon the hybridization with *Amycolatopsis orientalis* IMET7653's RNA.

Element	D x A - ROD x mm2	SD - ROD	Area - mm2	Bkgd	sRef	nDxA	S/N
A - 1	0.0011	0.0146	0.045	2.27E-05	8.10E-04	1.366	18.987
A - 2	0.0009	0.0109	0.045	2.76E-05	8.10E-04	1.095	14.946
A - 3	0.0011	0.014	0.045	3.39E-05	8.10E-04	1.284	10.929
A - 4	0.0014	0.0171	0.045	2.05E-05	8.10E-04	1.73	27.752
A - 5	0.0013	0.0166	0.045	2.27E-05	8.10E-04	1.553	24.917
A - 6	0.0016	0.0213	0.045	3.40E-05	8.10E-04	1.977	21.673
A - 7	0.0049	0.0744	0.045	8.69E-05	8.10E-04	5.934	11.253
A - 8	0.0037	0.0457	0.045	9.14E-05	8.10E-04	4.457	9.711
A - 9	0.0037	0.0513	0.045	3.94E-05	8.10E-04	4.551	48.909
A - 10	0.0046	0.0571	0.045	5.20E-05	8.10E-04	5.675	26.453
A - 11	0.0042	0.0515	0.045	3.75E-05	8.10E-04	5.115	56.641
A - 12	0.005	0.0706	0.045	4.37E-05	8.10E-04	6.076	39.009
A - 13	0.0026	0.0372	0.045	4.29E-05	8.10E-04	3.119	16.165
A - 14	0.0025	0.1196	0.045	3.52E-05	8.10E-04	3.102	38.075
A - 15	0.002	0.1151	0.045	7.09E-05	8.10E-04	2.385	4.532
A - 16	0.0023	0.026	0.045	3.49E-05	8.10E-04	2.754	33.253
A - 17	0.0025	0.0276	0.045	5.86E-05	8.10E-04	2.976	5.551
A - 18	0.0028	0.0305	0.045	3.48E-05	8.10E-04	3.442	30.372
B - 1	0.0003	0.0051	0.045	3.68E-05	8.10E-04	0.335	3.474
B - 2	0.0003	0.0062	0.045	3.56E-05	8.10E-04	0.313	3.512
B - 3	0.0004	0.0153	0.045	3.14E-05	8.10E-04	0.47	5.517
B - 4	0.0005	0.0069	0.045	2.53E-05	8.10E-04	0.595	8.408
B - 5	0.0005	0.0061	0.045	3.28E-05	8.10E-04	0.517	6.306
B - 6	0.0005	0.007	0.045	2.86E-05	8.10E-04	0.578	7.944
B - 7	0.001	0.0123	0.045	3.19E-05	8.10E-04	1.245	14.224
B - 8	0.001	0.0121	0.045	2.62E-05	8.10E-04	1.175	15.401
B - 9	0.001	0.0134	0.045	2.29E-05	8.10E-04	1.195	16.764
B - 10	0.0011	0.0147	0.045	3.44E-05	8.10E-04	1.29	16.414
B - 11	0.0011	0.0128	0.045	3.27E-05	8.10E-04	1.33	10.719
B - 12	0.0011	0.0146	0.045	2.93E-05	8.10E-04	1.317	17.282
B - 13	0.0015	0.0182	0.045	3.12E-05	8.10E-04	1.861	22.951
B - 14	0.0012	0.0156	0.045	3.02E-05	8.10E-04	1.487	19.663
B - 15	0.0011	0.0137	0.045	4.53E-05	8.10E-04	1.275	13.141
B - 16	0.0014	0.0171	0.045	3.73E-05	8.10E-04	1.736	20.132
B - 17	0.0016	0.0193	0.045	3.80E-05	8.10E-04	1.976	23.113
B - 18	0.0019	0.0228	0.045	3.90E-05	8.10E-04	2.308	19.818
C - 1	0.0074	0.097	0.045	6.42E-05	8.10E-04	9.042	37.369
C - 2	0.0063	0.0752	0.045	3.23E-05	8.10E-04	7.734	96.474
C - 3	0.0064	0.0842	0.045	3.14E-05	8.10E-04	7.912	96.735
C - 4	0.0072	0.0892	0.045	4.65E-05	8.10E-04	8.825	56.217
C - 5	0.0071	0.0894	0.045	3.83E-05	8.10E-04	8.727	81.197
C - 6	0.0088	0.1191	0.045	1.15E-04	8.10E-04	10.755	15.457

C - 7	0.0022	0.025	0.045	3.71E-05	8.10E-04	2.613	27.377
C - 8	0.0016	0.019	0.045	2.60E-05	8.10E-04	1.954	27.874
C - 9	0.0017	0.0187	0.045	3.93E-05	8.10E-04	2.009	17.528
C - 10	0.002	0.0223	0.045	4.45E-05	8.10E-04	2.445	13.708
C - 11	0.002	0.0215	0.045	5.36E-05	8.10E-04	2.432	14.915
C - 12	0.0024	0.0334	0.045	3.78E-05	8.10E-04	2.972	26.492
C - 13	0.0013	0.0162	0.045	4.28E-05	8.10E-04	1.561	14.625
C - 14	0.0012	0.0137	0.045	3.42E-05	8.10E-04	1.427	17.681
C - 15	0.0011	0.013	0.045	3.38E-05	8.10E-04	1.301	15.055
C - 16	0.0013	0.017	0.045	2.53E-05	8.10E-04	1.52	22.79
C - 17	0.0015	0.018	0.045	3.11E-05	8.10E-04	1.864	24.606
C - 18	0.0015	0.0184	0.045	3.97E-05	8.10E-04	1.811	19.357
D - 1	0.0018	0.0184	0.045	6.32E-05	8.10E-04	2.089	9.22
D - 2	0.0019	0.0208	0.045	4.23E-05	8.10E-04	2.278	21.659
D - 3	0.0019	0.0199	0.045	3.85E-05	8.10E-04	2.307	26.862
D - 4	0.003	0.0296	0.045	4.68E-05	8.10E-04	3.704	32.507
D - 5	0.0027	0.031	0.045	3.26E-05	8.10E-04	3.296	40.039
D - 6	0.0029	0.0285	0.045	4.16E-05	8.10E-04	3.522	22.294
D - 7	0.0002	0.006	0.045	3.33E-05	8.10E-04	0.261	3.421
D - 8	0.0002	0.0042	0.045	3.14E-05	8.10E-04	0.225	2.706
D - 9	0.0002	0.0038	0.045	3.37E-05	8.10E-04	0.201	2.434
D - 10	0.0002	0.0042	0.045	3.05E-05	8.10E-04	0.252	2.994
D - 11	0.0002	0.0045	0.045	3.81E-05	8.10E-04	0.256	2.048
D - 12	0.0003	0.005	0.045	3.75E-05	8.10E-04	0.297	2.121
D - 13	0.0021	0.0281	0.045	3.92E-05	8.10E-04	2.6	28.994
D - 14	0.0018	0.0218	0.045	3.61E-05	8.10E-04	2.185	28.141
D - 15	0.0017	0.0217	0.045	4.71E-05	8.10E-04	2.029	9.408
D - 16	0.0019	0.0253	0.045	3.21E-05	8.10E-04	2.348	29.035
D - 17	0.0018	0.0227	0.045	4.68E-05	8.10E-04	2.161	18.897
D - 18	0.0019	0.0248	0.045	3.78E-05	8.10E-04	2.271	26.76
E - 1	0.0005	0.0062	0.045	3.94E-05	8.10E-04	0.522	5.467
E - 2	0.0005	0.0067	0.045	4.51E-05	8.10E-04	0.613	6.251
E - 3	0.0006	0.0072	0.045	3.97E-05	8.10E-04	0.643	6.987
E - 4	0.0008	0.0098	0.045	4.04E-05	8.10E-04	0.971	10.027
E - 5	0.0008	0.0096	0.045	2.67E-05	8.10E-04	0.921	10.884
E - 6	0.0008	0.0182	0.045	3.59E-05	8.10E-04	0.922	10.829
E - 7	0.0002	0.0038	0.045	3.47E-05	8.10E-04	0.206	2.363
E - 8	0.0002	0.0039	0.045	4.27E-05	8.10E-04	0.227	2.541
E - 9	0.0002	0.0044	0.045	6.23E-05	8.10E-04	0.213	0.53
E - 10	0.0003	0.0047	0.045	3.90E-05	8.10E-04	0.303	2.992
E - 11	0.0003	0.0049	0.045	3.16E-05	8.10E-04	0.319	3.683
E - 12	0.0003	0.0051	0.045	2.05E-04	8.10E-04	0.091	0.026
E - 13	6.02E-05	0.0023	0.045	3.73E-05	8.10E-04	0.028	0.324
E - 14	5.35E-05	0.0019	0.045	3.44E-05	8.10E-04	0.024	0.295
E - 15	5.01E-05	0.0018	0.045	2.88E-05	8.10E-04	0.026	0.356
E - 16	4.96E-05	0.0019	0.045	3.40E-05	8.10E-04	0.019	0.224
E - 17	5.01E-05	0.0019	0.045	3.37E-05	8.10E-04	0.02	0.27

E - 18	6.26E-05	0.0023	0.045	2.71E-05	8.10E-04	0.044	0.644
F - 1	0.0003	0.0052	0.045	3.82E-05	8.10E-04	0.367	4.166
F - 2	0.0004	0.006	0.045	5.93E-05	8.10E-04	0.43	3.35
F - 3	0.0004	0.0051	0.045	3.73E-05	8.10E-04	0.394	4.734
F - 4	0.0007	0.0078	0.045	3.28E-05	8.10E-04	0.765	8.902
F - 5	0.0006	0.0074	0.045	2.74E-05	8.10E-04	0.674	9.067
F - 6	0.0006	0.0078	0.045	4.48E-05	8.10E-04	0.661	2.35
F - 7	7.74E-05	0.0024	0.045	3.94E-05	8.10E-04	0.047	0.539
F - 8	6.52E-05	0.002	0.045	3.80E-05	8.10E-04	0.034	0.424
F - 9	7.49E-05	0.0023	0.045	4.15E-05	8.10E-04	0.041	0.452
F - 10	8.35E-05	0.0024	0.045	4.15E-05	8.10E-04	0.052	0.568
F - 11	8.68E-05	0.0026	0.045	3.76E-05	8.10E-04	0.061	0.614
F - 12	8.67E-05	0.0027	0.045	3.70E-05	8.10E-04	0.061	0.734
F - 13	4.36E-05	0.002	0.045	3.30E-05	8.10E-04	0.013	0.156
F - 14	4.64E-05	0.0022	0.045	3.21E-05	8.10E-04	0.018	0.224
F - 15	4.56E-05	0.0017	0.045	3.90E-05	8.10E-04	0.008	0.085
F - 16	3.09E-05	0.0013	0.045	2.48E-05	8.10E-04	0.008	0.109
F - 17	2.80E-05	0.0012	0.045	3.14E-05	8.10E-04	0	0
F - 18	3.54E-05	0.0017	0.045	2.74E-05	8.10E-04	0.01	0.138
G - 1	0.0005	0.0075	0.045	4.39E-05	8.10E-04	0.602	6.127
G - 2	0.0005	0.0069	0.045	3.64E-05	8.10E-04	0.585	6.645
G - 3	0.0005	0.007	0.045	4.06E-05	8.10E-04	0.597	5.885
G - 4	0.0009	0.0099	0.045	3.33E-05	8.10E-04	1.034	6.898
G - 5	0.0008	0.0089	0.045	4.39E-05	8.10E-04	0.908	9.459
G - 6	0.0008	0.0093	0.045	3.77E-05	8.10E-04	0.935	11.185
G - 7	4.46E-05	0.0016	0.045	1.20E-04	8.10E-04	0	0
G - 8	3.93E-05	0.0015	0.045	2.79E-05	8.10E-04	0.014	0.179
G - 9	5.20E-05	0.002	0.045	2.97E-05	8.10E-04	0.027	0.343
G - 10	5.37E-05	0.002	0.045	3.99E-05	8.10E-04	0.017	0.175
G - 11	5.64E-05	0.002	0.045	3.59E-05	8.10E-04	0.025	0.273
G - 12	4.75E-05	0.0019	0.045	3.26E-05	8.10E-04	0.018	0.212
G - 13	4.36E-05	0.0032	0.045	3.52E-05	8.10E-04	0.01	0.127
G - 14	3.61E-05	0.0015	0.045	3.47E-05	8.10E-04	0.002	0.023
G - 15	3.68E-05	0.0017	0.045	3.23E-05	8.10E-04	0.005	0.067
G - 16	5.20E-05	0.0019	0.045	3.19E-05	8.10E-04	0.025	0.29
G - 17	4.12E-05	0.0016	0.045	2.65E-05	8.10E-04	0.018	0.233
G - 18	4.50E-05	0.0018	0.045	2.79E-05	8.10E-04	0.021	0.277
H - 1	0.0024	0.0271	0.045	5.28E-05	8.10E-04	2.936	11.529
H - 2	0.0025	0.0256	0.045	1.04E-04	8.10E-04	2.948	5.159
H - 3	0.0025	0.1138	0.045	1.65E-04	8.10E-04	2.909	3.744
H - 4	0.0042	0.0372	0.045	1.01E-04	8.10E-04	5.047	9.192
H - 5	0.004	0.0381	0.045	1.50E-04	8.10E-04	4.788	6.887
H - 6	0.0038	0.0336	0.045	1.01E-04	8.10E-04	4.629	9.829
H - 7	7.08E-05	0.0024	0.045	3.66E-05	8.10E-04	0.042	0.448
H - 8	6.35E-05	0.002	0.045	3.38E-05	8.10E-04	0.037	0.377
H - 9	7.76E-05	0.0023	0.045	3.48E-05	8.10E-04	0.053	0.412
H - 10	7.93E-05	0.0024	0.045	4.97E-05	8.10E-04	0.037	0.27

H - 11	0.0001	0.0037	0.045	3.16E-05	8.10E-04	0.085	1.084
H - 12	7.57E-05	0.0022	0.045	3.85E-05	8.10E-04	0.046	0.439
H - 13	0.0019	0.0163	0.045	5.06E-05	8.10E-04	2.223	9.157
H - 14	0.0015	0.0147	0.045	6.61E-05	8.10E-04	1.791	6.796
H - 15	0.0014	0.0133	0.045	4.09E-05	8.10E-04	1.711	16.089
H - 16	0.0001	0.0029	0.045	3.75E-05	8.10E-04	0.088	0.972
H - 17	0.0001	0.0027	0.045	3.68E-05	8.10E-04	0.085	0.96
H - 18	9.14E-05	0.0026	0.045	3.31E-05	8.10E-04	0.072	0.66
I - 1	0.0002	0.0261	0.045	3.42E-05	8.10E-04	0.199	2.272
I - 2	0.0001	0.0067	0.045	4.53E-05	8.10E-04	0.088	0.911
I - 3	0.0004	0.1148	0.045	4.81E-05	8.10E-04	0.447	1.325
I - 4	0.0002	0.0087	0.045	3.94E-05	8.10E-04	0.147	1.657
I - 5	0.0003	0.0188	0.045	3.80E-05	8.10E-04	0.268	2.903
I - 6	0.0005	0.1163	0.045	3.28E-05	8.10E-04	0.591	7.034
I - 7	8.62E-05	0.0053	0.045	1.26E-04	8.10E-04	0	0
I - 8	0.0001	0.0116	0.045	7.56E-05	8.10E-04	0.043	0.154
I - 9	6.86E-05	0.0066	0.045	7.64E-05	8.10E-04	0	0
I - 10	4.34E-05	0.0022	0.045	3.63E-05	8.10E-04	0.009	0.106
I - 11	3.21E-05	0.0013	0.045	3.28E-05	8.10E-04	0	0
I - 12	4.13E-05	0.0022	0.045	3.42E-05	8.10E-04	0.009	0.105
I - 13	0.0022	0.0193	0.045	4.50E-05	8.10E-04	2.667	18.556
I - 14	0.0019	0.0177	0.045	5.23E-05	8.10E-04	2.301	15.772
I - 15	0.0017	0.0161	0.045	5.30E-05	8.10E-04	2.071	11.018
I - 16	0.0001	0.0039	0.045	3.23E-05	8.10E-04	0.095	1.116
I - 17	9.50E-05	0.0027	0.045	2.57E-05	8.10E-04	0.086	1.274
I - 18	8.75E-05	0.0024	0.045	2.55E-05	8.10E-04	0.077	1.169
J - 1	3.87E-05	0.0017	0.045	1.36E-04	8.10E-04	0	0
J - 2	4.23E-05	0.0019	0.045	3.42E-05	8.10E-04	0.01	0.113
J - 3	3.08E-05	0.0014	0.045	2.64E-05	8.10E-04	0.005	0.075
J - 4	5.49E-05	0.0021	0.045	2.98E-05	8.10E-04	0.031	0.364
J - 5	3.76E-05	0.0015	0.045	2.62E-05	8.10E-04	0.014	0.208
J - 6	3.97E-05	0.0017	0.045	2.81E-05	8.10E-04	0.014	0.193
J - 7	6.91E-05	0.0023	0.045	3.41E-05	8.10E-04	0.043	0.389
J - 8	6.58E-05	0.0021	0.045	3.49E-05	8.10E-04	0.038	0.439
J - 9	8.30E-05	0.0033	0.045	4.33E-05	8.10E-04	0.049	0.415
J - 10	7.06E-05	0.0022	0.045	3.75E-05	8.10E-04	0.041	0.465
J - 11	8.15E-05	0.0023	0.045	3.07E-05	8.10E-04	0.063	0.822
J - 12	6.87E-05	0.0028	0.045	3.47E-05	8.10E-04	0.042	0.507
J - 13	0.0002	0.0036	0.045	3.49E-05	8.10E-04	0.17	2.098
J - 14	0.0002	0.0035	0.045	6.99E-05	8.10E-04	0.128	0.369
J - 15	0.0002	0.0032	0.045	4.39E-05	8.10E-04	0.143	1.403
J - 16	6.30E-05	0.0021	0.045	4.22E-05	8.10E-04	0.026	0.137
J - 17	6.12E-05	0.002	0.045	3.52E-05	8.10E-04	0.032	0.386
J - 18	6.25E-05	0.0019	0.045	3.35E-05	8.10E-04	0.036	0.435
K - 1	9.66E-05	0.0026	0.045	4.28E-05	8.10E-04	0.066	0.615
K - 2	0.0003	0.0173	0.045	3.16E-04	8.10E-04	0	0
K - 3	0.0001	0.0034	0.045	1.68E-04	8.10E-04	0	0

K - 4	0.0002	0.0062	0.045	6.18E-05	8.10E-04	0.198	0.978
K - 5	0.0002	0.0045	0.045	4.24E-05	8.10E-04	0.146	1.029
K - 6	0.0003	0.0207	0.045	5.23E-05	8.10E-04	0.323	2.317
K - 7	9.94E-05	0.0035	0.045	4.52E-05	8.10E-04	0.067	0.525
K - 8	8.02E-05	0.003	0.045	4.11E-05	8.10E-04	0.048	0.434
K - 9	6.56E-05	0.0022	0.045	3.59E-05	8.10E-04	0.037	0.407
K - 10	5.28E-05	0.002	0.045	5.03E-05	8.10E-04	0.003	0.026
K - 11	5.71E-05	0.002	0.045	3.73E-05	8.10E-04	0.024	0.265
K - 12	5.40E-05	0.0018	0.045	3.31E-05	8.10E-04	0.026	0.289
K - 13	0.0013	0.0116	0.045	5.44E-05	8.10E-04	1.494	8.379
K - 14	0.0012	0.0136	0.045	4.89E-05	8.10E-04	1.459	14.248
K - 15	0.001	0.0105	0.045	5.79E-05	8.10E-04	1.172	9.067
K - 16	4.69E-05	0.0019	0.045	3.04E-05	8.10E-04	0.02	0.26
K - 17	4.56E-05	0.0017	0.045	3.26E-05	8.10E-04	0.016	0.216
K - 18	4.92E-05	0.0017	0.045	2.39E-05	8.10E-04	0.031	0.406
L - 1	0.0008	0.0106	0.045	3.47E-05	8.10E-04	0.917	10.438
L - 2	0.0007	0.0099	0.045	3.59E-05	8.10E-04	0.848	10.191
L - 3	0.0008	0.0111	0.045	2.43E-05	8.10E-04	0.969	15.086
L - 4	0.0001	0.0032	0.045	2.83E-05	8.10E-04	0.132	1.736
L - 5	0.0001	0.0028	0.045	3.38E-05	8.10E-04	0.083	0.939
L - 6	0.0001	0.0026	0.045	2.88E-05	8.10E-04	0.093	1.276
L - 7	4.19E-05	0.0024	0.045	3.52E-05	8.10E-04	0.008	0.101
L - 8	4.96E-05	0.0043	0.045	4.18E-05	8.10E-04	0.01	0.106
L - 9	4.13E-05	0.002	0.045	3.23E-05	8.10E-04	0.011	0.136
L - 10	3.66E-05	0.0018	0.045	3.59E-05	8.10E-04	9.39E-04	0.011
L - 11	5.27E-05	0.0052	0.045	3.59E-05	8.10E-04	0.021	0.227
L - 12	3.56E-05	0.0016	0.045	4.41E-05	8.10E-04	0	0
L - 13	3.28E-05	0.0014	0.045	2.93E-05	8.10E-04	0.004	0.058
L - 14	3.86E-05	0.0016	0.045	3.28E-05	8.10E-04	0.007	0.094
L - 15	3.06E-05	0.0016	0.045	3.42E-05	8.10E-04	0	0
L - 16	2.70E-05	0.0013	0.045	3.45E-05	8.10E-04	0	0
L - 17	2.69E-05	0.0014	0.045	3.02E-05	8.10E-04	0	0
L - 18	3.68E-05	0.0016	0.045	2.90E-05	8.10E-04	0.01	0.116
M - 1	3.85E-05	0.0016	0.045	3.02E-05	8.10E-04	0.01	0.12
M - 2	3.47E-05	0.0016	0.045	2.93E-05	8.10E-04	0.007	0.095
M - 3	3.25E-05	0.0015	0.045	3.19E-05	8.10E-04	7.93E-04	0.01
M - 4	6.08E-05	0.002	0.045	3.37E-05	8.10E-04	0.033	0.25
M - 5	4.06E-05	0.0019	0.045	2.86E-05	8.10E-04	0.015	0.185
M - 6	4.46E-05	0.0017	0.045	1.56E-04	8.10E-04	0	0
M - 7	3.32E-05	0.0014	0.045	3.42E-05	8.10E-04	0	0
M - 8	3.49E-05	0.0016	0.045	3.66E-05	8.10E-04	0	0
M - 9	3.18E-05	0.0015	0.045	3.33E-05	8.10E-04	0	0
M - 10	3.64E-05	0.0016	0.045	2.55E-05	8.10E-04	0.013	0.185
M - 11	3.49E-05	0.0015	0.045	3.37E-05	8.10E-04	0.001	0.018
M - 12	3.56E-05	0.0016	0.045	7.12E-05	8.10E-04	0	0
M - 13	3.44E-05	0.0017	0.045	3.04E-05	8.10E-04	0.005	0.063
M - 14	3.78E-05	0.0016	0.045	3.94E-05	8.10E-04	0	0

M - 15	2.69E-05	0.0014	0.045	2.95E-05	8.10E-04	0	0
M - 16	2.55E-05	0.0013	0.045	2.24E-05	8.10E-04	0.004	0.063
M - 17	2.60E-05	0.0012	0.045	3.16E-05	8.10E-04	0	0
M - 18	2.84E-05	0.0013	0.045	3.31E-05	8.10E-04	0	0
N - 1	3.64E-05	0.0015	0.045	2.74E-05	8.10E-04	0.011	0.156
N - 2	4.29E-05	0.0017	0.045	2.24E-05	8.10E-04	0.025	0.41
N - 3	3.52E-05	0.0016	0.045	2.83E-05	8.10E-04	0.009	0.125
N - 4	0.0004	0.0067	0.045	3.66E-05	8.10E-04	0.478	5.452
N - 5	0.0004	0.0059	0.045	2.36E-05	8.10E-04	0.452	6.665
N - 6	0.0004	0.0057	0.045	4.05E-05	8.10E-04	0.41	3.317
N - 7	2.86E-05	0.0014	0.045	3.41E-05	8.10E-04	0	0
N - 8	3.42E-05	0.0014	0.045	3.02E-05	8.10E-04	0.005	0.06
N - 9	3.27E-05	0.0014	0.045	2.69E-05	8.10E-04	0.007	0.09
N - 10	3.29E-05	0.0017	0.045	2.79E-05	8.10E-04	0.006	0.078
N - 11	3.45E-05	0.0014	0.045	2.93E-05	8.10E-04	0.007	0.088
N - 12	2.93E-05	0.0013	0.045	3.39E-05	8.10E-04	0	0
N - 13	3.70E-05	0.0028	0.045	2.31E-05	8.10E-04	0.017	0.285
N - 14	2.24E-05	0.0013	0.045	2.67E-05	8.10E-04	0	0
N - 15	2.81E-05	0.0013	0.045	3.24E-05	8.10E-04	0	0
N - 16	1.85E-05	0.001	0.045	3.09E-05	8.10E-04	0	0
N - 17	2.52E-05	0.0013	0.045	3.16E-05	8.10E-04	0	0
N - 18	2.92E-05	0.0012	0.045	2.69E-05	8.10E-04	0.003	0.039
A. n	252	252	252	252	252	252	252
A. Mean	0.0009	0.0135	0.045	4.32E-05	8.10E-04	1.003	8.034
A. SD	0.0014	0.0226	0	3.02E-05	0	1.747	13.99
A. CV	166.707	168.0461	0	69.864	9.93E-06	174.297	174.134
A. Total	0.2149	3.3898	11.29	0.011	0.204	252.647	2024.528

Table 20. Results obtained upon the hybridization with *Streptomyces griseus* IMET40235's RNA.

Element	D x A - ROD x mm2	SD - ROD	Area - mm2	Bkgd	sRef	nDxA	S/N
A - 1	0.0002	0.0038	0.045	3.20E-05	9.63E-04	0.154	1.644
A - 2	0.0002	0.0041	0.045	2.25E-05	9.63E-04	0.176	2.036
A - 3	0.0002	0.0036	0.045	1.89E-05	9.63E-04	0.153	2.754
A - 4	0.0002	0.0039	0.045	2.27E-05	9.63E-04	0.145	2.539
A - 5	0.0001	0.003	0.045	1.63E-05	9.63E-04	0.112	2.741
A - 6	0.0001	0.0029	0.045	2.03E-05	9.63E-04	0.097	1.942
A - 7	0.0056	0.0686	0.045	6.55E-05	9.63E-04	5.704	13.571
A - 8	0.0042	0.0513	0.045	2.66E-05	9.63E-04	4.381	46.901
A - 9	0.0044	0.0497	0.045	2.65E-05	9.63E-04	4.592	68.362
A - 10	0.0055	0.0677	0.045	3.37E-05	9.63E-04	5.694	49.627
A - 11	0.006	0.0665	0.045	3.60E-05	9.63E-04	6.184	27.2
A - 12	0.008	0.1001	0.045	1.23E-04	9.63E-04	8.214	10.101
A - 13	0.0069	0.1354	0.045	3.60E-05	9.63E-04	7.163	76.266
A - 14	0.0048	0.0565	0.045	3.54E-05	9.63E-04	4.986	41.892
A - 15	0.005	0.0595	0.045	4.22E-05	9.63E-04	5.183	28.581
A - 16	0.0064	0.0738	0.045	5.01E-05	9.63E-04	6.565	15.637
A - 17	0.006	0.0684	0.045	8.55E-05	9.63E-04	6.102	10.918
A - 18	0.0088	0.1179	0.045	1.08E-04	9.63E-04	8.987	14.046
B - 1	0.0002	0.0033	0.045	2.20E-05	9.63E-04	0.134	2.33
B - 2	0.0002	0.0035	0.045	2.24E-05	9.63E-04	0.141	2.703
B - 3	0.0002	0.0036	0.045	1.25E-05	9.63E-04	0.152	3.966
B - 4	0.0002	0.0034	0.045	2.43E-05	9.63E-04	0.144	2.302
B - 5	0.0001	0.0028	0.045	1.84E-05	9.63E-04	0.09	1.601
B - 6	8.51E-05	0.0024	0.045	1.77E-05	9.63E-04	0.07	1.579
B - 7	0.0007	0.0091	0.045	1.63E-05	9.63E-04	0.696	14.156
B - 8	0.0006	0.008	0.045	2.39E-05	9.63E-04	0.591	9.776
B - 9	0.0006	0.0078	0.045	2.08E-05	9.63E-04	0.583	11.19
B - 10	0.0007	0.0087	0.045	2.13E-05	9.63E-04	0.677	11.88
B - 11	0.0007	0.0082	0.045	2.27E-05	9.63E-04	0.651	11.207
B - 12	0.0009	0.0104	0.045	3.63E-05	9.63E-04	0.849	4.469
B - 13	0.0019	0.0187	0.045	2.85E-05	9.63E-04	1.971	19.011
B - 14	0.002	0.1138	0.045	7.44E-05	9.63E-04	1.97	2.093
B - 15	0.0017	0.0171	0.045	2.69E-05	9.63E-04	1.705	23.244
B - 16	0.0022	0.0225	0.045	1.70E-05	9.63E-04	2.282	38.514
B - 17	0.0023	0.0214	0.045	2.60E-05	9.63E-04	2.33	37.65
B - 18	0.0022	0.0221	0.045	3.08E-05	9.63E-04	2.272	23.499
C - 1	0.0074	0.0995	0.045	7.43E-05	9.63E-04	7.645	13.469
C - 2	0.0065	0.076	0.045	2.46E-05	9.63E-04	6.761	102.102
C - 3	0.0068	0.081	0.045	4.32E-05	9.63E-04	7.034	24.814
C - 4	0.0078	0.0862	0.045	3.60E-05	9.63E-04	8.019	34.758
C - 5	0.0081	0.0913	0.045	5.08E-05	9.63E-04	8.371	28.563
C - 6	0.0139	0.324	0.045	3.99E-04	9.63E-04	14.039	7.184
C - 7	0.002	0.0233	0.045	2.70E-05	9.63E-04	2.061	24.504
C - 8	0.0016	0.0187	0.045	2.98E-05	9.63E-04	1.638	19.655

C - 9	0.0015	0.0205	0.045	3.26E-05	9.63E-04	1.484	12.557
C - 10	0.0021	0.0209	0.045	2.39E-05	9.63E-04	2.122	33.503
C - 11	0.0022	0.0238	0.045	2.91E-05	9.63E-04	2.276	25.807
C - 12	0.003	0.0338	0.045	3.46E-05	9.63E-04	3.034	21.736
C - 13	0.0009	0.0103	0.045	2.08E-05	9.63E-04	0.883	14.738
C - 14	0.0008	0.0092	0.045	2.10E-05	9.63E-04	0.758	14.018
C - 15	0.0008	0.0099	0.045	2.62E-05	9.63E-04	0.816	11.561
C - 16	0.0011	0.0113	0.045	2.27E-05	9.63E-04	1.085	19.256
C - 17	0.001	0.0109	0.045	2.48E-05	9.63E-04	0.977	15.778
C - 18	0.0009	0.0106	0.045	2.08E-05	9.63E-04	0.903	15.224
D - 1	0.0025	0.0232	0.045	2.76E-05	9.63E-04	2.54	36.865
D - 2	0.0025	0.0235	0.045	3.14E-05	9.63E-04	2.579	22.604
D - 3	0.0024	0.0237	0.045	3.02E-05	9.63E-04	2.425	20.249
D - 4	0.0034	0.0308	0.045	3.63E-05	9.63E-04	3.541	31.505
D - 5	0.0034	0.0316	0.045	5.86E-05	9.63E-04	3.44	11.853
D - 6	0.003	0.0293	0.045	3.61E-05	9.63E-04	3.074	25.051
D - 7	0.0002	0.0038	0.045	2.27E-05	9.63E-04	0.189	2.873
D - 8	0.0002	0.0034	0.045	2.53E-05	9.63E-04	0.156	2.579
D - 9	0.0002	0.0035	0.045	1.91E-05	9.63E-04	0.141	2.733
D - 10	0.0002	0.0041	0.045	2.20E-05	9.63E-04	0.183	3.178
D - 11	0.0002	0.0038	0.045	2.53E-05	9.63E-04	0.173	2.401
D - 12	0.0003	0.0047	0.045	2.06E-05	9.63E-04	0.241	4.199
D - 13	0.0036	0.0365	0.045	3.96E-05	9.63E-04	3.675	19.298
D - 14	0.0031	0.031	0.045	2.82E-05	9.63E-04	3.208	38.262
D - 15	0.0032	0.0314	0.045	2.20E-05	9.63E-04	3.34	63.123
D - 16	0.0043	0.0434	0.045	3.04E-05	9.63E-04	4.411	38.858
D - 17	0.0042	0.0408	0.045	2.68E-05	9.63E-04	4.32	48.788
D - 18	0.0049	0.0473	0.045	3.20E-05	9.63E-04	5.004	46.628
E - 1	0.0004	0.0057	0.045	2.15E-05	9.63E-04	0.389	6.821
E - 2	0.0003	0.0061	0.045	2.64E-05	9.63E-04	0.33	5.222
E - 3	0.0005	0.0062	0.045	2.15E-05	9.63E-04	0.451	8.255
E - 4	0.0006	0.0076	0.045	2.36E-05	9.63E-04	0.615	9.919
E - 5	0.0005	0.0072	0.045	2.64E-05	9.63E-04	0.528	8.846
E - 6	0.0006	0.0075	0.045	2.15E-05	9.63E-04	0.559	9.199
E - 7	0.0002	0.0035	0.045	2.03E-05	9.63E-04	0.16	3.051
E - 8	0.0002	0.0035	0.045	1.96E-05	9.63E-04	0.153	2.89
E - 9	0.0002	0.0035	0.045	2.62E-05	9.63E-04	0.132	1.969
E - 10	0.0002	0.0038	0.045	1.63E-05	9.63E-04	0.191	4.528
E - 11	0.0002	0.0041	0.045	1.94E-05	9.63E-04	0.207	3.822
E - 12	0.0002	0.0039	0.045	1.82E-05	9.63E-04	0.192	4.19
E - 13	3.29E-05	0.0016	0.045	1.58E-05	9.63E-04	0.018	0.4
E - 14	3.01E-05	0.0014	0.045	1.51E-05	9.63E-04	0.016	0.332
E - 15	3.27E-05	0.0015	0.045	1.58E-05	9.63E-04	0.017	0.361
E - 16	3.28E-05	0.0015	0.045	1.72E-05	9.63E-04	0.016	0.344
E - 17	4.00E-05	0.0024	0.045	2.08E-05	9.63E-04	0.02	0.377
E - 18	3.81E-05	0.0016	0.045	1.73E-05	9.63E-04	0.022	0.437
F - 1	0.0003	0.0044	0.045	1.70E-05	9.63E-04	0.259	5.833

F - 2	0.0003	0.006	0.045	2.08E-05	9.63E-04	0.32	5.936
F - 3	0.0003	0.005	0.045	2.36E-05	9.63E-04	0.309	5.521
F - 4	0.0005	0.0074	0.045	2.51E-05	9.63E-04	0.528	6.891
F - 5	0.0005	0.0059	0.045	2.13E-05	9.63E-04	0.465	8.42
F - 6	0.0004	0.0058	0.045	2.37E-05	9.63E-04	0.397	4.818
F - 7	5.63E-05	0.0022	0.045	2.05E-05	9.63E-04	0.037	0.723
F - 8	4.90E-05	0.0017	0.045	2.08E-05	9.63E-04	0.029	0.522
F - 9	4.89E-05	0.0018	0.045	1.87E-05	9.63E-04	0.031	0.57
F - 10	5.79E-05	0.002	0.045	2.13E-05	9.63E-04	0.038	0.681
F - 11	5.67E-05	0.002	0.045	1.82E-05	9.63E-04	0.04	0.795
F - 12	6.64E-05	0.0032	0.045	2.10E-05	9.63E-04	0.047	0.96
F - 13	2.19E-05	0.0013	0.045	1.54E-05	9.63E-04	0.007	0.162
F - 14	2.18E-05	0.0012	0.045	2.17E-05	9.63E-04	3.69E-05	6.75E-04
F - 15	2.19E-05	0.0011	0.045	2.13E-05	9.63E-04	6.44E-04	0.009
F - 16	6.19E-05	0.015	0.045	2.41E-05	9.63E-04	0.039	0.714
F - 17	2.02E-05	0.0012	0.045	1.77E-05	9.63E-04	0.003	0.053
F - 18	2.40E-05	0.0014	0.045	1.51E-05	9.63E-04	0.009	0.208
G - 1	0.0003	0.0047	0.045	1.98E-05	9.63E-04	0.297	5.572
G - 2	0.0004	0.0059	0.045	1.94E-05	9.63E-04	0.353	6.598
G - 3	0.0004	0.0055	0.045	1.77E-05	9.63E-04	0.348	7.771
G - 4	0.0005	0.0068	0.045	2.13E-05	9.63E-04	0.51	9.056
G - 5	0.0004	0.0064	0.045	2.29E-05	9.63E-04	0.399	6.233
G - 6	0.0003	0.0052	0.045	1.91E-05	9.63E-04	0.327	6.66
G - 7	3.13E-05	0.0014	0.045	1.87E-05	9.63E-04	0.013	0.261
G - 8	3.06E-05	0.0013	0.045	1.80E-05	9.63E-04	0.013	0.282
G - 9	2.38E-05	0.0012	0.045	2.08E-05	9.63E-04	0.003	0.054
G - 10	2.47E-05	0.0012	0.045	2.92E-05	9.63E-04	0	0
G - 11	2.06E-05	0.0011	0.045	1.98E-05	9.63E-04	7.47E-04	0.015
G - 12	2.72E-05	0.0014	0.045	2.27E-05	9.63E-04	0.005	0.078
G - 13	1.92E-05	0.001	0.045	1.51E-05	9.63E-04	0.004	0.102
G - 14	1.95E-05	0.0011	0.045	2.08E-05	9.63E-04	0	0
G - 15	2.21E-05	0.0012	0.045	2.17E-05	9.63E-04	3.67E-04	0.003
G - 16	3.83E-05	0.0015	0.045	2.27E-05	9.63E-04	0.016	0.274
G - 17	3.34E-05	0.0016	0.045	2.13E-05	9.63E-04	0.013	0.198
G - 18	4.32E-05	0.0023	0.045	1.91E-05	9.63E-04	0.025	0.441
H - 1	0.0026	0.0201	0.045	3.56E-05	9.63E-04	2.642	17.395
H - 2	0.0029	0.0254	0.045	4.47E-05	9.63E-04	2.984	16.948
H - 3	0.0031	0.0279	0.045	7.37E-05	9.63E-04	3.159	8.425
H - 4	0.0054	0.0401	0.045	1.14E-04	9.63E-04	5.451	8.275
H - 5	0.005	0.0378	0.045	9.85E-05	9.63E-04	5.077	10.941
H - 6	0.0039	0.0326	0.045	1.11E-04	9.63E-04	3.93	7.649
H - 7	4.29E-05	0.0017	0.045	1.91E-05	9.63E-04	0.025	0.462
H - 8	4.54E-05	0.0016	0.045	2.12E-05	9.63E-04	0.025	0.495
H - 9	4.90E-05	0.0018	0.045	2.01E-05	9.63E-04	0.03	0.567
H - 10	5.02E-05	0.0018	0.045	2.36E-05	9.63E-04	0.028	0.446
H - 11	3.74E-05	0.0016	0.045	1.89E-05	9.63E-04	0.019	0.392
H - 12	3.91E-05	0.0015	0.045	2.15E-05	9.63E-04	0.018	0.327

H - 13	0.0004	0.0055	0.045	3.08E-05	9.63E-04	0.36	3.868
H - 14	0.0004	0.0047	0.045	3.38E-05	9.63E-04	0.337	3.819
H - 15	0.0004	0.006	0.045	2.95E-05	9.63E-04	0.398	5.236
H - 16	0.0004	0.0059	0.045	3.31E-05	9.63E-04	0.38	4.411
H - 17	0.0003	0.005	0.045	2.32E-05	9.63E-04	0.338	4.528
H - 18	0.0004	0.0053	0.045	1.84E-05	9.63E-04	0.36	7.181
I - 1	5.23E-05	0.0033	0.045	2.55E-05	9.63E-04	0.028	0.44
I - 2	4.61E-05	0.0024	0.045	1.96E-05	9.63E-04	0.028	0.587
I - 3	6.92E-05	0.0043	0.045	2.55E-05	9.63E-04	0.045	0.686
I - 4	8.00E-05	0.0049	0.045	2.29E-05	9.63E-04	0.059	1.164
I - 5	0.0001	0.0067	0.045	2.38E-05	9.63E-04	0.084	1.487
I - 6	0.0001	0.0187	0.045	2.63E-05	9.63E-04	0.115	1.362
I - 7	5.27E-05	0.003	0.045	8.22E-05	9.63E-04	0	0
I - 8	4.46E-05	0.0023	0.045	4.71E-05	9.63E-04	0	0
I - 9	4.42E-05	0.0035	0.045	9.39E-05	9.63E-04	0	0
I - 10	2.12E-05	0.0012	0.045	1.82E-05	9.63E-04	0.003	0.06
I - 11	2.09E-05	0.0011	0.045	1.87E-05	9.63E-04	0.002	0.05
I - 12	2.35E-05	0.0012	0.045	2.20E-05	9.63E-04	0.002	0.028
I - 13	0.0013	0.0124	0.045	3.22E-05	9.63E-04	1.302	15.46
I - 14	0.0012	0.0122	0.045	3.44E-05	9.63E-04	1.233	8.087
I - 15	0.0013	0.0119	0.045	3.15E-05	9.63E-04	1.29	13.139
I - 16	0.0001	0.0031	0.045	1.56E-05	9.63E-04	0.118	2.796
I - 17	9.26E-05	0.0025	0.045	2.50E-05	9.63E-04	0.07	1.239
I - 18	8.95E-05	0.0024	0.045	1.54E-05	9.63E-04	0.077	1.734
J - 1	2.30E-05	0.0013	0.045	1.89E-05	9.63E-04	0.004	0.078
J - 2	2.58E-05	0.0013	0.045	1.98E-05	9.63E-04	0.006	0.121
J - 3	3.08E-05	0.0015	0.045	2.08E-05	9.63E-04	0.01	0.183
J - 4	2.57E-05	0.0013	0.045	1.91E-05	9.63E-04	0.007	0.148
J - 5	2.77E-05	0.0013	0.045	2.34E-05	9.63E-04	0.005	0.08
J - 6	3.11E-05	0.0015	0.045	2.24E-05	9.63E-04	0.009	0.156
J - 7	3.32E-05	0.0014	0.045	1.63E-05	9.63E-04	0.018	0.372
J - 8	3.45E-05	0.0015	0.045	1.94E-05	9.63E-04	0.016	0.328
J - 9	3.25E-05	0.0014	0.045	2.01E-05	9.63E-04	0.013	0.256
J - 10	2.33E-05	0.0011	0.045	1.68E-05	9.63E-04	0.007	0.13
J - 11	3.62E-05	0.0015	0.045	2.22E-05	9.63E-04	0.015	0.246
J - 12	3.75E-05	0.0016	0.045	1.82E-05	9.63E-04	0.02	0.432
J - 13	8.06E-05	0.0023	0.045	1.49E-05	9.63E-04	0.068	1.388
J - 14	6.85E-05	0.0021	0.045	1.72E-05	9.63E-04	0.053	1.246
J - 15	7.12E-05	0.0022	0.045	1.47E-05	9.63E-04	0.059	1.425
J - 16	4.97E-05	0.0017	0.045	1.84E-05	9.63E-04	0.032	0.676
J - 17	0.0002	0.0615	0.045	1.56E-05	9.63E-04	0.179	3.896
J - 18	4.52E-05	0.0022	0.045	1.42E-05	9.63E-04	0.032	0.722
K - 1	5.56E-05	0.0022	0.045	1.89E-05	9.63E-04	0.038	0.715
K - 2	5.43E-05	0.002	0.045	2.03E-05	9.63E-04	0.035	0.55
K - 3	5.64E-05	0.0019	0.045	2.29E-05	9.63E-04	0.035	0.574
K - 4	7.98E-05	0.0025	0.045	1.84E-05	9.63E-04	0.064	1.362
K - 5	7.67E-05	0.0022	0.045	1.63E-05	9.63E-04	0.063	1.276

K - 6	7.06E-05	0.0023	0.045	1.70E-05	9.63E-04	0.056	1.099
K - 7	3.66E-05	0.0016	0.045	2.05E-05	9.63E-04	0.017	0.32
K - 8	2.98E-05	0.0015	0.045	2.13E-05	9.63E-04	0.009	0.168
K - 9	3.47E-05	0.0015	0.045	2.31E-05	9.63E-04	0.012	0.213
K - 10	4.16E-05	0.0018	0.045	2.24E-05	9.63E-04	0.02	0.336
K - 11	3.59E-05	0.0016	0.045	3.68E-05	9.63E-04	0	0
K - 12	3.15E-05	0.0014	0.045	2.29E-05	9.63E-04	0.009	0.158
K - 13	0.0013	0.0126	0.045	2.63E-05	9.63E-04	1.341	16.85
K - 14	0.0014	0.0126	0.045	4.50E-05	9.63E-04	1.447	9.475
K - 15	0.0014	0.0136	0.045	4.34E-05	9.63E-04	1.415	9.116
K - 16	7.74E-05	0.0023	0.045	1.80E-05	9.63E-04	0.062	1.258
K - 17	6.27E-05	0.002	0.045	1.77E-05	9.63E-04	0.047	0.954
K - 18	7.18E-05	0.0022	0.045	1.21E-05	9.63E-04	0.062	1.569
L - 1	0.0008	0.01	0.045	2.08E-05	9.63E-04	0.797	14.856
L - 2	0.0009	0.0111	0.045	2.58E-05	9.63E-04	0.916	12.823
L - 3	0.0009	0.0125	0.045	3.15E-05	9.63E-04	0.925	10.634
L - 4	4.99E-05	0.0019	0.045	2.12E-05	9.63E-04	0.03	0.615
L - 5	4.33E-05	0.0018	0.045	1.65E-05	9.63E-04	0.028	0.559
L - 6	4.31E-05	0.0018	0.045	1.82E-05	9.63E-04	0.026	0.554
L - 7	1.92E-05	0.001	0.045	1.82E-05	9.63E-04	0.001	0.023
L - 8	2.09E-05	0.0012	0.045	1.99E-05	9.63E-04	0.001	0.019
L - 9	1.92E-05	0.0011	0.045	1.80E-05	9.63E-04	0.001	0.027
L - 10	2.11E-05	0.0011	0.045	1.80E-05	9.63E-04	0.003	0.063
L - 11	1.67E-05	0.0011	0.045	2.06E-05	9.63E-04	0	0
L - 12	1.83E-05	0.001	0.045	1.37E-05	9.63E-04	0.005	0.114
L - 13	2.12E-05	0.0012	0.045	2.08E-05	9.63E-04	4.85E-04	0.009
L - 14	2.38E-05	0.0012	0.045	1.96E-05	9.63E-04	0.004	0.085
L - 15	1.97E-05	0.0011	0.045	1.84E-05	9.63E-04	0.001	0.026
L - 16	1.66E-05	0.001	0.045	1.84E-05	9.63E-04	0	0
L - 17	1.65E-05	0.001	0.045	1.54E-05	9.63E-04	0.001	0.026
L - 18	1.78E-05	0.0011	0.045	1.56E-05	9.63E-04	0.002	0.049
M - 1	2.12E-05	0.0012	0.045	3.67E-05	9.63E-04	0	0
M - 2	2.23E-05	0.0012	0.045	2.15E-05	9.63E-04	7.92E-04	0.013
M - 3	2.64E-05	0.0014	0.045	2.51E-05	9.63E-04	0.001	0.02
M - 4	2.19E-05	0.0012	0.045	2.72E-05	9.63E-04	0	0
M - 5	2.55E-05	0.0014	0.045	2.15E-05	9.63E-04	0.004	0.066
M - 6	2.25E-05	0.0013	0.045	1.96E-05	9.63E-04	0.003	0.061
M - 7	2.31E-05	0.0014	0.045	1.56E-05	9.63E-04	0.008	0.187
M - 8	2.36E-05	0.0013	0.045	1.91E-05	9.63E-04	0.005	0.094
M - 9	1.90E-05	0.0011	0.045	2.08E-05	9.63E-04	0	0
M - 10	1.60E-05	0.001	0.045	1.89E-05	9.63E-04	0	0
M - 11	1.67E-05	0.0012	0.045	1.89E-05	9.63E-04	0	0
M - 12	2.18E-05	0.0012	0.045	1.82E-05	9.63E-04	0.004	0.068
M - 13	1.66E-05	0.0009	0.045	2.79E-05	9.63E-04	0	0
M - 14	2.11E-05	0.0011	0.045	2.32E-05	9.63E-04	0	0
M - 15	1.92E-05	0.0012	0.045	1.70E-05	9.63E-04	0.002	0.051
M - 16	1.78E-05	0.0011	0.045	2.08E-05	9.63E-04	0	0

M - 17	1.68E-05	0.0012	0.045	1.91E-05	9.63E-04	0	0
M - 18	2.00E-05	0.0011	0.045	1.35E-05	9.63E-04	0.007	0.171
N - 1	3.22E-05	0.0015	0.045	3.35E-05	9.63E-04	0	0
N - 2	4.79E-05	0.0029	0.045	2.32E-05	9.63E-04	0.026	0.405
N - 3	2.91E-05	0.0014	0.045	1.89E-05	9.63E-04	0.011	0.203
N - 4	0.0003	0.0048	0.045	2.46E-05	9.63E-04	0.257	3.05
N - 5	0.0003	0.0048	0.045	2.74E-05	9.63E-04	0.233	3.398
N - 6	0.0002	0.0042	0.045	2.05E-05	9.63E-04	0.203	3.867
N - 7	1.43E-05	0.0009	0.045	2.02E-05	9.63E-04	0	0
N - 8	1.94E-05	0.0011	0.045	1.58E-05	9.63E-04	0.004	0.073
N - 9	2.18E-05	0.0013	0.045	2.29E-05	9.63E-04	0	0
N - 10	2.09E-05	0.0012	0.045	2.30E-05	9.63E-04	0	0
N - 11	2.19E-05	0.0013	0.045	2.20E-05	9.63E-04	0	0
N - 12	1.58E-05	0.0009	0.045	1.82E-05	9.63E-04	0	0
N - 13	2.40E-05	0.0011	0.045	1.84E-05	9.63E-04	0.006	0.111
N - 14	2.00E-05	0.0011	0.045	1.91E-05	9.63E-04	9.43E-04	0.018
N - 15	1.95E-05	0.0011	0.045	2.31E-05	9.63E-04	0	0
N - 16	1.77E-05	0.0012	0.045	2.20E-05	9.63E-04	0	0
N - 17	2.14E-05	0.0012	0.045	1.68E-05	9.63E-04	0.005	0.1
N - 18	1.87E-05	0.0011	0.045	2.03E-05	9.63E-04	0	0
A. n	252	252	252	252	252	252	252
A. Mean	0.001	0.0134	0.045	2.81E-05	9.63E-04	1.001	7.601
A. SD	0.002	0.0297	0	2.88E-05	0	2.031	13.767
A. CV	199.4007	221.745	0	102.777	0	203.008	181.113
A. Total	0.2497	3.3799	11.29	0.007	0.243	252.169	1915.578

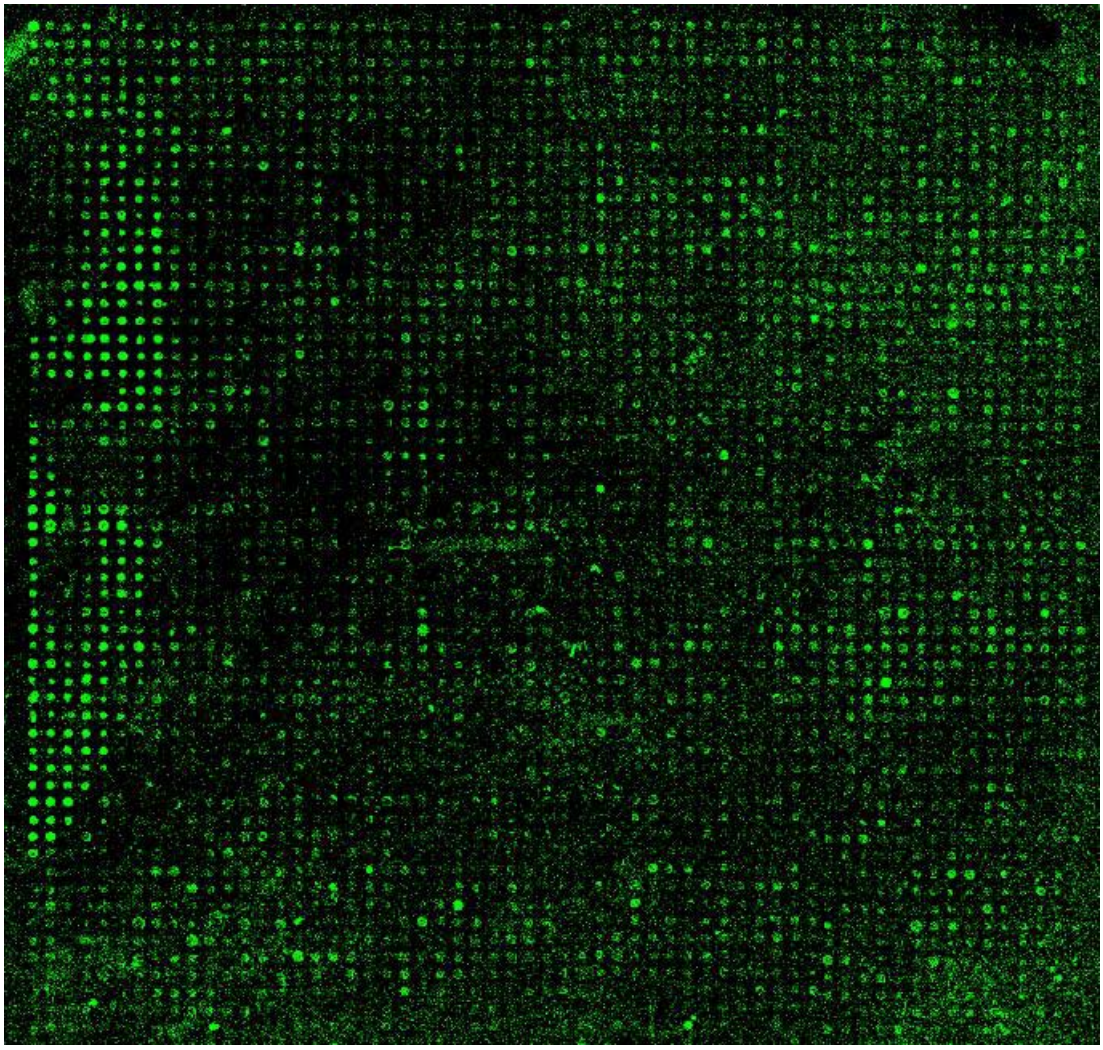

Figure 18. Signals detected in Cy3 channel upon hybridisation with *S.erythraea* DSM 41750 cDNA isolated from cells grown in rich and semi-synthetic media (experiment I).

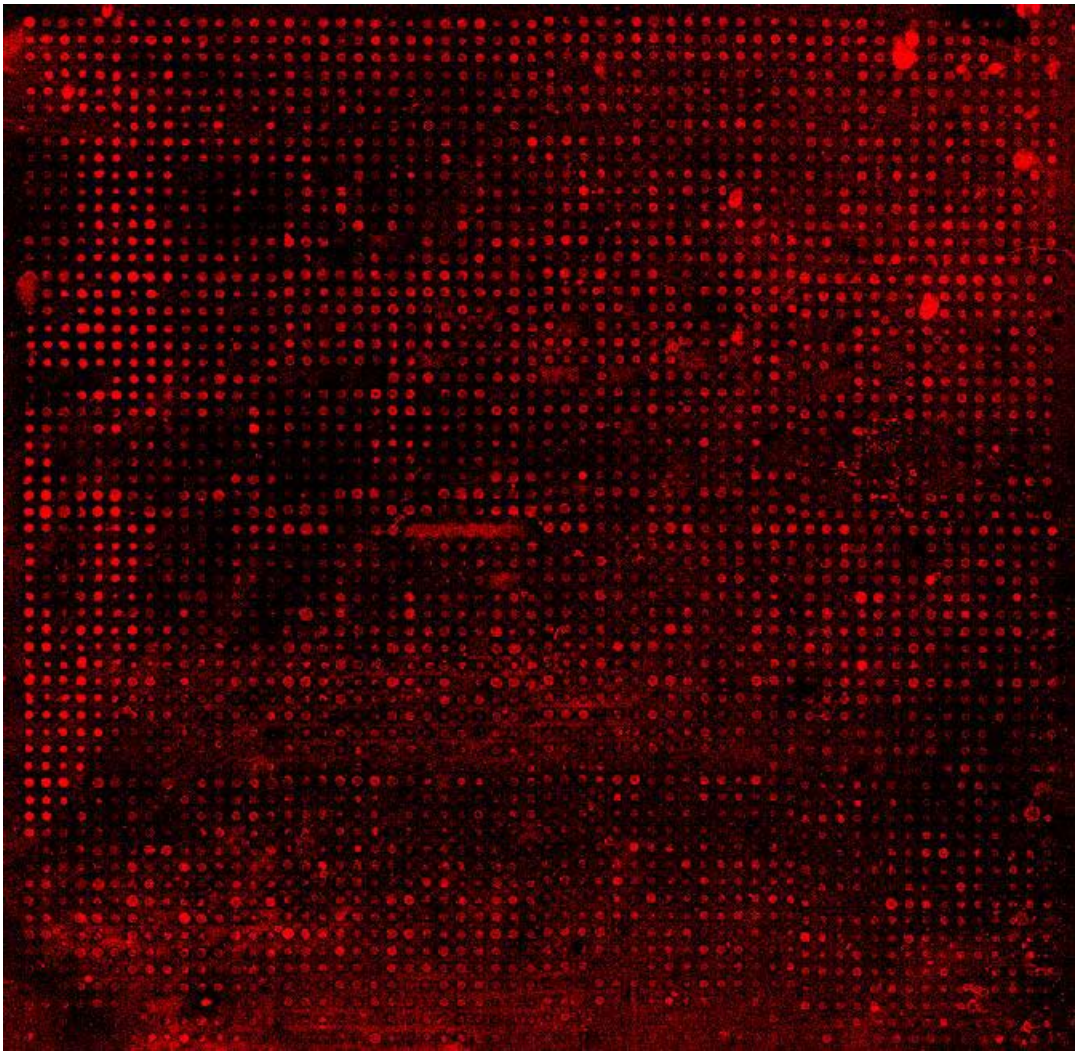

Figure 19. Signals detected in Cy5 channel upon hybridisation with *S.erythraea* DSM 41750 cDNA isolated from cells grown in rich and semi-synthetic media (experiment I).